

**EFFECT OF SUBDUCTION GROUND MOTIONS ON REGIONAL SEISMIC RISK
ASSESSMENT IN SELECTED LOCALITIES IN BRITISH COLUMBIA**

by

ANN ABRAHAM

B.Tech., National Institute of Technology Calicut, 2012

M.Sc., IUSS di Pavia & UJF-Grenoble 1, 2015

A THESIS SUBMITTED IN PARTIAL FULFILLMENT OF
THE REQUIREMENTS FOR THE DEGREE OF

DOCTOR OF PHILOSOPHY

in

THE FACULTY OF GRADUATE AND POSTDOCTORAL STUDIES
(Civil Engineering)

THE UNIVERSITY OF BRITISH COLUMBIA
(Vancouver)

April 2023

© Ann Abraham, 2023

The following individuals certify that they have read, and recommend to the Faculty of Graduate and Postdoctoral Studies for acceptance, the dissertation entitled:

Effect of subduction ground motions on regional seismic risk assessment in selected localities
in British Columbia

submitted by Ann Abraham in partial fulfilment of the requirements for

the degree of Doctor of Philosophy

In Civil Engineering

Examining Committee:

Carlos Ventura, Professor, Civil Engineering, UBC
Supervisor

Thomas Tannert, Professor, Wood Engineering, University of Northern British Columbia
Supervisory Committee Member

Tiegan Hobbs, Adjunct Professor, Earth, Ocean and Atmospheric Sciences, UBC
Supervisory Committee Member

Terje Haukaas, Professor, Civil Engineering, UBC
University Examiner

Stephanie Chang, Professor, Community and Regional Planning, UBC
University Examiner

Additional Supervisory Committee Members:

Liam Finn, Emeritus Professor, Civil Engineering, UBC
Supervisory Committee Member

Abstract

In this thesis, the effect of subduction ground motions on Regional Seismic Risk Assessment (RSRA) in British Columbia (BC), is studied. The primary objective of this study is to measure the increase in RSRA results when explicitly accounting for risk from the subduction events within the RSRA. Separate crustal and subduction fragility and vulnerability functions are introduced in RSRA to estimate risk from different seismic sources in 10 selected localities in BC, with varying subduction hazard. The resulting collapse and loss exceedance curves, average annual collapse fraction, average annual loss and loss ratios are used to measure the effect of subduction ground motions on RSRA.

Fragility and vulnerability functions are developed for predominant building typologies in BC (wood and concrete shear wall (C2)), for crustal and subduction events, using single-degree-of-freedom models that represent BC construction. New typologies are introduced to better classify BC wood buildings. Scenario risk analyses are done for Vancouver using these functions to determine the effect of the changes made, as compared to functions currently used to develop the first generation Canadian Seismic Risk Model (CanSRM1), before they are used to perform RSRA.

Most BC building typologies are weaker than the corresponding typologies used to develop the CanSRM1, implying that damage and loss estimates are higher when using BC-specific functions. Long duration effects of the subduction ground motions influence the fragility and vulnerability functions of newer constructions more, due to their larger inherent ductility. Subfloors and cripple walls increase the loss and damage estimates in low-rise residential wood construction. Scenario loss analyses in Vancouver shows that largest individual asset losses are

from C2, multi-family residential and commercial wood construction, while most of the total damage and loss comes from low-rise residential wood constructions. RSRA demonstrate that as the relative contribution of subduction hazard to total seismic hazard increases, generally, the influence of subduction ground motions on regional risk becomes significant. Therefore, using crustal functions alone for RSRA in sites within mainland BC will provide a good estimate of seismic risk, while it will be severely underestimated in sites on the islands off the mainland coast of BC.

Lay Summary

Earthquakes produced by different types of seismic sources generates different responses from the same structure. British Columbia can experience three types of earthquakes due to its proximity to crustal, subcrustal and subduction seismic sources. To understand the effect of subduction earthquakes - with typically longer duration of shaking- on the BC building stock over a long period of time, when compared to other types of earthquakes, we require appropriate functions that can estimate damage and losses to BC structures.

This thesis studies how subduction ground motions influence the estimations of damage and loss over a long period of time in 10 selected localities in BC, using fragility and vulnerability functions developed to estimate damage and loss to BC building types under crustal and subduction earthquakes. These findings can provide information essential to modify seismic risk maps for BC, to better include the effect of long duration subduction events.

Preface

This dissertation is the original work of Ann Abraham, conducted at the University of British Columbia in Vancouver, under the supervision of Prof. Carlos E. Ventura.

I am the primary author of this dissertation and conducted all the numerical analyses involved. Dr. Armin Bebamzadeh and Dr. Michael Fairhurst of UBC, provided the ground motion sets developed for the BC Seismic Retrofit Guidelines - 3rd edition (SRG3), which I used for Incremental Dynamic Analyses (IDAs). The source code for VMTK (Vulnerability Modellers Toolkit), used to develop the fragility and vulnerability functions in this study was provided by Dr. Luis Martins of the GEM Foundation. The OpenQuake (OQ) engine used to conduct seismic scenario analyses and regional seismic risk analyses was provided by the GEM Foundation.

A version of chapter 3 and chapter 4 has been published in the proceedings of the 12th Canadian Conference on Earthquake Engineering (CCEE), titled “Seismic vulnerability in Southwestern BC - impact of long duration subduction ground motions on wood typologies”. The paper was co-authored by Dr. Carlos E. Ventura and Dr. Armin Bebamzadeh. I conducted all the numerical analyses and wrote the manuscript. Dr. Armin Bebamzadeh and Dr. Michael Fairhurst of UBC, provided the ground motion sets developed for the BC Seismic Retrofit Guidelines - 3rd edition (SRG3), which I used for Incremental Dynamic Analyses (IDAs). Dr. Ventura offered advice during the analysis and writing of the manuscript. The RMTK (Risk Modellers Toolkit), used to develop the fragility functions was provided by the GEM Foundation.

A version of chapter 3 and chapter 4 has been published in the proceedings of the 17th World Conference on Earthquake Engineering (17WCEE), titled “Towards quantifying the effect

of long duration ground motions on regional seismic risk assessment in southwest British Columbia”. The paper was co-authored by Dr. Carlos E. Ventura and Dr. Armin Bebamzadeh. I conducted all the numerical analyses and wrote the manuscript. Dr. Armin Bebamzadeh and Dr. Michael Fairhurst of UBC, provided the ground motion sets developed for the BC Seismic Retrofit Guidelines - 3rd edition (SRG3), which I used for Incremental Dynamic Analyses (IDAs). Dr. Ventura offered advice during the analysis and writing of the manuscript. The source code for VMTK (Vulnerability Modellers Toolkit), used to develop the fragility and vulnerability functions, was provided by Dr. Luis Martins of the GEM Foundation. The OpenQuake engine used to conduct the scenario analyses was provided by the GEM Foundation.

The thesis has been drafted and revised by the author based on review comments from Dr. Carlos E. Ventura (supervisor), Dr. Thomas Tannert (co-supervisor), Dr. Tiegan Hobbs and Dr. Liam Finn.

Table of Contents

Abstract.....	iii
Lay Summary	v
Preface.....	vi
Table of Contents	viii
List of Tables	xiv
List of Figures.....	xvi
List of Abbreviations	xxviii
Acknowledgements	xxxii
Dedication	xxxiii
Chapter 1: Introduction	1
1.1 Seismic risk to infrastructure	1
1.2 Motivation and overview of previous work.....	3
1.3 Research needs.....	5
1.4 Research objectives	6
1.5 Organization of thesis	8
1.6 Scope and Limitations	9
Chapter 2: Background.....	12
2.1 Seismic hazard in Southwest BC	12
2.1.1.1 Crustal sources:.....	16
2.1.1.2 Subduction Interface sources	17
2.1.1.3 Subduction Intraslab sources	17

2.2	Effect of soil conditions at the site	18
2.3	Overview of building stock in Vancouver and Victoria	19
2.3.1	Vancouver	20
2.3.2	Victoria	21
2.4	Considered building typologies	22
2.4.1	Wood typologies	23
2.4.2	Concrete shear wall (C2) typologies	24
2.5	Methods to assess building stock vulnerability	24
2.6	Past research on fragility curves for BC wood and concrete shear wall typologies	27
2.7	Scenario Risk Analysis	28
2.8	Regional Seismic Risk Analysis (RSRA)	30
2.9	Summary	31
Chapter 3:	Methodology	33
3.1	Overview	33
3.2	Exposure model development for Vancouver and Victoria	36
3.3	Fragility and Vulnerability curve development and modifications	41
3.3.1	ESDOF models for BC construction.	41
3.3.1.1	Concrete shear wall typologies (C2): new capacity curves	42
3.3.1.2	Wood typologies: model development and capacity curve derivation	48
3.3.2	Development of crustal and subduction fragility functions	55
3.3.2.1	Representative models	57
3.3.2.2	Damping	59
3.3.2.3	Ground motion sets used	59

3.3.2.3.1	Crustal ground motion suites	62
3.3.2.3.2	Subduction ground motion suites.....	62
3.3.2.3.3	Duration characteristics of the ground motion suites.....	64
3.3.2.4	EDP and damage limit thresholds.....	69
3.3.2.5	Development of fragility functions.....	71
3.3.2.6	Limitations	71
3.3.2.6.1	Choice of structural models	71
3.3.2.6.2	Choice of ground motion sets	72
3.3.2.6.3	Choice of EDP	73
3.3.3	Development of crustal and subduction vulnerability functions	74
3.3.3.1	Consequence models used to develop vulnerability functions	75
3.3.3.2	Structural vulnerability functions	75
3.3.3.3	Non-structural vulnerability functions.....	76
3.3.3.4	Contents vulnerability functions.....	78
3.3.3.5	Assumption of ‘collapsed’ condition.....	79
3.3.4	Verification of vulnerability functions	79
3.4	Scenario Analysis	82
3.4.1	Crustal scenario: Georgia Strait shallow crustal earthquake M 7.3 (GSM7.3)	82
3.4.2	Subduction scenario: Cascadia Subduction earthquake M 9.0 (CSZ9.0)	83
3.5	Regional Seismic Risk assessment (RSRA)	84
3.5.1	Baseline assumption to measure the influence of subduction events on RSRA.....	87
3.5.2	RSRA runs	88
Chapter 4: Results.....		90

4.1	Exposure model developed for Vancouver and Victoria (objective 1)	90
4.2	Developing capacity curves for wood typologies in BC (objective 2)	91
4.2.1	Low-rise residential wood construction (W1): Pre-code	92
4.2.2	Mid-rise residential wood construction (W2): Pre-code	93
4.2.3	Commercial and Industrial wood construction (W3): Pre-code	94
4.2.4	Low-rise residential wood construction with subfloor (W4s): Pre-code	95
4.2.5	Low-rise residential wood construction with cripple wall (W4c): Pre-code	97
4.2.6	Wood Typologies: Summary of capacity curves developed for BC wood typologies	99
4.3	Comparison of current fragility functions to BC-specific crustal fragility functions (objective 3)	103
4.3.1	Concrete typologies	103
4.3.2	Wood typologies	106
4.4	Comparison of BC-specific crustal and subduction fragility functions (objective 3) .	109
4.4.1	Concrete typologies	109
4.4.2	Wood typologies	111
4.5	Comparison of BC-specific fragility curves in Vancouver and Victoria.....	114
4.6	Comparison of current vulnerability curves to BC-specific crustal vulnerability curves (objective 3)	116
4.6.1	Concrete typologies	116
4.6.2	Wood typologies	121
4.7	Comparison of BC-specific crustal and subduction vulnerability curves (objective 3)	126

4.7.1	Concrete typologies	127
4.7.2	Wood typologies	131
4.8	Verification of vulnerability functions (objective 3)	135
4.9	Scenario analysis for Vancouver (objective 4)	138
4.9.1	Crustal scenario (GSM7.3)	140
4.9.2	Subduction scenario (CSZ9.0)	148
4.10	Regional Seismic Risk Assessment (RSRA) (objective 5)	156
4.10.1	Compilation of RSRA results for 10 localities using the site's original exposure models	159
4.10.2	Compilation of RSRA results for 10 localities using Ucluelet exposure model	167
4.10.3	General summaries drawn from RSRA results	177
Chapter 5: Conclusion		181
5.1	Summary of results	181
5.2	Key Findings	182
5.2.1	Key findings regarding exposure	182
5.2.2	Key findings regarding fragility and vulnerability functions	183
5.2.3	Key findings from scenario analysis	185
5.2.4	Key findings from Regional Seismic Risk Analysis (RSRA)	186
5.3	Conclusions	187
5.4	Significant contributions	189
5.5	Recommendations for future research	191
Bibliography		193
Appendices		207

Appendix A : HAZUS definitions and consequence models	207
A.1 HAZUS building type classification.....	207
A.2 Detailed description of W1, W2 and C2 HAZUS typologies [Source: HAZUS]...	208
Wood, Light Frame (W1):	208
A.3 HAZUS building occupancy class definition	210
A.4 HAZUS damage limit state definition [Source: HAZUS]	211
Appendix B : Pinching4 Material	214
Appendix C : Ground motion suites used for development of fragility and vulnerability functions.....	216
C.1 Crustal ground motion suites	216
C.2 Subduction ground motion suites	220
C.3 D ₅₋₉₅ and SED characteristics of SRG3 ground motion suites.....	224
Appendix D : Additional tables and figures	229
D.1 Comparison of damage state thresholds	229
D.2 Consequence Models	231
D.3 Capacity curves and fragility functions for C2-MC typology	233
D.4 Building taxonomy description in CanSRM1.....	235

List of Tables

Table 2.1 Summary of all seismic sources within CanadaSHM5.....	14
Table 2.2 Summary of all seismic sources within CanadaSHM5 (Continuation of Table 2.1)....	15
Table 2.3 Summary of all seismic sources within CanadaSHM5 (Continuation of Table 2.2)....	16
Table 2.4 Site classification based on average shear wave velocity in NBCC 2015.....	18
Table 3.1 Summary of HAZUS and new BC wood structural typology definitions	37
Table 3.2 Summary of design code level for C2, W2 and W3 typologies	39
Table 3.3 Summary of design code level for low-rise wood typologies	40
Table 3.4 Summary of modal heights used in HAZUS, GEM and this study (BC-specific) for C2 typologies.....	46
Table 3.5 Pinching4 material model parameters accounting for cyclic degradation (Vamvatsikos, 2011)	59
Table 3.6 Summary of the mean D_{5-95} and SED of the crustal and subduction ground motion suites	68
Table 3.7 Floor acceleration limits to assign nonstructural damage states (source: HAZUS)	77
Table 3.8 GMPEs and weights used in GSM7.3 scenario analysis	83
Table 3.9 GMPEs and weights used in CSZ9.0 scenario analysis.....	84
Table 3.10 GMPEs and weights used to develop NBCC2015_AA13_interface_central	84
Table 3.11 Contributions of crustal, subcrustal and subduction hazard to total seismic hazard at a locality.....	87
Table 4.1 Summary of modal heights for GEM and BC-specific Wood typologies.	102

Table 4.2 Comparison of AALR values for wood building typologies in Vancouver, using GEM and BC-specific vulnerability functions	136
Table 4.3 Comparison of AALR values for C2 building typologies in Vancouver, using GEM and BC-specific vulnerability functions	137
Table 4.4 Summary of seismic sources that contribute to the seismic hazard at Chilliwack, Masset, Port Hardy, Prince Rupert and Princeton (based on CanadaSHM5 seismic source model)	157
Table 4.5 Summary of seismic sources that contribute to the seismic hazard at Daajing Giids (QCC), Sooke, Ucluelet, Vancouver and Victoria (based on CanadaSHM5 seismic source model)	157

List of Figures

Figure 2.1 Seismic sources affecting seismic hazard in southwest BC [Source: United States Geological Survey / Public Domain]	12
Figure 2.2 Crustal sources closest to Vancouver, defined within CanadaSHM5, for southwestern BC (VC Structural Dynamics, 2019)	16
Figure 2.3 Subduction interface sources closest to Vancouver, defined within CanadaSHM5, for southwestern BC (VC Structural Dynamics, 2019)	17
Figure 2.4 Subduction Intralab sources closest to Vancouver, defined within CanadaSHM5, for southwestern BC (VC Structural Dynamics, 2019)	18
Figure 2.5 NEHRP site classification for the city of Vancouver	19
Figure 2.6 Distribution of building stock based on construction material for Vancouver and Victoria	20
Figure 2.7 An illustration of where the cumulative damage function (CDF) (fragility curves) meets with various intensities of ground shaking [Source: HAZUS (FEMA, 2014)]	26
Figure 2.8 Components for scenario damage and loss analysis in OpenQuake	29
Figure 3.1 Flowchart of Methodology followed	36
Figure 3.2 Recommendation used to adjust the design code levels in the exposure model for Vancouver based on seismic hazard and year of construction- extracted from (Hobbs et al., 2022b)	40
Figure 3.3 Comparison of MLCC for HAZUS C2H of all code levels (The LC and PC MLCC overlaps)	42

Figure 3.4: Factored base shear calculations for a C2 building in Vancouver (a) 2-storey (b) 5-storey (c) 10-storey	44
Figure 3.5: Comparison of MLCC for BC-specific C2 typologies of all design code levels as suggested by the Concrete group of the Buildings at Risk Sub-Committee (a) C2L (b) C2M (c) C2H. The LC and PC MLCC overlaps for all BC C2 typologies.....	45
Figure 3.6 Comparison between capacity curves- GEM, HAZUS and BC-specific for: (a) C2L-PC (b) C2L-HC (a) C2M-PC (b) C2M-HC (a) C2H-PC (HAZUS and BC MLCC overlaps) (b) C2H-HC	47
Figure 3.7 Distribution of W2 buildings per number of stories in the City of Vancouver (a) W2 PC/LC (b)W2 MC/HC	49
Figure 3.8 Schematic for three storey W2-PC	49
Figure 3.9 Analytical model for W2-PC LRFS developed in OpenSees.....	49
Figure 3.10 Distribution of W3 buildings per number of stories in the City of Vancouver.....	52
Figure 3.11 Distribution of W1 buildings per number of stories in the City of Vancouver.....	53
Figure 3.12 Schematic for two storey W1-PC	53
Figure 3.13 Analytical model for W1-PC LRFS developed in OpenSees.....	53
Figure 3.14 Schematic for two storey house with 1m cripple wall	54
Figure 3.15 Reference displacements from monotonic test: 2ft cripple wall (CUREE W-17, 2002)	54
Figure 3.16 Schematic for two storey house with 1.8m subfloor above grade.....	55
Figure 3.17 Crustal ground motion records for Vancouver (Bebamzadeh et al., 2015).....	62
Figure 3.18 Subduction ground motion records for Vancouver (Bebamzadeh et al., 2015)	63

Figure 3.19 Comparison of the mean of the SRG3 crustal (Cr) and subduction (Subd) ground motion suites to the 2% in 50 years Vancouver site class C UHS (2015)	64
Figure 3.20 Distribution of D_{5-95} of the records in the Vancouver crustal and subduction ground motion suites conditioned at 1.0s, across relevant magnitudes.	66
Figure 3.21 Plot of D_{5-95} vs. SED of the records in the Vancouver crustal and subduction ground motion suites conditioned at 1.0s.....	67
Figure 3.22 Distribution of D_{5-95} vs. SED of the records in the Vancouver crustal and subduction ground motion suites conditioned at 1.0s, across relevant magnitudes.	67
Figure 3.23 Comparison of AALR for prominent building classes in Vienna, Lisbon and Oakland (Martins & Silva, 2020)	80
Figure 3.24 Seismic hazard obtained from GEM's Global Seismic Hazard (a) Vancouver (b) Lisbon [Source: (Pagani et al., 2018)]	81
Figure 3.25 Location of selected cities	85
Figure 3.26 Comparison of building stock distribution between the selected cities in the BC exposure model developed by NRCan.....	86
Figure 4.1 Distribution of wood and concrete shear wall building stock for Vancouver and Victoria	90
Figure 4.2 Distribution of concrete shear wall building stock in Vancouver and Victoria	91
Figure 4.3 Distribution of wood and concrete shear wall building stock based on design code level for Vancouver and Victoria.....	91
Figure 4.4 Shear spring assigned at each floor.	92
Figure 4.5 Mode shapes of W1-PC.....	92
Figure 4.6 Pushover curve of W1-PC	93

Figure 4.7 Capacity curve for first mode SDOF.....	93
Figure 4.8 Shear spring assigned at each floor.	94
Figure 4.9 Mode shapes of W2-PC.....	94
Figure 4.10 Pushover curve of W2-PC.....	94
Figure 4.11 Capacity curve for first mode SDOF.....	94
Figure 4.12 Shear spring assigned at each floor	95
Figure 4.13 Mode shapes of W3-PC.....	95
Figure 4.14 Pushover curve of W3-PC.....	95
Figure 4.15 Capacity curve for first mode SDOF.....	95
Figure 4.16 Shear spring assigned at each floor	96
Figure 4.17 Mode shapes of W4s-PC	96
Figure 4.18 Pushover curve of W4s-PC	96
Figure 4.19 Capacity curve for first mode SDOF.....	96
Figure 4.20 Shear spring assigned at each floor	97
Figure 4.21 Mode shapes of W4c-PC	97
Figure 4.22 Mode shapes for W4c-PC when cripple wall softens.....	98
Figure 4.23 Pushover curve of W4c-PC	98
Figure 4.24 Capacity curve for first mode SDOF.....	98
Figure 4.25 Comparison between capacity curves-GEM, HAZUS and BC-specific for typology: (a)W1-PC (b)W1-HC (c)W2-PC (d)W2-HC	99
Figure 4.26 Comparison between capacity curves-GEM, HAZUS and BC-specific for typology (a)W3-PC (b) W3-HC.....	100

Figure 4.27 Comparison between capacity curves-GEM, HAZUS and BC-specific for typology:

(a)W4s-PC (b)W4c-PC 101

Figure 4.28 Comparison of current fragility curves (GEM-) to new BC specific fragility curves

(Van-): (a) C2L-PC (b) C2L-HC (c) C2M-PC (d) C2M-HC (e) C2H-PC and (f) C2H-HC 104

Figure 4.29 Comparison of current fragility curves (GEM-) to new BC specific fragility curves

(Van-): (a)W1-PC (b)W1-HC 106

Figure 4.30 Comparison of current fragility curves (GEM-) to new BC specific fragility curves

(Van-): (a)W4s-PC (b)W4c-PC 107

Figure 4.31 Comparison of DS4 fragility curves for pre-code low-rise residential wood structures

..... 107

Figure 4.32 Comparison of current fragility curves (GEM-) to new BC specific fragility curves

(Van-): (a)W2-PC (b) W2-HC (c) W3-PC (d) W3-HC 108

Figure 4.33 Comparison of crustal fragility curves (Cr-) to subduction fragility curves (Subd-):

(a) C2H-PC (b) C2H-HC (c) C2M-PC (d) C2M-HC (e) C2L-PC and (f)C2L-HC 110

Figure 4.34 Comparison of crustal fragility curves (Cr-) to subduction fragility curves (Subd-):

(a)W1-PC (b) W1-HC (c) W4s-PC and (d) W4c-PC..... 112

Figure 4.35 Comparison of crustal fragility curves (Cr-) to subduction fragility curves (Subd-):

(a)W2-PC (b) W2-HC (c) W3-PC and (d) W3-HC 113

Figure 4.36 Comparison of crustal fragility curves for Vancouver and Victoria (a) C2L-PC

(b)C2L-HC (c) C2H-PC (d) C2H-HC (e)W1-PC and (f)W1-HC..... 115

Figure 4.37 Comparison of GEM structural vulnerability curves (GEM-) to BC crustal structural

vulnerability curves (Van-): (a)C2L-PC (b) C2L-HC (c) C2M-PC (d) C2M-HC (e) C2H-PC (f)

C2H-HC 117

Figure 4.38 Comparison of GEM non-structural vulnerability curves (GEM-) to BC crustal non-structural vulnerability curves (Van-): (a)C2L-PC (b) C2L-HC (c) C2M-PC (d) C2M-HC (e) C2H-PC (f) C2H-HC	118
Figure 4.39 Comparison of GEM contents vulnerability curves (GEM-) to BC contents non-structural vulnerability curves (Van-): (a)C2L-PC (b) C2L-HC (c) C2M-PC (d) C2M-HC (e) C2H-PC (f) C2H-HC	119
Figure 4.40 Comparison of GEM structural vulnerability curves (GEM-) to BC crustal structural vulnerability curves (Van-): (a)W1-PC (b) W1-HC(c)W2-PC (d) W2-HC (e)W3-PC (f) W3-HC	122
Figure 4.41 Comparison of GEM non-structural vulnerability curves (GEM-) to BC crustal non-structural vulnerability curves (Van-): (a)W1-PC (b) W1-HC(c)W2-PC (d) W2-HC (e)W3-PC (f) W3-HC	123
Figure 4.42 Comparison of GEM contents vulnerability curves (GEM-) to BC crustal contents vulnerability curves (Van-): (a)W1-PC (b) W1-HC(c)W2-PC (d) W2-HC (e)W3-PC (f) W3-HC	124
Figure 4.43 Comparison of structural vulnerability curves of W4c, W4s and W1 PC typologies	126
Figure 4.44 Comparison of BC-specific crustal (Cr-) and subduction (Subd-) structural vulnerability curves (Van-): (a)C2L-PC (b) C2L-HC (c) C2M-PC (d) C2M-HC (e) C2H-PC (f) C2H-HC	128
Figure 4.45 Comparison of BC-specific crustal (Cr-) and subduction (Subd-) non-structural vulnerability curves for Vancouver: (a)C2L-PC (b) C2L-HC (c) C2M-PC (d) C2M-HC (e) C2H-PC (f) C2H-HC	129

Figure 4.46 Comparison of BC-specific crustal (Cr-) and subduction (Subd-) contents vulnerability curves for Vancouver: (a)C2L-PC (b) C2L-HC (c) C2M-PC (d) C2M-HC (e) C2H- PC (f) C2H-HC	130
Figure 4.47 Comparison of BC-specific crustal (Cr-) and subduction (Subd-) structural vulnerability curves for Vancouver for (a)W1-PC (b) W1-HC(c)W2-PC (d) W2-HC (e)W3-PC (f) W3-HC	132
Figure 4.48 Comparison of BC-specific crustal (Cr-) and subduction (Subd-) nonstructural vulnerability curves for Vancouver for (a)W1-PC (b) W1-HC(c)W2-PC (d) W2-HC (e)W3-PC (f) W3-HC	133
Figure 4.49 Comparison of BC-specific crustal (Cr-) and subduction (Subd-) contents vulnerability curves for Vancouver for (a)W1-PC (b) W1-HC(c)W2-PC (d) W2-HC (e)W3-PC (f) W3-HC	134
Figure 4.50 Vancouver building stock distribution per per typology based on (a) year of construction (b) general occupancy class	138
Figure 4.51 Geographic distribution of prominent BC-typologies in Vancouver. (a) C2H (b) C2M (d) C2L (d) W1 and W4s (e)W2 and W3 and (f) W4c	139
Figure 4.52 GSM7.3 Complete damage state distribution map for Vancouver, using GEM fragility functions.....	141
Figure 4.53 GSM7.3 Distribution of highest assets losses that make 50% of total loss, using GEM fragility functions	141
Figure 4.54 GSM7.3 Complete damage state distribution map for Vancouver, using BC-specific fragility functions, without accounting for W4s and W4c.....	143

Figure 4.55 GSM7.3 Distribution of highest assets losses that make 50% of total loss, using BC-specific fragility functions, without accounting for W4s and W4c.	143
Figure 4.56 GSM7.3 Complete damage state distribution map for Vancouver, using BC-specific fragility functions, accounting for W4s and W4c.	145
Figure 4.57 GSM7.3 Distribution of highest assets losses that make 50% of total loss, using BC-specific fragility functions, accounting for W4s and W4c.	145
Figure 4.58 Total damage distribution based on building damage state for (a) Case 1 (b) Case 2 (3) Case 3	147
Figure 4.59 DS4 distribution across building typologies for (a) Case 1 (b) Case 2(3) Case 3..	147
Figure 4.60 Total loss distribution across different building typologies for (a) Case 1 (b) Case 2 (3) Case 3	147
Figure 4.61 CSZ9.0 Complete damage state distribution map for Vancouver, using GEM fragility functions.....	150
Figure 4.62 CSZ9.0 Distribution of highest assets losses that make 50% of total loss, using GEM fragility functions.....	150
Figure 4.63 CSZ9.0 Complete damage state distribution map for Vancouver, using BC-specific fragility functions, without accounting for W4s and W4c.....	152
Figure 4.64 CSZ9.0 Distribution of highest assets losses that make 50% of total loss, using BC-specific fragility functions, without accounting for W4s and W4c.	152
Figure 4.65 CSZ9.0 Complete damage state distribution map for Vancouver, using BC-specific fragility functions, accounting for W4s and W4c.	154
Figure 4.66 CSZ9.0 Distribution of highest assets losses that make 50% of total loss, using BC-specific fragility functions, accounting for W4s and W4c.	154

Figure 4.67 Total damage distribution based on building damage state for (a) Case 1 (b) Case 2 (3) Case 3	155
Figure 4.68 DS4 distribution across building typologies for (a) Case 1 (b) Case 2(3) Case 3..	155
Figure 4.69 Total loss distribution across different building typologies for (a) Case 1 (b) Case 2 (3) Case 3	156
Figure 4.70 Collapse exceedance curve: Princeton	159
Figure 4.71 Loss exceedance curve: Princeton.....	159
Figure 4.72 Collapse exceedance curve: Chilliwack	159
Figure 4.73 Loss exceedance curve: Chilliwack.....	159
Figure 4.74 Collapse exceedance curve: Vancouver	160
Figure 4.75 Loss exceedance curve: Vancouver.....	160
Figure 4.76 Collapse exceedance curve: Victoria.....	160
Figure 4.77 Loss exceedance curve: Victoria.....	160
Figure 4.78 Collapse exceedance curve: Sooke.....	160
Figure 4.79 Loss exceedance curve: Sooke	160
Figure 4.80 Collapse exceedance curve: Ucluelet	161
Figure 4.81 Loss exceedance curve: Ucluelet.....	161
Figure 4.82 Collapse exceedance curve: Port Hardy	161
Figure 4.83 Loss exceedance curve: Port Hardy	161
Figure 4.84 Collapse exceedance curve: Prince Rupert.....	161
Figure 4.85 Loss exceedance curve: Prince Rupert	161
Figure 4.86 Collapse exceedance curve: Masset	162
Figure 4.87 Loss exceedance curve: Masset.....	162

Figure 4.88	Collapse exceedance curve: QCC	162
Figure 4.89	Loss exceedance curve: QCC	162
Figure 4.90	Summary of AACF at selected BC localities for Cr-All and Cr+Subd cases when using the locality's exposure model.....	163
Figure 4.91	Summary of AAL at selected BC localities for Cr-All and Cr+Subd cases when using the locality's exposure model.....	164
Figure 4.92	Summary of AALR at selected BC localities for Cr-All and Cr+Subd cases when using the locality's exposure model.....	164
Figure 4.93	Absolute increase in AACF for 10 selected BC sites when using the site's exposure model.....	165
Figure 4.94	Absolute increase in AAL for 10 selected BC sites when using the site's exposure model.....	165
Figure 4.95	Absolute increase in AALR for 10 selected BC sites when using the site's exposure model.....	165
Figure 4.96	Relative increase in AACF across 10 selected BC localities using the site's exposure model.....	167
Figure 4.97	Relative increase in AALR across 10 selected BC localities using the site's exposure model.....	167
Figure 4.98	Collapse exceedance curve: Princeton	168
Figure 4.99	Loss exceedance curve: Princeton.....	168
Figure 4.100	Collapse exceedance curve: Chilliwack	168
Figure 4.101	Loss exceedance curve: Chilliwack.....	168
Figure 4.102	Collapse exceedance curve: Vancouver	168

Figure 4.103	Loss exceedance curve: Vancouver.....	168
Figure 4.104	Collapse exceedance curve: Victoria.....	169
Figure 4.105	Loss exceedance curve: Victoria.....	169
Figure 4.106	Collapse exceedance curve: Sooke.....	169
Figure 4.107	Loss exceedance curve: Sooke	169
Figure 4.108	Collapse exceedance curve: Ucluelet	169
Figure 4.109	Loss exceedance curve: Ucluelet.....	169
Figure 4.110	Collapse exceedance curve: Port Hardy	171
Figure 4.111	Loss exceedance curve: Port Hardy	171
Figure 4.112	Collapse exceedance curve: Prince Rupert.....	171
Figure 4.113	Loss exceedance curve: Prince Rupert	171
Figure 4.114	Collapse exceedance curve: Masset	172
Figure 4.115	Loss exceedance curve: Masset.....	172
Figure 4.116	Collapse exceedance curve: QCC	172
Figure 4.117	Loss exceedance curve: QCC	172
Figure 4.118	Summary of AACF for 10 selected BC localities for Cr-All and Cr+Subd cases using the Ucluelet exposure model.	173
Figure 4.119	Summary of AAL for 10 selected BC localities for Cr-All and Cr+Subd cases using the Ucluelet exposure model.	173
Figure 4.120	Summary of AALR for 10 selected BC localities for Cr-All and Cr+Subd cases using the Ucluelet exposure model.	174
Figure 4.121	Absolute increase in AACF for 10 selected BC sites when using the Ucluelet exposure model.	174

Figure 4.122 Absolute increase in AAL for 10 selected BC sites when using the Ucluelet exposure model.	175
Figure 4.123 Absolute increase in AALR for 10 selected BC sites when using the Ucluelet exposure model.	175
Figure 4.124 Relative increase in AACF across 10 selected BC localities using the Ucluelet exposure model.	176
Figure 4.125 Relative increase in AALR across 10 selected BC localities using the Ucluelet exposure model.	176
Figure 4.126 Grouping of localities	179

List of Abbreviations

AACF	:	Average Annual Collapse Fraction
AAL	:	Average Annual Loss
AALR	:	Average Annual Loss Ratio
ATC	:	Applied Technology Council
BC	:	British Columbia
BCBC	:	British Columbia Building Code
C2	:	Concrete shear wall structure
C2H	:	High-rise Concrete shear wall structure
C2L	:	Low-rise Concrete shear wall structure
C2M	:	Mid-rise Concrete shear wall structure
CanSRM1	:	First generation Canadian Seismic Risk Model
CanadaSHM5	:	Fifth generation Canadian Seismic Hazard Model
CanadaSHM6	:	Sixth generation Canadian Seismic Hazard Model
CS	:	Conditional Spectrum
CSZ9.0	:	Cascadia Subduction Zone Magnitude 9.0
CUREE	:	Consortium of Universities for Research in Earthquake Engineering
DPM	:	Damage Probability Matrix
DS	:	Damage State
EDP	:	Engineering Demand Parameter
ESDOF	:	Equivalent Single Degree of Freedom
FEMA	:	Federal Emergency Management Agency
GEM	:	Global Earthquake Model Foundation
GMPE	:	Ground Motion Prediction Equation
GSC	:	Geological Survey of Canada
GSM7.3	:	Georgia Strait Crustal Scenario Magnitude 7.3
HAZUS	:	FEMA Methodology for estimating potential losses from disasters
HC	:	High-code

IDA	:	Incremental Dynamic Analysis
IDR	:	Inter-storey Drift Ratio
IM	:	Intensity Measure
LC	:	Low-code
LFRS	:	Lateral Force Resisting System
MC	:	Moderate-code
MDOF	:	Multi degree of freedom
MLCC	:	Multi-linear Capacity Curve
NBCC	:	National Building Code of Canada
NEHRP	:	National Earthquake Hazard Reduction Program
NLTHA	:	Nonlinear Time History Analysis
NRCan	:	Natural Resources Canada
OQ	:	OpenQuake
OSB	:	Oriented Strand Board
PBSD	:	Performance-Based Seismic Design
PC	:	Pre-code
PGA	:	Peak Ground Acceleration
PO	:	Pushover
PSHA	:	Probabilistic Seismic Hazard Analysis
QCC	:	Queen Charlotte City
RC	:	Reinforced Concrete
RSRA	:	Regional Seismic Risk Analysis
Sa(T)	:	Spectral acceleration at a specific period T
SDOF	:	Single degree of freedom
SED	:	Specific Energy Density
SF	:	Scaling Factor
SRG3	:	Seismic Retrofit Guidelines 3rd edition
UBC	:	The University of British Columbia
UBC-SAWS	:	Structural models developed for Canadian wooden houses by UBC
UHS	:	Uniform Hazard Spectrum

USA	:	United States of America
USGS	:	United States Geological Survey
W1	:	Low-rise wood residential buildings
W2	:	Mid-rise wood residential buildings
W3	:	Commercial and Industrial wood buildings
W4	:	W1 with cripple wall or subfloor
W4c	:	W1 with cripple wall
W4s	:	W1 with subfloor

Acknowledgements

This research was funded through a Research Affiliate Program (RAP) Bursary, provided by the Natural Resources Canada (NRCan).

I would like to express my gratitude to my supervisor Prof. Carlos E. Ventura for his encouragement and his patient guidance throughout my Ph.D. My sincere gratitude for his timely advices and support throughout my PhD, that motivated me to do my best and helped solidify my work. I am grateful to my co-supervisor, Prof. Thomas Tannert, not only for all the time and energy he dedicated in helping edit this thesis, but also for helping me stay on track regarding the goals of this work. My sincerest thanks to Dr. Armin Bebamzadeh, for sharing his immense knowledge and experience in the field of earthquake engineering throughout my research work, for feedback regarding the fragility functions developed, and for providing me with the ground motion suites used in this work.

I am truly thankful to Dr. Luis Martins for his immense help and guidance during the development of the fragility and vulnerability functions, for taking time to sort out my queries and providing me with the source code for developing these functions. I also thank Dr. Anirudh Rao for his insights into the results of my work, and the discussions that left me understanding this research work better.

I would also like to extend my gratitude to Dr. Tiegan Hobbs, as my supervisor from NRCan, for helping edit and review this thesis, for her patience in helping me understand how the results of my work influence the work NRCan is doing in Vancouver and Canada, and for her willingness to discuss the results obtained from different seismic scenarios analyses and regional

seismic risk assessments. I thank Nicky Hastings, for her support and helping me understand where my work stands as part of a much bigger picture of assessing risk in BC.

To my wonderful parents, Dr. Abraham George and Dr. Susan Abraham, I owe my deepest gratitude. They are the greatest blessing in my life. I could not have come this far, without their unconditional love, constant prayers, support, and encouragement throughout my years of education. A special thanks to my husband, Jubin Tom George, for his love, prayers and support and helping me see my work to the end. I cannot thank enough, my sister, Dr. Evelyn Abraham, who encouraged me during the course of my research, for her love and prayers and for always having my back.

Above all, I thank Jesus Christ, my LORD and personal savior, for His mercy and never-ending grace in making this dissertation a reality.

Dedication

Dedicated to:

El Shaddai,

My Rock,

My Redeemer.

Chapter 1: Introduction

1.1 Seismic risk to infrastructure

Seismic risk refers to the damage and losses to infrastructure, life, property etc. when exposed to an earthquake. It represents not only structural damages but also the likely financial, societal and built environmental impacts of different possible earthquake scenarios that could occur in a specified period of time (seismic hazard) at a given site. When the probable seismic risk (damage and loss) is evaluated for a region, over a long period of time, it is referred to as Probabilistic Seismic Risk Assessment or Regional Seismic Risk Assessment (referred to as RSRA in this study). Proper execution of seismic risk assessment is an important step towards minimizing financial losses, damages and casualties during possible earthquakes in the region.

The Cascadia region in south-western British Columbia (BC), Canada, is one of the most tectonically complex regions in the world. The seismic hazard is dominated by three earthquake types – Crustal, Subduction Intraslab (referred to as subcrustal in this study) and Subduction Interface (referred to as subduction in this study). All three types of earthquakes have distinct characteristics that set them apart from each other, and these characteristics determine how the same structure would behave differently under each earthquake. For example, subduction earthquakes are rare, can have large magnitudes ($M > 8.0$) and are characterized by long duration of shaking (could be several minutes) and a richer low frequency content, making them more damaging for long period structures such as tall buildings, bridges and dams. Crustal earthquakes on the other hand, tend to be frequent, of lower magnitudes ($5.0 < M < 7.5$), have a rich high frequency content and a much shorter duration (often less than a minute), making them more damaging for short period structures. As such, the same structure will display different levels of

damage when subjected to a crustal or a subduction earthquake. The effect of these earthquakes during regional seismic risk assessment must be properly accounted for, to get a proper idea of damages and losses expected.

Existing methods for assessing regional risk rely on the availability of appropriate fragility and vulnerability functions that can estimate damage and losses to the building stock the at the site of interest respectively. Development of these functions requires creation of building models representing the building types unique to the investigated region, relevant exposure models and continuous refinement of hazard models. The OpenQuake Engine (GEM, 2022; Pagani et al., 2014; Silva et al., 2014) created by the Global Earthquake Model (GEM) Foundation, Italy, offers a platform for seismic hazard and risk assessment at a global scale. GEM and their partners work to update and replace fragility and vulnerability functions, exposure models, and seismic source models. While it has a similar methodology to HAZUS (FEMA, 2014)-developed for USA, OQ has probabilistic modelling capability and does a rigorous job of handling uncertainties in modelling seismic risk. In recent years, many agencies like the GEM Foundation and HAZUS, have been moving towards strategies for regional damage and loss assessment, the former at a global scale and the latter, specifically for USA.

To evaluate regional seismic risk in BC, where seismicity sources involve complex tectonic regions, a study towards creating a proper regional damage and loss assessment model is required. Towards this, the unavailability of a relevant set of fragility and vulnerability functions for BC-specific construction which could be used develop regional scale risk reduction strategies for different building typologies specific to BC has to be fixed. The focus of such a study is not the

probabilistic risk assessment for a specific building, but rather a portfolio analysis at a regional level for a specific building typology.

1.2 Motivation and overview of previous work

Long duration earthquakes may instigate structural collapse or unacceptable displacements at lower intensity of ground motion shaking levels as compared to short duration ground motions, thus increasing the damage potential and collapse risk of various types of structures. This was proved true during the large magnitude events like the 2010 Chile and 2011 Tohoku earthquakes (Capraro, 2018), emphasizing the importance of considering duration effects in seismic design and seismic risk assessment.

The National Building Code of Canada (NBCC, 2015) building design procedure is based on the elastic response spectrum of the representative linear single degree of freedom (SDOF) system and an assumed ductility and overstrength. However, the response spectrum only reflects the intensity (or amplitude) and frequency content of the ground motions. The duration of the ground motion is not captured in the elastic response spectra, and hence, the duration effect of ground motions is not addressed within the current and previous versions of NBCC. While the use of an elastic response spectra is sufficient for building design in regions where short duration earthquakes like crustal earthquakes dominate the seismic hazard, in regions where subduction earthquakes dominate the hazard, as is the case of southwest BC, designing structures against the elastic response spectrum could result in insufficient seismic resistance against collapse.

Studies show that duration can have a significant impact on the collapse capacity of structures, and it depends on the hysteretic energy dissipation capacity of the system. In the more recent comprehensive works done, care has been given so that models used captured cyclic

deterioration of strength and stiffness (Chandramohan, 2016; Fairhurst, 2021; Pan, 2018). The effect of duration on collapse capacity has been studied in detail for concrete structures (Capraro, 2018; Chandramohan et. al., 2016b) wood frame structures (Pan, 2018; Pan et al., 2020) and steel structures (Chandramohan et. al., 2016a). These studies show that realistic deteriorating structural models and careful ground motion selection are required to get a robust assessment of duration effects. These studies have been done for specific buildings, and comprehensive work has not been carried out to account for duration effects of earthquakes at a regional scale.

The most inclusive RSRA in BC was carried out by Tuna Onur (Ventura et al., 2005; Onur, 2001; Onur et al., 2005; Onur et al., 2006) for the cities of Vancouver and Victoria and used Modified Mercalli intensity-based damage matrices to link ground shaking intensity with expected damage and assessed the damage level of structural and non-structural building components. In more recent work for wood structures in Canada, a nationwide earthquake risk model was developed (Goda, 2019; Goda & Yoshikawa, 2013; Goda et al., 2021). This was done by integrating Probabilistic Seismic Hazard Analysis (PSHA) results provided by the Geological Survey of Canada (GSC) with fragility functions derived from Incremental Dynamic Analysis (IDA) on the UBC-SAWS (White & Ventura, 2006) structural models, developed and validated by the University of British Columbia (UBC). The loss estimation for older Reinforced Concrete (RC) building construction in Victoria during subduction events have also been studied (Teshamariam & Goda, 2015a, 2015b). It is crucial to the accuracy of a RSRA to consider how subduction ground motions with long durations influence RSRA. However, none of the above RSRA for BC have included its effects.

1.3 Research needs

The current first generation Canadian Seismic Risk Model (CanSRM1) (Hobbs et al., 2022a; Hobbs et al., 2022b) was developed using OQ, where the damage and loss assessment is based on a single set of fragility and vulnerability functions that were developed by the GEM Foundation, Pavia, using the FEMA P695 ground motions, considering records from all tectonic source types and for building models developed based on HAZUS. However, their validity for use in southwest BC — with different building typologies and where there is a nearby subduction seismic source contributing to total seismic hazard — has not been studied in detail. To more accurately reflect the likely impact of shaking from subduction earthquakes, new fragility and vulnerability functions have to be developed specifically for predominant building typologies in BC (will be explained in detail in Chapter 2). A method to properly represent the effect of subduction ground motions on RSRA in BC is required, as well as suggestions on RSRA metrics that can properly quantify this effect.

When studying previous research works on the RSRA in BC and Canada, certain knowledge gaps were identified. Fragility curves for the building typologies present in the BC building stock have not been developed for crustal and subduction ground motions. The current building typologies, defined in HAZUS, do not contain all of the representative building typologies in BC. The current fragility functions used for the development of the CanSRM1 do not account for the effect of higher modes, as well as for possible period elongation, as the accumulated damage in a structure during a long duration event increase. The consideration of soil-site effects within the soil model used has not been verified. A method to classify localities within a study region based on the severity of the effect of long duration ground motions in RSRA has not been investigated.

Of the knowledge gaps cited above, the issues addressed in this work are as follows. For crustal and subduction events, fragility and vulnerability functions for the most predominant building typologies present in the BC building stock needs to be developed. These building typologies should reflect the structural properties of the median representative building of the corresponding building typology in BC. The building typologies defined in HAZUS, which are currently adopted for use in Canada, do not completely reflect the entirety of the BC building stock. For example, the HAZUS building typologies does not account for half-storey cripple walls (or crawl spaces) and buildings with sub-floors (or basements). To account for these buildings, it is necessary to introduce new typologies. It is also noted here that the fragility functions of different building typologies were created for structures which were designed for extremely high base shears in regions of high seismicity like California, which is not applicable for BC. As such the fragility curves for these prominent building typologies should be modified such that the median capacity curves are representative of the Canadian building stock, by lowering the building capacity of the median building to more closely match, the capacities of buildings in BC.

1.4 Research objectives

The main objective of this research is to investigate the influence of subduction ground motions (typically with long durations of shaking) on probabilistic regional seismic risk (damage and loss) assessment within chosen localities in BC, with various contributions of subduction hazard to total hazard at the site. Towards this, the Vancouver and Victoria building stocks are studied in detail to understand the prominent BC building typologies and new building typologies needed to represent the entirety of the BC building stock is introduced. Subduction and crustal fragility and vulnerability functions are then developed for the predominant BC building typologies identified.

Vancouver is chosen for scenario risk assessment (deterministic seismic risk assessment) because of the availability of a detailed high-resolution building-by-building exposure model — developed from a building survey conducted by UBC for Vancouver. Ten localities within BC are chosen for RSRA (probabilistic seismic risk assessment) - using the OQ event-based damage and loss calculators.

The specific research objectives include:

1. Developing a uniform exposure model for Vancouver and Victoria - as representative localities in BC, to understand the building stock distribution and identify prominent building typologies for further study.
2. Developing single-degree-of-freedom (SDOF) models for representative wood and concrete shear wall buildings in BC.
3. Developing crustal and subduction fragility and vulnerability functions for the most prominent building typologies in BC.
4. Investigating the difference between the seismic scenario damages and losses estimated using the BC-specific fragility and vulnerability functions and that estimated by current functions -used to develop the first generation Canadian Seismic Risk Model (CanSRM1), for a crustal and a subduction scenario in Vancouver. As part of this, the additional damages and losses incurred when including new low-rise wood typologies with cripple walls and sub-floors when running the scenario analyses, has to be investigated.
5. Investigating the effect of explicitly including subduction fragility and vulnerability functions on probabilistic seismic risk assessment through OQ event-based risk analysis for selected localities in southwest BC.

1.5 Organization of thesis

To achieve the research objectives cited above, this thesis is organized as follows:

Chapter 2 provides insight into the seismic hazard in BC, modelled within the 2015 GSC Seismic Hazard Model (Halchuk et al., 2014, 2015, 2016), adopted into OQ (Allen et al., 2020), followed by a brief review of the soil conditions in Vancouver. Next, an overview of the building stock of Victoria and Vancouver (summarized from the building-by-building survey carried out in the two localities by UBC) is provided, followed by an introduction to the most prominent building typologies in these two localities, which will be covered in this study. This is followed by an outline of how fragility and vulnerability functions are developed and a brief review of the research done on fragility curves for the typologies considered in BC and a description of scenario analysis and RSRA in OQ.

Chapter 3 presents the methodology to study the effect of subduction earthquakes on RSRA in selected localities in BC. It starts out describing the development of the exposure model, followed by explaining how the representative SDOF systems for the predominant building typologies in BC are developed. Then, the development of crustal and subduction fragility curves and vulnerability curves is described and is succeeded by an account of how the vulnerability functions are verified. This is followed by a description of the scenario analyses carried out for Vancouver (crustal and subduction) to study the effect of the changes made in the fragility and vulnerability functions in scenario damage and loss estimation. The subsequent section explains the methodology proposed to identify the effect of subduction ground motions on RSRA in selected localities in BC.

Chapter 4 summarizes the results obtained on following the methodology described in Chapter 3. It starts off comparing the exposure models developed for Vancouver and Victoria. This is followed by a summary of the capacity curves developed example BC typologies (pre-code wood typologies), following the methodology in Chapter 3. The subsequent section summarizes and describes the crustal and subduction fragility curves and vulnerability curves developed for BC-specific building typologies and then verifies these vulnerability functions for Vancouver. Following this, the results from the scenario analyses for Vancouver (crustal and subduction) are summarized, and then, the results from implementing the methodology proposed in Chapter 3 to identify the effect of subduction ground motions on RSRA in 10 selected localities in BC.

Chapter 5 summarizes the main findings and contributions of this work, conclusions arrived at, and proposes recommendations for future research work.

1.6 Scope and Limitations

- In this study, not all building typologies are considered. Only the most prevalent typologies in the representative cities - Vancouver and Victoria i.e., concrete shear wall (C2) and wood constructions are studied. For all deterministic and probabilistic analyses done in this work, it is assumed that wood and concrete shear wall structures constitute 100% of the building stock at any site.
- In this study, SDOF models for the first mode of the representative buildings of each BC building typologies -accounting for strength and stiffness degradation - are considered for IDA. Spectral acceleration at a specific period - $S_a(T)$ - is chosen to relate the ground shaking intensity to probability of damage level exceedance and loss assessment. Given a linear oscillator with a definite natural period and

damping ratio, $S_a(T)$ represents the maximum acceleration that an earthquake ground motion generates in it. As such, higher mode effects and period lengthening effects due to non-linearity of structures have not been considered in this study, and is beyond the scope of this work.

- Deterministic seismic risk analysis, to understand the impact of the modifications made to the BC fragility and vulnerability functions, is carried out in Vancouver. The exposure model for Vancouver was developed from a comprehensive building-by-building survey conducted by UBC, that identified low-rise residential wood structures with cripple wall and subfloor construction. Even within such a detailed survey, there was much missing information, including floor area, building height and building replacement costs.
- The RSRA for the 10 selected localities studied herein uses the exposure model for BC developed by Natural Resources Canada (NRCan) (Journey et al., 2022) to create CanSRM1. This exposure model is not as detailed as the building-by-building exposure model, as can be seen on comparison with the Vancouver and Victoria exposure models developed in this study. More accurate exposure models yield a better estimate of true damage and loss analysis.
- This thesis aims to understand the influence of subduction ground motions on regional risk (damage and loss) assessment at specific localities in BC, and not to quantify it based on subduction hazard contribution at the site. This study also aims to identify metrics that can best measure this influence. To quantify the effect of subduction ground motions on RSRA, further work is necessary to compute the

contribution of subduction hazard at a site at all periods significant to the building stock, at which the fragility and vulnerability functions are developed. This is beyond the scope of this work.

- This study began in 2017, when the design code in effect was NBCC 2015. Therefore, the ground motion suites used for the creation of fragility and vulnerability functions are selected and scaled to match the requirements of NBCC 2015. The Ground Motion Prediction Equations (GMPEs) suggested in Atkinson & Adams (2013) (with additional modifications made for NBCC2015) (Atkinson & Adams, 2013) are used to estimate the intensity of ground shaking from the seismic scenarios considered. For RSRA, the 5th Generation Canadian Seismic Hazard Model (CanadaSHM5) (Halchuk et al., 2014) used by NBCC 2015, is chosen in this study.

Chapter 2: Background

2.1 Seismic hazard in Southwest BC

The expected earthquake ground motion at a given location, over a specified time period of interest, is referred to as the seismic hazard at the site. The characteristics of the seismic sources that can cause earthquakes at a given location and how far they are, the amplification or deamplification of the seismic waves from the epicenter to the location, the local geology and soil conditions determine the ground shaking intensity at a site.

The seismicity in the Pacific Northwest is due to the interaction of four tectonic plates (the Pacific plate, the North American plate, the Juan de Fuca plate and the Explorer plate), creating three tectonic regions - Queen Charlotte region, the offshore region off the Pacific coast and the continental region (Filiatrault et al., 2013). The continental region (where southwest BC lies) is where the oceanic Juan de Fuca plate and the Explorer plate diverges from the Pacific plate which are being subducted underneath the continental North American plate as shown in Figure 2.1.

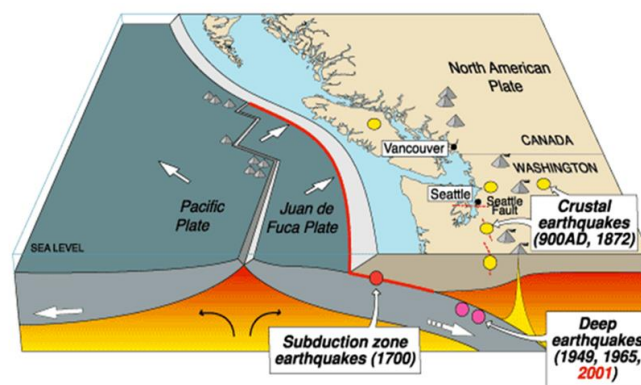


Figure 2.1 Seismic sources affecting seismic hazard in southwest BC [Source: United States Geological Survey / Public Domain]

The Cascadia subduction zone (CSZ) extends from California in the south to the Northern tip of Vancouver Island in BC. The subduction process drives three types of earthquakes that contribute to the seismic hazard in southwest BC. Large magnitude subduction earthquakes (megathrust earthquakes) at the interface between the Juan de Fuca and the North American plates (e.g., Goldfinger et al., 2012) ; shallow crustal events from faults in the overlying crust within the North American plate; and deep Inslab earthquakes in the subducting Juan de Fuca plate along the west coast of Vancouver Island and beneath Puget Sound. The subduction earthquakes are very powerful and rare, reaching moment magnitudes of 9.0 with a return period of around 475 years. The last recorded event occurred in January 1700 (Satake, 2003; Wang et al., 2013). Most of the frequent crustal earthquakes are very small. However larger magnitude events are also possible, like the M6.9 earthquake of 1918 on Vancouver Island (Cassidy, 1986), and can cause substantial damage and economic losses in nearby cities of Vancouver and Victoria. The latest significant inslab event in the CSZ was the M6.8 earthquake beneath Nisqually, Washington State, USA in 2001 that was felt in Seattle, Victoria and Vancouver (Molnar, 2004; Molnar et al., 2004).

The CanadaSHM5 (Halchuk et al., 2014) was developed in OQ (Allen et al., 2017; Allen et al., 2020), and is used in this work. Within this, the seismic sources are modelled as area sources when identification and classification of a single fault geometry is difficult. Seismic sources modelled as a simple fault source are described by a surface trace, depth, dip and rake. A simple fault source is a well-defined source and is mostly used to describe shallow faults. Complex faults allow a user to specify the geometry of the top, middle, and bottom of a non-planar or curved fault, and are used to model subduction interface faults (GEM, 2022).

A summary of all the seismic sources considered within the CanadaSHM5 is tabulated in Table 2.1 Summary of all seismic sources within CanadaSHM5., including their corresponding tectonic region types.

Table 2.1 Summary of all seismic sources within CanadaSHM5.

Source Type	ID	Name	Tectonic Region Type
areaSource	BRO	Brooks Peninsula	Active Shallow Crust
areaSource	CAS	Cascade Mountains	Active Shallow Crust
areaSource	CST	Coastal Mountains	Active Shallow Crust
areaSource	EXP	Explorer Plate Bending	Active Shallow Crust
areaSource	FHL	Flathead Lake	Active Shallow Crust
areaSource	HEC	Hecate Strait	Active Shallow Crust
areaSource	JDFF	Juan De Fuca Plate Bending, offshore	Active Shallow Crust
areaSource	NBC	Northern British Columbia	Active Shallow Crust
areaSource	NOFR	Nootka Fault	Active Shallow Crust
areaSource	OLM	Olympic Mountains	Active Shallow Crust
areaSource	PGT	Puget Sound Shallow	Active Shallow Crust
areaSource	ROCN	Rocky Mountain Fold/Thrust Belt North	Active Shallow Crust
areaSource	ROCS	Rocky Mountain Fold/Thrust Belt South	Active Shallow Crust
areaSource	SBC	Southern British Columbia	Active Shallow Crust
areaSource	VICM	Vancouver Island Coast Mountains	Active Shallow Crust

Table 2.2 Summary of all seismic sources within CanadaSHM5 (Continuation of Table 2.1)

Source Type	ID	Name	Tectonic Region Type
simpleFaultSource	QCSS00	Queen Charlotte - Strike Slip Beta = 0	Active Shallow Fault
simpleFaultSource	QCSS08	Queen Charlotte - Strike Slip Beta = 1.84	Active Shallow Fault
simpleFaultSource	FWF00	Fairweather Fault Beta = 0	Active Shallow Fault
simpleFaultSource	FWF08	Fairweather Fault Beta = 1.84	Active Shallow Fault
areaSource	QCFA	Queen Charlotte Fault - Area	Active Shallow Fault
areaSource	FWFA	Fairweather Fault - Area	Active Shallow Fault
areaSource	OFS	Offshore	Active Shallow Offshore
areaSource	FTH	Foothills	Stable Shallow Crust
areaSource	SCCWCH	Stable Cratonic Core Western Canada, H model	Stable Shallow Crust
areaSource	SCCECH W	Stable Cratonic Core Eastern Canada, H model - Williston Basin Cut Out	Stable Shallow Crust
areaSource	WLB	Williston Basin	Stable Shallow Crust
complexFaultSource	CIS-15, CIS-22	Cascadia Interface Source	Subduction Interface
simpleFaultSource	EISO-22	EISO - outboard estimate of rupture - 16 km depth	Subduction Interface
simpleFaultSource	EISB-22	EISB - best estimate landward extent of rupture - 22 km depth	Subduction Interface
simpleFaultSource	EISI-22	EISI - inboard estimate of rupture - 28 km depth	Subduction Interface
simpleFaultSource	HGT00	Haida Gwaii Thrust Beta=0	Subduction Interface
simpleFaultSource	HGT08	Haida Gwaii Thrust Beta=1.84	Subduction Interface

Table 2.3 Summary of all seismic sources within CanadaSHM5 (Continuation of Table 2.2)

Source Type	ID	Name	Tectonic Region Type
simpleFaultSource	WIN00	Winona Thrust Beta=0	Subduction Interface
simpleFaultSource	WIN08	Winona Thrust Beta=1.84	Subduction Interface
areaSource	JDFN	Juan De Fuca Plate Bending, Onshore (Deep)	Subduction IntraSlab30
areaSource	GTP	Georgia Strait/Puget Sound (Deep)	Subduction IntraSlab50

2.1.1.1 Crustal sources:

The geographic distribution of the active shallow crustal sources defined in CanadaSHM5 model for southwestern BC, with respect to Vancouver and Victoria, are shown in Figure 2.2 and tabulated in Table 2.1 and Table 2.2.

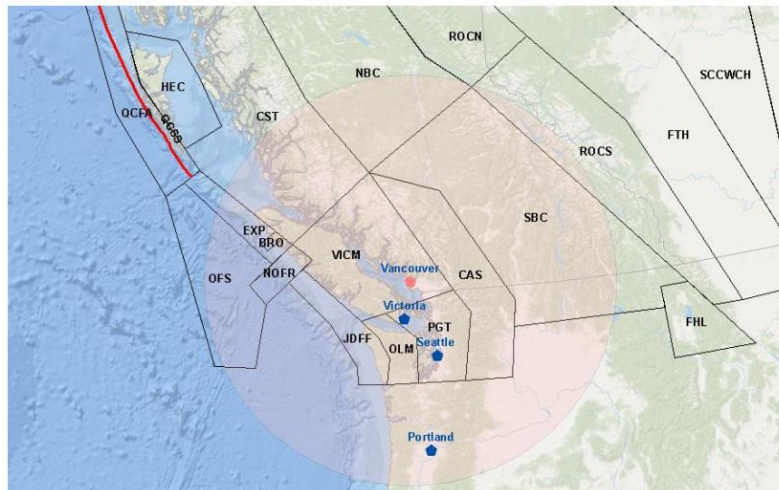


Figure 2.2 Crustal sources closest to Vancouver, defined within CanadaSHM5, for southwestern BC (VC Structural Dynamics, 2019)

2.1.1.2 Subduction Interface sources

The subduction interface sources defined in CanadaSHM5 for southwestern BC are the Cascadia Interface Source (the Juan de Fuca segment of the CSZ), the EISO, EISB and EISI (the Explorer segment of the CSZ) and two thrust fault sources: the Haida Gwaii Thrust and The Winona Thrust Fault (Table 2.2 and Table 2.3). The geographic distribution of these sources with respect to Vancouver and Victoria, is shown in Figure 2.3.

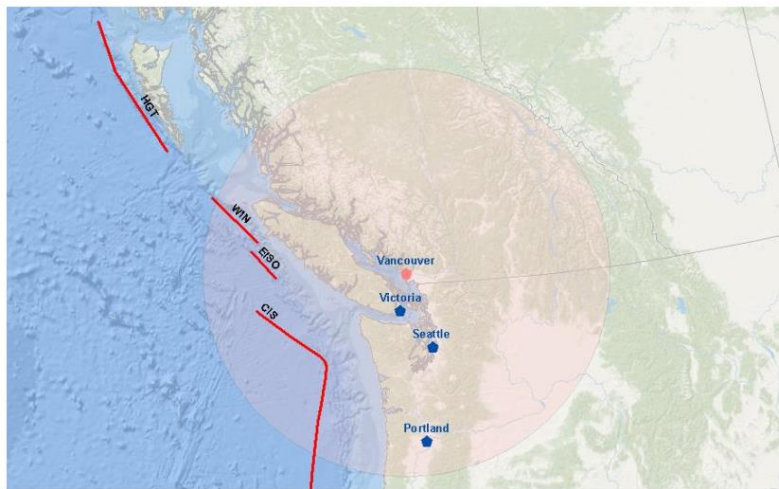


Figure 2.3 Subduction interface sources closest to Vancouver, defined within CanadaSHM5, for southwestern BC (VC Structural Dynamics, 2019)

2.1.1.3 Subduction Intraslab sources

The Subduction Intraslab sources defined in the CanadaSHM5 model for southwestern BC are the Juan de Fuca Plate Onshore and the Georgia Strait/Puget Sound that captures the seismicity at different depths within the Juan de Fuca plate (Table 2.3) The geographic distribution of these sources with respect to Vancouver and Victoria, is shown in Figure 2.4.

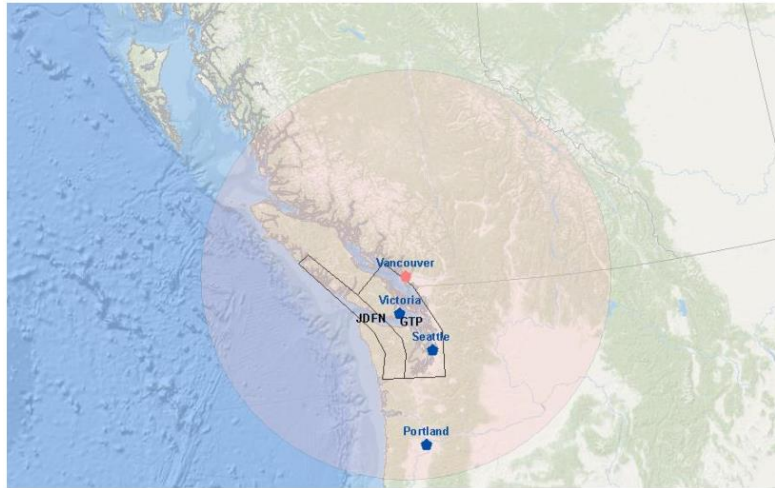


Figure 2.4 Subduction Intraslab sources closest to Vancouver, defined within CanadaSHM5, for southwestern BC (VC Structural Dynamics, 2019)

2.2 Effect of soil conditions at the site

The local soil conditions of the site will influence the seismic hazard, since the soil's properties can amplify or de-amplify the intensity of ground shaking. NBCC 2015 classifies the soils into different site classes (A to F in decreasing order of shear wave velocity) from recorded shear wave velocity (V_{s30}) in the top 30 meters of soil or rock at the site as summarized in Table 2.4 .

Table 2.4 Site classification based on average shear wave velocity in NBCC 2015

Site Class	Ground Profile Name	Average Shear Wave Velocity, V_{s30} in m/s
A	Hard rock	$V_{s30} > 1500$
B	Rock	$760 < V_{s30} \leq 1500$
C	Very dense soil and soft rock	$360 < V_{s30} < 760$
D	Stiff soil	$180 < V_{s30} < 360$
E	Soft soil	$V_{s30} < 180$
F	Other soils	Site-specific evaluation required

Ground shaking intensifies at sites with soft soil and abates at sites with stiff soils or rock, respectively, and this in turn influences the seismic response of the structure located at the site. Based on the site class described in Table 2.4 , NBCC classification amplifies the seismic demand on structures at the site of interest.

The National Earthquake Hazard Reduction Program (NEHRP) V_{s30} site classification for Vancouver (Turner et al., 1998) is shown in Figure 2.5. This soil site classification information at the site of interest is then used by the GMPEs defined in the seismic hazard analysis, to calculate the intensity of ground shaking.

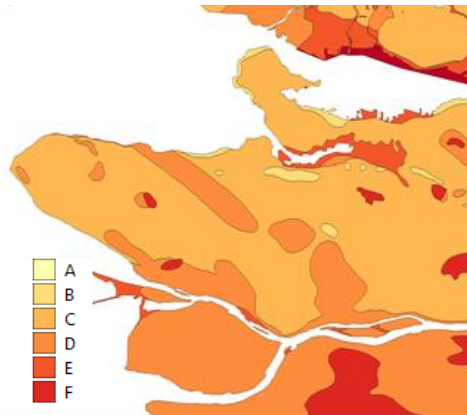


Figure 2.5 NEHRP site classification for the city of Vancouver

2.3 Overview of building stock in Vancouver and Victoria

A combination of high population density, high building density, an aging building stock, and relatively high seismic hazard makes Vancouver and Victoria crucial study areas to identify the issues of fragility models currently used to conduct seismic risk assessments. ‘Building stock’ refers to the total number of buildings in a specific country, region, province etc., classified based on several distinguishing features. Choosing Vancouver and Victoria as representative regions for

BC, their building stock are studied from an extensive building survey conducted by UBC in these two cities. The classification was based on construction material used (Figure 2.6), occupancy type, lateral force resisting system, age of construction etc.

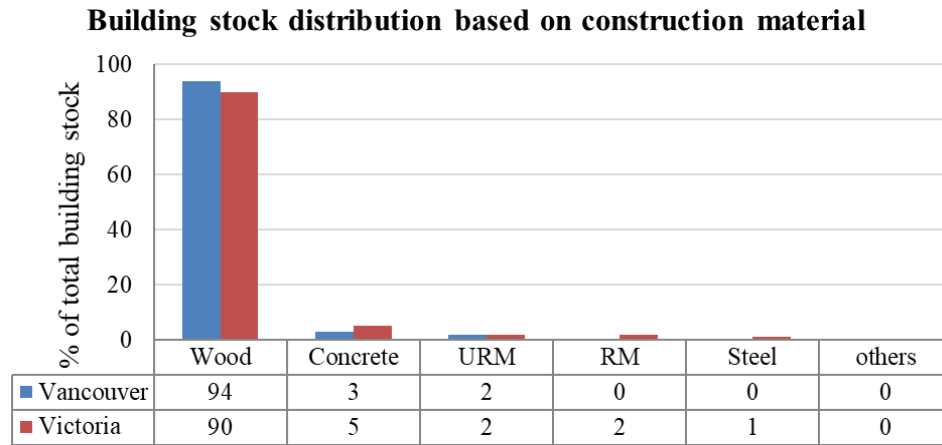


Figure 2.6 Distribution of building stock based on construction material for Vancouver and Victoria

The building stock distribution in Vancouver and Victoria in Figure 2.6 shows that wood is the main construction material of choice followed by concrete and masonry in these two cities. The building structural typologies and occupancy classes were initially assigned based on the HAZUS building typology definitions (defined in Appendix A, Table A. 1) and the HAZUS (FEMA, 2014) building occupancy classes (defined in Appendix A, Table A. 3), respectively.

2.3.1 Vancouver

The City of Vancouver 2018 Building Inventory Report records about 95,000 addresses from the building survey conducted by UBC. Virtual and sidewalk surveys were used to confirm or update data to merge with the 2011 UBC database which had ~ 25,000 addresses. The buildings were then classified based on construction material, building height (when available), year of construction, occupancy, number of stories and area of the building (when available), preliminarily based on the HAZUS building typology classification (Appendix A, Table A. 1, Table A. 3).

Regions outside the Vancouver downtown contain mostly residential and commercial wood buildings including single family houses, multi-storey wood apartments (3-4 stories), and low-rise masonry commercial buildings. 94% of the buildings surveyed in the city are wood construction. Single family wood houses make ~80,000 buildings of the total building stock, with approximately half of them having sub-floors or cripple walls. About 50,000 were built before 1972, of which, approximately 27,000 were single family wood construction. Concrete is the second common construction material (3%), while masonry construction (2.3%) and steel (0.3%) follow. Mid-rise and high-rise construction is dominated by concrete and steel. The concrete and masonry buildings make up the majority of the downtown core, with the highest density of commercial and residential structures, including almost all the concrete high rises in Vancouver. The masonry buildings are mostly unreinforced older buildings. About 1,157 buildings are concrete shear wall constructions built before 1972 which could show non-ductile behavior, as compared to those designed to newer building codes. Concrete shear wall constructions and wood constructions together make about 97 %, and single-storey light frame wood houses alone makes about 92 % of Vancouver's building stock. More than half of the city's building stock (~57 %) were built before 1972, when seismic design was not accounted for.

2.3.2 Victoria

The building stock for Victoria is developed by merging BC Assessment's 2016 Building Inventory report with a database of the buildings inventory in Victoria that was compiled in the mid-1900s and updated in 2010 by UBC (Ventura & Bebamzadeh, 2016). Virtual investigations and sidewalk surveys were conducted by UBC students to verify and update information within the database. The building survey of ~13,300 buildings show that with around 90% of the surveyed buildings, wood is the most frequently used construction material. Of this, 84% are low rise

residential wood construction with 1-2 stories height, and around 6% are multi-storey wood construction of 3 to 4 stories height, both commercial and residential. Of the about 12,000 wood buildings, 84% were built before 1972, which makes 72% of Victoria's building stock, low rise residential wood construction built prior to 1972. With ~700 (5%) buildings made of concrete, it is the second common construction material, of which 43% are built before 1972. Concrete shear wall construction dominates the concrete building stock. Masonry construction (4%) and steel (1%) follows as other most used construction materials. Mid-rise and high-rise construction are dominated by concrete. Studying the spread of the different building stock, it is seen that concrete and masonry (unreinforced and reinforced) constructions are concentrated in downtown and most of them are built prior to 1972, while other areas are dominated by wood construction.

2.4 Considered building typologies

It is assumed that the Vancouver and Victoria building stock is reflective of the BC building stock, meaning that the BC building stock is dominated by wood, concrete and unreinforced masonry structures. For the current study, the choice was made to develop fragility and vulnerability curves, targeting the 'most prominent' building typologies in the representative regions in BC, which refers to building types that make up at least 95% of the building stock. Creating damage and loss functions for all structural building typologies is an immense task, and 95% of the building stock could give a realistic estimate of predicted damage and losses. The major typologies in Vancouver (~97%) and Victoria (~95%) are wood structures and concrete shear walls construction, and this study will focus on them.

2.4.1 Wood typologies

HAZUS (FEMA, 2014) classifies wood typologies into W1 (light frame wood construction of floor area less than 5000 sq.ft.) and W2 (wood construction of floor area greater than 500 sq.ft.) (full HAZUS definition is provided in Appendix A, section A.2).

In BC, the main wood typologies that are seen are light frame residential low-rise, light frame residential mid-rise and commercial and industrial constructions. More than half of the light frame residential low-rise buildings have a basement (referred to as subfloor in this study), and some have a crawl space (referred to as cripple wall in this study). A detailed description of these main wood typologies seen in BC will be presented in Chapter 3.

Cripple walls are mostly wood-frame stud walls that run along the perimeter of the buildings' base, creating a gap between the foundation and first floor joists, called crawl space. The crawl space is not livable and are built to resist the vertical building weight, but with not enough lateral strength capacity to resist seismic loads. Past earthquakes prove that cripple walls can collapse under a moderately strong earthquake, and under a strong earthquake, they are the first structural element to fail (CUREE, 2002). The house falls even if the upper floors are fastened to the cripple wall, and the cripple wall to the foundation, making this failure more dangerous and expensive.

Houses with basements are usually of two types. One, with the first-floor framing set directly over a concrete/brick foundation wall, with no "short wall" in between and second, where the concrete/brick basement walls extend only partially up to the first-floor framing and have a wooden "short wall" above them. The first case will be considered a light frame residential low-rise buildings without cripple wall or subfloor, and the latter as a light frame residential low-rise

buildings with a subfloor. Unlike crawl spaces, basements are mandated to have openings for windows and external access to satisfy BC Building Code (BCBC) requirements and are considered livable spaces.

2.4.2 Concrete shear wall (C2) typologies

HAZUS defines concrete shear wall (C2) structures as those where the vertical components of the lateral-force-resisting system (LFRS) are RC shear walls, which also act as the load bearing walls. It provides resistance against lateral loads like earthquakes and wind, while also providing stiffness and strength under service loads in an RC shear wall building. Shear walls can differ from building to building based on building height, geometry, building usage and architectural designs. The design of LFRS in Canada at the time of this study, followed NBCC 2015, where the nonlinear response of the building is not clearly accounted for, as this code edition did not consider performance-based seismic design. Most C2 buildings before 1990 have extensive shear walls that are lightly reinforced, while newer C2 building have limited, but well-detailed and properly reinforced shear walls. C2 is classified into three typologies based on number of stories: Low-rise C2 (C2L) structures have stories in the range of 1 to 3; Mid-rise C2 (C2M) structures in the range of 4 to 7 stories; and high-rise C2 (C2H) with more than 8 stories (Appendix Table A.1).

2.5 Methods to assess building stock vulnerability

The probable damage and losses to the building stock in a region of interest can be estimated from the predicted intensity of ground shaking at the location using fragility (Porter, 2021) and vulnerability functions, respectively. Structural fragility and vulnerability functions define the probability of a structure attaining or exceeding a structural damage state or loss ratio respectively, for a given level of ground shaking - quantified in this study by the spectral

acceleration at the effective period of the structure ($S_a(T)$). They account for variability and uncertainty associated with structural properties of the buildings and ground motions used, which in turn accounts for variability in structural response of the system. These fragility and vulnerability functions can be developed either empirically - from damage and loss data recorded from past earthquake events- or analytically, when the quantity and quality of field data is scarce, as is the case for BC. Analytical fragility functions are developed by subjecting representative structural models to selected ground motion records to evaluate their response, correlating the ground motion intensity to the probability of exceeding a damage state (defined by appropriate damage threshold criteria) and fitted to a cumulative distribution function through regression analysis. They are converted into vulnerability functions using suitable consequence (damage-to-loss) models.

Structural characteristics of buildings classified under a given typology can vary across individual buildings. When this is represented as a distribution function, the building that embodies the median properties given a typology is referred to as a median building. Representative structural models for median buildings are realized through an equivalent-single-degree-of-freedom (ESDOF) system with a defining capacity curve. This ESDOF model represents the first mode behavior of the building.

A capacity curve is a plot of spectral displacement versus spectral acceleration, developed from a non-linear pushover (PO) curve. The PO curve (plot of roof displacement versus base shear) is obtained through a PO analysis of the median building model using a structural analysis software or empirically, through experimental laboratory tests or from observational data during previous seismic events. A set of non-linear SDOF models which are represented by capacity curves, using

a probability distribution, are developed and damage state thresholds are defined to designate damage states that the buildings will be in. The capacity curves used to develop the damage and loss functions used to create the CanSRM1 are developed from HAZUS static capacity curves.

The damage state of the structure is assigned based on damage limit thresholds, set as specific structural response values like structural displacement, drift, acceleration etc. Four damage states are assigned to represent the degree of damage to a structure: Slight (DS1), Moderate (DS2), Extensive (DS3), and Complete (DS4). Appendix A, section A.5 provides physical descriptions of these damage states in wood and concrete shear wall constructions as documented in HAZUS. An example of how the damage state of the structure is determined based of the level of ground shaking is shown in Figure 2.7.

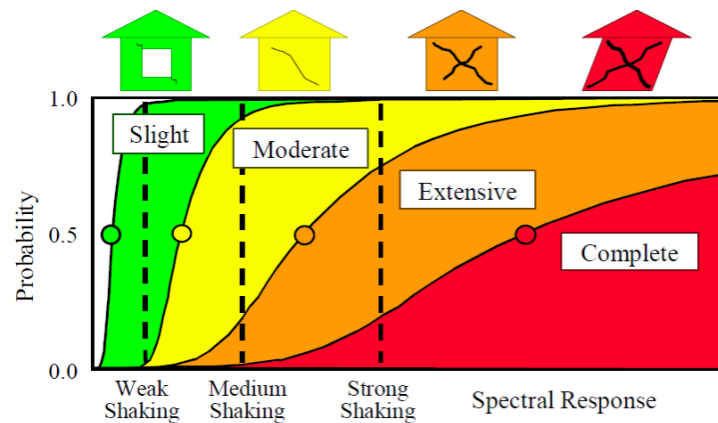


Figure 2.7 An illustration of where the cumulative damage function (CDF) (fragility curves) meets with various intensities of ground shaking [Source: HAZUS (FEMA, 2014)]

Once the damage states are defined, the ESDOFs are subjected to nonlinear time history analyses (NLTHA) to determine the extent of damage to the representative building models. The intensity of ground motion shaking and probability of exceedance of a given damage state are correlated and the fragility functions are conventionally fitted as lognormal distributions, through

regression analysis. Consequence models are used to convert fragility functions into vulnerability functions, that helps estimate the encumbered losses, relating the physical damage (structural, non-structural, contents) to a measure of fraction of loss (say in % of building replacement costs).

2.6 Past research on fragility curves for BC wood and concrete shear wall typologies

Globally, extensive research has been done to determine the fragility and vulnerability functions of different building types like wood and C2 construction - both at the building level and at the regional level - in an effort to quantify the responses of these building types during seismic events. HAZUS has developed the most extensive collection of fragility and vulnerability curves for the different building typologies in US construction, including C2L, C2M and C2H, W1 and W2 (FEMA, 2020b).

In recent years, FEMA has also expanded the fragility curves for wood, to include specific wood typologies like one-storey, two-storey wood (FEMA P-1100-3, 2019), multi-family dwellings, commercial wood structures, multi-storey wood buildings with weak first stories (FEMA P-807, 2012) and wood structures built over cripple walls, basements etc (Welch et.al., 2020). GEM foundation has a very extensive collection of fragility and vulnerability curves from across the globe in its repository (Yepes-Estrada et al., 2016).

In BC, the major studies pertaining to concrete shear wall buildings were done by Nazari, where fragility curves for 2-storey (C2L), 5-storey (C2M) (Nazari et. al., 2017) and 10-storey shear wall buildings in Vancouver (Nazari, 2017) built in 1965 and in 2010 were developed. Fairhurst et al., (2019) studies the effect of long duration ground motions on high-rise RC shear wall buildings in Vancouver. Chin et al., (2015) studied the effect of long duration ground motions on low-rise RC shear wall buildings in Vancouver.

UBC has studied the seismic performance of wood-frame residential construction in BC (White & Ventura, 2006). A series of studies done by Goda based on the UBC-SAWS models - developed in the study cited above- provides extensive research on RSRA for low-rise residential wood structures in BC (Goda, 2019), especially in Victoria (Goda & Sharipov, 2021; Goda et al., 2021; Zhang et al., 2020). Recently, work has also been done to quantify the effects of long-duration subduction ground motion on wood structures (Jafari et al., 2022; Mulder et al., 2017; Pan, 2018; Pan et al., 2020).

2.7 Scenario Risk Analysis

A seismic scenario is a realization of a specific earthquake of a defined magnitude, created from rupture in a given location, with intensities of ground shaking calculated using different GMPEs. A seismic scenario analysis is a means to analyze the risk (damage and loss) accumulated in a site of interest due to a specific earthquake event. While a scenario damage assessment refers to the calculation of the damage distribution statistics from a single earthquake rupture scenario, considering the aleatory and epistemic ground-motion variability at a site of interest, for the building portfolio at the site, scenario loss assessment refers to the corresponding calculation of the incurred loss (structural, non-structural and contents).

Once a set of fragility and vulnerability functions are developed (to be discussed in sections 3.3.1 and 3.3.2), they can be used to develop the scenario damage and loss estimates respectively. The components required by the OQ scenario calculator to carry out a scenario analysis are: the exposure model (to be discussed in section 3.2), the rupture model, a list of GMPEs (to be discussed section 3.4) and corresponding weights, and the soil data (section 2.2) at the site, in addition to the fragility and vulnerability functions. This is shown in Figure 2.8.

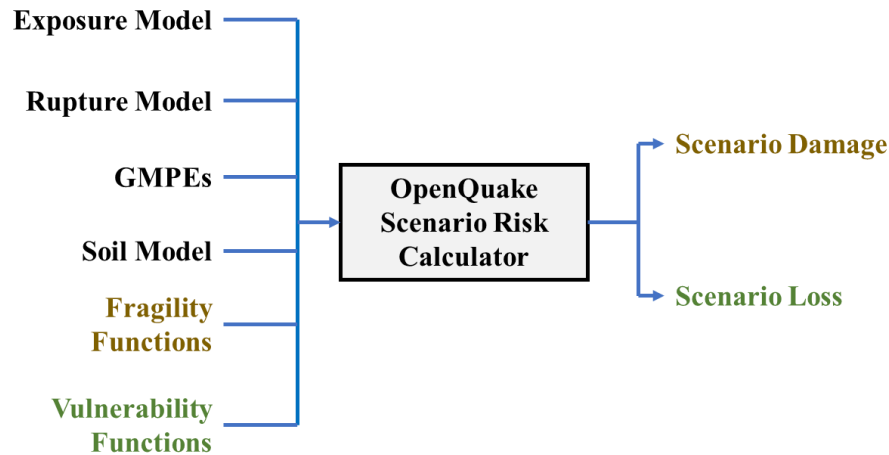


Figure 2.8 Components for scenario damage and loss analysis in OpenQuake

Seismic scenario damage analysis is a good tool to understand the geographical distribution of different building typologies with a given level of damage, under predicted levels of ground shaking in forecasted seismic events arising from known ruptures near or farther away from the site of interest. It helps to identify extremely vulnerable neighbourhood pockets where the more susceptible buildings are, give a general idea of building typologies most susceptible to damage (which needs to be considered for retrofitting) and understand, roughly, the performance of buildings built to various design codes levels. Buildings not designed to carry seismic loads will undergo higher levels of damage, and could collapse, causing monetary losses and casualties. Combined with a casualties' consequence function, it can also give an idea of the fatalities that should be considered for emergency evacuation purposes. Scenario loss assessment, similarly, gives a general picture of the building typologies that are most susceptible to losses, and where measures are to be taken to reduce such losses. Both scenario damage and scenario loss assessment is a means to empirically validate the fragility and vulnerability functions developed, when there is recorded damage and loss data from historical damaging events at the site of interest.

Many seismic scenario analyses have aimed to understand the effect of fragility curves developed (Goda & Sharipov, 2021; Goda & Yoshikawa, 2013; Goda et al., 2021; Liu & Hong, 2017; Ploeger et al., 2010) .The city of Vancouver and NRCan uses scenario analysis to develop its earthquake preparedness exercises (Bird et al., 2022). Recently, the GSC has put together a list of seismic scenarios to be considered for government planning purposes (Hobbs, 2021) as well as an earthquake scenario catalogue for Canada (Hobbs et al., 2021b)

2.8 Regional Seismic Risk Analysis (RSRA)

While the scenario analysis is helpful to understand the building portfolio behavior, during a specific seismic scenario, a RSRA statistically compiles impact from all relevant seismic sources that can drive the seismic damage and losses over a given time period. The most comprehensive work on RSRA in BC was by Tuna Onur (Ventura et al., 2005; Onur, 2001; Onur et al., 2005, 2006) , and studies the regional damage and loss assessment in Vancouver and Victoria. Another RSRA study done for Victoria studied the damage and loss estimated in Victoria (VC Structural Dynamics, 2016), for the entire Victoria building stock.

Within OQ, ‘Stochastic Event Based Probabilistic Seismic Risk Analysis’ (henceforth called event-based risk analysis) is used to develop event loss tables from stochastic event sets, and calculate loss exceedance curves. As per GEM (2022), a stochastic event set “*represents a potential realisation of the seismicity (i.e., a list of ruptures) produced by the set of seismic sources considered in the analysis over the time span fixed for the calculation of hazard*”.

OQ has a powerful event-based damage calculator that “*employs an event-based Monte Carlo simulation approach to probabilistic damage assessment in order to estimate the damage distribution for individual assets and aggregated damage distribution for a spatially distributed*

portfolio of assets within a specified time period” (GEM, 2022) . It can be used to calculate the probabilistic damage metrics such as damage-state exceedance curves for different return periods, both at the asset level and also at the aggregated level. The inputs for the calculator include the exposure model of the region of study, a fragility model for each typology within the exposure model and a stochastic event set that characterizes the seismicity of the region of study (created by the OQ probabilistic event-based hazard calculator) for a chosen time period. For each event in the stochastic event set, a ground motion field realization is generated, using the assigned logic trees to implement the uncertainty of the seismic source model and GMPEs chosen for different tectonic regions. Then, using the fragility functions assigned to each typology within the exposure model, the probability of being in a specific damage state is assigned to each asset within the exposure model, and this is used to calculate the damage estimate, over the investigation time, and damage exceedance curves.

The event-based risk calculator in OQ, which calculates the loss distributions instead of damage distributions, works similar to the event-based damage calculator, but utilizes vulnerability functions introduced within the calculation to assign loss ratios for each asset within the exposure model. From these loss metrics, the average annual loss (AAL), average annual loss ratios (AALR) and loss exceedance curves can be calculated. OQ has been used by the GSC to develop the CanSRM1 (Hobbs, 2022; Hobbs et al., 2022a; Hobbs et al., 2022b) and to develop a retrofit scheme for CanSRM1 (Hobbs et al., 2021a).

2.9 Summary

The seismic hazard at BC was studied, including sources that contribute to seismic hazard in BC, to understand the contributing sources modelled within the CanadaSHM5 seismic source

model used for RSRA studies within this work. The soil conditions at Vancouver were studied to understand how the soil model used within OpenQuake scenario and regional risk analysis will influence the predicted ground motion values at different sites. The Vancouver and Victoria building stock were studied to identify prominent building typologies that would be the focus of this work. The prominent wood and concrete shear wall building types in BC were discussed, and building typologies will be assigned to these building types in Chapter 3. Past research on these prominent building types in BC were discussed along with the methods to assess the vulnerability of a building stock. Finally, scenario risk analysis and RSRA within OpenQuake is discussed. This background information, was the basis for developing the methodology discussed in Chapter 3.

Chapter 3: Methodology

3.1 Overview

To quantify regional seismic damage and loss, a thorough understanding of the region's building stock, seismic hazard, soil characteristics and appropriate fragility and vulnerability functions for the building typologies are needed. The assumptions made in creating the exposure model for Vancouver (used for scenario analysis) and Victoria, reclassifying representative building typologies and the development of their fragility and vulnerability curves for the crustal and subduction events are discussed here. A method to verify the vulnerability functions, their application to scenario analysis and finally, their application to RSRA and to study the influence of subduction ground motions on RSRA is also included.

The fragility and vulnerability functions currently used to develop the CanSRM1, by NRCan (Hobbs et al., 2022b) are henceforth referred to as GEM functions - as they have been developed by the GEM Foundation for use in Canada.

The methodology followed in this study is detailed below:

1. Develop an exposure model of Vancouver and Victoria from UBC building surveys, to identify the predominant BC typologies. (To be discussed in Section 3.2)
2. Develop SDOF models for BC-specific median buildings that reflect the predominant BC building typologies. (To be discussed in Section 3.3.1)
 - a. For C2 typologies, the capacity curve for each BC building typology is provided by the Concrete group of the Buildings at Risk Sub-Committee (part of the Seismic Policy Advisory Committee of the City of Vancouver).

- b. For the wood typologies, the Wood group of the Buildings at Risk Sub-Committee (part of the Seismic Policy Advisory Committee of the City of Vancouver) provided the backbone curve for a single storey for each typology. These are used to develop multi-storey models for the different BC specific wood typologies and the capacity curve for each wood building typology is determined from a PO analysis result.
- 3. Develop crustal and subduction fragility and vulnerability functions for the most prominent building typologies in BC. (To be discussed in Section 3.3.2 and Section 3.3.3)
 - a. Prepare the ground motions (crustal and subduction) for IDA from the BC Seismic Retrofit Guidelines 3rd edition (SRG3) ground motion suites developed for Vancouver and Victoria (Bebamzadeh et al., 2015).
 - b. Develop crustal and subduction fragility and vulnerability functions for the most prominent building typologies in BC (C2 and wood) using the SDOFs developed in step 2 for Vancouver and Victoria.
 - c. Verify the vulnerability curves, by calculating the Average Annual Loss Ratio (AALR) for C2 and wood typologies and checking if they yield realistic values for Vancouver. (To be discussed in Section 3.3.4)
- 4. Carry out deterministic seismic analysis for Vancouver, and evaluate the implications of the modifications made for the BC-specific functions. Crustal and subduction scenarios are run for Vancouver for three cases and the results are compared for each scenario. (To be discussed in Section 3.4)
 - a. Case 1: GEM's fragility and vulnerability functions for Canada are used with the Vancouver exposure model.

- b. Case 2: BC-specific fragility and vulnerability functions are used with the Vancouver exposure model assuming that the low-rise residential wood buildings do not have cripple walls or subfloors
 - c. Case 3: BC-specific fragility and vulnerability functions are used with the Vancouver exposure model, distinguishing between low-rise residential wood construction having cripple walls and sub-floors, and those that do not.
- 5. Investigate the effect of explicitly including subduction fragility and vulnerability functions in RSRA, for multiple locations across BC. (To be discussed in Section 3.5)
 - a. Carry out probabilistic seismic risk analysis (RSRA) for 10 selected localities, considering only the C2 and wood buildings in the site's building stock for two cases to study the influence of subduction ground motions in BC.
 - i. Case 1: Stochastic damage and loss analysis is carried out using only the crustal fragility and vulnerability functions, for all seismic events.
 - ii. Case 2: Stochastic damage and loss analysis is carried out using crustal fragility and vulnerability functions for crustal and subcrustal events and subduction fragility and vulnerability functions for subduction events.
 - b. To better assess the influence of the exposure model, it is desirable to use a uniform exposure model for the 10 selected localities to carry out RSRA studies. So, the Ucluelet exposure model (as it is the smallest in terms of area) is applied at the 10 selected localities and step 5a is repeated.

The methodology explained above is depicted as a flowchart in Figure 3.1

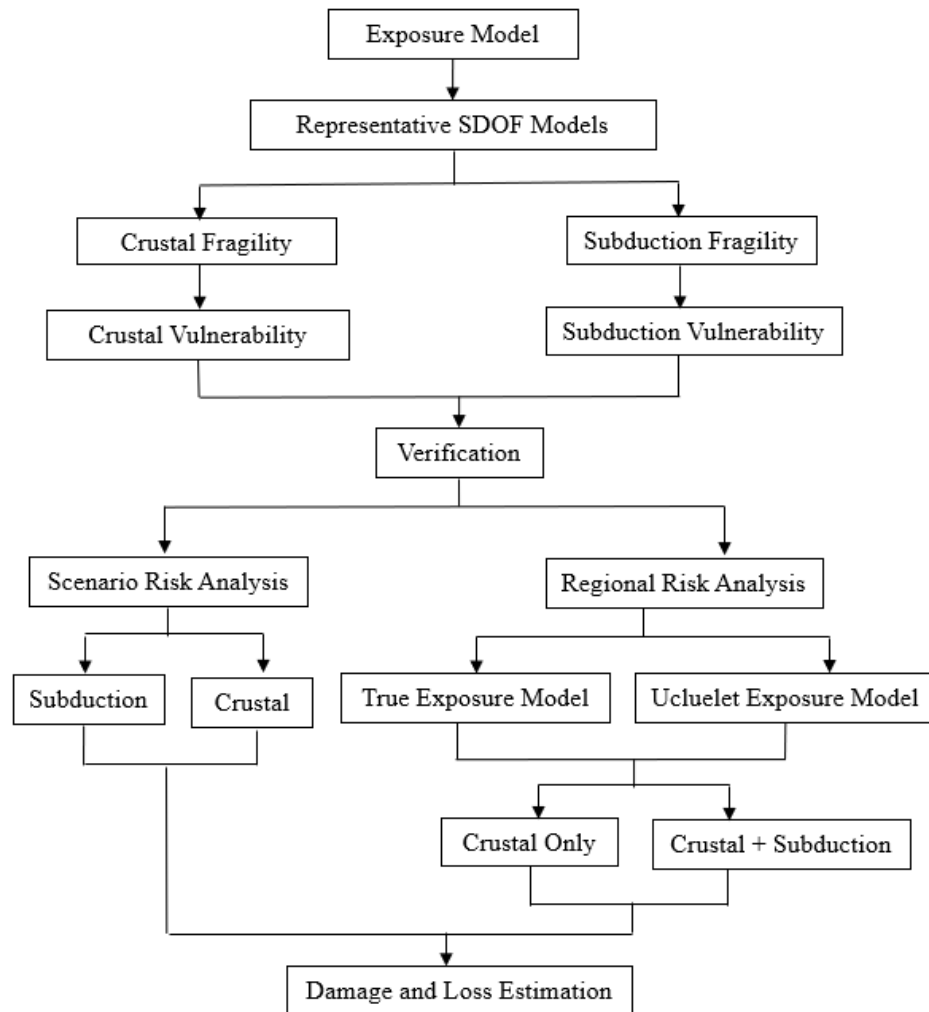




Figure 3.1 Flowchart of Methodology followed

3.2 Exposure model development for Vancouver and Victoria

Using UBC’s building survey data for Vancouver and Victoria as input, an ‘exposure model’ is developed for each locality. This requires proper classification of the BC building typologies. The HAZUS classification of wood typology into two (W1 and W2) did not accurately reflect the BC wood construction and was deemed insufficient to reflect BC wood buildings. Three new building typologies are introduced on joint discussion with the Wood group of the Buildings at Risk Sub-Committee as shown in Table 3.1.

Table 3.1 Summary of HAZUS and new BC wood structural typology definitions

HAZUS building taxonomy	Updated BC building taxonomy	Picture
W1: Wood, Light Frame ($< 5,000$ sq. ft.) Storey Range 1 - 2	W1: Wood, Low-rise residential, Light Frame Storey Range 1 - 2	 <p>[Source: Smallworks, 2022]</p>
	W4c: Wood, Low-rise residential, Light Frame, with cripple wall Storey Range 1 – 2	 <p>[Source: Carolina Custom Homes, 2023]</p>
	W4s: Wood, Low-rise residential, Light Frame, with sub-floor Storey Range 1 – 2	 <p>[Source: Drummond House Plans, 2015]</p>
	W2: Wood, Mid-rise residential, Light Frame Storey Range 3 - 6	 <p>[Source: Business in Vancouver, 2015]</p>
W2: Wood, Commercial and Industrial ($> 5,000$ sq. ft.) Storey Range All stories	W3: Wood, Commercial and Industrial, Heavy Frame Storey Range 1 - 4	 <p>[Source: naturally:wood, 2022]</p>

W1 are light frame residential low-rise buildings built of wood. This classification includes single-family detached homes and attached townhouses, usually one or two stories high, with a footprint area generally in the range of 70-350 m², without a crawl space or basement. Cripple wall in this study refers to the stud wall that runs along the perimeter of the building's base, between the foundation and the first storey flooring, which is not designed to resist lateral loading. Subfloor in this study refers to the wood part of the basement above grade which is properly designed (with better strength and stiffness) to resist lateral loads, as part of the wood building. A short wall that surrounds the basement, which is not designed for lateral loading is classified as a cripple wall in this study, if they are weak to lateral loading. W4c refers to W1 built above a cripple wall. These buildings usually have 1 or 2 stories above a cripple wall. W4s refers to W1 built above a sub-floor. These buildings usually have 1 or 2 stories above a livable basement. As previously mentioned, the building database for Vancouver put together by UBC was created on visual evaluation from physical onsite street walk and using virtual tools like Google Maps. Distinguishing between low-rise wood construction with sub-floors and cripple walls cannot be done accurately just by looking from the outside. With limited access into these residential buildings, the discernment between W4c and W4s was made such that, the presence of a window on the short wall assigned the structure as a sub-floor case (W4s) and if not, it was classified as a cripple wall case (W4c).

W2 refers to light frame residential mid-rise wood constructions that includes multi-unit residential buildings with an average footprint area of 1500 m². Those built before the early 1970s usually do not have underground parking, while in later cases, they are often built over an underground concrete parking level.

W3 refers to commercial and industrial wood constructions, usually from 80 to 600 m² in footprint area. While the ground level of commercial building types commonly has extensive glazing to set up a storefront, the industrial building types does not.

The concrete shear wall typologies were updated to reflect the code-based strength and drift levels expected over the evolution of the Canadian concrete code (Canadian Standards Association (CSA) A23.3). While the structural typology definition for concrete shear wall typologies (C2L, C2M, C2H) remains the same as in HAZUS (Table A.1), the designation of design code level has been updated as explained below.

The building's year of construction can be used to classify them into different strength bins or seismic design levels. This is because the building's year of construction can be used as a proxy for the building's design level, based on significant changes during the evolution of the building code and seismic hazard level at the building site. Design code levels for C2 structures are assigned based on the classification provided by the Concrete group of the Buildings at Risk Sub-Committee (of the Seismic Policy Advisory Committee of the City of Vancouver) (Table 3.2). Design code levels for wood typologies are assigned based on the classification provided by the Wood group of the Buildings at Risk Sub-Committee (of the Seismic Policy Advisory Committee of the City of Vancouver) (Table 3.3 for low-rise wood typologies, and Table 3.2 for W2 and W3 typologies).

Table 3.2 Summary of design code level for C2, W2 and W3 typologies

Design code level	Year of construction
High Code (HC)	2005 and newer
Moderate code (MC)	1990-2004
Low code (LC)	1973-1989
Pre-Code (PC)	before 1973

Table 3.3 Summary of design code level for low-rise wood typologies

Design code level	Year of construction
High Code (HC)	2001 and newer
Moderate code (MC)	1990-2000
Low code (LC)	1973-1989
Pre-Code (PC)	before 1973

This design code level is then adjusted based on recommendations from GSC for different seismic zones in Canada, as shown in Figure 3.2. Vancouver falls within Seismic Zone 3 and site seismic category 4.

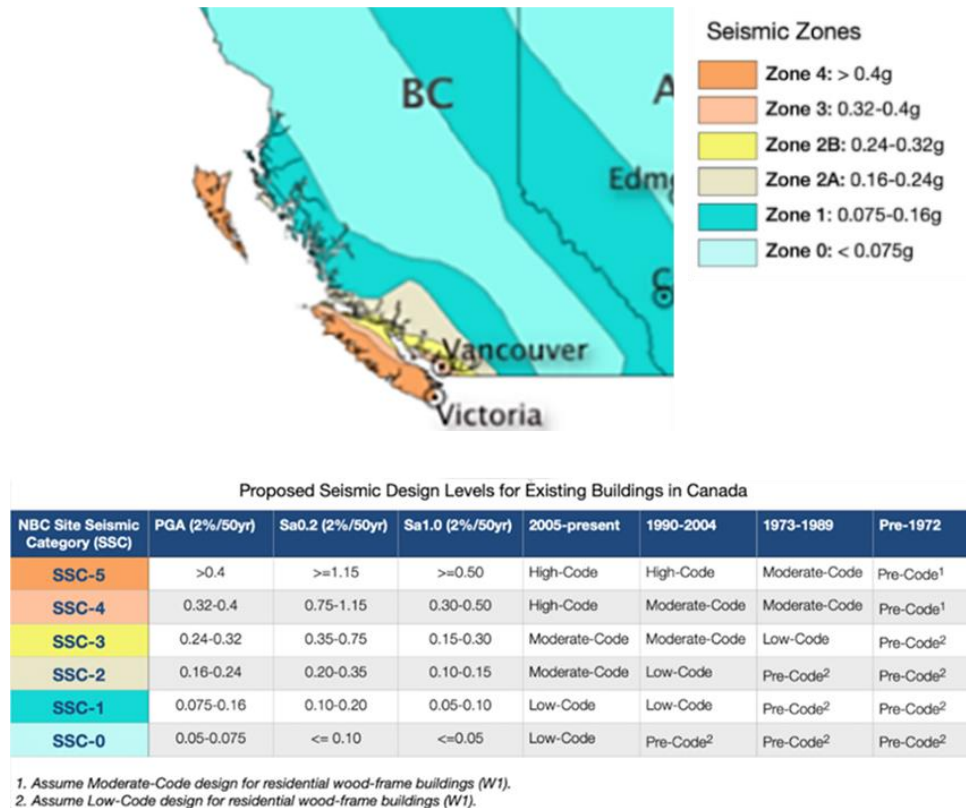


Figure 3.2 Recommendation used to adjust the design code levels in the exposure model for Vancouver based on seismic hazard and year of construction- extracted from (Hobbs et al., 2022b)

The replacement costs for the assets in the exposure model were calculated from corresponding replacement costs that was developed by NRCan within the exposure model for BC. NRCan developed these replacement cost values based on empirical data gathered from the San Francisco retrofit program (estimated from industry-standard construction costs published yearly, (Journeay et al., 2022)). Unit costs (\$CAD/sqft) are derived per taxonomy and were used to estimate replacement costs in the Vancouver exposure model, based on building floor area, recorded by the UBC building survey.

3.3 Fragility and Vulnerability curve development and modifications

In this study, fragility and vulnerability functions for generic building typologies are developed to estimate seismic risk on a regional level in a relatively simple manner. Such fragility functions are less accurate than building-specific fragility functions when calculating the damage to a single building, but provide reliable estimates of damage and loss in RSRA. To better estimate damage and losses in a region, fragility and vulnerability functions must be developed to reflect region-specific construction practices and based on site-specific seismic hazard. This section summarizes the main components to developing fragility and vulnerability curves: the ESDOF models, ground motion sets used, damage state threshold definitions and consequence models.

3.3.1 ESDOF models for BC construction.

The ESDOFs used to develop the GEM functions (especially for wood and concrete shear wall typologies) are concluded to not adequately reflect the BC building construction (will be discussed in detail in this section), as they were developed based on HAZUS building typologies. The Seismic Policy Advisory Committee of the City of Vancouver arranged the Buildings at Risk Sub-Committee, comprising of academia and industry personnel to modify the capacity curves

that represent the median building per BC building typology, accounting for BC construction types and practices over the years.

3.3.1.1 Concrete shear wall typologies (C2): new capacity curves

The Concrete group of the Buildings at Risk Sub-Committee developed BC-specific capacity curves for C2L, C2M and C2H, to reflect the changes in the strength and drift capacities expected over the years, based on the evolution of the seismic design provisions in the NBCC (Mitchell et al., 2010).

The HAZUS C2 building typologies display a large increase in base-shear and drift capacity across increasing different design code levels (PC to HC). For example, the multilinear capacity curves (MLCC) were developed for the C2H building typology from static curvilinear capacity curves recorded in HAZUS for all code levels using the methodology developed by Ryu et al. (2008), as shown in Figure 3.3.

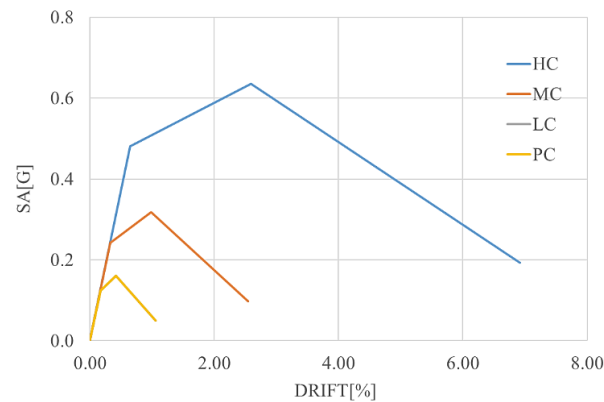
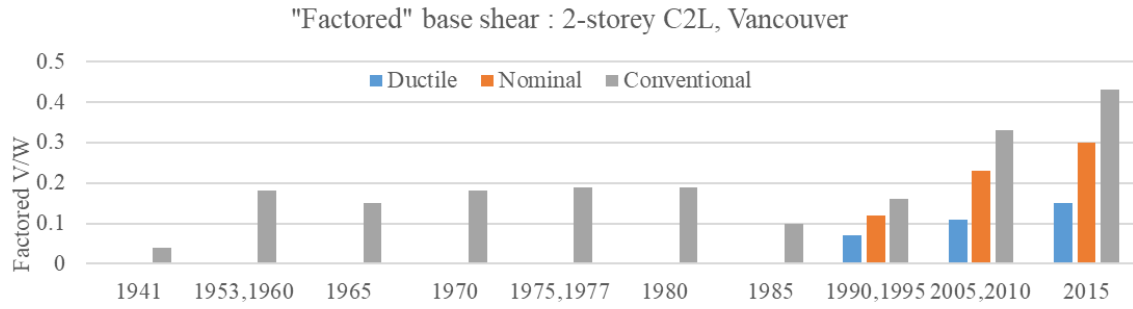


Figure 3.3 Comparison of MLCC for HAZUS C2H of all code levels (The LC and PC MLCC overlaps)

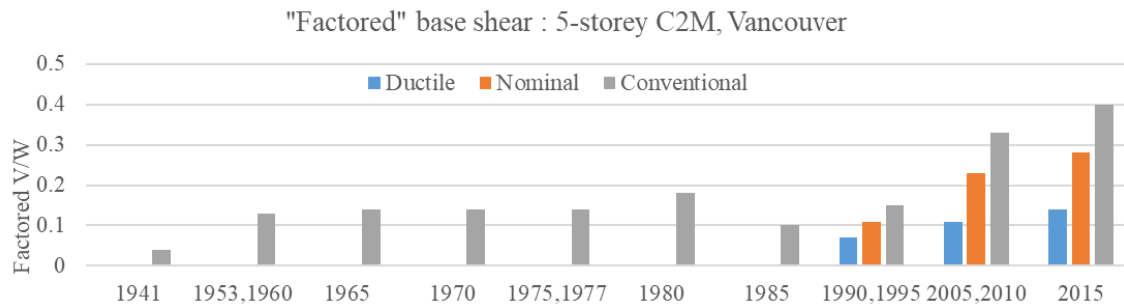
A MLCC is developed for NLTHA as an alternative to the curvilinear capacity curve documented in HAZUS, which are proposed to be used for the capacity spectrum method, rather than for NLTHA. Figure 3.3. shows that in HAZUS, the maximum base shear capacity for pre-

code and low-code C2H structures are the same which implies that the design base shear remained the same. For C2H-MC structures, the maximum design base shear is almost double that for PC and LC, and quadruples when considering C2H-HC. This increase in strength capacity is also followed by an increase in displacement capacity due to the large ductility introduced in newer design codes.

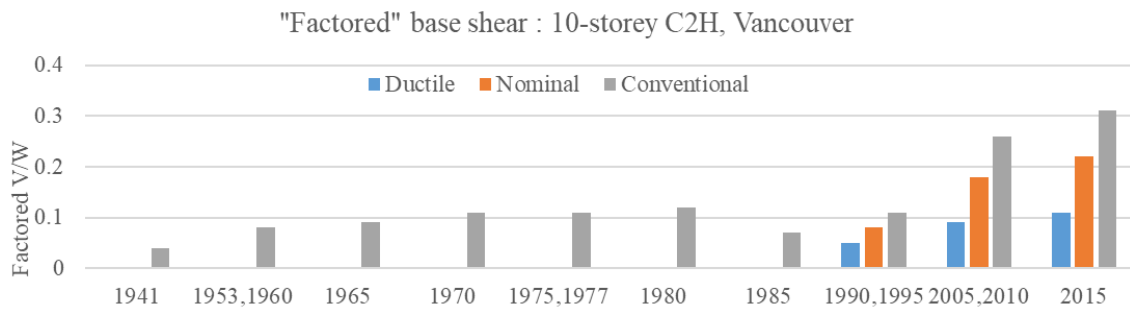
On studying the evolution of seismic design provisions in Canada (Mitchell et al., 2010), it is seen that the strength capacity of C2 buildings has not significantly changed over the years. Taking this into account, the factored design base shear is calculated for a 2-storey, 5-storey and 10-storey shear wall building built in Vancouver during the different years when the seismic design provisions in NBCC were updated. The buildings are assumed to have a storey height of 3.5m, and lateral dimension of 30m. C2 buildings built between 1941 and 1990 are assumed as mostly being nonductile (Yathon et al., 2014) and those built after 1990, as either ductile or moderately ductile in nature. Figure 3.4 shows the factored base shear calculated for a 2-storey, 5-storey and 10-storey shear wall building in Vancouver, from 1994 to 2015, respectively, accounting for the evolution of the seismic design provisions in NBCC (Mitchell et al., 2010).



(a)



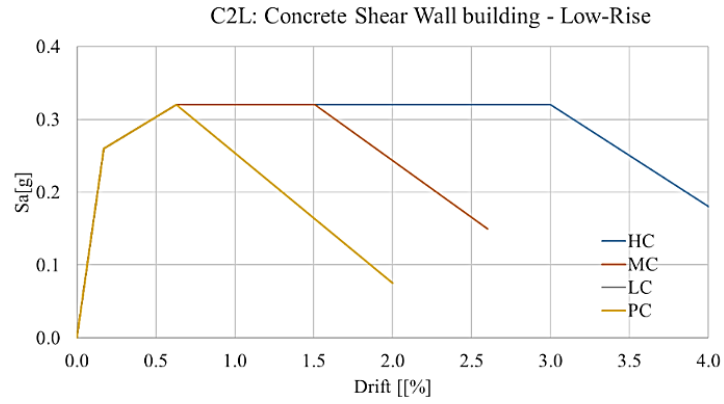
(b)



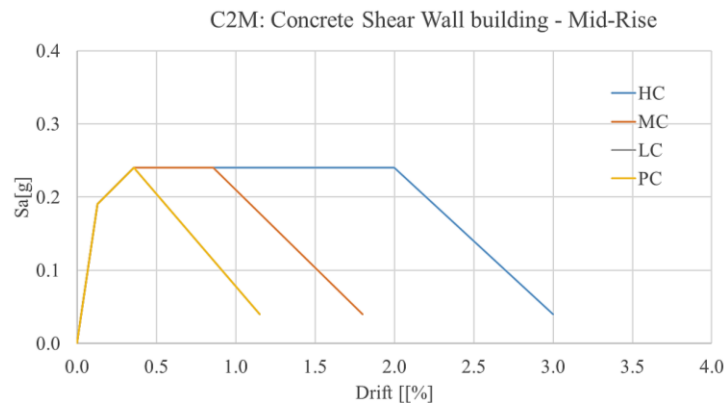
(c)

Figure 3.4: Factored base shear calculations for a C2 building in Vancouver (a) 2-storey (b) 5-storey (c) 10-storey

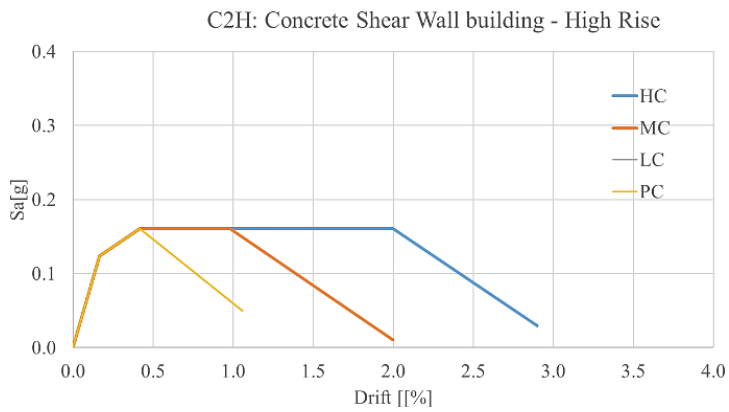
It can be seen that across the years 1941 to 1995, the factored base shear remains almost the same for C2L (0.2g), C2M (0.15g) and C2H (0.1g). Assuming an overstrength factor of 1.6, an ultimate shear capacity of 0.32g, 0.24g and 0.16g is assumed for C2L, C2M and C2H typologies respectively, across the years (PC, LC, MC, HC) as can be seen in Figure 3.5.



(a)



(b)



(c)

Figure 3.5: Comparison of MLCC for BC-specific C2 typologies of all design code levels as suggested by the Concrete group of the Buildings at Risk Sub-Committee (a) C2L (b) C2M (c) C2H. The LC and PC MLCC overlaps for all BC C2 typologies.

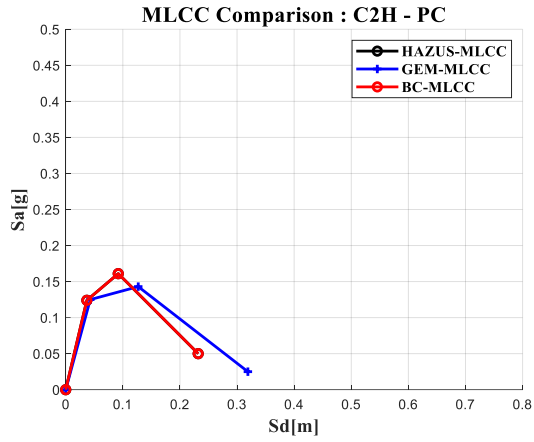
While the shear walls themselves could reach higher drift limits, as better and more stringent detailing requirements as NBCC evolved, it ensured better ductility in newer constructions and hence higher drift capacity in the newer buildings. The Concrete group of the Buildings at Risk Sub-Committee opted for more conservative values of drift capacity in the concrete shear wall building typologies. This is because from their expert opinion, in the concrete shear wall buildings designed in downtown Vancouver, before any form of shear wall failure (flexural or shear failure) occurs, other forms of damages occur. This includes structural damage initiated by the failure of adjacent gravity columns, diaphragm failure of the slab system and punching shear failure of the RC slabs subjected to high localized forces, occurring at column support points. This was observed during the Northridge earthquake (Mitchell et al., 1995).

These BC-specific capacity curves are compared to HAZUS capacity curves and the current capacity curves used by GEM to develop fragility functions for the CanSRM1 and comparison plots are drawn for representative concrete typologies. A summary of the modal heights used by HAZUS, GEM and this study is summarized in Table 3.4.

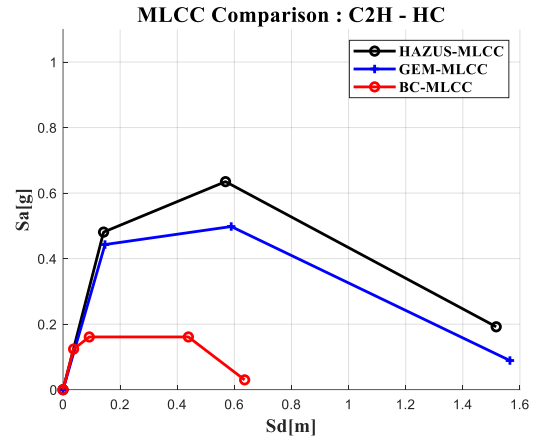
Table 3.4 Summary of modal heights used in HAZUS, GEM and this study (BC-specific) for C2 typologies

	HAZUS and BC-specific	GEM
Typology	modal height [m]	modal height [m]
C2L	4.6	5.6
C2M	11.4	14
C2H	21.9	36.4

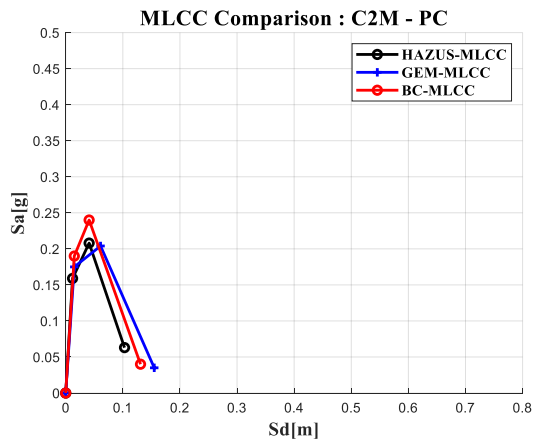
Figure 3.6 compares the MLCC developed from HAZUS to those used by GEM and those provided by the concrete subcommittee, for PC and HC design levels for C2 structures.



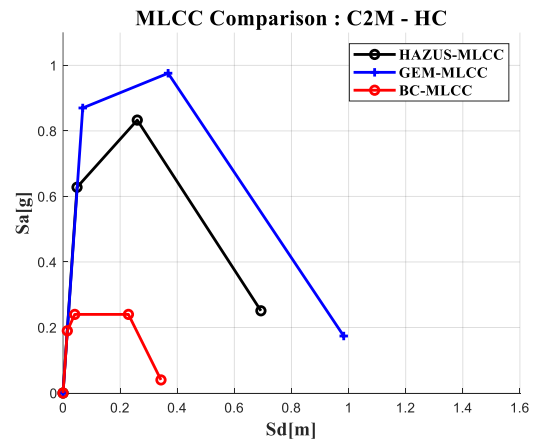
(a)



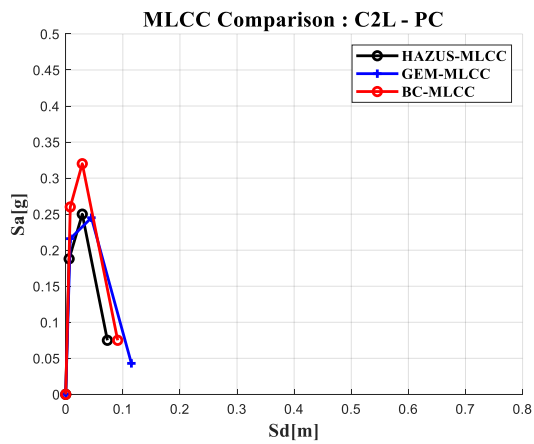
(b)



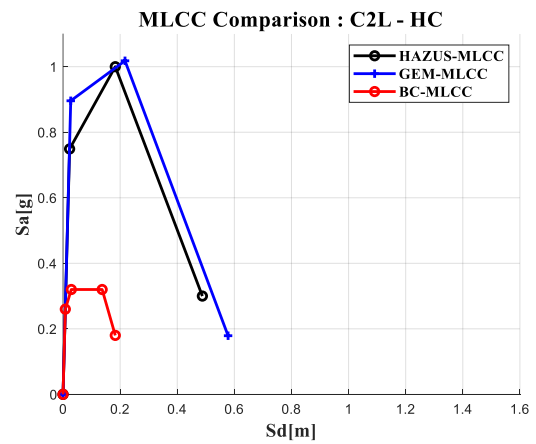
(c)



(d)



(e)



(f)

Figure 3.6 Comparison between capacity curves- GEM, HAZUS and BC-specific for: (a) C2L-PC (b) C2L-HC (c) C2M-PC (d) C2M-HC (e) C2H-PC (HAZUS and BC MLCC overlaps) (f) C2H-HC

A similar comparison for Moderate-code (MC) is provided in Appendix D (Section D.3). The HAZUS MLCC for C2H-PC overlaps with its BC-specific counterpart. The strength and displacement capacity of the C2-HC structures constructed in BC are much lower than their corresponding GEM ESDOF models. Figure 3.6a, c and e, illustrates that the BC-specific C2L-PC, C2M-PC and C2H-PC is 32%, 18% and 12% stronger than that corresponding GEM typologies. For C2 construction built after 2005, the GEM C2L-HC, and C2H-HC are about three times stronger than corresponding BC typologies, C2M -HC, about 4 times stronger.

3.3.1.2 Wood typologies: model development and capacity curve derivation

The Wood group of the Buildings at Risk Sub-Committee provided backbone curves of the wood typologies, updated for BC-specific wood construction practices, from experimental results from the FPI Innovations lab, for a single storey. Simplified building models for median buildings of each wood typologies (W1, W2, W3, W4c and W4s) was developed in OpenSees for varying code levels, with single storey properties provided, assigned per storey to these models (the number of storeys chosen for each typology is explained later in the section). Corresponding ESDOF models were derived from PO analysis of the above models and were used as the median backbone curves of their representative typologies when developing fragility and vulnerability functions.

Multi-storey/ mid-rise residential wood typology (W2)

W2 in BC had a height restriction of 4 storeys until 2009 and in BC Building Code (BCBC) 2009, this height limit was increased to 6 storeys. W2 distribution per number of stories in Vancouver (Figure 3.7) shows that median W2 construction built before 1990 can be modeled for 3 storeys and after 1990 as 4 storeys, as recommended by FPI innovations.

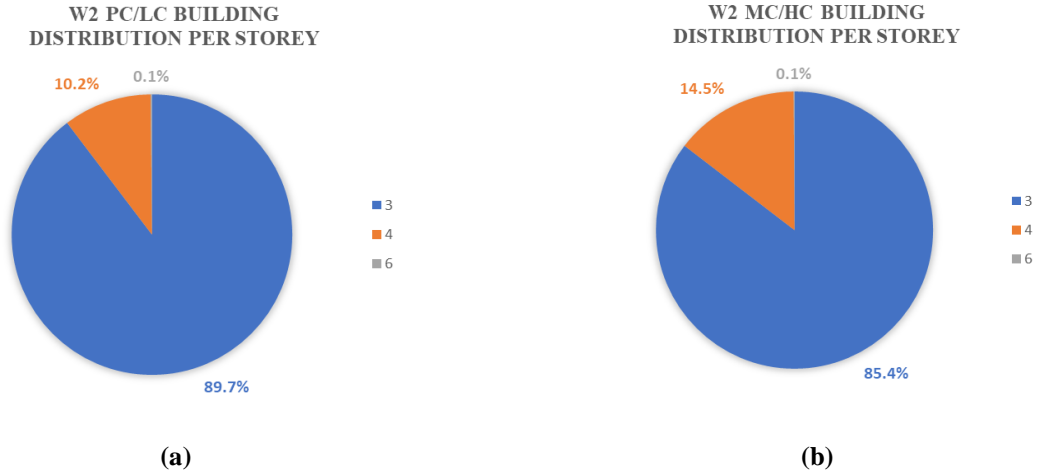


Figure 3.7 Distribution of W2 buildings per number of stories in the City of Vancouver (a) W2 PC/LC (b)W2 MC/HC

The process used to generate the ESDOF properties of W2-PC, using the single storey capacity curve provided by FPI Innovations, is described hereon. To develop the ESDOF capacity curves for W2-PC, the representative three-storey model based on the schematic in Figure 3.8, was developed in OpenSees as a three-story lumped mass model. Figure 3.9 depicts the analytical model for the W2-PC Lateral Force Resisting System (LFRS) used.

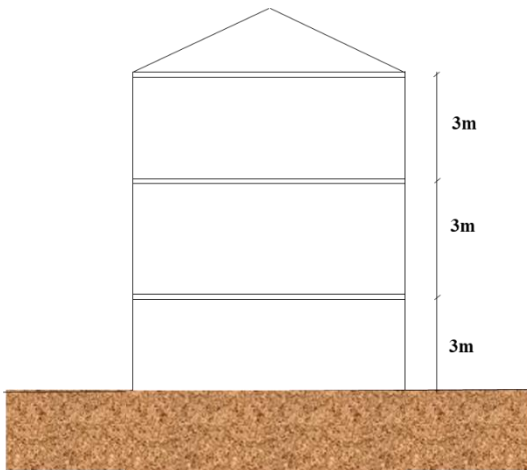


Figure 3.8 Schematic for three storey W2-PC

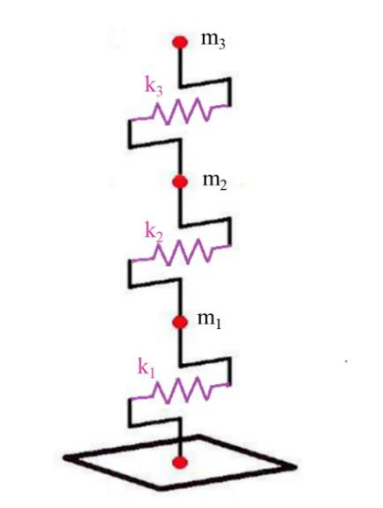


Figure 3.9 Analytical model for W2-PC LRFS developed in OpenSees

This is modeled with connecting rigid beams and columns and connected by zero length elements that simulate springs that account for the structure's nonlinear behavior. The lumped mass model has masses assigned at each floor. Each adjacent floor is connected by a rigid column with a shear spring (modeled using a zero-length element) at the middle of each storey. This shear spring is designed to replicate the backbone curve behavior of a single storey (provided by FPI innovations) at each floor. The mass per floor of the structure is assumed as 1000kg. The capacity of the shear spring at each storey is based on total design shear force for each corresponding storey, as described in NBCC 2015. A leaning column with gravity loads is linked to the lumped mass model by rigid beams to simulate any P-Delta effects in the model. The leaning columns are modeled as rigid columns that are connected to the beam-column joint by zero length rotational springs with very small stiffness so as to not draw large moments towards it. These rotational springs are provided at the top of the leaning column at each floor except the top floor. The height of each storey is set as 3.0m, and the leaning column line is located 1.0m away from the lumped mass main column. The lumped mass column is fixed at the base and the leaning column is pinned at the base.

This OpenSees model is first analyzed under gravity loads, and then a pushover analysis is done to get the pushover curve of the structure. For the first part, gravity loads are assigned to the floor joint nodes, half on the main column and half on the p-delta column and are applied as a plain load pattern with a constant time series. For the PO analysis, lateral loads are distributed across the height of the main structure using the methodology of ASCE 7-10 (ASCE 7-10, 2010) and applied to each floor, as a plain load pattern of lateral load application, where loads increase with time. The pushover analysis is run using a displacement-controlled static analysis, with the

displacement control node taken as the topmost floor node, with maximum displacement of pushover taken as 10% of the roof drift.

Once the PO curve for the whole structure is obtained, this PO curve of the MDOF system is converted to its equivalent SDOF capacity curve, considering the first mode of vibration alone. The PO curve of the three-storey structure (in terms of base shear and roof displacement) is converted into an ESDOF capacity curve, which is in terms of spectral acceleration and spectral displacement. The roof displacement of the three-storey model is normalized by the participation factor of the first mode of vibration to get S_d (spectral displacement) and base shear is normalized by the modal mass of the first mode to get S_a (spectral acceleration), used to describe the capacity curve of the resulting ESDOF, as described in ATC-40 (ATC-40, 1996) and FEMA-440 (FEMA-440, 2005) . The properties of the ESDOF model correspond to the properties of the first mode of vibration of the three-storey structure. The ESDOF acceleration S_{a-cap} and displacement S_{d-cap} are calculated as:

$$S_{a-cap} = \frac{V_{b-po}}{M_1^* g} \quad (3.1)$$

$$S_{d-cap} = \frac{\Delta_r}{\Gamma_1 \phi_{1-r}} \quad (3.2)$$

Where V_{b-po} is the total base shear from the pushover analysis of the three-storey model, M_1^* is the effective modal mass of its first mode, g is acceleration due to gravity, Δ_r is the displacement of the roof, Γ_1 is the modal participation factor of the first mode and ϕ_{1-r} is the roof displacement in the first mode. The modal participation factor and effective modal mass of the first mode of the model are calculated as below, where m_i is the mass of storey i , N is the number of storeys and ϕ_{i-1} is the displacement of storey i in the first mode.

$$\Gamma_1 = \frac{\sum_{i=1}^N m_i \phi_{i-1}}{\sum_{i=1}^N m_i \phi_{i-1}^2} \quad (3.3)$$

$$M_1^* = \frac{(\sum_{i=1}^N m_i \phi_{i-1})^2}{\sum_{i=1}^N m_i \phi_{i-1}^2} \quad (3.4)$$

Commercial and industrial wood typology (W3)

For commercial and industrial wood construction (W3), the height restriction was up to 4 stories until 2016, and with BCBC 2016 the height limit was increased up to 6 storeys. However, the number of commercial six-storey W3 buildings are negligible, if any. The distribution of commercial and industrial wood construction per number of stories in Vancouver is shown in Figure 3.10. So, median W3 built before 1990 are modeled in OpenSees for 2 storeys and those built after 1990 as 3 storeys, with storey height of 3.0m.

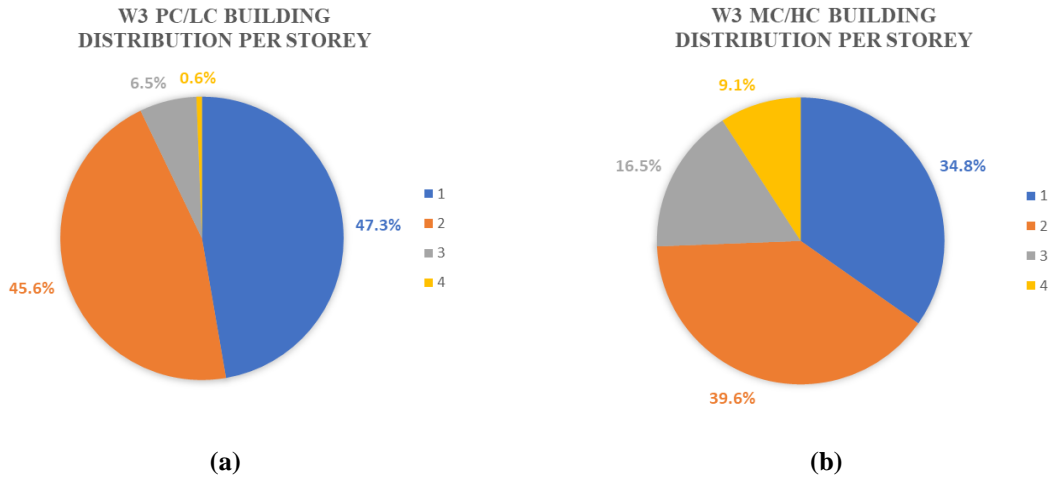


Figure 3.10 Distribution of W3 buildings per number of stories in the City of Vancouver.

Low-rise residential wood typology without cripple wall or subfloor (W1)

Low-rise residential wood constructions without cripple wall or subfloor (W1) among the BC building stock has an average of 2 stories, across different design code levels (Figure 3.11).

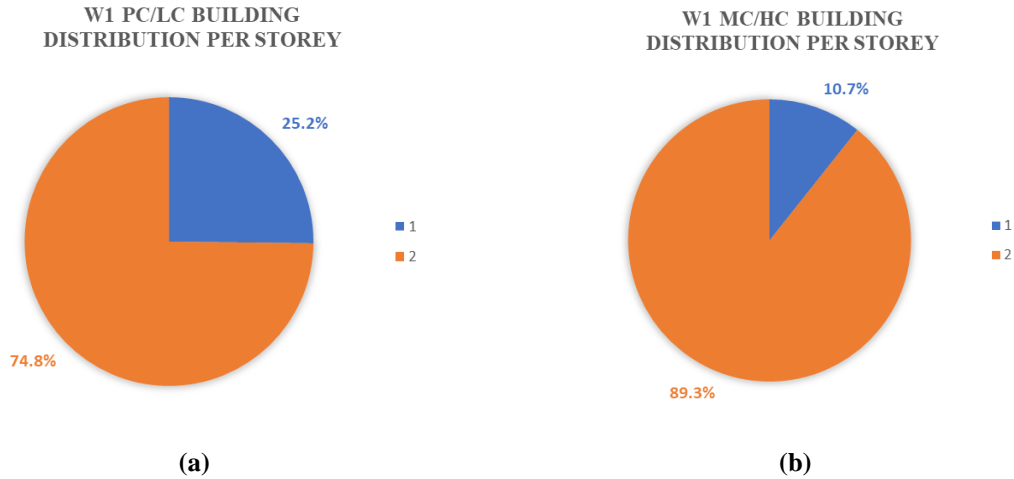


Figure 3.11 Distribution of W1 buildings per number of stories in the City of Vancouver.

For W1, the ESDOF characteristics are determined from a two-storey model developed in OpenSees, with storey height of 3.0m, as shown in Figure 3.12 and Figure 3.13. As explained before, the two-storey median building model has its shear spring properties at each floor derived from the single storey backbone properties provided by FPI innovations.

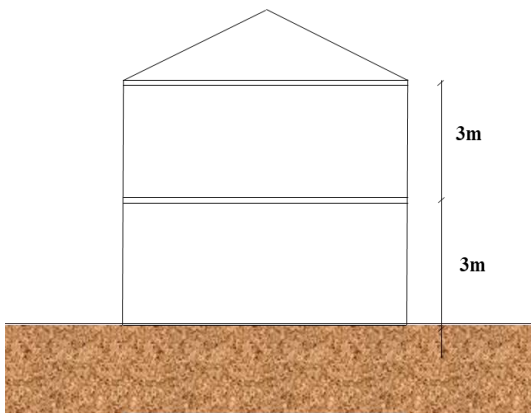


Figure 3.12 Schematic for two storey W1-PC

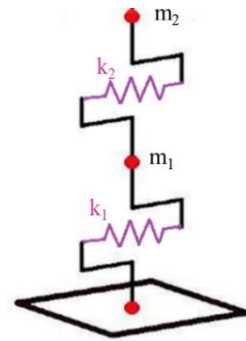


Figure 3.13 Analytical model for W1-PC LFRS developed in OpenSees

Low-rise residential wood construction with cripple wall (W4c)

Cripple walls are shorter than the wood frame walls of the upper storeys, varying from about 0.6m to 1.8m. FPI Innovations recommended the use of a 1.0m cripple wall for modelling purposes in BC. To derive the ESDOF properties for W4c, the models are developed as having 2 stories of 3.0m each, over a 1.0m cripple wall, as shown in Figure 3.14. The cripple wall properties used in this study are derived from the PO curve results from the CUREE-Caltech Wood frame Project (CUREE W-17, 2002), reproduced in Figure 3.15. Figure 3.15 documents the pushover curve for a two-storey residential building resting over a 2ft (0.6096 m) cripple wall of 12ft length. It is assumed that a gravity compression of 450 lbs/ft is applied over the length of the cripple wall (about 1200 kg per floor). The ultimate displacement of the cripple wall is 7.2cm, equivalent to about 12% drift. For the 1.0m cripple wall, the displacements are adjusted to maintain the same drift ratio as the 2ft cripple wall.

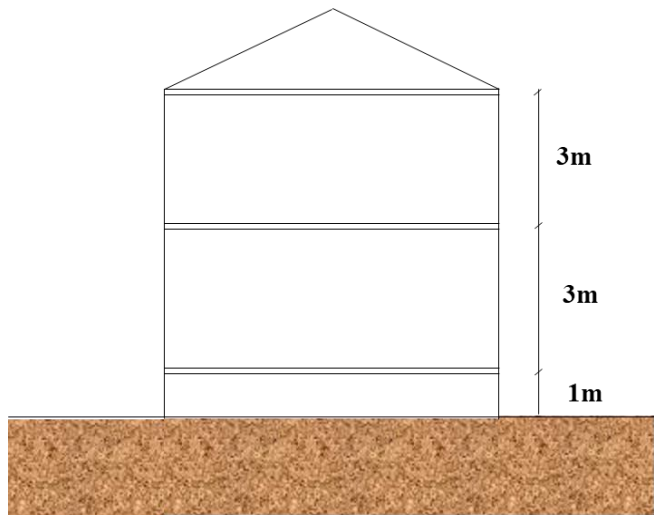


Figure 3.14 Schematic for two storey house with 1m cripple wall

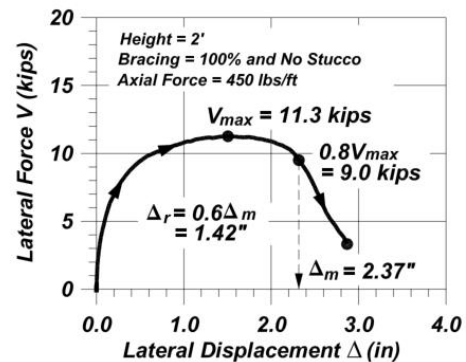


Figure 3.15 Reference displacements from monotonic test: 2ft cripple wall (CUREE W-17, 2002)

Low-rise residential wood construction with sub-floor (W4s)

As per the BCBC 2018, sentence 9.10.8.9, in terms of height and occupancy, a crawl space is considered a basement if it exceeds 1.8m in height between the floor bottom and the ground or is used for any occupancy. As such, to derive the ESDOF properties for W4s, the models are developed as having 2 stories of 3.0m each, over a 1.8m subfloor, as shown in Figure 3.16. Built as part of the superstructure, the wood part of the basement floor is assumed as well-designed, like the floors above it.

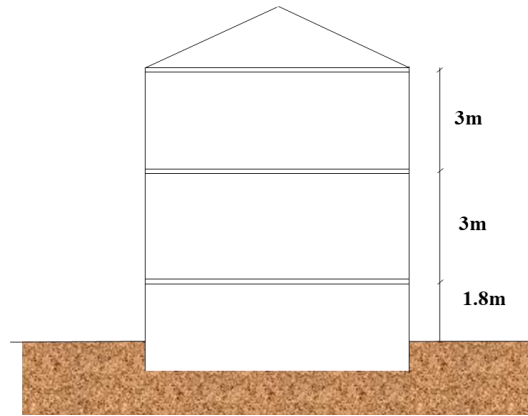


Figure 3.16 Schematic for two storey house with 1.8m subfloor above grade

3.3.2 Development of crustal and subduction fragility functions

Crustal and subduction ground motions vary in their duration and frequency content. This contributes to the varying structural responses from structures subjected to such ground motions. It is not easy to separate the effect of duration from other ground motion characteristics while developing fragility functions. This difference in spectral shape and duration is implicitly accounted for within the crustal and subduction ground motion suites used in this study.

In IDA, each selected ground motion is typically linearly scaled to increasing levels of intensity, approaching collapse conditions. Since this linear scaling process will not affect the

spectral shape and significant duration of the ground motions, IDA is used to develop the different fragility functions, while investigating possible effects of duration from within the subduction functions. The 5% damped spectral acceleration at a period of interest, $S_a(T)$, is chosen as the intensity measure (IM). This is because $S_a(T)$ is most widely used, has readily available GMPEs, is efficient enough for use when large part of the portfolio is made of older deficient buildings (D'Ayala et al., 2015) and because the structural response of each building in the portfolio is represented by reducing it to the structural response of an equivalent SDOF. The structural response of the ESDOF is observed via its maximum displacement. A lognormal cumulative distribution function is generally used to define a fragility function. The cumulative probability of occurrence of the damage equal to or higher than the specified damage state threshold is given as Equation 3.5

$$P(D \geq ds | IM = x) = \Phi \left[\frac{\ln(x/\theta)}{\beta} \right] \quad (3.5)$$

where $P(D \geq ds | IM = x)$ represents the probability that a ground motion with $IM = x$ will cause a structure to reach damage state “ds” or higher; $\Phi[\quad]$ is the standard normal cumulative distribution function; θ is the median value of the probability distribution and β is the standard derivation of $\ln IM$.

In this study, the initial versions of fragility and vulnerability functions were developed using the RMTK (Risk Modeller's Toolkit) (Silva et al., 2017) developed by the GEM Foundation. Within the RMTK, Monte Carlo sampling was used to create multiple (150) equivalent SDOF systems (defined around the median) which are representative of the Vancouver building stock, to account for the building-to-building variability (Villar-Vega et al., 2017) . Then, IDA were carried out on them, using the representative ground motions suites (crustal and subduction) for

Vancouver. Based on the four damage limit thresholds defined, the structures were assigned damage states depending on their structural response (engineering demand parameter (EDP)). These results were recorded into a damage probability matrix (DPM) and a simple regression analysis was carried out to calculate the mean and standard deviation of the cumulative log-normal distribution i.e., fragility curves that relate a ground motion intensity measure to probability of exceedance of a damage state. However, the computational time required to create the fragility functions for each typology is large.

As such, the fragility and vulnerability functions recorded in this dissertation are developed using the source code of VMTK (Vulnerability Modeller's Toolkit) developed by GEM (Martins et al., 2021), modified to suit the requirements of this work. It is used in the current study to ease time and computation limitations. Within the VMTK, representative SDOF models for median buildings of each BC building typology is defined and subjected to IDA, developed from appropriate ground motions suites. From these structural analyses, the VMTK develops a distribution of EDP vs. IM levels, using which, fragility functions are developed using the cloud analysis approach proposed by Jalayer et al., (2015). Then, a censored regression analysis (Stafford, 2008) is carried out, based on a defined EDP threshold (i.e., maximum displacement or acceleration). This process is detailed in (Martins & Silva, 2020).

3.3.2.1 Representative models

Owing to the recurring loading and unloading cycles, ground-motion duration impacts the structural strength and stiffness, accumulating damage and affecting the peak response of the structure in turn. On modelling cyclic degradation within the SDOF model, the damage (and resulting degradation) that accumulates as the SDOF is loaded, unloaded, and reloaded cyclically

is accounted for. Cyclic degradation includes both strength and stiffness degradation. Strength degradation refers to the structure's loss in ability to resist peak loads after multiple cycles of damage. Stiffness degradation refers to the structure's loss of stiffness due to multiple cycles of damage. Within the OpenSees framework, the *Pinching4* material model considers unloading, reloading, and strength degradation, using a pinched backbone curve to replicate structures which display a pinching behavior (Ab-Kadir et al., 2014; Mohammad Noh et al., 2017; Shen et al., 2013) and uses energy (area under the force-displacement curve) or cycles (total number of loading/unloading cycles) to define damage.

In this study, the capacity of the typical median structure of each BC building typology is defined through a multilinear backbone curve (Martins et al., 2021) that characterizes the representative SDOF model, introduced in its ADRS (acceleration-displacement response spectrum) format. The nonlinear behavior of the SDOF is modelled using a *Pinching4* uniaxial material to simulate the hysteretic behavior and capture strength and stiffness degradation under the imposed cyclic loading. The load-deformation response envelope within the *Pinching4* model is defined through the capacity curve of the representative SDOF model. The implementation of degradation follows `simpleSDOF4.tcl` by Vamvatsikos (2011) adopted within the VMTK, accounting for cyclic degradation as reloading stiffness degradation, unloading stiffness degradation, and strength degradation. These parameters are tabulated in Table 3.5. Further explanation of these parameters is provided in Appendix B.

Table 3.5 Pinching4 material model parameters accounting for cyclic degradation (Vamvatsikos, 2011)

Constant	Value	Constant	Value	Constant	Value	Constant	Value
gK1	0.00	gD1	0.00	gF1	0.00	gE	10.00
gK2	0.10	gD2	0.10	gF2	0.40	rDispP/ rDispP	0.50
gK3	0.00	gD3	0.00	gF3	0.00	rForceP/ rForceP	0.25
gK4	0.00	gD4	0.00	gF4	0.40	uForceP/ uForceP	0.50
gKLim	0.20	gDLim	0.20	gFLim	0.90		

3.3.2.2 Damping

The total damping in a system includes hysteretic damping and elastic damping. The hysteretic damping is activated in the NLTHA from the hysteresis model used to model the structure's behavior. Studies have shown that the damping of concrete structures decreases as height increases (Cruz & Miranda, 2017). For low-rise concrete shear wall structures (say median building height ~10m) and mid-rise concrete shear wall structures (say median building height ~20m), a damping of 5.0% is assumed. For high-rise concrete shear wall structures (say median building height ~60m), a damping of 3.0% is assumed. For wood structures, a damping of 5.0% is assumed, except for commercial wood buildings, where a damping of 3.0% is assumed, owing to the large open spaces, and reduced mass of the structures.

3.3.2.3 Ground motion sets used

The SDOF defined in section 3.3.2.1 is subjected to NLTHA in the form of IDA, within the VMTK to determine its structural response. The characteristic features of the ground motions that affect structural response include ground motion intensity, frequency content of the ground motion and duration of shaking.

The primary focus of this study is to develop hazard-consistent subduction and crustal fragility and vulnerability functions that can be used for RSRA studies in BC. Therefore, it is required to develop hazard-consistent crustal and subduction ground motion record suites, to develop corresponding fragility and vulnerability functions, which are necessary to study the effect of subduction ground motions on RSRA in BC. Long duration is a characteristic feature of large magnitude ground motions originating from subduction tectonic sources like the Cascadia Subduction Zone. Because the BC sites are far from the subduction sources, and predicted to be subjected to large magnitude events, we expect that most of the subduction ground motions would have a long duration of shaking. As such, the fragility and vulnerability functions are expected to reflect the effect of long duration ground motions characteristic of the crustal and subduction ground motions in BC.

The primary selection criterion for ground motion selection is the tectonic region type of its source: Crustal vs. Subduction. This criterion leads towards developing crustal and subduction fragility and vulnerability functions for BC-specific building typologies. Recognizing that the database for subduction events is limited, the secondary criterion set, is that the suite of subduction ground motions will include majority of characteristic long duration subduction ground motions. Similarly, the suite of crustal ground motions will include majority of characteristic short duration crustal ground motions. In other words, this work studies the effect of subduction ground motions on RSRA in BC, with the consideration that majority of such ground motions have a long duration.

The criteria for selecting the ground motion suites for this study were set as:

1. The ground motions are selected primarily based on the tectonic region type of its source (subduction source vs. crustal source).

2. Not more than 10% of the ground motions within the subduction ground motions suite should qualify as short duration. Similarly, not more than 10% of the ground motions within the crustal ground motion suite should qualify as long duration.
3. Use D_{5-95} of 30s (Pan, 2018) to distinguish between short and long duration ground motions.

The IDA ground motion sets used in this study are developed from the crustal and subduction ground motion record suites developed as part of the SRG3 (Seismic Retrofit Guidelines 3rd edition) project (Bebamzadeh et al., 2015). The SRG3 implements the 2015 GSC seismic hazard model, and uses the conditional spectra (CS) for record selection and scaling of an appropriate set of ground motion records to match corresponding mean and variance of the developed CS (SRG3, 2016). Further details on the procedure followed to develop the ground motion suites are documented within Appendix O of the SRG3 report (SRG3, 2016).

This catalogue of ground motion records includes crustal, subcrustal and subduction earthquakes that are selected to match the geophysical parameters (distance, depth, magnitude, and site conditions) for the crustal, subcrustal and subduction sources contributing to seismic hazard at the site of interest respectively. The range of these determining parameters are chosen based on seismic hazard deaggregation results obtained at the sites of interest. Since mean spectral values and their variance also has to be matched when selecting records to match a CS, appropriate record-to-record variability is accounted for (NEHRP, 2011) and can be used for development of fragility and vulnerability functions for RSRA, for a portfolio of structures.

3.3.2.3.1 Crustal ground motion suites

From deaggregation results for Vancouver and Victoria conducted as part of SRG3, it is seen that crustal events occurring close to the surface (less than 30km deep) with magnitudes ranging from ~5.5-7.5, at distances of about 80km or less contribute towards seismic hazard at the two sites. These parameters were used to select crustal ground motion records in SRG3. SRG3 documents two crustal ground motion suites each for Vancouver and Victoria, one conditioned at 0.5s, and another at 1.0s. These ground motion records are summarized in Appendix C. The SRG3 crustal ground motion suite for Vancouver conditioned at 1.0s and its mean is shown in Figure 3.17. Other crustal ground motion suites are documented within Appendix O of the SRG3 Report (SRG3, 2016).

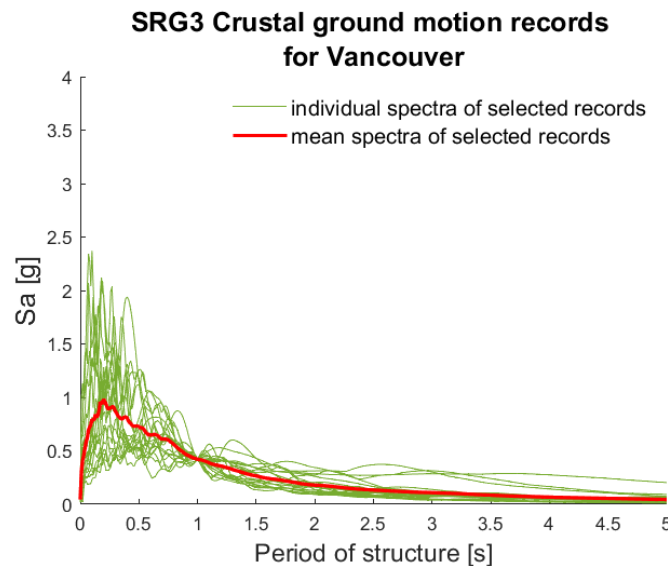


Figure 3.17 Crustal ground motion records for Vancouver (Bebamzadeh et al., 2015)

3.3.2.3.2 Subduction ground motion suites

From deaggregation results for Vancouver and Victoria conducted as part of SRG3, it is seen that subduction events occurring at depths less than 50km, with magnitudes greater than 8.0,

at distances of about 50 to 250km, contribute towards seismic hazard at the two sites. These parameters were used to select subduction ground motion records in SRG3. SRG3 documents two subduction ground motion suites each for Vancouver and Victoria, one conditioned at 0.5s, and another at 1.0s. These ground motion records are summarized in Appendix C. The SRG3 subduction ground motion suite for Vancouver conditioned at 1.0s and their mean is shown in Figure 3.18. Other subduction ground motion suites are documented within Appendix O of the SRG3 Report (SRG3, 2016).

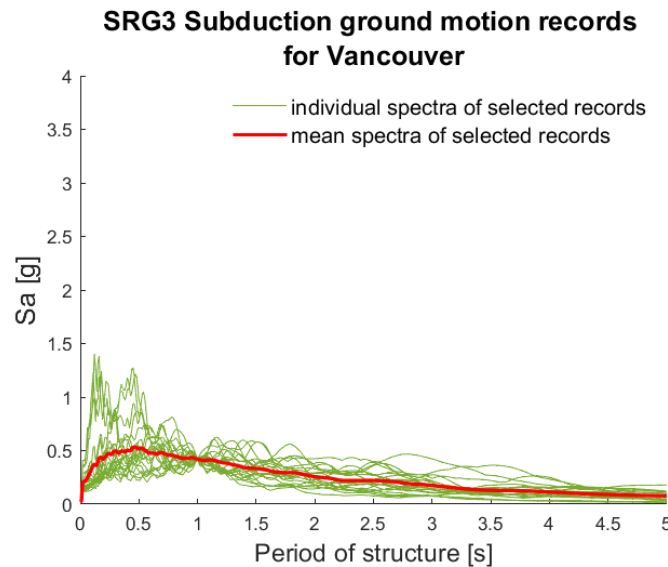


Figure 3.18 Subduction ground motion records for Vancouver (Bebamzadeh et al., 2015)

Figure 3.19 compares the mean of the crustal and subduction ground motion suites, conditioned at the 0.5s and 1.0s to the UHS at Vancouver for NBCC 2015. Such a comparison for the other ground motion suites used in this study is documented in Appendix O (SRG3, 2016).

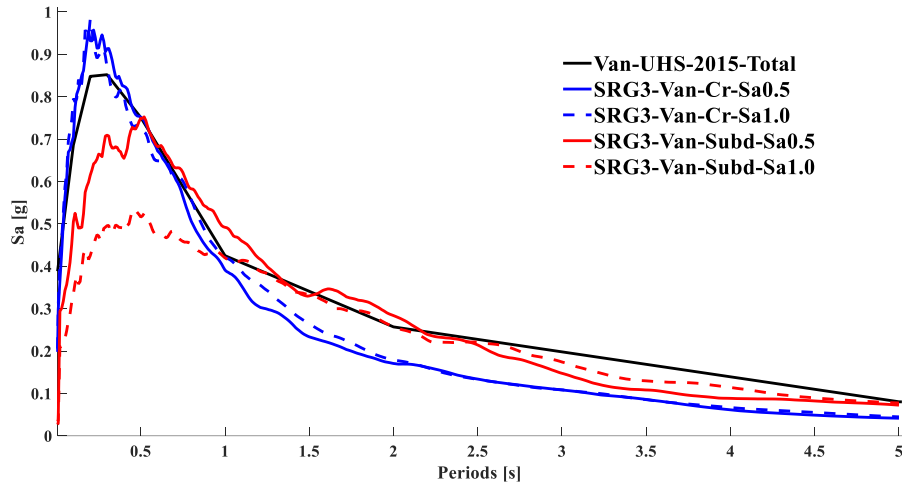


Figure 3.19 Comparison of the mean of the SRG3 crustal (Cr) and subduction (Subd) ground motion suites to the 2% in 50 years Vancouver site class C UHS (2015)

3.3.2.3.3 Duration characteristics of the ground motion suites

The duration of a ground motion record depends on the characteristics of the tectonic region type of the source from which the event originates, and increases with the distance of the recording site from the source, due to the scattering and dispersion of seismic waves along its travel path. While duration of a ground motion record depends on the soil conditions at the source, it also depends on soil conditions at the recording site. Ground motion records from large subduction interface events at sites far from the source typically have longer durations and more energy than those from close, small magnitude crustal events, more so, if the site is on soft soil (due to repeated seismic wave reflections within the softer layers).

Many intensity metrics are documented within literature to quantify the duration of a ground motion record (reference). Fairhurst (2021) reports that the best metrics for the SDOF hysteretic models were the specific energy density and 5-95% significant duration. It concluded that duration metrics obtained from integration of the length of a time history are most correlated with the collapse of the SDOF model, independent of the hysteretic model considered, as long as

cyclic degradation is accounted for in the numerical model. Because there is no fixed consensus on what duration metric should be used to define a ground motion record as long or short, Specific Energy Density (SED) and Significant Duration are considered in this study due to their better correlation with the response of SDOF systems (Fairhurst, 2021).

Specific Energy Density (SED) is the integral of the square of the velocity of the record, calculated over the record length. It is calculated as:

$$SED = \int_0^{t_{max}} v(t)^2 dt$$

where v is the velocity of the record and t_{max} is the record length. Significant Duration is the time interval over which a specified amount of energy in the ground motion record is accumulated. In this setting, energy is calculated as the integral of the square of the acceleration (normalized Arias Intensity): $\int a^2 dt$. Significant duration is usually calculated over ranges of 5 to 95% (D_{5-95}) and 5 to 75% (D_{5-75}). This study will use D_{5-95} .

Since there is no consensus on what defines long duration, this study chooses to classify long duration ground motions as those with $D_{5-95} > 30s$ (Pan, 2018). Rather than studying individual ground motion duration characteristics, this study focuses on the characteristics of the suites as a whole.

Figure 3.20 shows the distribution of significant duration of the ground motions, across all relevant magnitudes for the crustal and subduction ground motion records suites developed for Vancouver, conditioned at 1.0s. The figure shows the mean D_{5-95} of the crustal and subduction ground motion suites. The ground motions not conforming to the criteria set for long and short duration ground motions in terms of D_{5-95} are emphasized as: the blue points are crustal ground

motions with $D_{5-95} < 30s$, the magenta points are crustal ground motions with $D_{5-95} > 30s$, the black points are subduction ground motions with $D_{5-95} > 30s$ and the red points are subduction ground motions with $D_{5-95} < 30s$. This representation of the scatter plot is followed in Figures 3.20, 3.21 and 3.22.

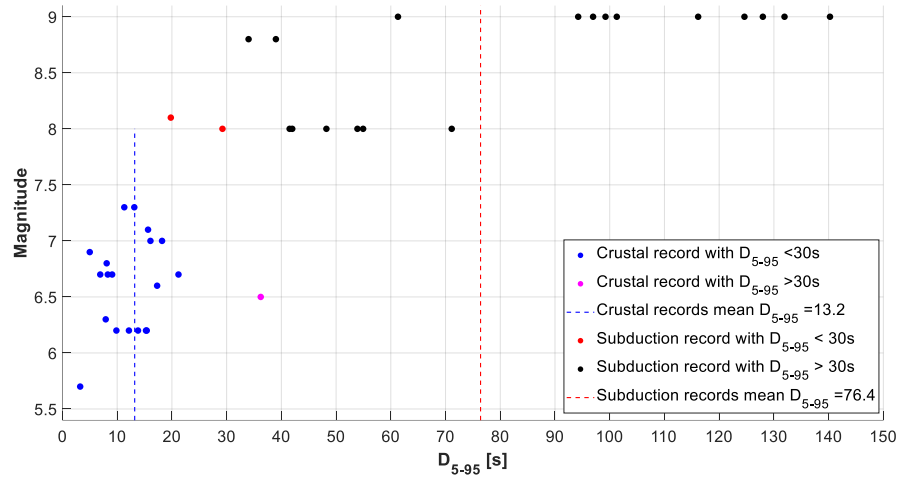


Figure 3.20 Distribution of D_{5-95} of the records in the Vancouver crustal and subduction ground motion suites conditioned at 1.0s, across relevant magnitudes.

Next, the distribution of SED - for each record within the crustal and subduction ground motion records suites developed for Vancouver, conditioned at 1.0s - is studied against corresponding significant duration of the record (Figure 3.21).

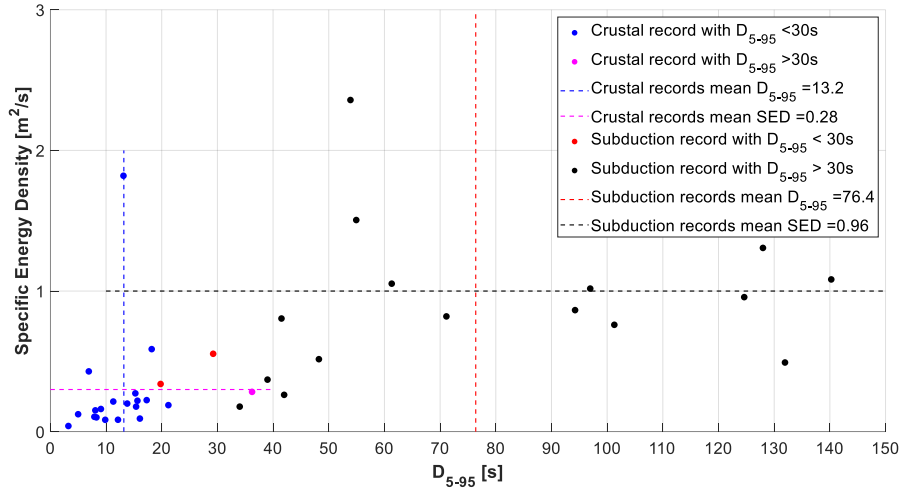


Figure 3.21 Plot of D_{5-95} vs. SED of the records in the Vancouver crustal and subduction ground motion suites conditioned at 1.0s

To understand the implications of D_{5-95} in the context of parameters like SED, the distribution of D_{5-95} vs. SED of the ground motions, across all relevant magnitudes within the crustal and subduction ground motion suites developed for Vancouver, conditioned at 1.0s is also plotted (Figure 3.22).

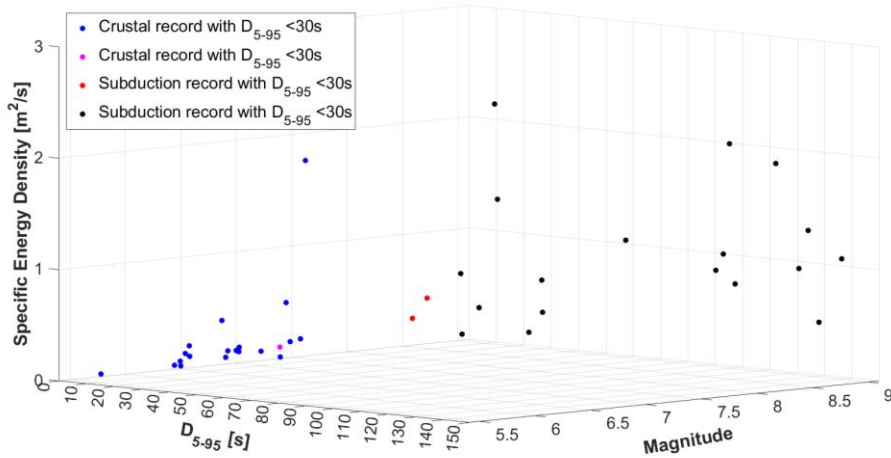


Figure 3.22 Distribution of D_{5-95} vs. SED of the records in the Vancouver crustal and subduction ground motion suites conditioned at 1.0s, across relevant magnitudes.

It is seen from Figures 3.20-22 that the Vancouver crustal ground motion suite has one record that is greater than 30s (36.2s) — the Imperial Valley earthquake (M6.5) of 1979. The Vancouver subduction ground motion suite has two records that are less than 30s (19.8s and 29.2s). As for the two subduction ground motion records with $D_{5-95} < 30$ s their response spectra shows that there is a significant demand in the long periods. So, these records are accepted as valid for my analysis. The subduction record with D_{5-95} of 19.8s is from the Michoacan Earthquake (M8.1) of 1985 of total record length of 62s long with many cycles of low amplitude.

The mean D_{5-95} and SED of the crustal and subduction ground motion suites developed for Vancouver and Victoria are tabulated in Table 3.6.

Table 3.6 Summary of the mean D_{5-95} and SED of the crustal and subduction ground motion suites

Site	Conditioning Period [s]	Tectonic Region Type	Mean D_{5-95} [s]	Ratio of D_{5-95}	Mean SED [m2/s]	Ratio of SED
Vancouver	0.5	Crustal	11.20	5.30	0.23	4.20
		Subduction	59.10		0.96	
	1.0	Crustal	13.20	5.80	0.28	3.40
		Subduction	76.40		0.96	
Victoria	0.5	Crustal	11.70	4.80	0.44	4.50
		Subduction	55.70		1.96	
	1.0	Crustal	11.80	4.80	0.70	2.80
		Subduction	56.10		1.97	

Although the criteria for long duration definition was set as 30s or higher and there are two outliers within the subduction suite, on evaluating the whole suite of records, the D_{5-95} of the subduction suite exceeds 76s, which meets the criteria set. Similarly, for the crustal suite, the D_{5-95} value is around 13s meaning that the suite is primarily made of short duration records. From the

SED value for the Vancouver crustal and subduction ground motion suites conditioned at 1.0s, it is seen that the crustal suite has a mean SED of 0.28 m²/s and the subduction suite, a mean SED of 0.96 m²/s. The ratio of SED between the subduction and crustal ground motion suites is 3.4, depicting a clear difference in the SED characteristics of the ground motion suites.

It is reported that when considering the ratios between the mean significant duration of long- and short-duration ground motion record suites, even at values as low as 1.40, the effect of duration is found to be significant and obvious (Du et al., 2020). From Table 3.6, the ratio of D_{5-95} between the subduction and crustal ground motion suites is 5.8. As such, noticeable effects of duration on the nonlinear structural performance of the SDOFs are expected between the subduction and crustal ground motion suites. This effect of duration will translate into the resulting fragility and vulnerability functions. Similar studies were done on the other crustal and subduction ground motion suites developed within the SRG3, and is recorded in Appendix C.

3.3.2.4 EDP and damage limit thresholds

An Engineering Demand Parameter (EDP) is a measure of structural response that is used to assess the damage of a structure. This study uses spectral displacement as the EDP used to assign structural and non-structural drift sensitive damage states to the SDOF models. Spectral acceleration is chosen as the EDP used to assign contents and non-structural acceleration sensitive damage states to the SDOF models.

Based on the damage limit thresholds (defined in terms of spectral displacement), damage states are assigned to the SDOFs, based on its structural response under a NLTHA. Five damage states are assigned to the structure, based on four EDP thresholds that are defined, and a single definition of damage states is used per typology. In this study, while the definition of the damage

states follows HAZUS definitions, explained in Appendix A (A.3), the damage limit thresholds used to allocate the damage states, are defined differently. In this study, the damage limit thresholds defined are tied to the capacity curves, and are set as factors of the ultimate displacement (Sd_u) and the yielding displacement (Sd_y), of the corresponding building typology (Martins & Silva, 2020). The damage to structural components in a building during a seismic event is assumed as being displacement-sensitive. The slight damage threshold (DS1) is selected as Sd_y (Spectral displacement at the yield point). This is because, before reaching Sd_y , the structure only undergoes elastic deformation without significant damages. The complete damage (DS4) threshold is designated as Sd_u (spectral displacement at ultimate point). Two equally-spaced points between DS1 and DS4 are selected as moderate damage threshold (DS2) and extensive damage state (DS3).

The slight damage (DS1) threshold is identified as Sd_y on the global capacity curve (Lagomarsino & Giovinazzi, 2006). For concrete structures in BC built after 1990, the DS1 is chosen as the starting point of the inelastic deformation plateau. This is because, these concrete shear wall structures built after 1990 are designed according to strict code that usually control the usability of structure. Also, the capacity curves for C2-MC and C2-HC buildings are very conservative in terms of drift capacity, and there is larger inherent ductility in the concrete shear wall system. As such, assuming slight damage to occur at 0.2% drift is too small and a higher drift was assumed (displacement at which inelastic deformation starts), since these buildings are expected to perform better and thus show lower damage in an early stage. The spectral displacement at the four damage state thresholds used by GEM and in this study is tabulated in Table D.1. for C2 typologies and in Table D.2 for wood typologies.

3.3.2.5 Development of fragility functions

The VMTK utilizes the cloud analysis approach to derive fragility curves, where a best fit curve, whose parameters are calculated based on a censored regression method, is defined between the log of an intensity measure (IM) and log of an EDP.

When developing fragility and vulnerability curves in the VMTK, the record-to-record variability was introduced in the process through the ground motion suites used for the NLTHA. The building-to-building variability is accounted for by adding to the record-to-record variability (σ_{rr}), a building-to-building variability (σ_{bb}) of 0.3 according to Equation 3.5.

$$\sigma_{total} = \sqrt{(\sigma_{rr}^2 + \sigma_{bb}^2)} \quad (3.5)$$

The fragility and vulnerability curves are developed for Sa (0.3s), Sa (0.6s) and Sa (1.0s). The period assignment -between 0.3s, 0.6s or 1.0s - is chosen in such a way that the optimal time period (time period where the correlation to damage is highest) of the building typology is closest to one of the three periods. This was done to reduce the periods at which ground motion fields are developed within the OQ during scenario analysis and RSRA.

3.3.2.6 Limitations

Limitations regarding the choice of structural models, ground motion suites used and choice of EDP are discussed in this section.

3.3.2.6.1 Choice of structural models

The SDOF model is a less accurate representation of a 3D structure and assumes that higher vibration modes are irrelevant to the seismic response of a structure. It is widely used when there is scarce information of the specific structural characteristics of a building that it does not justify the effort of detailed modelling. Though an SDOF is an inaccurate representation of individual

structures - especially those with plan and stiffness irregularities and high-rise structures - for portfolio damage and loss assessment (where information on all buildings is not available, or is enormous and requires comprehensive modelling), we can only draw a compromise between the scope of the output and the computational effort required. An ESDOF model as a representation of a median model of a building typology for portfolio risk assessment, has been proven to provide fairly good estimates of portfolio risk assessment. Adopting experience based simplified models that represents the probable dominant characteristics of a building typology is a practical way to approach portfolio risk assessment (D'Ayala et al., 2015).

Since the VMTK is meant to be a generalized method for all possible building typologies, irrespective of construction type, the SDOF model considered is a general model. This assumption has provided good estimates for scenario and regional risk assessment (validated and verified extensively by GEM Foundation in their many global projects) and because an appropriate model for different building typologies that inspired confidence do not exist currently in literature, it was decided to use the generic pinching4 model developed by Vamvatsikos (2011), which was found to be appropriate for use when a general building typology is defined. This model was deemed feasible for use in developing fragility and vulnerability functions for regional risk assessment studies, and has been proven to work (validated and verified extensively by GEM Foundation in their many global projects).

3.3.2.6.2 Choice of ground motion sets

To properly study the effect of ground motion duration, we require the development of ground motion suites that reflect the seismic hazard at the site, as well as the subjected duration characteristics. This means isolating the effect of duration from other ground motion

characteristics like amplitude and frequency content - in any tectonic context (both crustal and subduction). To solve this, it was suggested to isolate the effect of duration from the effects of ground motion amplitude and response spectral shape by developing sets of “spectrally equivalent” long and short-duration records (Chandramohan, 2016). This method has been implemented in many studies involving comparative nonlinear dynamic analyses (Chandramohan et al., 2013, 2016b; Fairhurst et al., 2019; Jafari et al., 2022; Pan et al., 2020) and fragility and vulnerability functions derivation. For site-specific, hazard-consistent analysis, the generalized conditional intensity measure approach (Bradley, 2010; Otárola et al., 2023) of selecting ground-motion records, where ground-motion duration and spectral shape is accounted for is yet another option. Future studies could consider the use of this method to study the effect of long duration ground motions on RSRA in BC. However, due to the unavailability of a comprehensive database for long duration subduction ground motions that could be used to develop seismic hazard consistent subduction fragility and vulnerability functions for BC were not available, a suitable criteria for subduction and crustal record selection was chosen.

3.3.2.6.3 Choice of EDP

Most of the experimental tests studied within (Hancock & Bommer, 2006) – a complete review on the effect of ground motion duration on structural damage - noted a high correlation between the number of loading cycles and structural damage. Numerical studies have shown that peak-based EDPs do not generally show a strong correlation with ground-motion duration (Cosenza et al., 2004; Iervolino et al., 2006) whereas cumulative-based demands (e.g., dissipated hysteretic energy) show a much stronger correlation with structural damage (Chai, 2005; Stephens & Yao, 1987). However, these results may be due to limitations in the numerical models used, which did not always properly account for cyclic strength and stiffness degradation. Recent studies

on structures conducted using OpenSees (Mazzoni et al., 2007) which employed advanced nonlinear modeling strategies, incorporating cyclic strength and stiffness degradation coupled with leaning PDelta columns, on the other hand, have reported a good correlation between duration and maximum response measure (Chandramohan et al., 2016b, 2016a; Raghunandan & Liel, 2013).

As such, spectral displacement and spectral acceleration obtained from NLTHA of the ESDOF representing the first mode of vibration are chosen as the EDPs for this study, while cyclic degradation is properly accounted for within the SDOF models, in reflection to the severity and the number of inelastic cycles the system could undergo. Because the results of this work are also meant to be used by NRCan in the development of the risk maps for BC, it was decided to use S_d and S_a as the EDPs, to be consistent with what is currently used by the GEM Foundation.

3.3.3 Development of crustal and subduction vulnerability functions

While fragility functions estimate the probability of damage exceedance, vulnerability functions estimate monetary loss ratio (structural, non-structural, contents) as a function of ground shaking intensity at a site. Vulnerability functions are developed from corresponding fragility functions as by multiplying the probabilities of the structure in each damage state -obtained from the fragility functions given IM- with the corresponding damage-to-loss ratios, and adding them together to get the loss ratio at each intensity level of ground shaking. This can be mathematically expressed as:

$$LR|IM = \sum_{i=1}^{nDS} P[DS = ds_i|IM] * cons_{ds_i} \quad (3.6)$$

Where $LR|IM$ is the mean loss ratio of the vulnerability functions at each intensity measure level, $P[DS = ds_i|IM]$ is the probability of structure being in structural damage state ds_i given IM, and $cons_{ds_i}$ is the damage-to-loss or consequence model for damage state ds_i , based on occupancy

class of the typology. Separate vulnerability functions are developed per building occupancy class to assign losses due to structural components and contents. For non-structural components, a single vulnerability function is developed per occupancy class by combining the acceleration sensitive and drift sensitive non-structural components vulnerability curves for each occupancy class.

3.3.3.1 Consequence models used to develop vulnerability functions

To ensure compatibility with the fragility model, the consequence models used in this study are developed from the existing models for the USA in the HAZUS technical manual (FEMA, 2014, 2020b), under the assumption that construction costs are similar in Canada and the US. The different consequence models provided in the HAZUS documentation are normalized for each occupancy class, such that the component (structural, non-structural or contents) repair cost for a building in DS4 would equal its full component replacement cost. That is, the building if estimated to be in DS4, would need to be torn down and rebuilt, including non-structural and contents elements in the building. It should be noted that the exposure model separately assigns the structural, non-structural and contents cost for each asset.

3.3.3.2 Structural vulnerability functions

Section 3.3.2 describes how fragility functions are developed in this study, with section 3.3.2.3 describing the damage limit thresholds used to assign structural damage states to the structure. Once the structural fragility functions are developed, they are combined with a structural consequence model (damage-to-loss model) to develop the structural vulnerability curves (Equation 3.6). The structural consequence model used in this study to develop structural vulnerability functions, is the structural repair costs ratio table tabulated in HAZUS, normalized

to the repair cost of the complete damage state. This structural consequence model is tabulated in Appendix D, section D.2.

3.3.3.3 Non-structural vulnerability functions

Non-structural damage to a building originates from damage to drift-sensitive non-structural elements and acceleration sensitive non-structural elements. Since the nonstructural drift-sensitive components start getting damaged before structural damages begins, the slight damage limit threshold for non-structural components is adjusted to start assigning damage states before the structure yields. DS1 (Slight Damage) is defined at $0.75S_{dy}$, while the rest of the damage thresholds are as defined for structural damage thresholds defined in section 3.3.2.3, and are used to develop corresponding fragility curves.

The consequence model used to develop the drift-sensitive non-structural vulnerability curves are provided in the drift sensitive non-structural repair costs tabulated in HAZUS, normalized to the repair cost of the complete damage state, as in Appendix D, section D.4.

To develop acceleration-sensitive non-structural fragility functions, the damage state thresholds for the acceleration-sensitive nonstructural elements are assumed as that recorded in Table 5.12 in HAZUS (FEMA, 2014), and is tabulated in Table 3.7.

Table 3.7 Floor acceleration limits to assign nonstructural damage states (source: HAZUS)

Seismic Design Level	Floor acceleration at the threshold of nonstructural damage (g)			
	DS1	DS2	DS3	DS4
HC	0.3	0.6	1.2	2.4
MC	0.25	0.5	1.0	2.0
LC	0.2	0.4	0.8	1.6
PC	0.2	0.4	0.8	1.6

The accelerations felt by the non-structural components are restricted to the maximum shear capacity of the building (i.e., once the SDOF reaches maximum shear capacity, the accelerations no longer increase with intensity of ground motion). As such, a structure might not be assigned higher damage states once its maximum shear capacity is reached. This is especially so for the BC building typologies- especially those built after 1990- which have a much lower shear capacity than corresponding structures in California (for which HAZUS has recommended the values tabulated in Table 3.7). Once the non-structural fragility curves are developed, to appropriately model the non-structural acceleration sensitive vulnerability functions, it is assumed that the structural damage state and acceleration-sensitive non-structural damage state are statistically independent. Then, the acceleration sensitive non-structural elements loss is accounted for within the total non-structural loss as ¹:

$$E[LR|IM]_{ns} = wt_{dr} * E[LR|IM]_{dr} + wt_{acc} * (P[DS4] + (1 - P[DS4]) * E[LR|IM]_{acc}) \quad (3.7)$$

Where $E[LR|IM]_{ns}$ is the combined loss ratio of the non-structural components and $E[LR|IM]_{dr}$ and $E[LR|IM]_{acc}$ are the loss ratio of the drift-sensitive and acceleration -sensitive

¹ Personal correspondence, Dr. Luis Martins, GEM Foundation

non-structural components respectively. wt_{dr} and wt_{acc} are relative economic value of drift-sensitive non-structural components, and acceleration-sensitive non-structural components as compared to the total economic value of all non-structural components, respectively, and $P[DS4]$ is the probability of the structure being in complete damage state. The consequence model used to develop the acceleration-sensitive non-structural vulnerability curves are provided in the acceleration-sensitive non-structural repair costs tabulated in HAZUS, normalized to the repair cost of the complete damage state. This is tabulated in Appendix D, section D.5. It is assumed that all acceleration-sensitive components are lost if the building is in DS4.

3.3.3.4 Contents vulnerability functions

The damage state threshold definitions for contents are the same as that for acceleration sensitive non-structural components explained in section 3.3.3.3. Once the contents fragility curves are developed, the contents vulnerability functions are appropriately developed by account for the fact that the contents in typologies with lower shear capacity never reach higher damage states, while the structure itself has collapsed, as² :

$$E[LR|IM]_{cts} = (P[DS4] + (1 - P[DS4]) * E[LR|IM]_{acc}) \quad (3.8)$$

Where $E[LR|IM]_{cts}$ is the updated contents loss ratio. The consequence model used is the contents damage ratios tabulated in table 15.5 of HAZUS, normalized to DS4, assuming that contents cannot be retrieved when building is in DS4. It is tabulated in Appendix D, section D.6.

² Personal correspondence, Dr. Luis Martins, GEM Foundation

3.3.3.5 Assumption of ‘collapsed’ condition

The HAZUS definitions for complete damage state for the different building typologies investigated in this study is recorded in Appendix A, section A.3. Of the buildings estimated to be in complete damage state, a fraction of them is expected to have collapsed. HAZUS definitions of damage states (Appendix A, section A.3) states that approximately 3% of the total area of low-rise residential and commercial and industrial wood in DS4 is expected to be collapsed. Similarly, approximately 13%, 10% and 5% of the total area of C2L, C2M, and C2H buildings in complete damage state is expected to be collapsed, respectively. Because OQ reports damages as aggregate damages, in this study, for all wood typologies, 3% of the wood buildings in DS4 is assumed as collapsed. Similarly, for C2L, 5%, C2M, 10% and C2H, 13% are the percentage of building assumed as collapsed, given the building is in complete damage (DS4).

3.3.4 Verification of vulnerability functions

Average annual (AAL) refers to the mean loss per year over a large enough time span, assessed due to direct seismic losses (structural and non-structural losses) to the building stock in the region of interest. The AAL normalized by the total asset replacement cost due to the region’s building stock is referred to as the average annual loss ratio (AALR). Calculating the AALR is a good way to go about an initial verification of the vulnerability functions, and implicitly, the fragility functions, to isolate overly vulnerable building typologies, and get a general idea of the relative vulnerability between the same. In a global study (Martins & Silva, 2020), the expected AALR for thirteen locations across USA, South America and Europe with distinct seismic hazard levels were calculated, and three locations with distinct seismic hazard levels Vienna (low seismicity: PGA between 0.08g and 0.13g), Lisbon (moderate seismicity: PGA between 0.2g and

0.35g) and Oakland (high seismicity: PGA between 0.55g and 0.9g) with a 10% probability of being exceeded in 50 years were compared as in Figure 3.23.

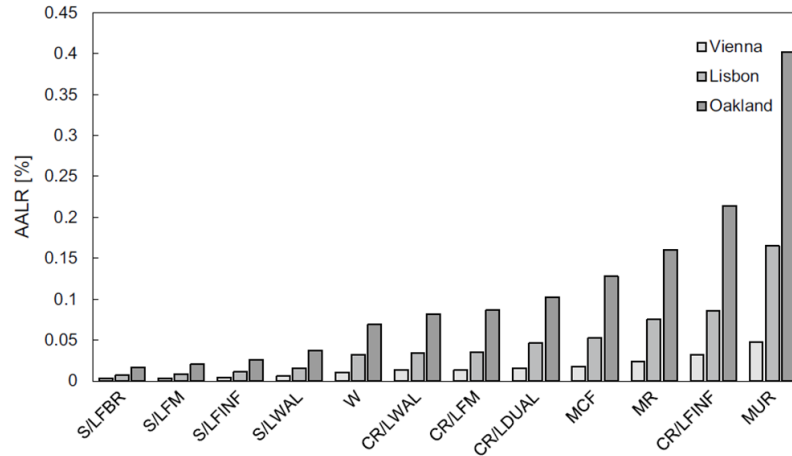


Figure 3.23 Comparison of AALR for prominent building classes in Vienna, Lisbon and Oakland (Martins & Silva, 2020)

GEM's Global Seismic Hazard map (Pagani et al., 2018; Pagani et al., 2020) depicts a geographical distribution of the Peak Ground Acceleration (PGA) with a 10% in 50 years probability of exceedance, for reference rock conditions around the world. This map combines existing national and regional probabilistic seismic hazard models and those developed by GEM, and was used to check the similarity in seismic hazard between Vancouver and the three locations above. Of the three locations, the intensity of seismic hazard in Lisbon looks most similar to Vancouver - both being in moderate seismic zones (Figure 3.24).

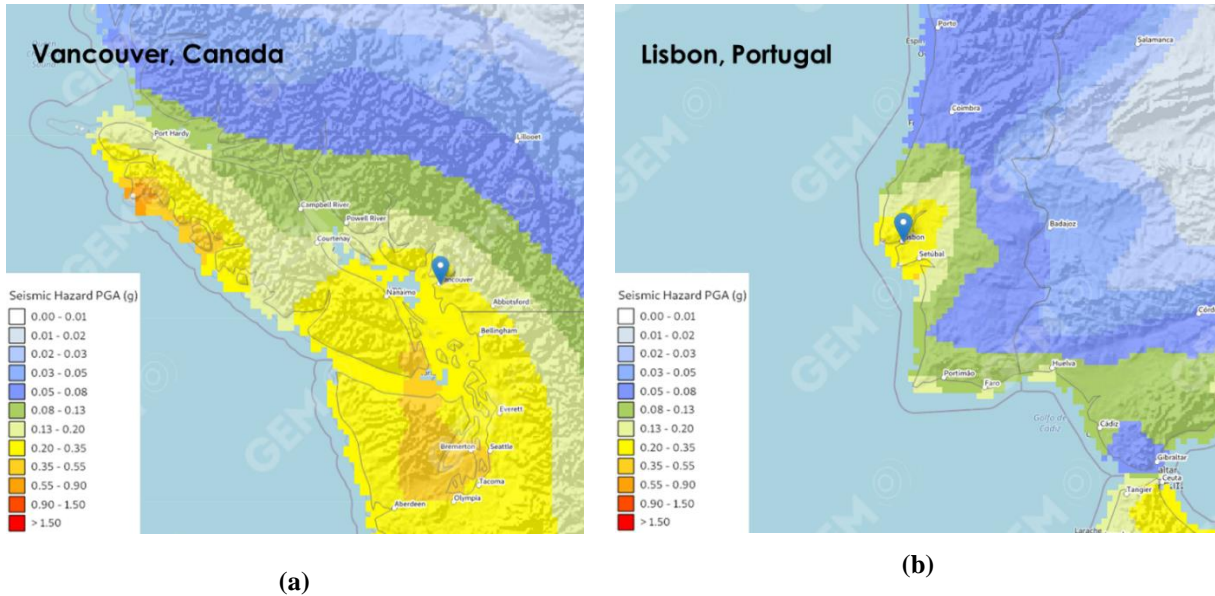


Figure 3.24 Seismic hazard obtained from GEM's Global Seismic Hazard (a) Vancouver (b) Lisbon [Source: (Pagani et al., 2018)]

Using the values of AALR seen at Lisbon as a reference, for wood construction AALR slightly higher than 0.03% is seen, for Concrete shear wall structures, an AALR of about 0.04% is noted and for URM, a high AALR is seen, of almost 0.16%. From studies across the world of every possible typology, it was seen that the worst case of AALR seen for the worst possible construction at a high seismic site should still be less than 1% (Martins & Silva, 2020).

Keeping these figures in mind, two OQ event-based regional risk assessment is run using the 2015 GSC seismic hazard model for Canada, at Vancouver for the building typologies of interest (C2 and Wood), for an investigation time of one year. The first run will use the GEM vulnerability functions and the second run, the BC-specific vulnerability functions. It is assumed that the contribution from structural and non-structural (acceleration and drift sensitive components) loss toward total repair costs of the building is equal, to calculate the AALR per building typology. The AALR at Vancouver for the BC building typologies, obtained when using

both the GEM vulnerability functions and the BC-specific vulnerability functions will be compared to values obtained in Lisbon, to verify the vulnerability functions and indirectly, the fragility functions.

3.4 Scenario Analysis

To understand urban seismic risk, develop immediate earthquake response plans, seismic policy development, earthquake mitigation plans and retrofitting strategies, the city of Vancouver uses three earthquake scenarios in the city's seismic exercises. Of the three, the subduction and crustal scenarios used are the Cascadia Subduction zone 'megathrust' earthquake of magnitude 9.0 (CSZ9.0) and the Georgia Strait shallow crustal earthquake of magnitude 7.3 (GSM7.3), respectively. These scenarios, developed in OQ by NRCan, were shared with the author.

These two scenarios will be analyzed for the city of Vancouver, to check the reasonability of the developed fragility and vulnerability curves. The changes brought in the scenario analyses on modifying the representative BC building typologies, introducing new building typologies, modifying the damage limit thresholds and updating the definition of loss functions is studied.

3.4.1 Crustal scenario: Georgia Strait shallow crustal earthquake M 7.3 (GSM7.3)

For the shallow crustal earthquake scenario, a rupture of the Georgia Strait, with its hypocenter around 30 km west of Vancouver, off the coast, at a depth of 5 km is modelled using a simple fault geometry. This rupture has a length of about 40 km on the Strait of Georgia could produce a seismic event of magnitude 7.3 or higher. OQ implements the ground motion models (GMM) of the 5th generation seismic hazard model of Canada (Allen et al., 2017; Allen et al., 2020; Halchuk et al., 2014), used in the NBCC 2015, as a GMPE table. The GMPEs used to develop this western crustal scenario in OQ are described as in (Atkinson & Adams, 2013), with

additional modifications made for NBCC 2015. Being an active shallow fault, Table 3.8 summarizes the GMPE models and weights used to predict ground shaking intensity due to the assumed rupture, which is then used to determine damage states of buildings on respective sites.

Table 3.8 GMPEs and weights used in GSM7.3 scenario analysis

GMPE model	weight
NBCC2015_AA13_activecrustFRjb_low	0.2
NBCC2015_AA13_activecrustFRjb_central	0.5
NBCC2015_AA13_activecrustFRjb_high	0.3

The Georgia strait rupture produces very destructive levels of ground shaking due to its proximity to the City of Vancouver and shallow depth. Although a very rare event (occurring with a return period of about 10,000 years), since the epicenter is close to Vancouver, the GSM7.3 is likely to cause greater direct damages and losses to the city than a larger magnitude earthquake that could occur further away. Therefore, this scenario is chosen as a catastrophic event.

3.4.2 Subduction scenario: Cascadia Subduction earthquake M 9.0 (CSZ9.0)

The Cascadia subduction events occur at the interface between subducting Juan de Fuca Plate and North America Plate and can cause large magnitude earthquakes, inducing intensive and destructive levels of ground shaking in nearby BC. The Cascadia Subduction Zone (CSZ) is fully ruptured over a rupture area 1020 km long and 125 km wide, extending between Northern California, till northern Vancouver Island to get a magnitude 9.0 earthquake scenario. The GMPEs used to develop this western subduction interface scenario in OQ are described as in (Atkinson & Adams, 2013), with additional modifications made for NBCC2015. Table 3.9 summarizes the GMPE models and weights used to predict intensity of ground shaking due to the assumed rupture

and is consequently used to determine damage states of buildings on respective sites. The CSZ9.0 has a return period of around 500 years and has much lower levels of ground shaking intensity (almost one-third in the lower periods), when compared to the GSM7.3 scenario. The central GMPE for the subduction interface events is developed as shown in Table 3.10.

Table 3.9 GMPEs and weights used in CSZ9.0 scenario analysis

GMPE model	weight
NBCC2015_AA13_interface_low	0.2
NBCC2015_AA13_interface_central	0.5
NBCC2015_AA13_interface_high	0.3

Table 3.10 GMPEs and weights used to develop NBCC2015_AA13_interface_central

GMPE model	weight
AM09 (Atkinson & Macias, 2009)	0.5
GA13 (Ghofrani & Atkinson, 2014)	0.2
2A&al13 (Abrahamson et al., 2016)	0.2
Z&al06 (Zhao et.al., 2006)	0.1

3.5 Regional Seismic Risk assessment (RSRA)

To understand the effect of subduction ground motions on RSRA, ten cities in BC were chosen (Figure 3.25), where the influence of subduction seismic sources on the total seismic hazard at the site varies. Princeton, Chilliwack and Vancouver within mainland BC; Victoria, Sooke, Ucluelet and Port Hardy on the Vancouver Island; Queen Charlotte city (Daajing Giids) and Masset in the Haida Gwaii archipelago; and Prince Rupert, close to mainland BC are the chosen localities.

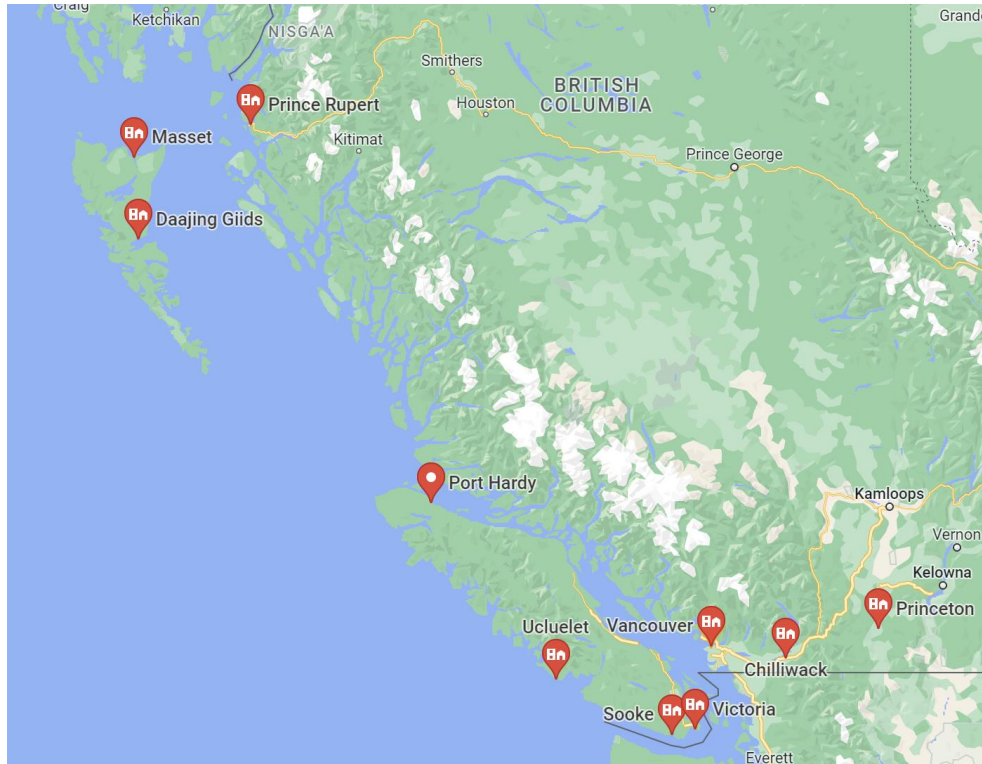


Figure 3.25 Location of selected cities

The exposure model for these cities were extracted from the exposure model for BC, developed by NRCan (Journey et al., 2022). For Vancouver and Victoria, where UBC had conducted a detailed building to building survey, it was recorded that wood buildings constitute ~94% and ~90% of the total building stock, respectively. However, on studying the coarser exposure model for the 10 localities developed by NRCan, it is noted that Vancouver and Victoria record significantly smaller percentage of wood buildings (Figure 3.26). Because this study is focused on the concrete shear wall and wood building typologies, only these typologies within the building stock in all ten cities will be considered. That is, for the purposes of this study, is considered that C2 and wood buildings together make 100% of the building stock in each of the ten selected localities.

**General building stock distribution for selected cities in the BC exposure model
developed by NRCan**

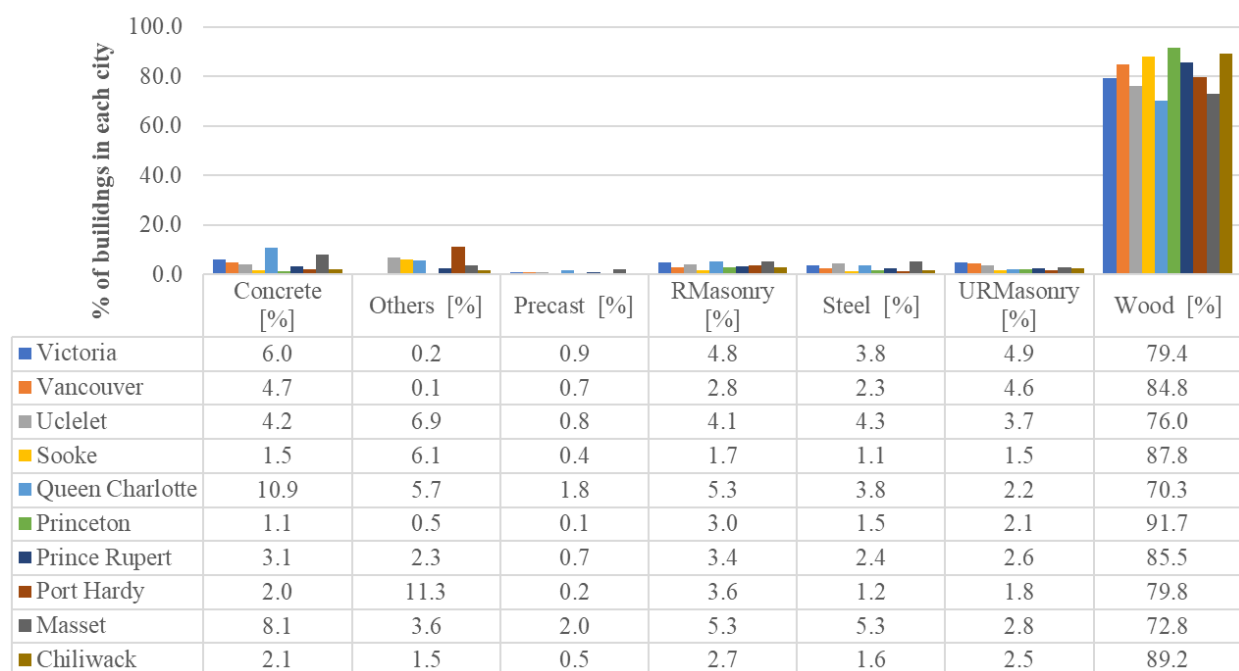


Figure 3.26 Comparison of building stock distribution between the selected cities in the BC exposure model developed by NRCan

Other than the exposure model, these ten localities have a varied contribution from the three different seismic sources to the total seismic hazard at each site. To understand this, Table 3.11 summarizes the relative contribution of hazard from the three types of seismic sources to the total seismic hazard at the 10 selected localities. This table was developed based on values reported within the SRG3 document. The 10 localities are presented in increasing order of relative contribution of subduction hazard to total seismic hazard at the site of interest.

Table 3.11 Contributions of crustal, subcrustal and subduction hazard to total seismic hazard at a locality

Locality	Crustal Hazard	Subcrustal Hazard	Subduction Hazard
Prince Rupert	Low	None	Moderate
Masset	Moderate	None	High
Daajing Giids (Queen Charlotte City (QCC))	High	None	Very High
Port Hardy	Moderate	None	High
Ucluelet	Moderate	Moderate	Very High
Vancouver	Moderate	High	Moderate
Chilliwack	Moderate	Moderate	Low
Princeton	Low	Moderate	Very Low
Sooke	Moderate	High	Very High
Victoria	High	High	High

In this study, to quantify the effect of varying fragility and vulnerability functions, it is required to compute the aggregated damage and loss statistics (per aggregation zone, building typology, etc) for the distributed portfolio of assets in each selected locality. Therefore, the use of event-based damage and event-based risk calculators developed in the OQ engine is chosen to run RSRA. It simulates damage states and corresponding losses for each building in an asset for each seismic event in the seismic event catalogue. Event-based damage and loss assessment was carried out for each of the selected cities using Canada's 5th Generation seismic source model developed in OQ platform (Allen et al., 2017).

3.5.1 Baseline assumption to measure the influence of subduction events on RSRA

This thesis aims to study the effect of subduction events on RSRA in BC. In other words, the increase in the metrics that describe the RSRA results (loss exceedance curves, collapse exceedance curves, AACF, AAL, AALR), when subduction fragility and vulnerability functions

are explicitly used to estimate the damage and loss from subduction events in RSRA. Since all individual seismic events in the stochastic seismic events set in the RSRA are independent of each other, quantification of the effects of subduction events on RSRA at a site will not depend on the baseline used to identify the increase in the metrics concerned.

The seismic source model for southwest BC has crustal, subcrustal and subduction seismic sources, and the seismic events originating from these sources are independent of each other. To further explain the assumption made in this study to define the baseline case: Say two baseline cases are considered to measure the increase in the metrics of introducing subduction fragility and vulnerability curves in RSRA. The first baseline case uses the crustal fragility and vulnerability functions to estimate damage and losses from all seismic events within the RSRA. The second baseline case combines the results using the crustal fragility and vulnerability functions to estimate damage and losses from crustal and subduction events and subcrustal fragility and vulnerability functions to estimate damage and losses from subcrustal events within the RSRA respectively. To these two baselines, the damage and losses from the subduction events are added by introducing subduction fragility and vulnerability functions in RSRA. Because the seismic events are independent, the increase in the metrics, from the baseline, due to the subduction events will not be influenced by whether or not subcrustal damage and loss is included to establish the baseline. As such, in this study, crustal fragility and vulnerability functions alone are used to establish the baseline (represented by ‘Cr-All’).

3.5.2 RSRA runs

Once a decision was made on the baseline case, first, RSRA is carried at the 10 sites using their respective exposure models. Two RSRA cases are run:

1. **Case 1 (Cr-All) (baseline case):** For each of the selected cities, an event-based damage and loss analysis is carried out using only the crustal fragility and vulnerability curves to determine the damage and losses for seismic events from all seismic sources.
2. **Case 2 (Cr+Subd):** For each of the selected cities, event-based damage and loss analysis is carried out using crustal fragility and vulnerability functions to calculate damage and losses from crustal events and sub-crustal events and using subduction fragility and vulnerability functions for subduction events. To do this, the seismic sources are first separated into crustal and sub-crustal sources and subduction sources. Individual event-based analysis is carried out for these two sets of seismic sources separately. Because the seismic events are independent from each other, the results are then combined to get the results of regional seismic damage and loss assessment considering the effect of subduction ground motions explicitly.

From the event-based damage and loss analyses for Cr-All and Cr+Subd cases, collapse exceedance curves, loss exceedance curves, average annual collapse fraction (AACF), AAL, and AALR are calculated for each case. These metrics are compared to understand the effect of subduction ground motions on RSRA in the selected locations, depending on the contribution of subduction seismic sources to the seismic hazard at the site.

Finally, to remove any effect that the variation in exposure models have on the results above, a uniform exposure model is chosen for all 10 localities, and the above process is repeated. The exposure model of Ucluelet is chosen to redo the RSRA for the 10 selected sites, by moving the Ucluelet assets to each of the sites.

Chapter 4: Results

4.1 Exposure model developed for Vancouver and Victoria (objective 1)

The result of the exposure model developed for Vancouver and Victoria (where UBC has done a building-by-building survey), based off the modifications explained in section 3.2 is documented in this section. Only C2 and Wood typologies are discussed. In Vancouver they account for 97.2 % of the building stock and 95.0% in Victoria. While the Vancouver building survey had recorded the buildings with and without subfloors and cripple walls, the Victoria building survey did not have such a means of identification. Hence, the wood construction in Victoria is only classified between W1, W2 and W3, as shown in Figure 4.1.

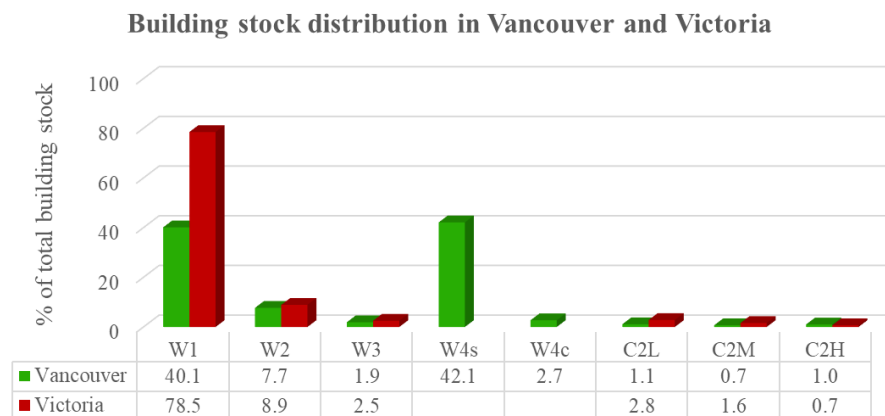


Figure 4.1 Distribution of wood and concrete shear wall building stock for Vancouver and Victoria

A summary of the distribution of C2 building stock in Vancouver and Victoria is shown in Figure 4.2. While Vancouver has an almost even distribution of high-rise, mid-rise and low-rise C2 buildings, Victoria has more low-rise and mid-rise C2 buildings than high-rise C2 buildings.

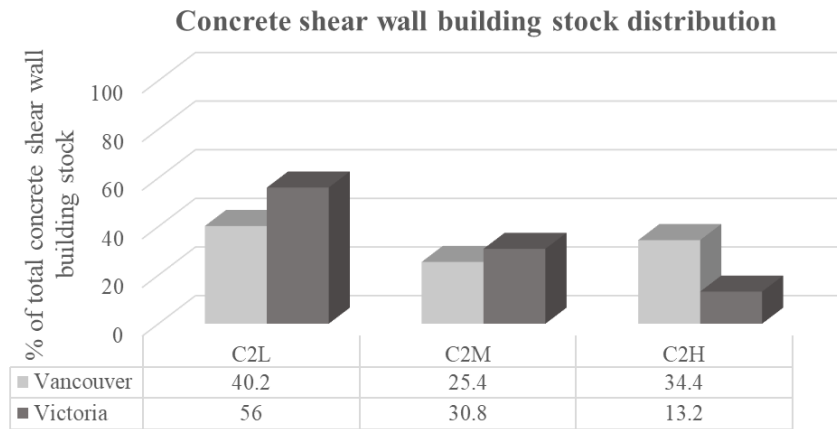


Figure 4.2 Distribution of concrete shear wall building stock in Vancouver and Victoria

Figure 4.3 summarizes the distribution of these C2 and wood buildings based on building age in Vancouver and Victoria, and observes that both cities have an aging building stock (built prior to 1972), more so in Victoria, where around 78% of the building stock are pre-code. These buildings are more susceptible to larger seismic damage.

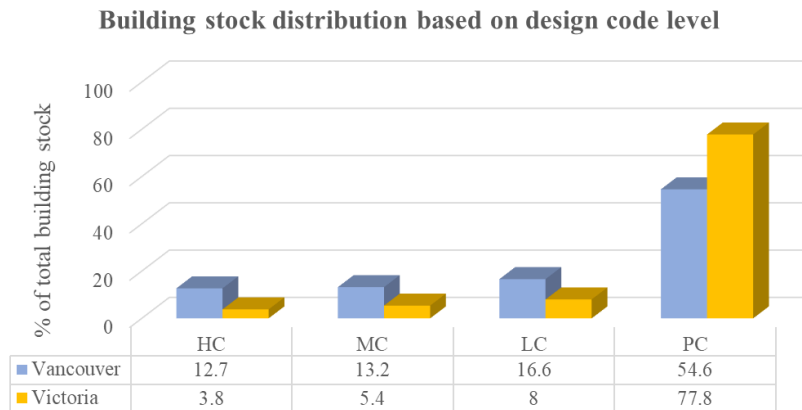


Figure 4.3 Distribution of wood and concrete shear wall building stock based on design code level for Vancouver and Victoria

4.2 Developing capacity curves for wood typologies in BC (objective 2)

While the concrete subcommittee provided the capacity curves for the median low-rise, mid-rise and high-rise C2 buildings through their expert opinion (section 3.3.1.1), the wood

committee provided the backbone curves for wood typologies for a single story, developed from experimental results in the FPI Innovations lab. Capacity curves representing the full structure for each wood building typology had to be developed as explained in section 3.3.1.2. These results - for PC constructions alone- are summarized in this section. It is seen that W4s constructions have highest base shear capacity due to the stiff short wall subfloor wall, but at the cost a reduced displacement capacity. The base shear and displacement capacity of buildings with cripple wall depend on the properties on the cripple wall, since the cripple wall introduces a soft-storey effect in the building. W3-PC typology has the lowest base shear capacity.

4.2.1 Low-rise residential wood construction (W1): Pre-code

The capacity curve development results for W1-PC are documented in this section. The shear spring properties assigned at each floor level, developed from the single-story backbone curves FPI innovations provided, as per NBCC 2015 are summarized in Figure 4.4. The mode shapes of the W1-PC typology model are shown in Figure 4.5.

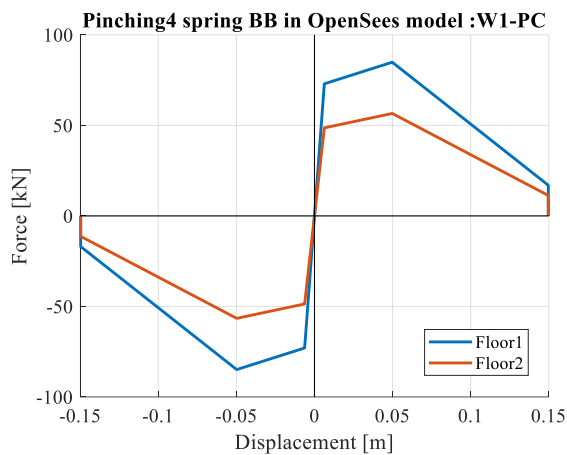


Figure 4.4 Shear spring assigned at each floor.

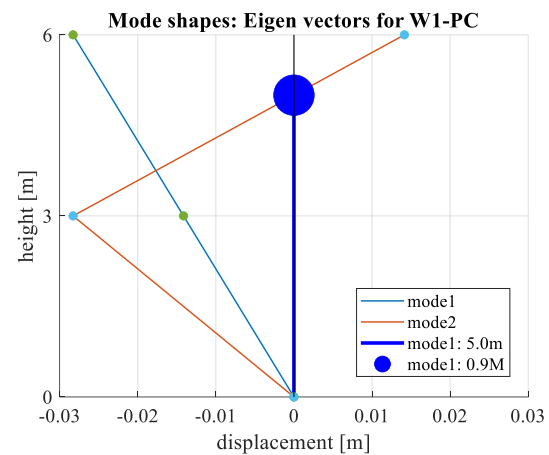


Figure 4.5 Mode shapes of W1-PC

Using the properties of the first mode (model1), a PO analysis is carried out for the structure following the ASCE 7-10 lateral load distribution, along the height of the structure. The resulting PO curve of the W1-PC model is shown in Figure 4.6. From the PO curve, Sa-Sd capacity curve for the first mode SDOF is developed as explained in section 3.3.1.2 and is shown in Figure 4.7. This capacity curve will be used as the median building of the W1-PC typology for fragility curve development. The modal height of first mode is 5.0m with period of the first mode being 0.32s.

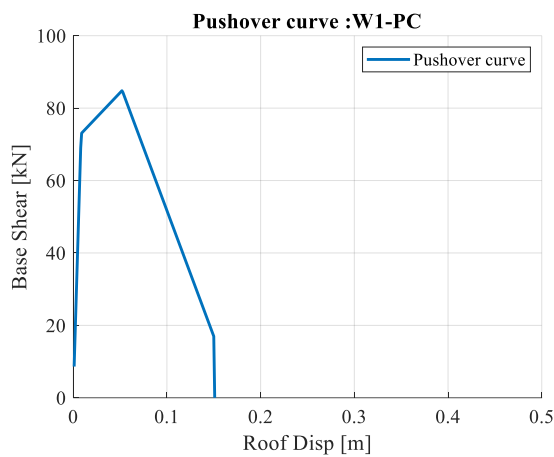


Figure 4.6 Pushover curve of W1-PC

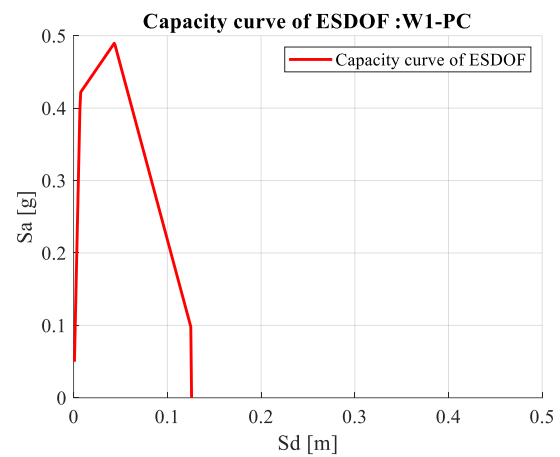


Figure 4.7 Capacity curve for first mode SDOF

4.2.2 Mid-rise residential wood construction (W2): Pre-code

The capacity curve development results for W2-PC construction are documented in this section. The shear spring properties assigned at each floor are summarized in Figure 4.8, and the mode shapes, in Figure 4.9. The pushover curve of the three-story W2-PC model is shown in Figure 4.10, and the Sa-Sd capacity curve for the first mode SDOF is shown in Figure 4.11.

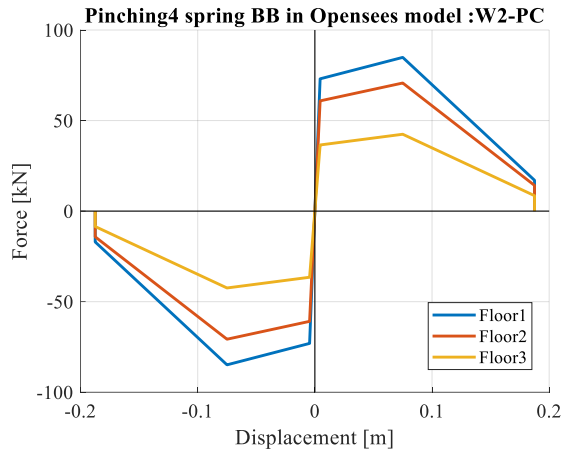


Figure 4.8 Shear spring assigned at each floor.

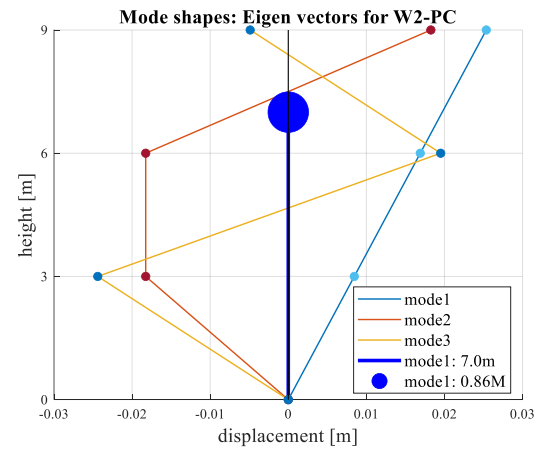


Figure 4.9 Mode shapes of W2-PC

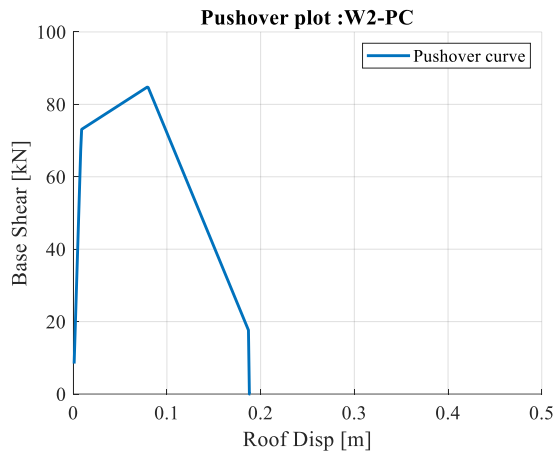


Figure 4.10 Pushover curve of W2-PC

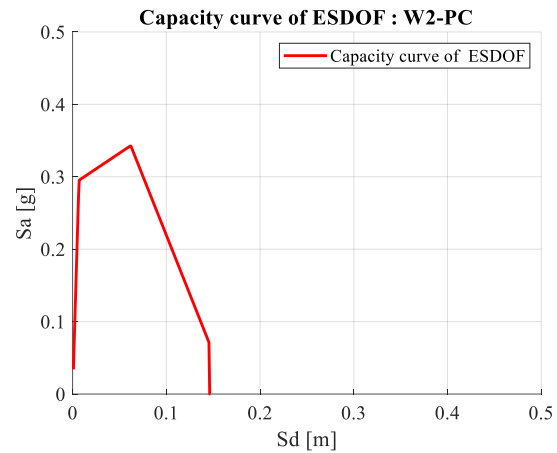


Figure 4.11 Capacity curve for first mode SDOF

4.2.3 Commercial and Industrial wood construction (W3): Pre-code

The capacity curve development results for W3-PC construction are documented in this section. The shear spring properties assigned at each floor are summarized in Figure 4.12. The mode shapes of the W3-PC typology model are shown in Figure 4.13. The pushover curve of the two-story W3-PC model is shown in Figure 4.14, and the Sa-Sd capacity curve for the first mode SDOF is shown in Figure 4.15.

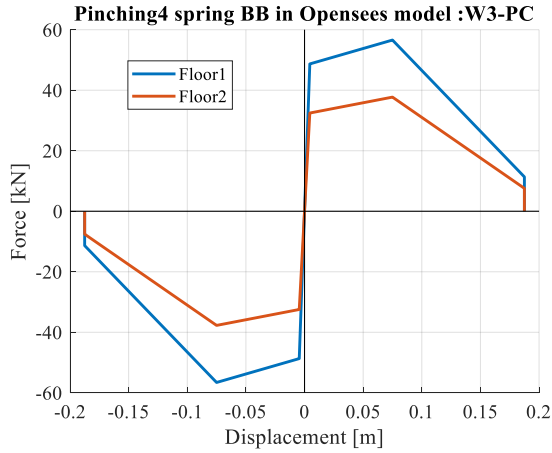


Figure 4.12 Shear spring assigned at each floor

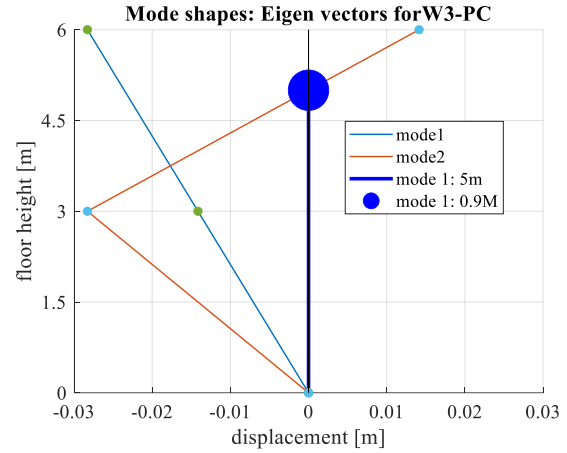


Figure 4.13 Mode shapes of W3-PC

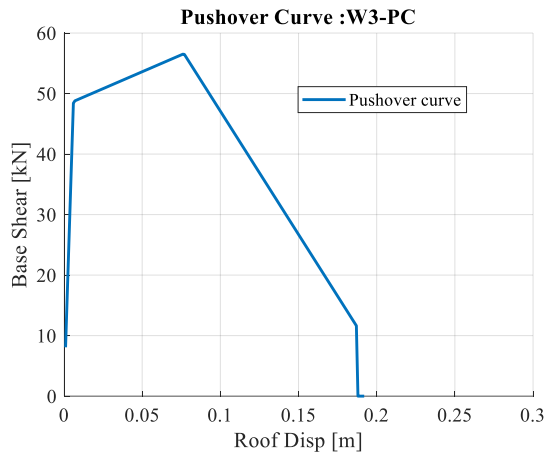


Figure 4.14 Pushover curve of W3-PC

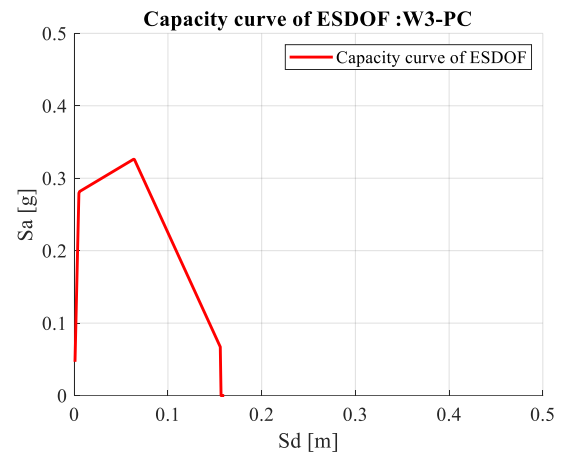


Figure 4.15 Capacity curve for first mode SDOF

4.2.4 Low-rise residential wood construction with subfloor (W4s): Pre-code

The capacity curve development results for W4s-PC construction are documented in this section. The 1.8m subfloor is assumed to have been designed as having the same strength capacities as the two 3.0m floors above it, but with a reduced displacement capacity, as seen for a shorter wall, to maintain the drift capacity across stories. The backbone curve properties assigned per floor of the W4s-PC typology is assumed as that for a single story W1-PC, provided by FPI

innovations. The displacement capacity provided is divided by the height ratio (height of the regular wall divided by the height of the subfloor) when assigned to the subfloor portion. The shear spring properties assigned at each floor are summarized in Figure 4.16. The mode shapes of the W4s-PC typology model are shown in Figure 4.17. The modal height of first mode is 6.0m with period of the first mode being 0.33s. The PO curve of the W4s-PC model is shown in Figure 4.18, and the Sa-Sd capacity curve for the first mode SDOF is shown in Figure 4.19.

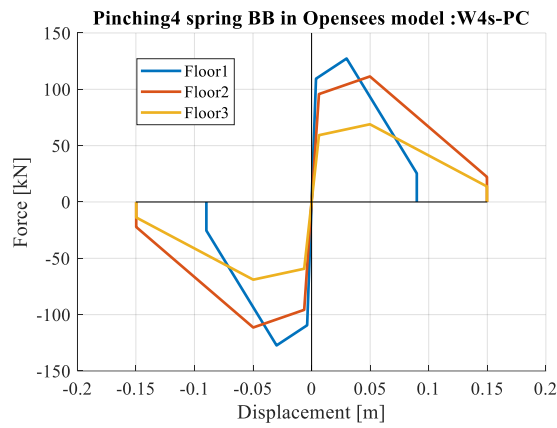


Figure 4.16 Shear spring assigned at each floor

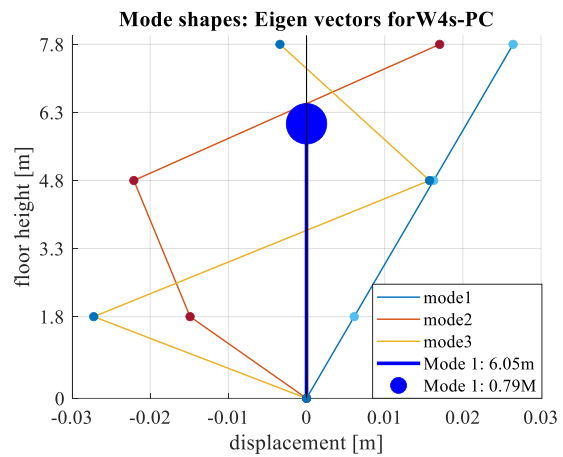


Figure 4.17 Mode shapes of W4s-PC

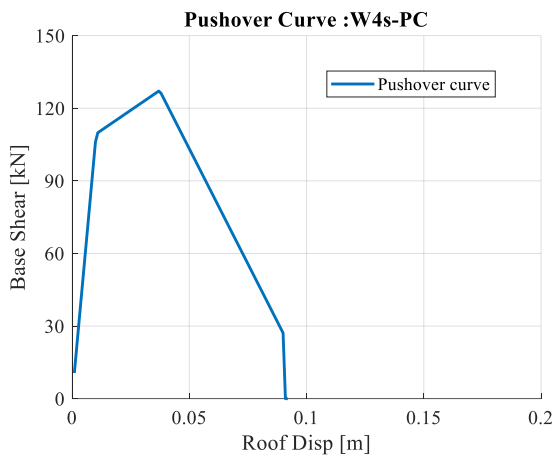


Figure 4.18 Pushover curve of W4s-PC

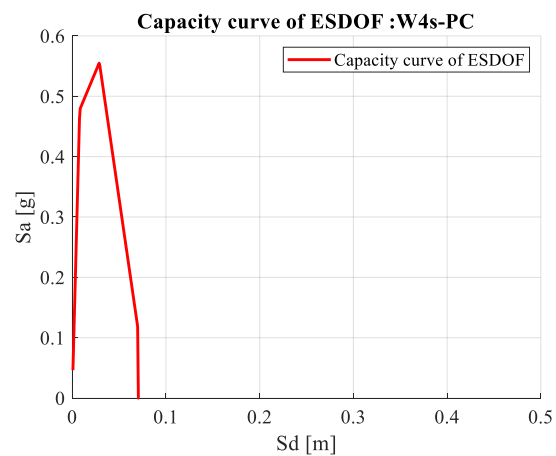


Figure 4.19 Capacity curve for first mode SDOF

The reduced displacement capacity of the short subfloor wall subsequently reduces the displacement capacity of the structure. However, the overall strength capacity of the structure increases due to a stiffness concentration created at the subfloor level.

4.2.5 Low-rise residential wood construction with cripple wall (W4c): Pre-code

The capacity curve development results for W4c-PC construction are documented in this section. The backbone curve properties of the two stories above the cripple wall is assumed as that for a single story W1-PC provided by FPI innovations, while the cripple wall properties are assigned as described in section 3.3.1.2. The shear spring properties assigned at each floor are summarized in Figure 4.20 and the mode shapes of the model are shown in Figure 4.21.

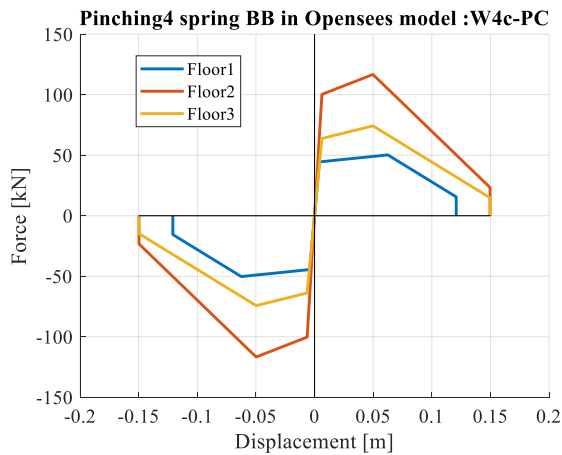


Figure 4.20 Shear spring assigned at each floor

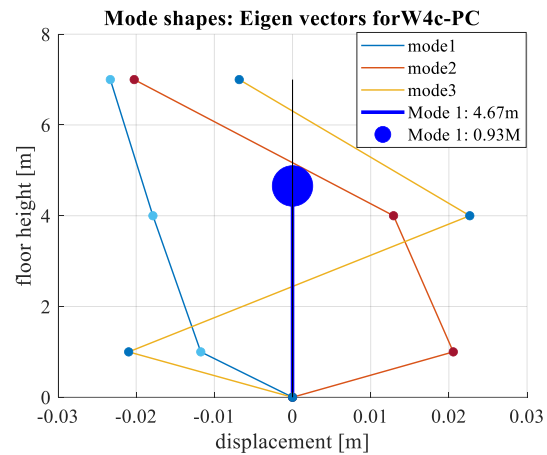


Figure 4.21 Mode shapes of W4c-PC

When the soft-story is not developed in the cripple wall, the effective mass of first mode is $0.93M$, where M is the total mass of the structure, and height of first mode is $4.6m$. From the modal analysis of the W4c-PC MDOF, the first mode shows that the structure closely resembles a base-isolated system as the cripple wall progressively ‘softens’, with a rigid mass above the cripple wall, as shown in Figure 4.22. As the structure softens, the resulting first mode SDOF would have

the height of the cripple wall and a mass equivalent to the mass of the stories above at the cripple wall height. The PO curve of the W4c-PC model is shown in Figure 4.23, and Sa-Sd capacity curve for the first mode SDOF is shown in Figure 4.24. The strength capacity of W4c-PC is verified against values recorded for two-storey cripple wall houses in USA (V/W for 2 storey pre-1945 unretrofitted as 0.16g and for those built between 1956-1970 as 0.29g) (Welch & Deierlein, 2020).

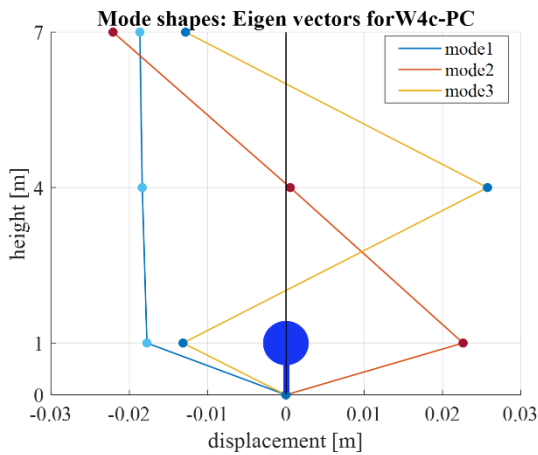


Figure 4.22 Mode shapes for W4c-PC when cripple wall softens

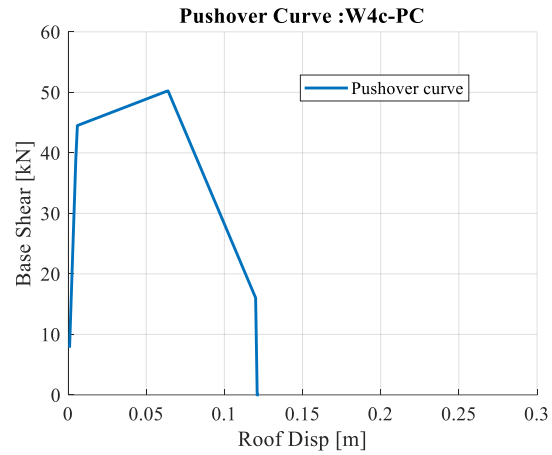


Figure 4.23 Pushover curve of W4c-PC

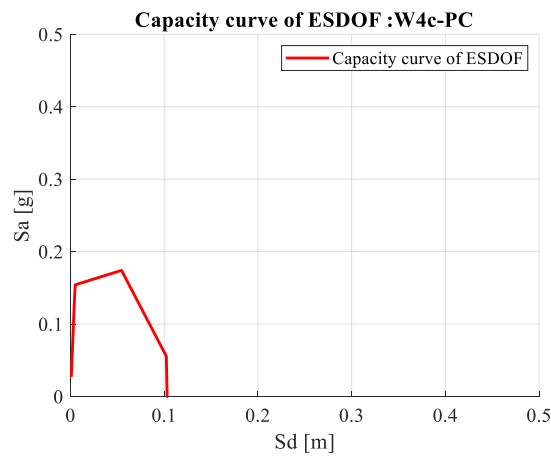


Figure 4.24 Capacity curve for first mode SDOF

4.2.6 Wood Typologies: Summary of capacity curves developed for BC wood typologies

The BC-specific capacity curves are compared to MLCC developed from HAZUS capacity curves and those used by GEM, for representative wood typologies (Figure 4.25 and Figure 4.26).

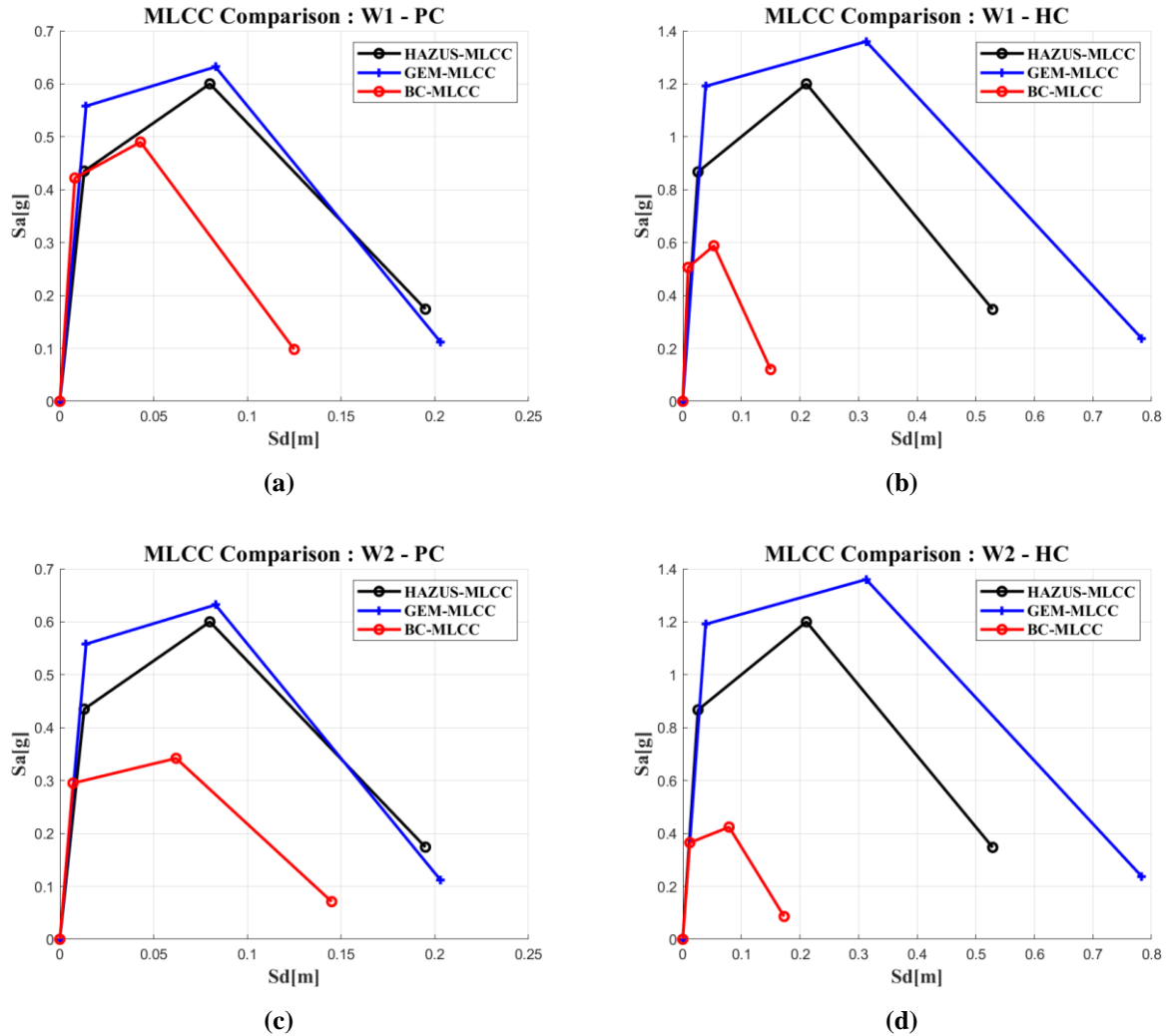


Figure 4.25 Comparison between capacity curves-GEM, HAZUS and BC-specific for typology: (a)W1-PC (b)W1-HC (c)W2-PC (d)W2-HC

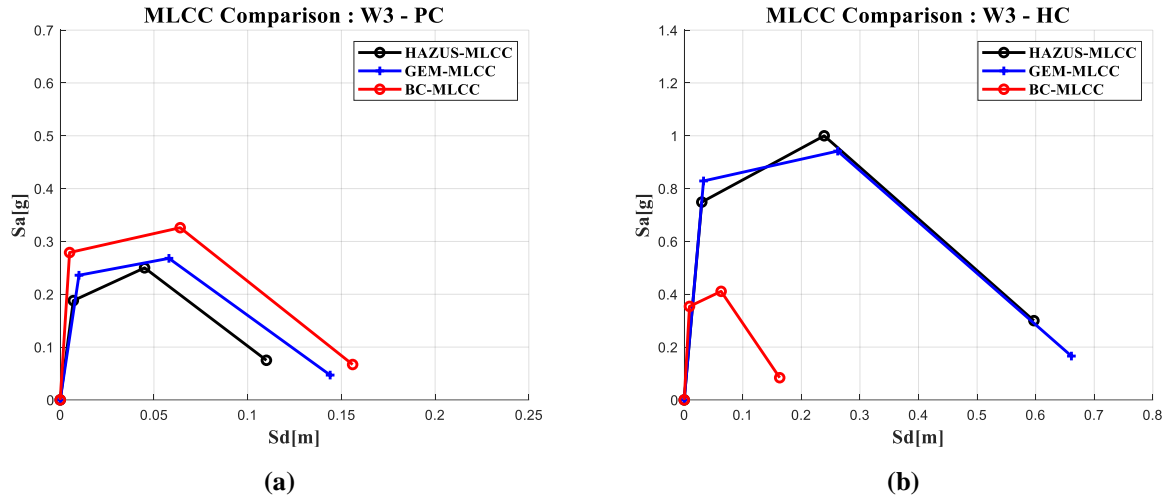


Figure 4.26 Comparison between capacity curves-GEM, HAZUS and BC-specific for typology (a)W3-PC (b) W3-HC

There is a notable difference in the strength and drift capacities between the MLCCs, with the BC specific wood construction (except for W3-PC) showing smaller values than corresponding HAZUS and GEM capacity curves, meaning that the BC wood building stock is weaker than those built in California, especially for wood buildings built after 1990.

The GEM W1-PC typology is about 30% stronger than the BC W1-PC typology, with 62% higher displacement capacity (Figure 4.25a). This difference is much more pronounced in W1-HC, where the maximum shear and displacement capacity of the GEM typology is 3.2 times and 4.5 times higher than the W1-HC BC typology (Figure 4.25b). While the GEM W2-PC shear capacity is 85% higher than the BC W2-PC, meaning the multi-family dwellings in BC, built before 1973 are weaker than those in California (Figure 4.25c), the BC commercial and industrial wood typology (W3-PC) has 18% higher shear capacity than GEM W3-PC (Figure 4.26a). W2 and W3 built after 2005 in BC have much lower strength capacity than corresponding GEM typologies (Figure 4.25d, Figure 4.26b) (0.29 times and 0.42 times lower respectively).

Figure 4.27 compares the MLCCs of W4s-PC and W4c-PC used by HAZUS, GEM and this study. It is noted that HAZUS and GEM do not recognize this typology, and the comparison is drawn between W1 (HAZUS and GEM) with BC-specific W4s and W4c. The capacity curve for W4c-PC for BC-specific typology is developed for an ESDOF of height 1.0m, with total mass concentrated at cripple wall height. For W4s, it is noted that the stiff short wall increases the overall shear capacity of the structure, but reduces the displacement capacity, since it increases the stiffness of the system. The presence of a sub-floor in W1-PC construction increases the shear capacity of the system, reducing the difference from 30% to 14%, when compared to GEM W1-PC typology, at the cost of severely reducing the ultimate displacement capacity (0.38 times lower) (Figure 4.27a). As such, the damage estimated for this type of construction will be higher than for W1-PC, and careful consideration should be given to this typology, as the building survey done in Vancouver estimated that about 50% of the low-rise residential wood structures have a subfloor.

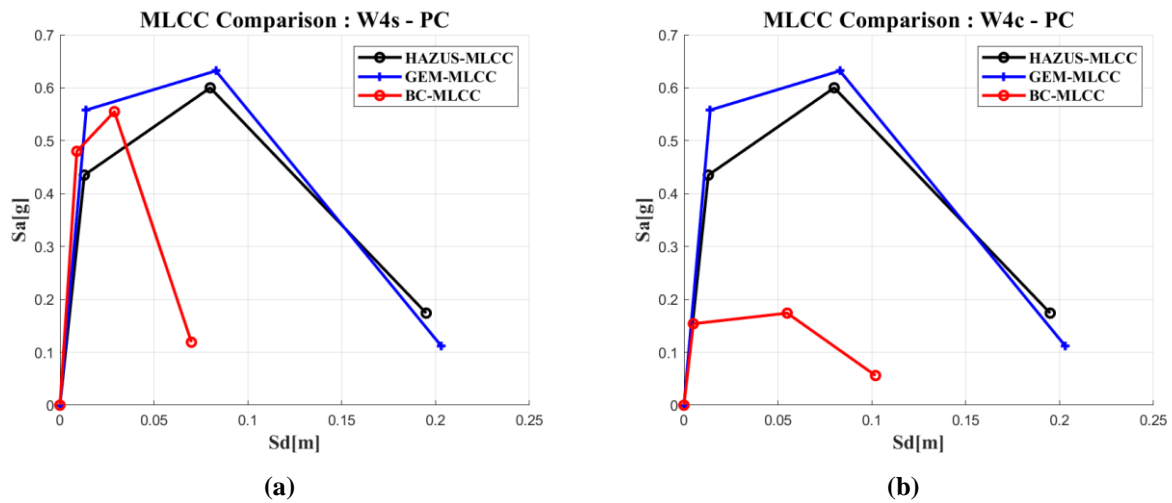


Figure 4.27 Comparison between capacity curves-GEM, HAZUS and BC-specific for typology: (a)W4s-PC (b)W4c-PC

Though smaller in number (~2700 buildings), low-rise wood construction with cripple walls (W4c-PC) are about 2.8 times weaker than W1-PC, making these typologies highly

susceptible to seismic damage. These typologies must be specifically studied, as there are pockets within Vancouver, where they are concentrated. Table 4.1 summarizes the model heights obtained for the BC-specific wood typologies, and model heights used by GEM wood typologies.

Table 4.1 Summary of modal heights for GEM and BC-specific Wood typologies.

Typology	modal height [m]	Typology	modal height [m] (estimated from modal analysis)
GEM		BC-specific	
W1	5.6	W1	5.0
		W2-HC	9.0
		W2-PC	7.0
		W4s	6.0
		W4c	1.0
W2	8.4	W3-HC	7.0
		W3-PC	5.0

To make a comparison between the capacity curves obtained from this study to that present in literature, the low-rise wood capacity curves are compared to those from experimental works done at UBC (White & Ventura, 2006). This work classifies the low-rise residential wood construction -with two storeys, each of height 2.75m- into 4 types: House 1(with stucco/engineered OSB/GWB), House 2 (with engineered OSB/GWB), House 3 (with non-engineered OSB/GWB), House 4 (with horizontal boards/GWB). The capacity curves for W1-PC/LC and W1-HC/MC developed in this study, in terms of strength capacity, are comparable with House 3 and House 2, but have a better displacement capacity. The capacity curves for W2 and W3 are compared to capacity curves developed for wood multi-family dwelling (MFD) archetypes and commercial building archetypes respectively, provided in FEMA P-2139-2 (FEMA, 2020a). FEMA P-2139-2 documents the shear capacity vs. roof drift pushover curves for 2 storey and 4 storeys for wood

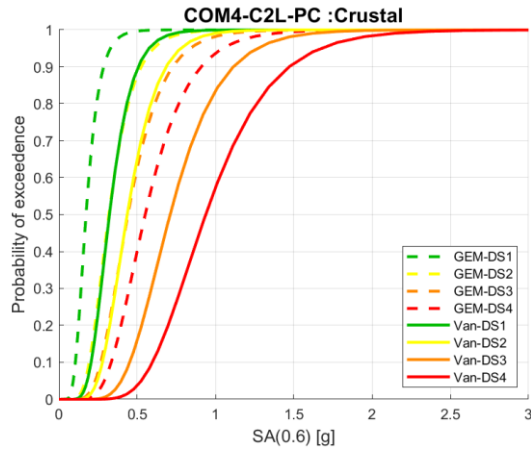
single family dwelling, multi-family dwelling archetypes and commercial building archetypes. The shear capacity of 2 storey commercial wood building (W3) was recorded as about 0.44g, while that for 4 storey, as around 0.3g, and the shear capacity of 2 storey MFD (W2) as about 0.65g while that of a 4 storey MFD, about 0.35g, in ranges similar to the capacity of the BC W2 and W3 buildings. However, both US typologies recorded better drift capacities, since the 1 storey roof drift capacities recorded in FEMA P-2139-2 for the US W2 and W3 typologies is more than double that recorded for 1 storey BC W2 and W3 typologies.

4.3 Comparison of current fragility functions to BC-specific crustal fragility functions (objective 3)

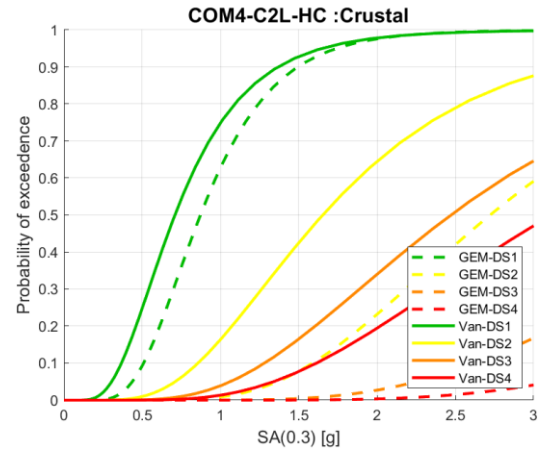
In this section, the effect of considering BC construction practices and its changes over the years, when modeling median buildings towards developing fragility and vulnerability functions for different building typologies, is discussed. The GEM functions are referred to by the prefix GEM-, and the BC-specific, by the prefix Van- (BC-specific fragility functions developed for Vancouver). It should be noted that the GEM fragility functions are developed using FEMAp695 ground motions from all three tectonic sources, while the BC fragility curves, using the SRG3 crustal ground motion set developed for Vancouver (Bebamzadeh et al., 2015). The GEM fragility functions are used to run scenario analysis and RSRA by NRCan.

4.3.1 Concrete typologies

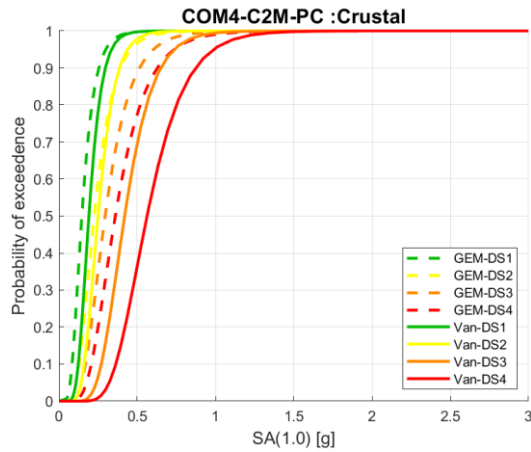
The comparison between the GEM fragility curves and BC-specific crustal fragility curves for C2L, C2M and C2H for PC and HC are shown in Figure 4.28.



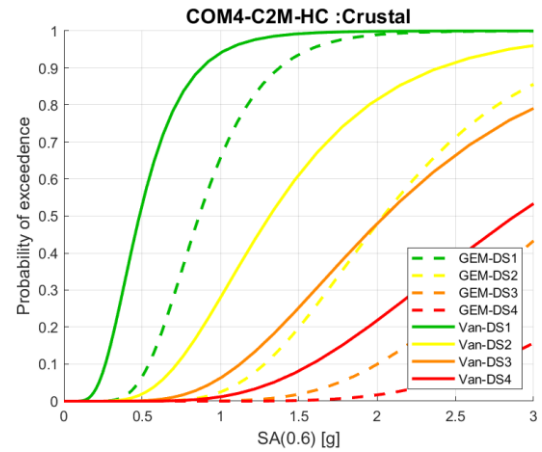
(a)



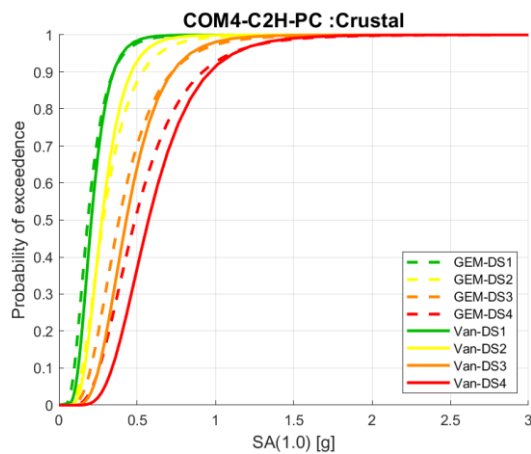
(b)



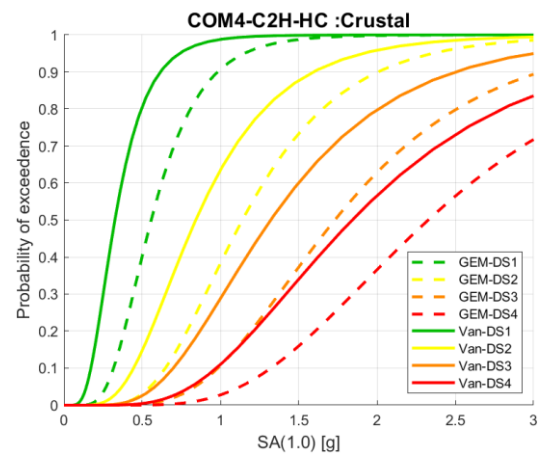
(c)



(d)



(e)



(f)

Figure 4.28 Comparison of current fragility curves (GEM-) to new BC specific fragility curves (Van-): (a) C2L-PC (b) C2L-HC (c) C2M-PC (d) C2M-HC (e) C2H-PC and (f) C2H-HC

Figure 4.28a, c, e illustrates that the damage estimated for BC C2 typologies built before 1973 are lower than those estimated by the corresponding GEM fragility functions. The median DS4 capacity (defined as the spectral acceleration at 50% of probability of exceedance of DS4) predicted by the GEM fragility functions are 41%, 34% and 15% lower than BC-specific crustal fragility functions for C2L-PC, C2M-PC and C2H-PC typologies respectively, when the capacity curves are modified for BC-specific construction. The UHS at Vancouver city hall at 0.6s according to NBCC 2015 shows a spectral acceleration of about 0.685g, at which, the BC C2L-PC fragility curves estimate ~20% DS4, while the GEM fragility curves estimate around 72% DS4. The UHS at Vancouver city hall at 1.0s according to NBCC 2015 shows a spectral acceleration of about 0.425g, at which, while the BC-specific C2M-PC and C2H-PC fragility curves estimate ~18% and 23% complete damage and the GEM fragility curves, around 62% and 40% DS4 respectively.

However, for C2 construction built after 2005, the GEM capacity curves (developed from HAZUS) for C2L and C2H are about three times stronger and for C2M, about 4 times stronger than the corresponding BC typology. The ultimate displacement capacities of the GEM C2 typologies are also more 2 times that of the corresponding BC typologies. Hence, Figure 4.28b, d, f shows that BC-specific C2 HC fragility curves estimate higher damages than corresponding GEDM C2-HC typologies. The median DS4 capacity predicted by the BC crustal fragility functions are 84%, 51.4% and 25% lower than GEM fragility functions for C2L-HC, C2M-HC and C2H-HC typologies respectively, when the capacity curves are modified for BC-specific construction.

4.3.2 Wood typologies

As discussed in section 4.2.6, the capacity curves for BC wood typologies are considerably lower than corresponding GEM typologies in terms of strength and displacement capacity, except for W3-PC. The backbone curves provided by FPI Innovations record that shear and displacement capacity for PC and LC BC-specific wood construction are similar, as is MC and HC. This means that fragility and vulnerability curves for PC and LC BC-specific wood typologies overlap, as do for MC and HC wood typologies. The comparison between the GEM and BC-specific crustal fragility curves for W1-PC and HC are shown in Figure 4.29.

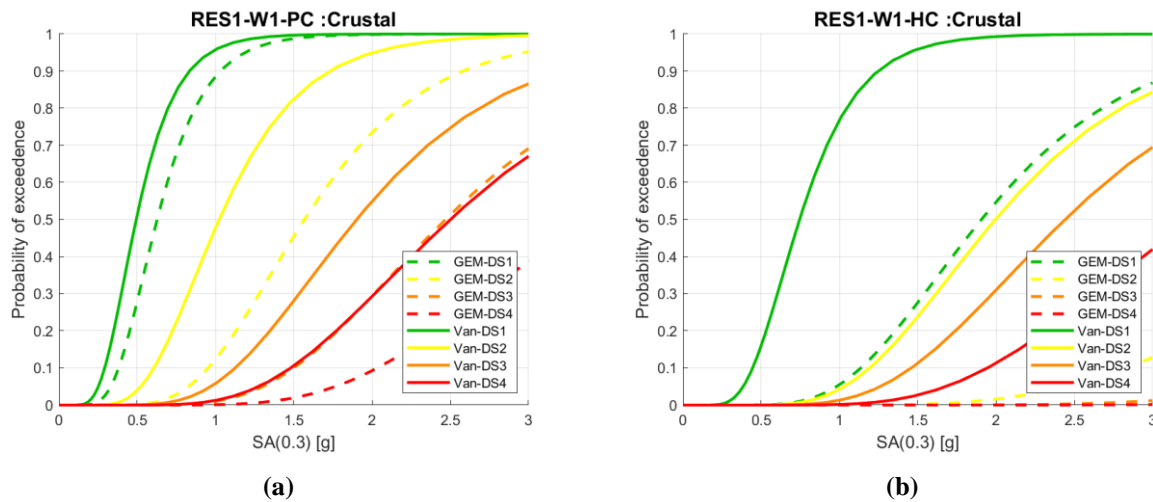


Figure 4.29 Comparison of current fragility curves (GEM-) to new BC specific fragility curves (Van-):
(a)W1-PC (b)W1-HC

The median DS4 capacity predicted by the BC W1-PC and W1-HC crustal fragility functions are 27.5% and 96% lower than GEM W1-PC and W1-HC fragility functions respectively. The GEM W1-HC typology is unrealistically strong when considered for use in BC. The implication of this is that in a region like Vancouver - where more than 80% of its large wood building stock being low-rise wood construction - when using the BC W1 fragility functions to

estimate damage than the GEM functions, a very large number of buildings will be estimated to be in higher forms of damage. The comparison between BC W4s-PC and W4c-PC and GEM W1-PC fragility curves is shown in Figure 4.30 (GEM typologies do not account for subfloor or cripple walls). Figure 4.31 illustrates how the DS4 fragility curve for low-rise residential wood structures change when accounting for cripple wall or subfloor.

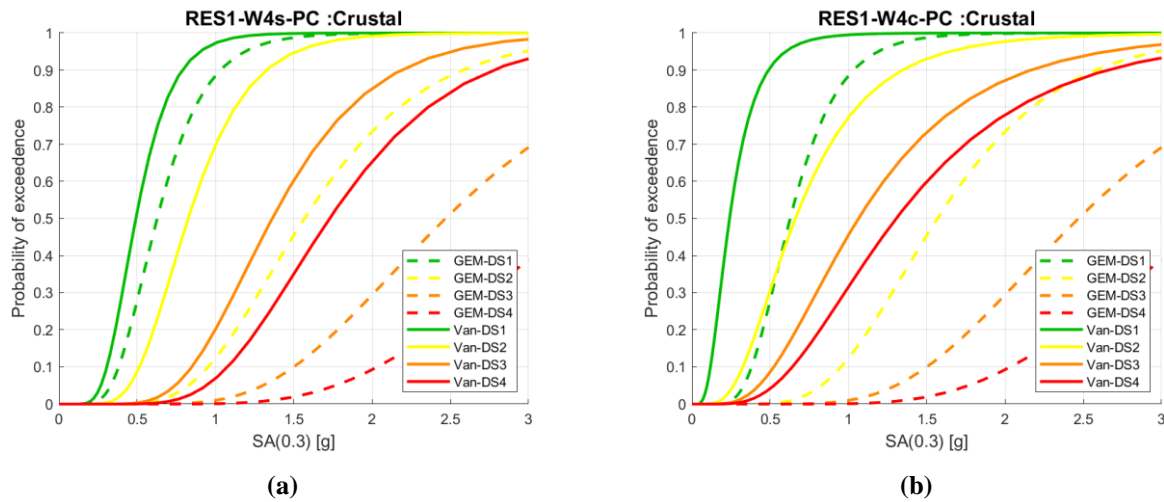


Figure 4.30 Comparison of current fragility curves (GEM-) to new BC specific fragility curves (Van-): (a)W4s-PC (b)W4c-PC

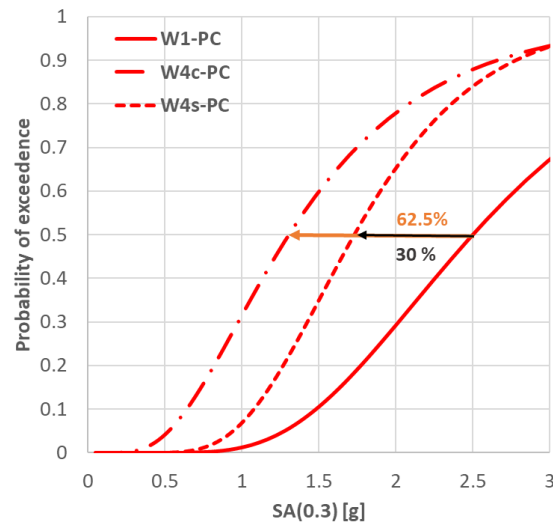


Figure 4.31 Comparison of DS4 fragility curves for pre-code low-rise residential wood structures

From Figure 4.30, for $S_a(0.3)$ of 0.85g (UHS at Vancouver city hall at 0.3s according to NBCC 2015) the probability of exceeding DS4 increases from 0.4% to 2.5% to 21% for W1-PC, W4s-PC and W4c-PC when compared to GEM W1-PC DS4 fragility curve. The median DS4 capacity, is reduced by 62.5% and 30% when accounting for a cripple wall or subfloor as shown in Figure 4.31. The comparison between the GEM and BC-specific crustal fragility curves for W2-PC and HC and W3-PC and HC are shown in Figure 4.32.

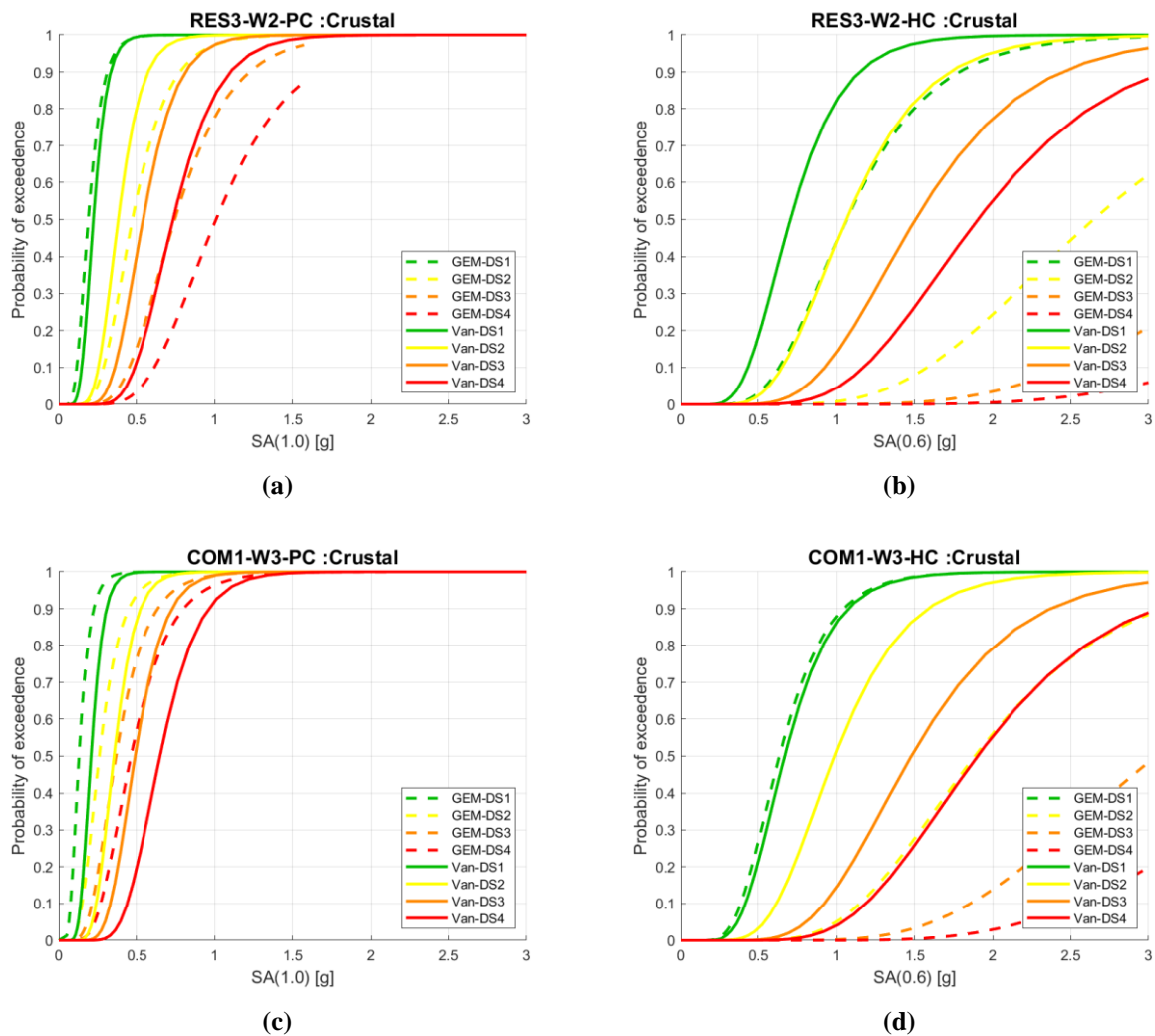


Figure 4.32 Comparison of current fragility curves (GEM-) to new BC specific fragility curves (Van-):
(a)W2-PC (b) W2-HC (c) W3-PC (d) W3-HC

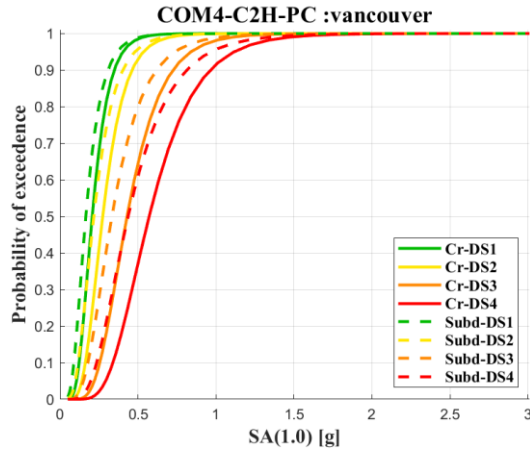
It should be noted that GEM uses ‘W2’ to represent commercial and industrial wood typology and ‘W1’ to represent low-rise residential and mid-rise multi-family dwellings. Figure 4.32 compares BC W2 typology to GEM W1 typology and BC W3 typology to GEM W2 typology. The median DS4 capacity predicted by the BC W2-PC and W2-HC crustal fragility functions are 24% and 95% lower than corresponding GEM fragility functions. The median DS4 capacity predicted by the BC W3-PC and W3-HC crustal fragility functions are 28.5% higher and 56% lower than corresponding GEM fragility functions.

4.4 Comparison of BC-specific crustal and subduction fragility functions (objective 3)

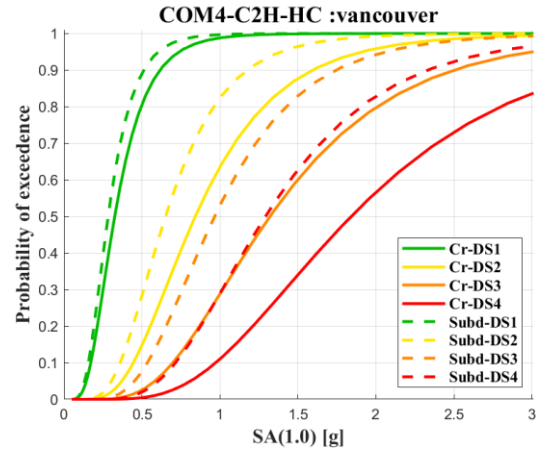
The crustal and subduction fragility curves developed for BC building typologies are documented in this section and how the characteristics of the subduction ground motions effect the damage estimated for the building typologies is discussed. The duration of shaking impacts the energy dissipation capacity of the structure, pushing it faster into its inelastic behavior, thus increasing its collapse potential under subduction events, compared to crustal events.

4.4.1 Concrete typologies

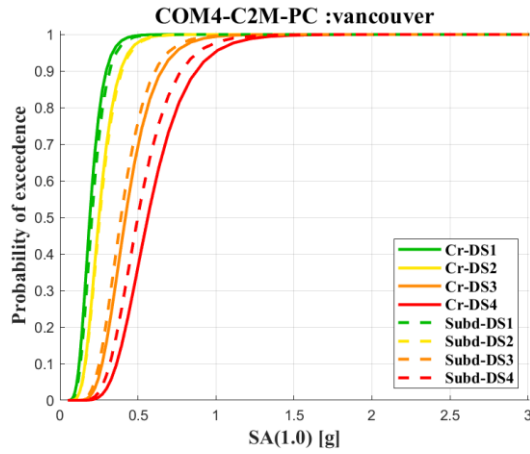
The comparison between the BC-specific crustal (Cr-) and subduction (Subd-) fragility curves for C2L, C2M and C2H, PC and HC typologies are shown in Figure 4.33. It is seen that for subduction DS4 fragility curves, the median DS4 capacity (spectral acceleration at which the probability of exceedance of DS4 reaches 50%) decreases by 13%, 11% and 23% as compared to crustal DS4 fragility curves for BC C2L, C2M and C2H pre-code typology, from Figure 4.33a, c, e. The subduction ground motions push these structures to collapse at a lower intensity of ground shaking than crustal ground motions. This influence increases to 43%, 25% and 29% for C2L, C2M and C2H high-code construction.



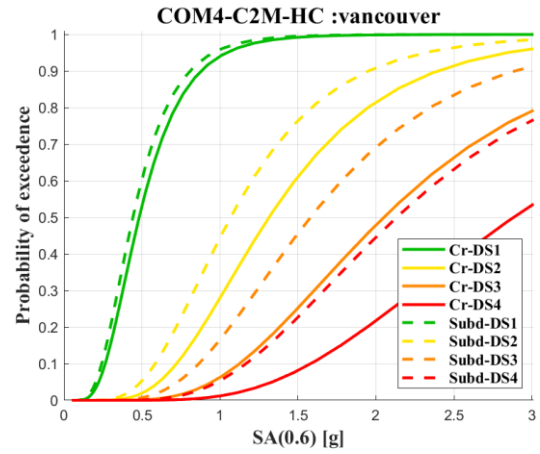
(a)



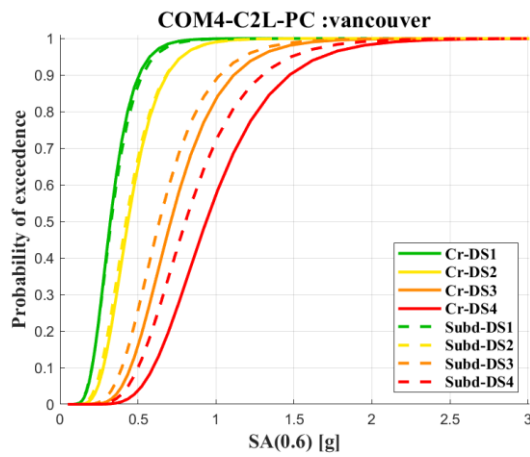
(b)



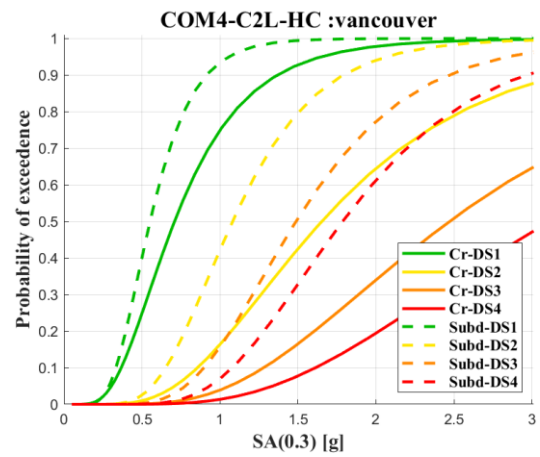
(c)



(d)



(e)



(f)

Figure 4.33 Comparison of crustal fragility curves (Cr-) to subduction fragility curves (Subd-): (a) C2H-PC (b) C2H-HC (c) C2M-PC (d) C2M-HC (e) C2L-PC and (f)C2L-HC

The influence of the subduction ground motions in imparting damage is felt more by the low-rise concrete structures. For all C2 typologies, the long duration effects tend to increase the damage potential of the structures and shifts the fragility curves to the left. This becomes more evident for newer construction (MC and HC structures with more ductility than those built before 1990, where seismic design was not well implemented within the Canadian building codes), where the effect of long duration ground shaking is more pronounced, especially at higher damage states.

4.4.2 Wood typologies

The comparison of BC-specific crustal (prefix: Cr-) and subduction fragility curves (prefix: Subd-) for W1-PC and HC and W4s-PC and W4c-PC are shown in Figure 4.34. Figure 4.34 shows that the influence of subduction ground motions on W1 typology is higher than on W4s typology, but lower than W4c typology. The influence of subduction ground motion on low-rise wood construction are similar, whether it be pre-code or high-code. It is seen that for subduction DS4 fragility curves, the median DS4 capacity decreases by 36% to 38% as compared to crustal DS4 fragility curves for BC W1-PC and W1-HC typologies respectively. For W4s-PC the subduction fragility curves median DS4 capacity decreases by 28%, while for W4c-PC, it decreases by 38.5% as compared to crustal DS4 fragility curves for BC W4s-PC and W4c-PC typologies respectively. Low-rise wood construction in BC with cripple walls is most susceptible to damage, followed by those with subfloors and then by W1 structure during a subduction seismic scenario.

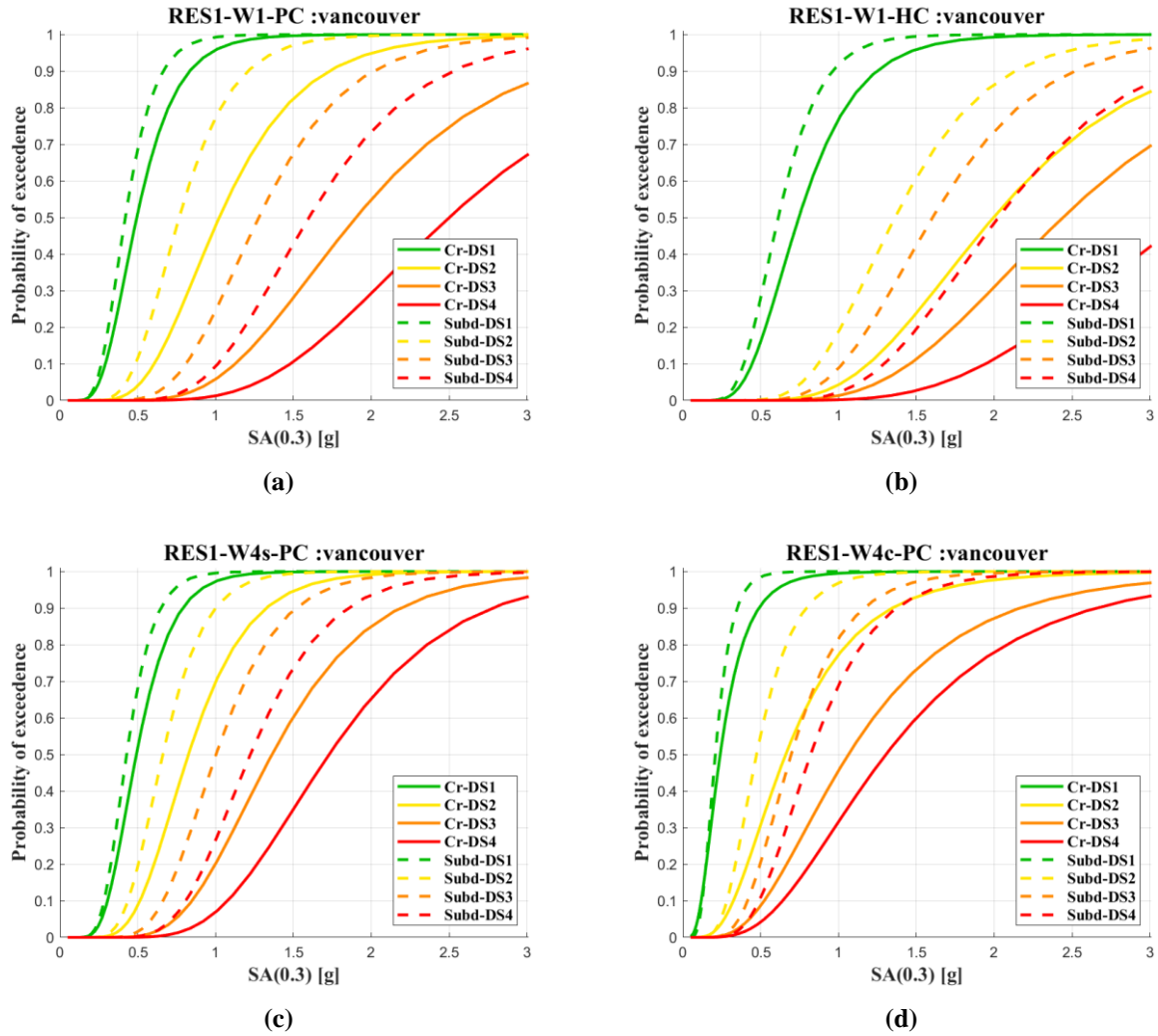


Figure 4.34 Comparison of crustal fragility curves (Cr-) to subduction fragility curves (Subd-): (a)W1-PC (b) W1-HC (c) W4s-PC and (d) W4c-PC

Comparing the BC-specific crustal and subduction fragility curves for W2 and W3 PC and HC as shown in Figure 4.35, it is seen that the subduction ground motions only very slightly influence the fragility curves for the W2 and W3 PC typologies (Figure 4.35a, c). However, subduction ground motions influence the newer (MC and HC) W2 and W3 construction more, decreasing the median DS4 capacity by 16% for a four storey multi-family wood dwelling, and for a three-storey commercial and industrial wood building by 14% from crustal DS4 fragility functions. At lower intensity measure levels and for lower damage states (slight and moderate

damage state), crustal events tend to estimate a slightly higher damage than subduction events for W2 and W3 PC typologies.

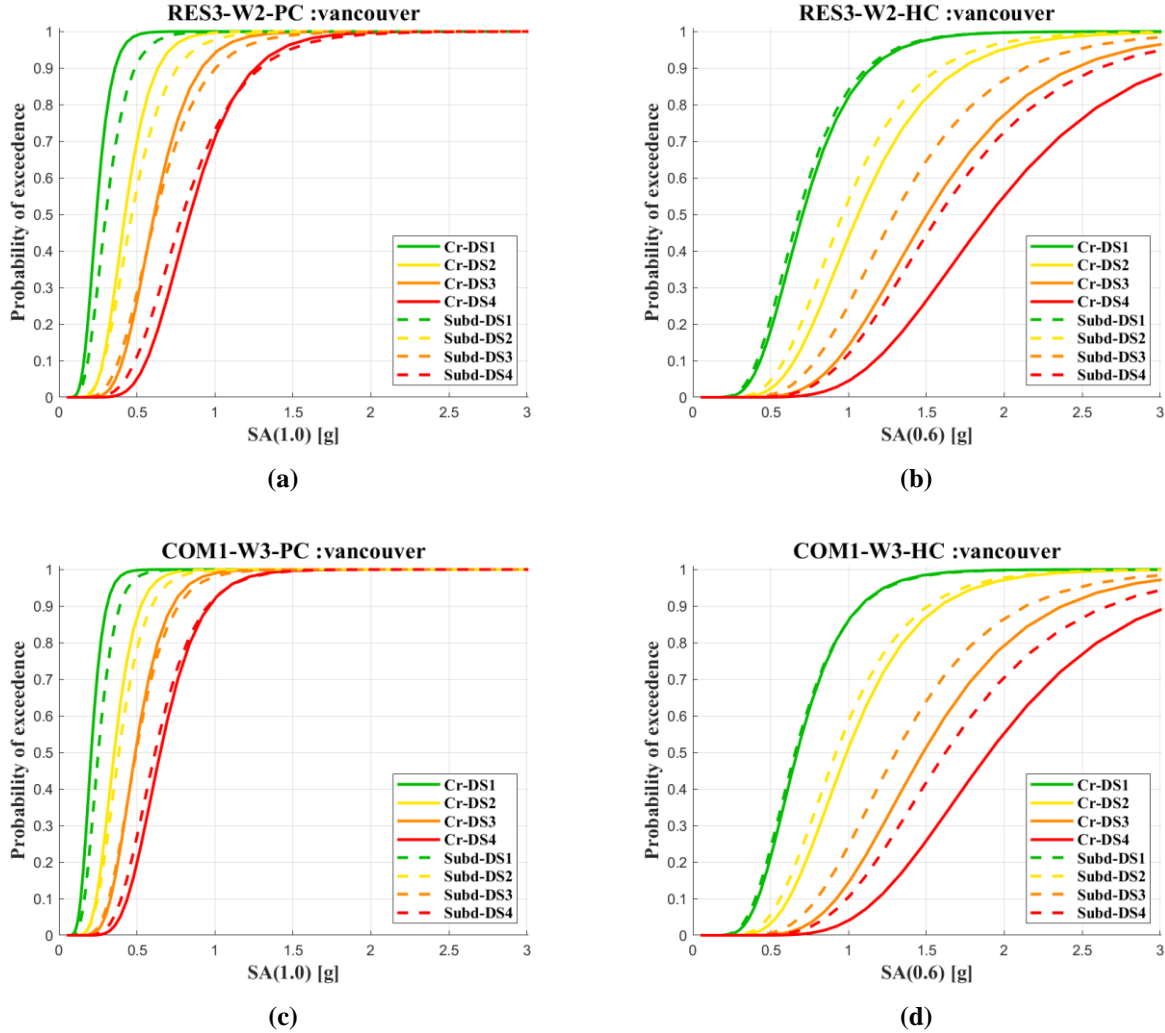


Figure 4.35 Comparison of crustal fragility curves (Cr-) to subduction fragility curves (Subd-): (a)W2-PC (b) W2-HC (c) W3-PC and (d) W3-HC

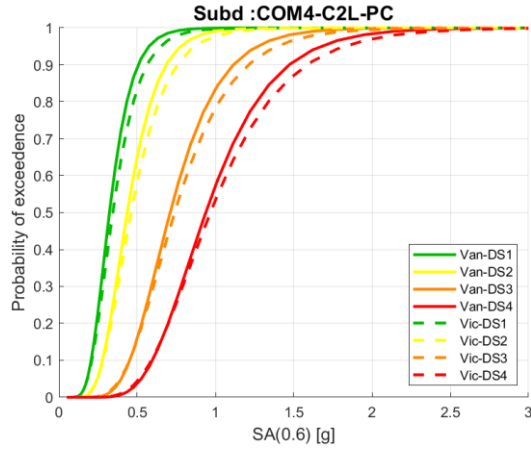
From section 4.4.1 and 4.4.2, it was seen that the damage estimated at a ground shaking intensity level by crustal fragility curves are lower than that estimated by subduction fragility curves. The difference between the crustal and subduction damage estimates increases as the intensity of ground shaking increases. It is also noted that long duration ground motions

significantly influence DS4, but its effect diminishes as the damage state lowers. That is to say, slight damage state is least influenced by long duration effects. It is also noted that higher the ductility of the system, higher the influence of long duration ground motions on probability of exceedance of a given damage state.

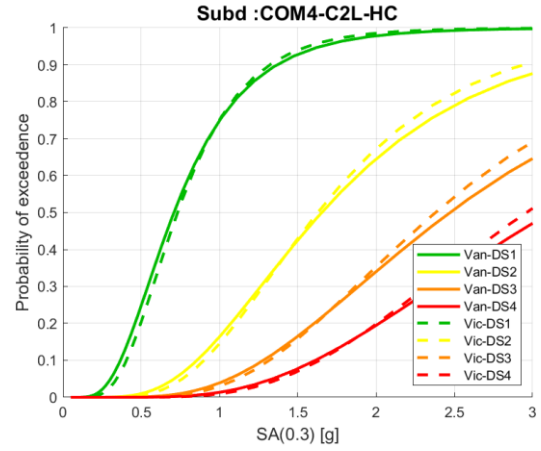
4.5 Comparison of BC-specific fragility curves in Vancouver and Victoria

This section compares the fragility curves developed at Vancouver and Victoria for crustal and subduction events, for some representative typologies. It is noted that at low intensities, the damage estimated for different building typologies in Vancouver and Victoria are similar for crustal and subduction events. But, this changes at higher intensities, depending on the relative shape of the Vancouver and Victoria crustal and subduction spectra at the period at which the fragility functions are developed for a typology, as is seen in Figure 4.36 for C2L, C2H and W1 pre-code and high-code typologies.

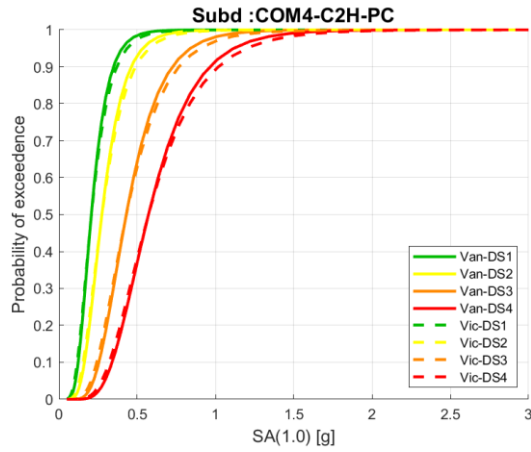
At lower periods, as intensity of ground shaking increases, Victoria fragility curves estimates more damage, especially for W1 (Figure 4.36e, f). At higher periods, the Victoria fragility curves estimate slightly lower damage estimates (Figure 4.36a, b, c, d). But since in this study we do not come across such high intensities spoken of, further research into this phenomenon is out of the scope of this work.



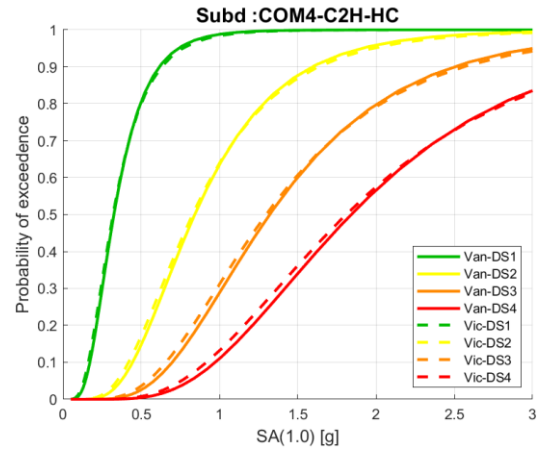
(a)



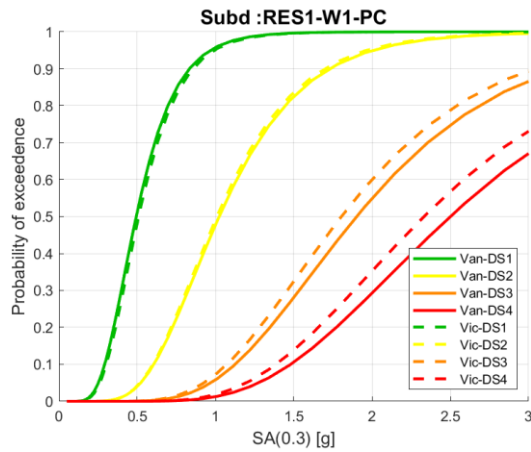
(b)



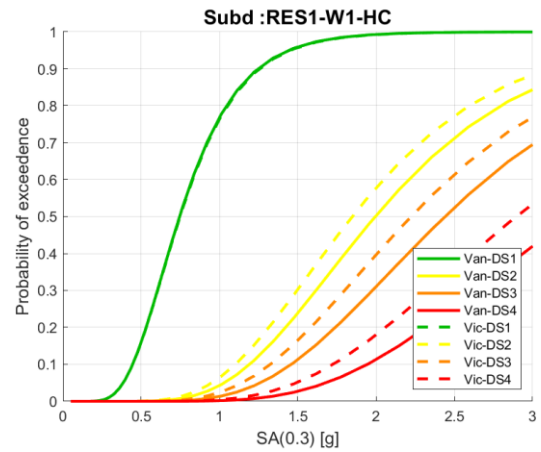
(c)



(d)



(e)



(f)

Figure 4.36 Comparison of crustal fragility curves for Vancouver and Victoria (a) C2L-PC (b)C2L-HC (c) C2H-PC (d) C2H-HC (e)W1-PC and (f)W1-HC

4.6 Comparison of current vulnerability curves to BC-specific crustal vulnerability curves (objective 3)

The major changes in the vulnerability curves comes from modifying the fragility curves, and from altering the way in which non-structural and contents vulnerability functions are developed. In this section, the effect of these modifications in developing vulnerability curves is discussed.

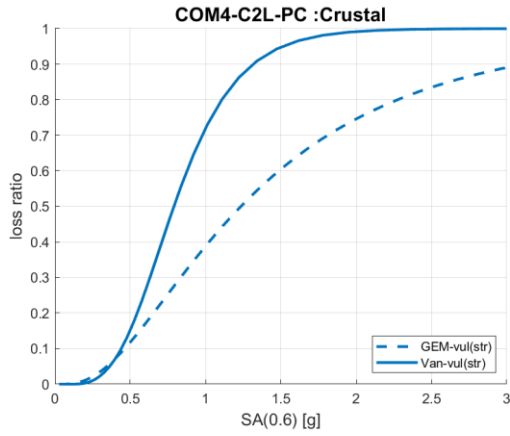
This section compares the GEM vulnerability functions (prefix: GEM-) to BC-specific vulnerability functions (prefix: Van-). Generally, the BC-specific C2 vulnerability curves estimate more loss than their corresponding GEM functions, while BC-specific wood vulnerability curves estimate lower losses than their corresponding GEM functions (except for low-rise wood with cripple wall). For all typologies, there is a large difference in the estimated loss ratios between buildings built before 1990 and those built after 1990, with PC structures estimating much higher losses, due to their low ductility.

4.6.1 Concrete typologies

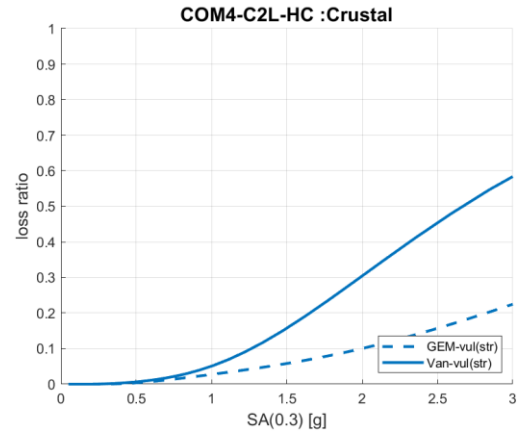
Figure 4.37 compares the GEM structural vulnerability functions to corresponding crustal BC-specific functions for all C2 PC and HC typologies, respectively.

Figure 4.38 compares the GEM non-structural vulnerability functions to corresponding crustal BC-specific functions for all C2 PC and HC typologies, respectively.

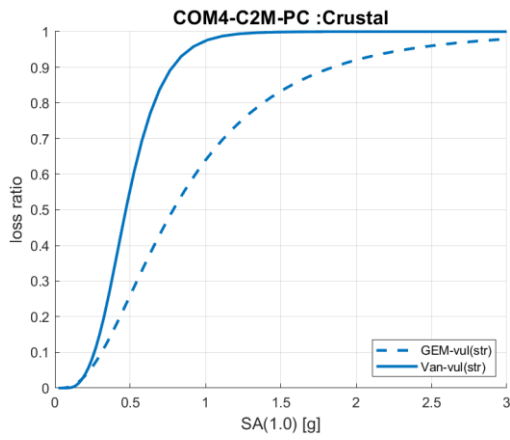
Figure 4.39 compares the GEM contents vulnerability functions to corresponding crustal BC-specific functions for all C2 PC and HC typologies, respectively.



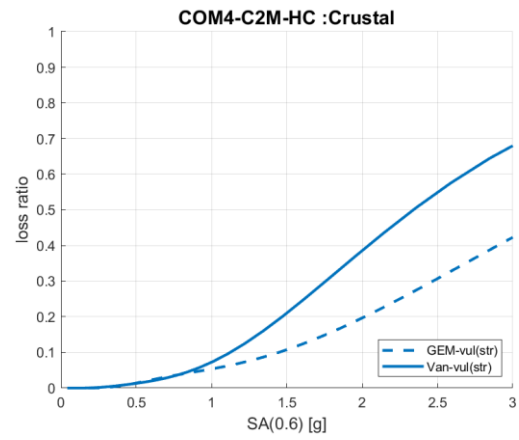
(a)



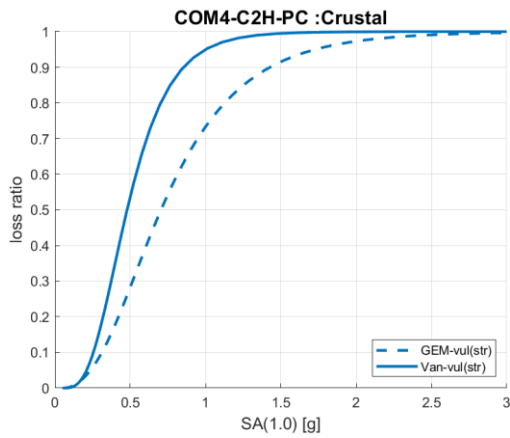
(b)



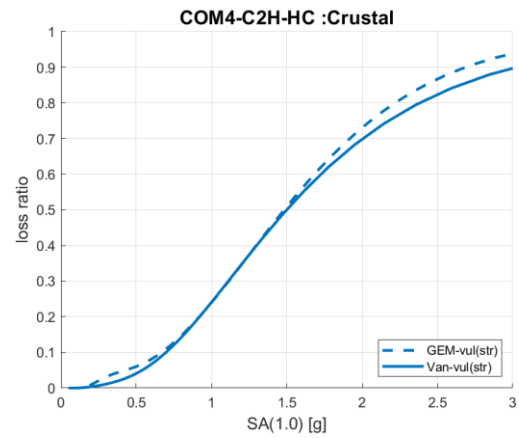
(c)



(d)

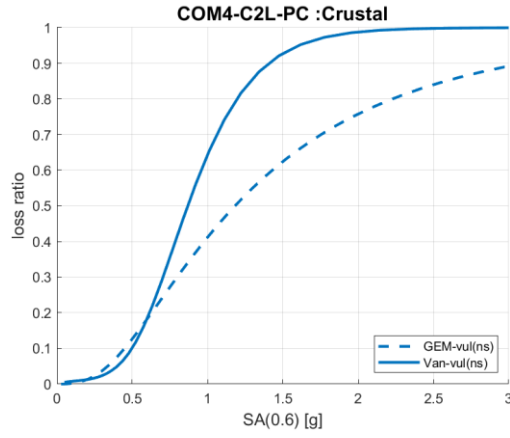


(e)

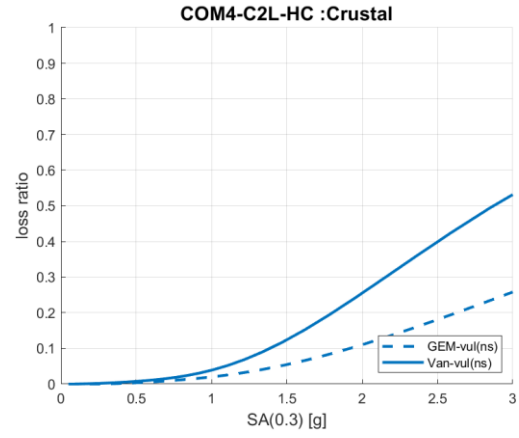


(f)

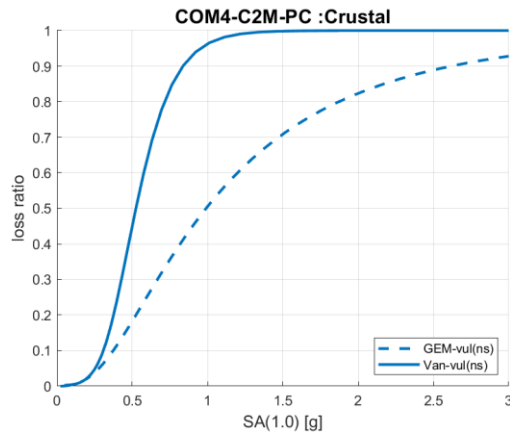
Figure 4.37 Comparison of GEM structural vulnerability curves (GEM-) to BC crustal structural vulnerability curves (Van-): (a)C2L-PC (b) C2L-HC (c) C2M-PC (d) C2M-HC (e) C2H-PC (f) C2H-HC



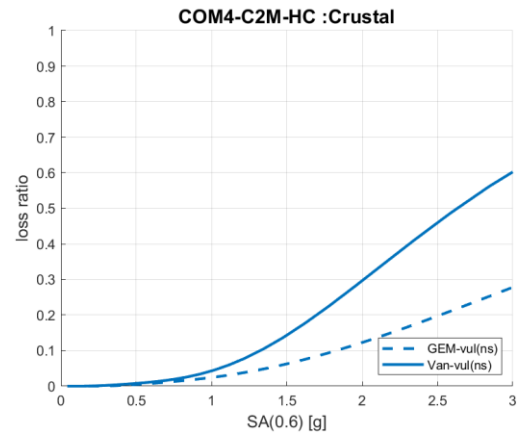
(a)



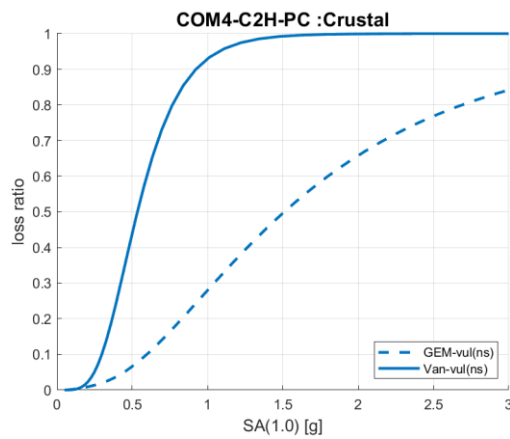
(b)



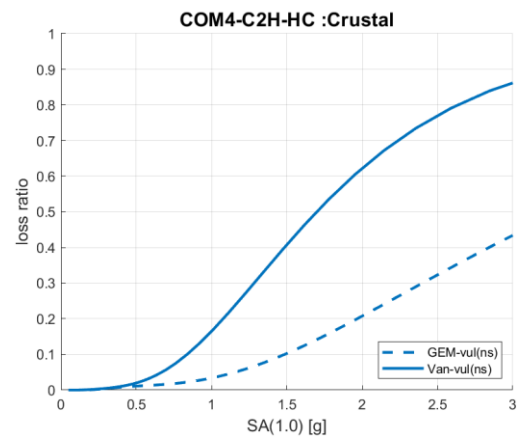
(c)



(d)

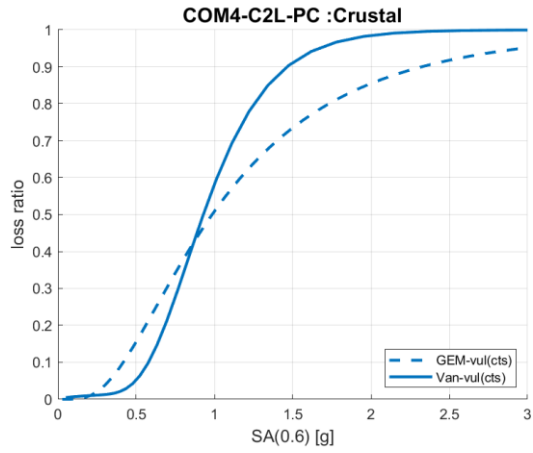


(e)

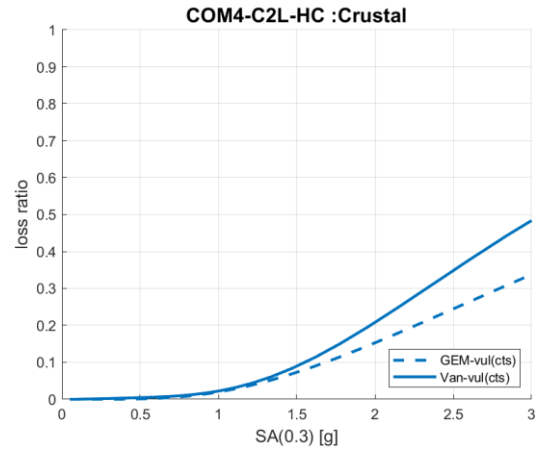


(f)

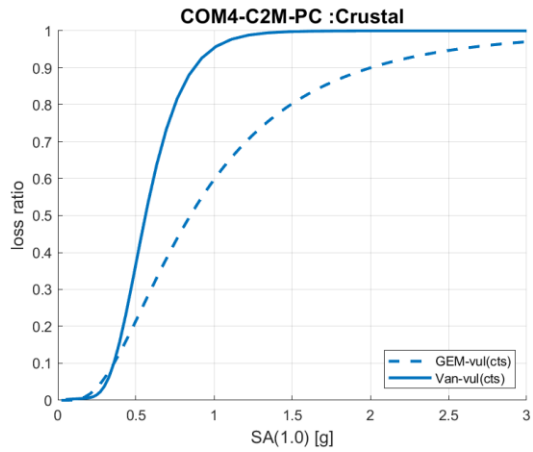
Figure 4.38 Comparison of GEM non-structural vulnerability curves (GEM-) to BC crustal non-structural vulnerability curves (Van-): (a)C2L-PC (b) C2L-HC (c) C2M-PC (d) C2M-HC (e) C2H-PC (f) C2H-HC



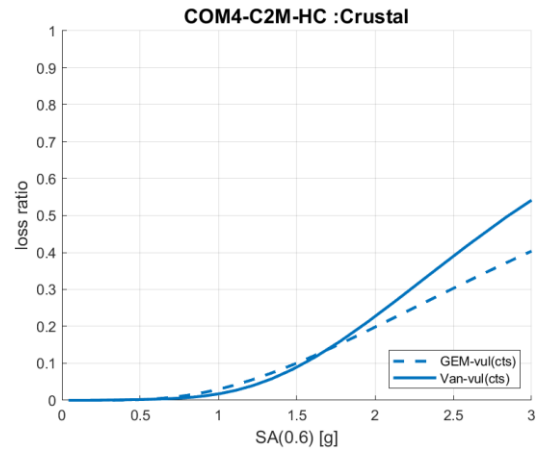
(a)



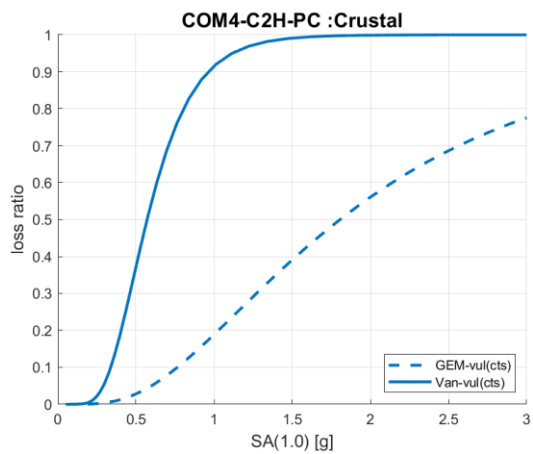
(b)



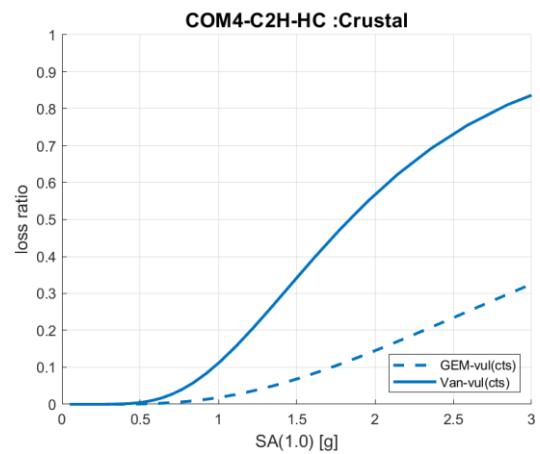
(c)



(d)



(e)



(f)

Figure 4.39 Comparison of GEM contents vulnerability curves (GEM-) to BC contents non-structural vulnerability curves (Van-): (a)C2L-PC (b) C2L-HC (c) C2M-PC (d) C2M-HC (e) C2H-PC (f) C2H-HC

Structural vulnerability functions comparison: Other than for C2H-HC, BC-specific crustal structural vulnerability functions tend to estimate higher losses than corresponding GEM functions at a given intensity of ground shaking, as is seen in Figure 4.37. Figure 4.37a-e shows that the median structural loss ratio capacity (spectral acceleration at which a structural loss ratio of 50% is reached) for GEM functions are relatively higher than that of BC-specific functions. The median structural loss ratio capacity decreases by 35%, 40 % and 31% for BC C2L-PC, C2M-PC and C2H-PC typologies and by 36% and 42% for BC C2L-HC and C2M-HC typologies as compared to corresponding GEM typologies. However, Figure 4.37f shows that GEM C2H-HC structural vulnerability functions estimate slightly higher loss ratios than their BC counterpart. At $S_a(1.0)$ of 0.425g in Vancouver, -according to NBCC 2015- the GEM structural vulnerability function estimates twice (0.05%) the losses than the BC structural vulnerability function (0.025%). The median structural loss ratio capacity for BC-specific C2H-HC is 1.1% lower than that for GEM C2H-HC.

Non-structural vulnerability functions comparison: Figure 4.38 shows that BC-specific crustal non-structural vulnerability functions tend to estimate higher losses than corresponding GEM functions at a given intensity of ground shaking. The median non-structural loss ratio capacity for BC functions is lower than corresponding GEM functions by 27% ,47% and 65% for C2L-PC, C2M-PC and C2H-PC typologies (Figure 4.38a, c, e) and by 38%, 40% and 48% for C2L-HC, C2M-HC and C2H-HC typologies Figure 4.38b, d, f). A large difference in estimated non-structural loss will be seen when using BC C2H-PC and C2H-HC crustal non-structural vulnerability functions, as compared to when using corresponding GEM functions.

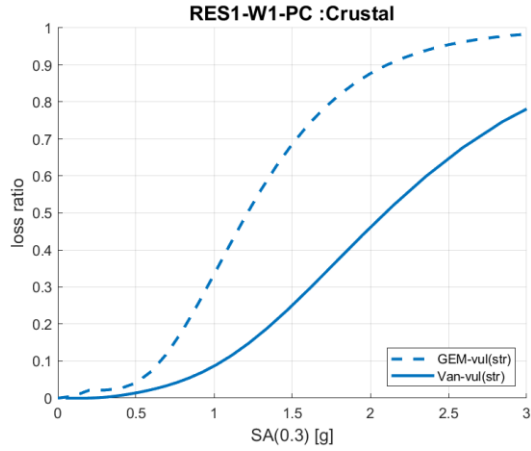
Contents vulnerability functions comparison: Figure 4.39 shows that BC-specific crustal contents vulnerability functions tend to estimate higher losses than corresponding GEM functions at a given intensity of ground shaking, except for C2L-PC, C2M-PC and C2M-HC typologies at low intensity of ground shaking (Figure 4.39a, c, d). The median non-structural loss ratio capacity for BC functions is lower than corresponding GEM functions by 6%, 33% and 69% for C2L-PC, C2M-PC and C2H-PC typologies (Figure 4.39a a, c, e) and by 23%, 19% and 55% for C2L-HC, C2M-HC and C2H-HC typologies (Figure 4.39b, d, f). This means that a large difference in estimated contents loss will be seen when using BC C2H-PC and C2H-HC crustal contents vulnerability functions, as compared to when using corresponding GEM functions.

4.6.2 Wood typologies

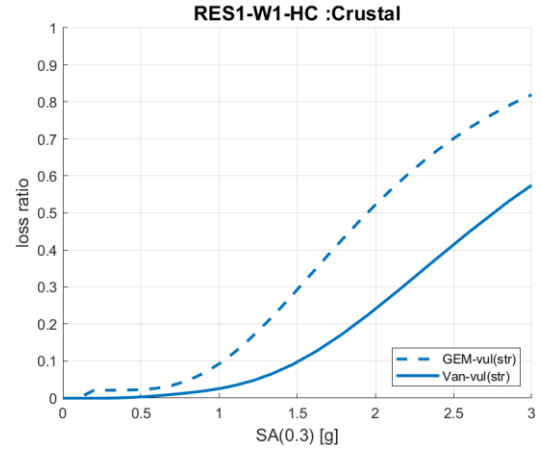
Figure 4.40 compares the GEM structural vulnerability functions to corresponding crustal BC-specific functions for W1, W2 and W3 PC and HC typologies respectively.

Figure 4.41 compares the GEM non-structural vulnerability functions to corresponding crustal BC-specific functions for W1, W2 and W3 PC and HC typologies respectively.

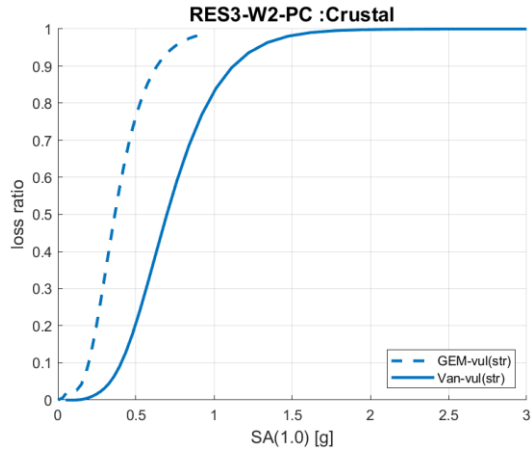
Figure 4.42 compares the GEM contents vulnerability functions to corresponding crustal BC-specific functions for W1, W2 and W3 PC and HC typologies respectively.



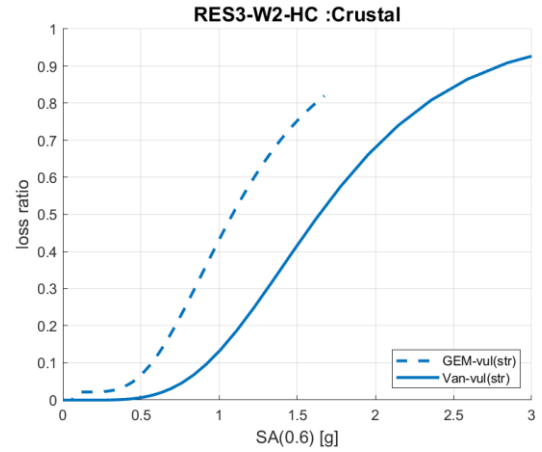
(a)



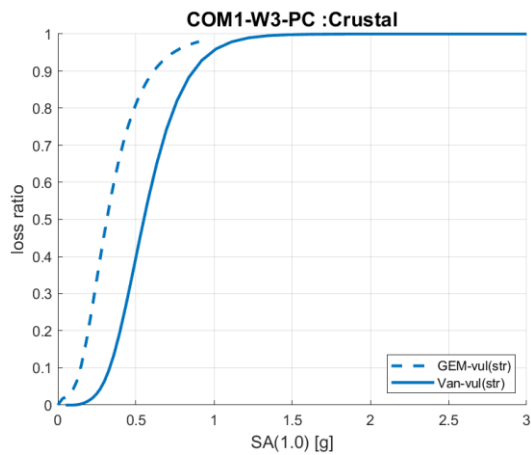
(b)



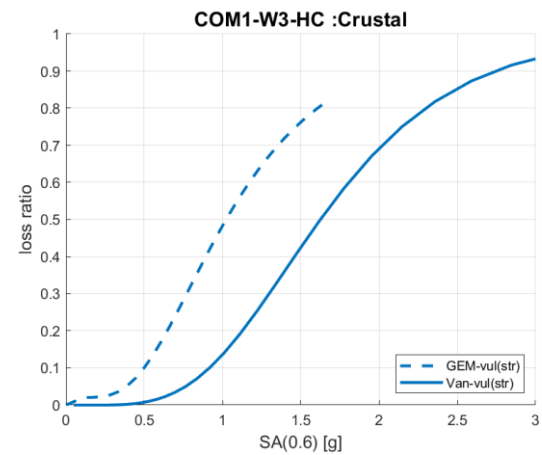
(c)



(d)

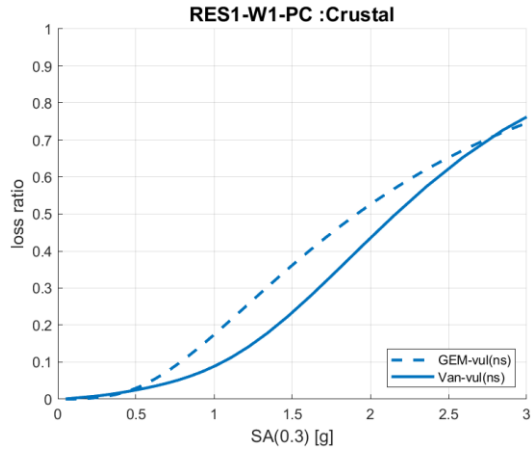


(e)

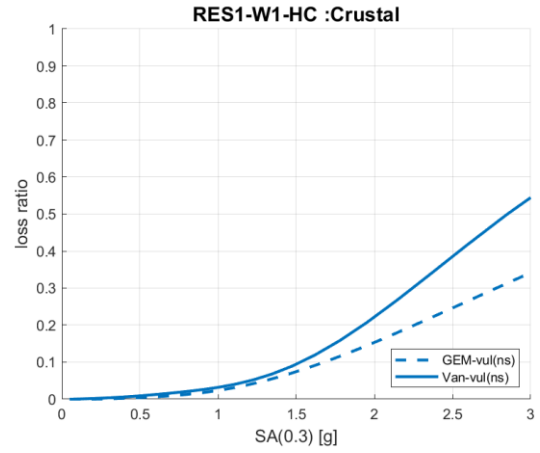


(f)

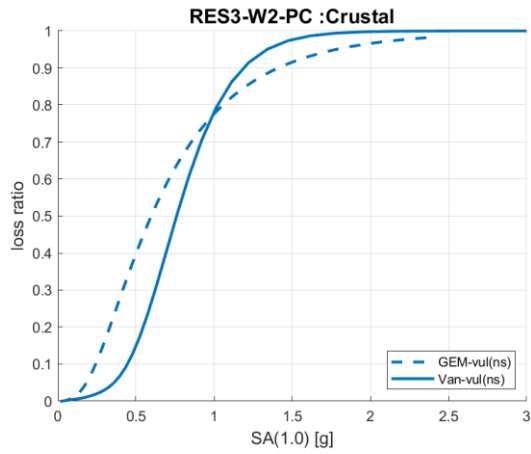
Figure 4.40 Comparison of GEM structural vulnerability curves (GEM-) to BC crustal structural vulnerability curves (Van-): (a)W1-PC (b) W1-HC(c)W2-PC (d) W2-HC (e)W3-PC (f) W3-HC



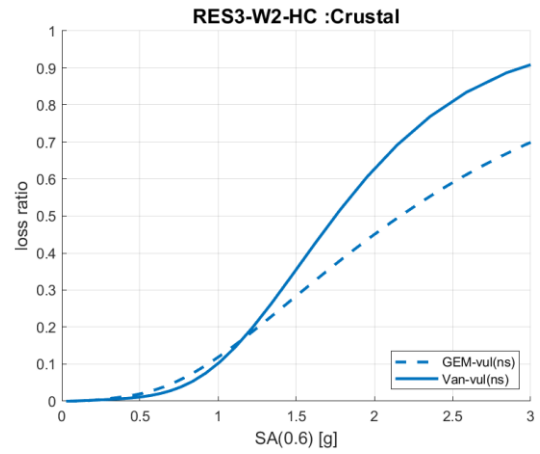
(a)



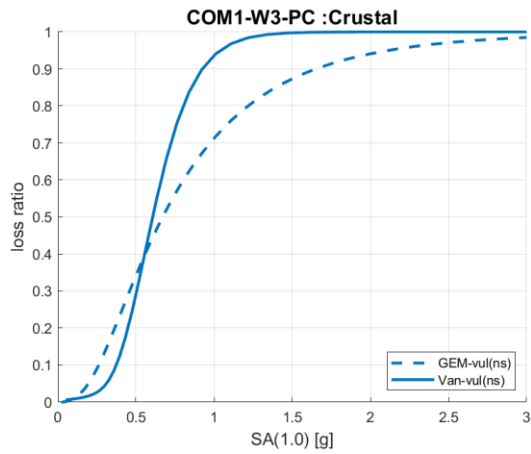
(b)



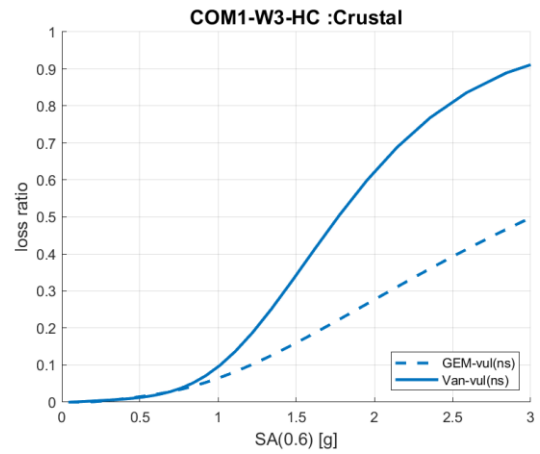
(c)



(d)

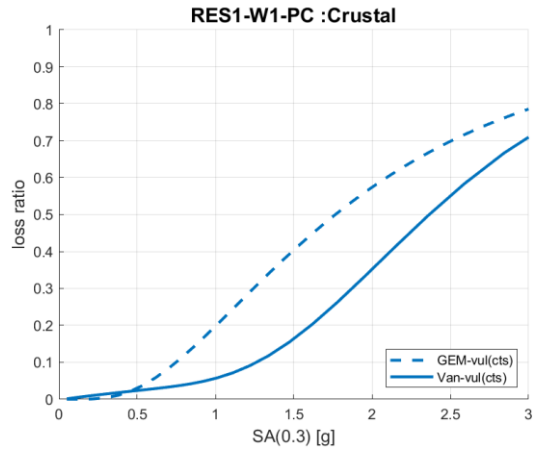


(e)

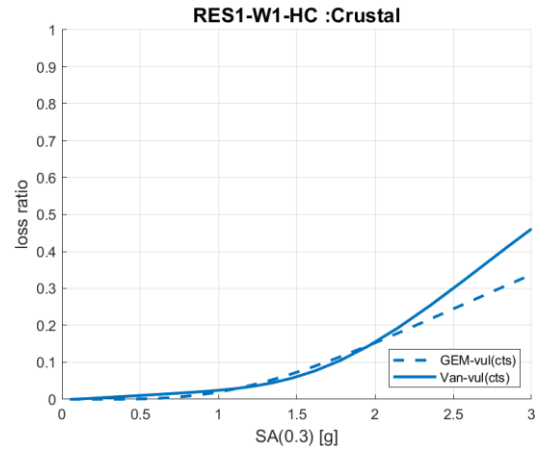


(f)

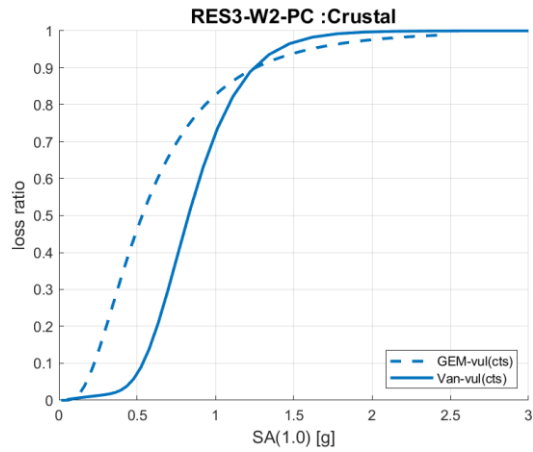
Figure 4.41 Comparison of GEM non-structural vulnerability curves (GEM-) to BC crustal non-structural vulnerability curves (Van-): (a)W1-PC (b) W1-HC(c)W2-PC (d) W2-HC (e)W3-PC (f) W3-HC



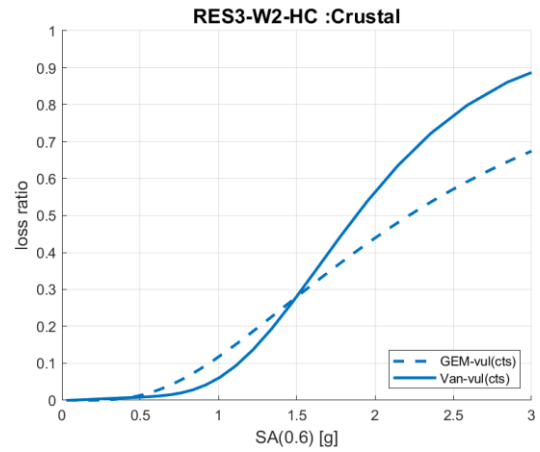
(a)



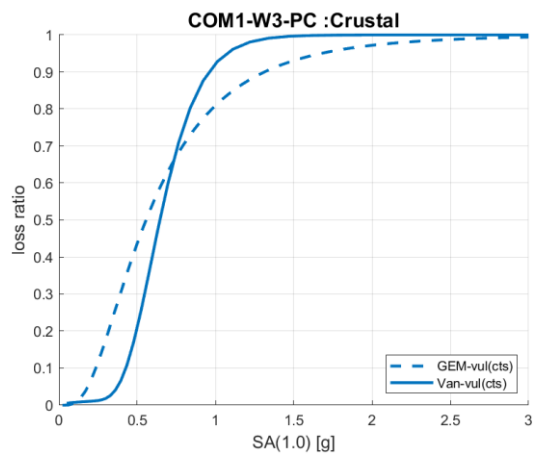
(b)



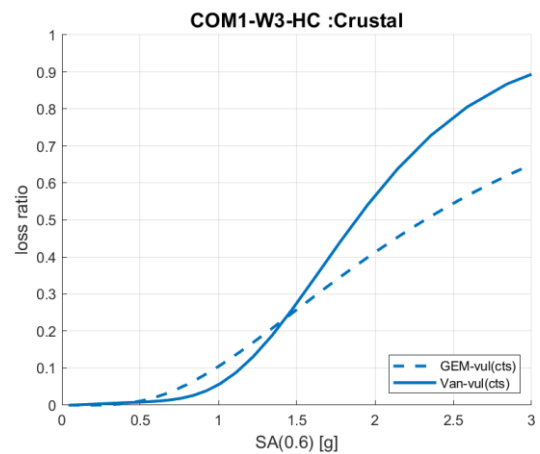
(c)



(d)



(e)



(f)

Figure 4.42 Comparison of GEM contents vulnerability curves (GEM-) to BC crustal contents vulnerability curves (Van-): (a)W1-PC (b) W1-HC(c)W2-PC (d) W2-HC (e)W3-PC (f) W3-HC

Structural vulnerability functions comparison: Other than for W4c-PC, GEM crustal structural vulnerability functions tend to estimate higher losses than corresponding BC functions at a given intensity of ground shaking, as is seen in Figure 4.40. The median structural loss ratio capacity for BC-specific functions is relatively higher than that of GEM functions. The median structural loss ratio capacity decreases by 71.8% 93.5% and 75% for GEM W1-PC, W2-PC and W3-PC typologies and by 41.9%, 52.2% and 58.7% for W1-HC, W2-HC and W3-HC typologies as compared to corresponding BC typologies. The median structural loss ratio capacity decreases by 8.3% for BC W4c-PC as compared to corresponding GEM typologies.

Non-structural vulnerability functions comparison: Figure 4.41 shows that except for W1, W2 and W3 PC, BC-specific crustal non-structural vulnerability functions tend to estimate higher losses than corresponding GEM functions at a given intensity of ground shaking. For HC wood structures, median non-structural loss ratio capacity for BC functions is lower than corresponding GEM functions by 38%, 23% and 71% for W1-HC, W2-HC and W3-HC typologies (Figure 4.41b, d, f). For W1, W2 and W3 PC, at the ground shaking intensities of interest, the GEM non-structural vulnerability functions estimate higher losses than corresponding BC functions. For PC wood structures, median non-structural loss ratio capacity for GEM functions is lower than corresponding BC functions by 13% and 27% for W1-PC and W2-PC typologies (Figure 4.41a, e), and higher by 10.2% for W3-PC typology (Figure 4.41f).

Contents vulnerability functions comparison: Figure 4.42 shows that pre-code BC crustal contents vulnerability functions tend to estimate lower losses than corresponding GEM functions at a given intensity of ground shaking. The median non-structural loss ratio capacity for pre-code GEM contents vulnerability functions is lower than corresponding BC functions by 37%

56% and 17% for W1-PC, W2-PC and W3-PC typologies (Figure 4.42a, c, e). The median non-structural loss ratio capacity for high-code BC contents vulnerability functions is lower than corresponding BC functions by 26.5%, 18.4% and 23.3% for W1-HC, W2-HC and W3-HC typologies (Figure 4.42b, d, f).

Figure 4.43 summarizes how the structural vulnerability curves for low-rise residential wood construction changes as it accounts for a subfloor or a cripple wall. Since W4c is more susceptible to damage than a subfloor, with W1 being least damage prone under the same intensity of ground shaking, loss ratio of low-rise residential wood buildings with a cripple wall is higher than from that with a subfloor. It is seen that the median loss ratio decreases by 45% in the presence of a cripple wall, and by 28% in the presence of a subfloor, as compared to W1-PC.

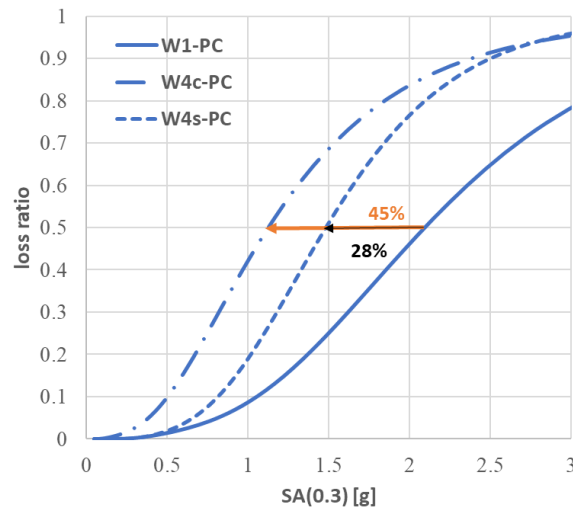


Figure 4.43 Comparison of structural vulnerability curves of W4c, W4s and W1 PC typologies

4.7 Comparison of BC-specific crustal and subduction vulnerability curves (objective 3)

The BC-specific crustal and subduction vulnerability functions are compared and the effects of the long duration subduction ground motions on the vulnerability curves for

representative building typologies are discussed hereon. As in the case for the DS4 fragility curves, the loss ratio estimated under subduction ground motions is higher than the loss ratio estimated by crustal vulnerability curves, given an intensity of ground motion. The effects of the long duration subduction ground motions on the vulnerability curves are more pronounced in buildings built after 1990 (i.e., MC and HC).

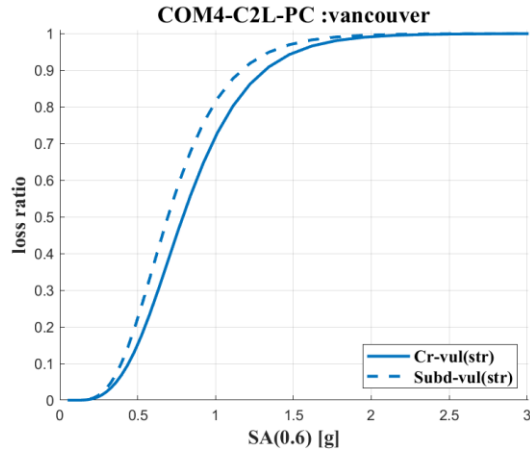
4.7.1 Concrete typologies

Figure 4.44, compares the BC-specific concrete shear wall (C2) crustal (prefix: Cr-) structural vulnerability functions to corresponding BC-specific subduction (prefix: Subd-) functions for PC and HC typologies, respectively.

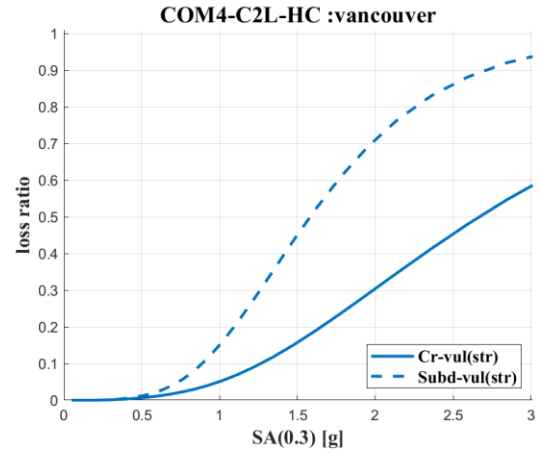
Figure 4.45, compares the BC-specific concrete shear wall (C2) crustal (prefix: Cr-) non-structural vulnerability functions to corresponding BC-specific subduction (prefix: Subd-) functions for PC and HC typologies, respectively.

Figure 4.46, compares the BC-specific concrete shear wall (C2) crustal (prefix: Cr-) contents vulnerability functions to corresponding BC-specific subduction (prefix: Subd-) functions for PC and HC typologies, respectively.

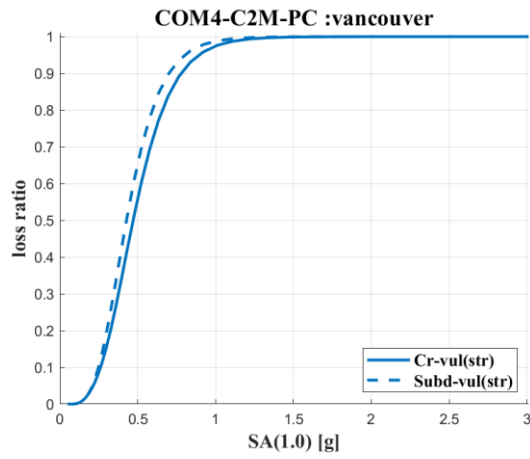
These figures show that C2 BC-specific subduction vulnerability curves estimate higher losses than corresponding BC-specific crustal vulnerability functions, given an intensity of ground shaking.



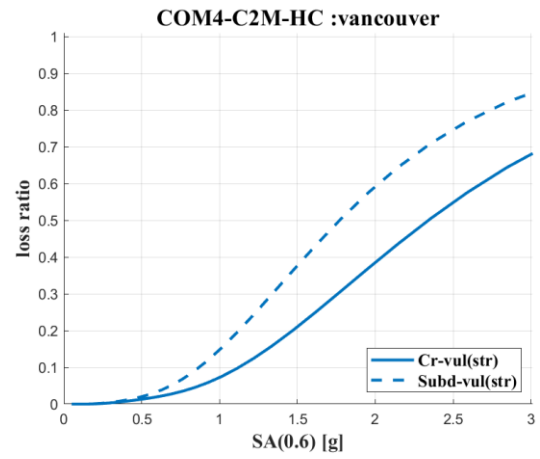
(a)



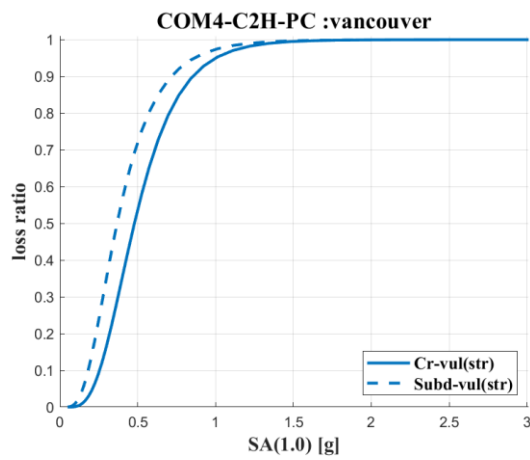
(b)



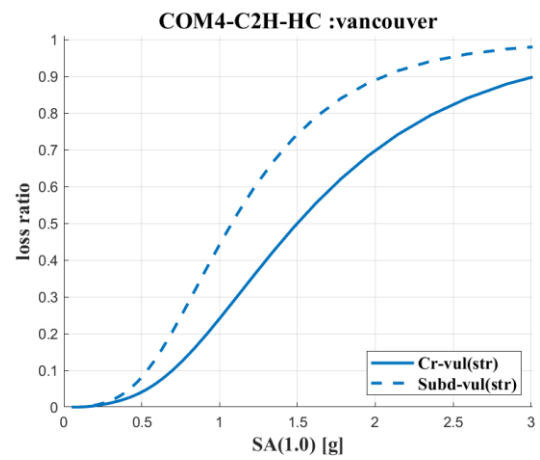
(c)



(d)

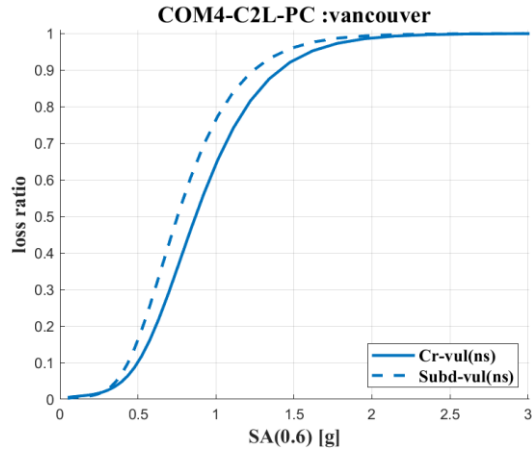


(e)

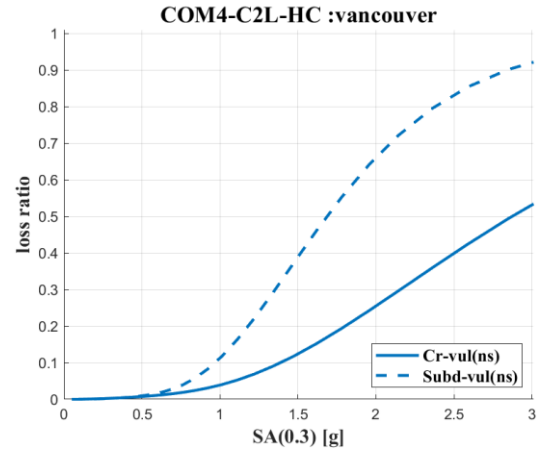


(f)

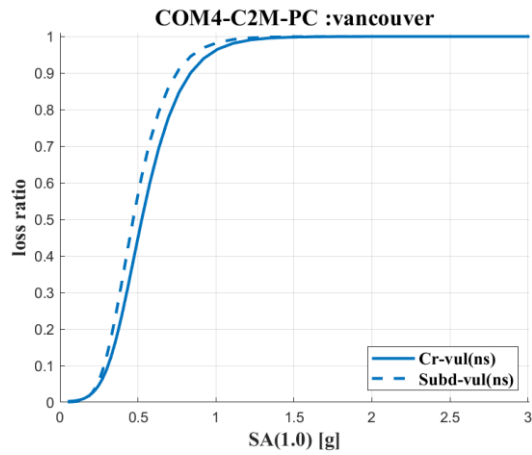
Figure 4.44 Comparison of BC-specific crustal (Cr-) and subduction (Subd-) structural vulnerability curves (Van-): (a)C2L-PC (b) C2L-HC (c) C2M-PC (d) C2M-HC (e) C2H-PC (f) C2H-HC



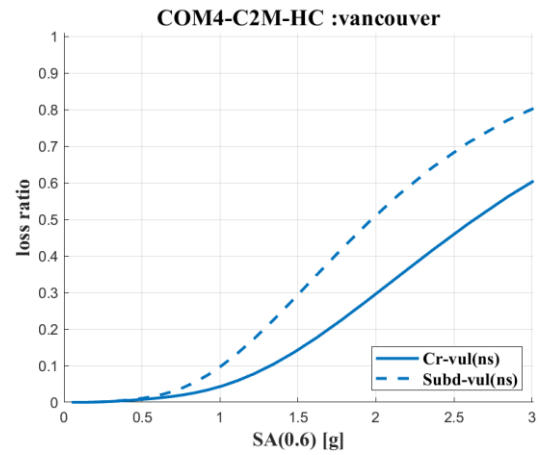
(a)



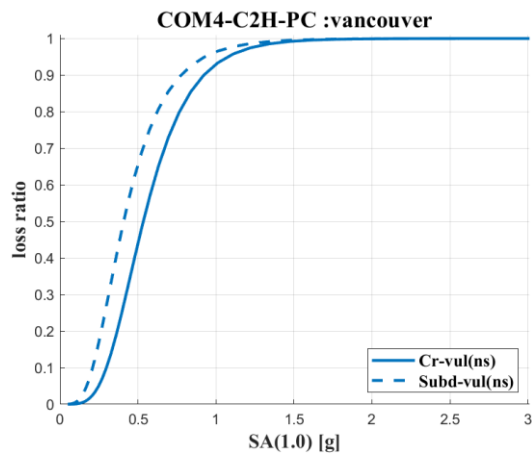
(b)



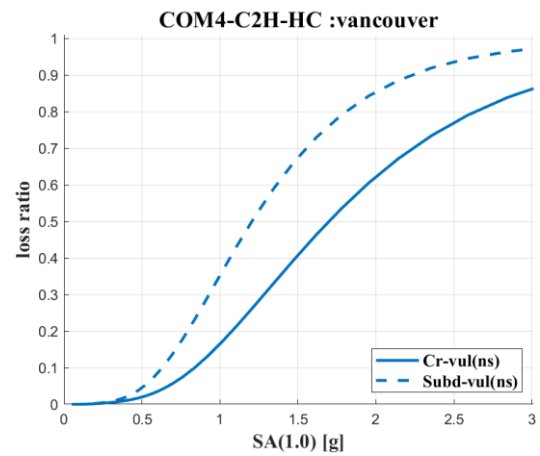
(c)



(d)

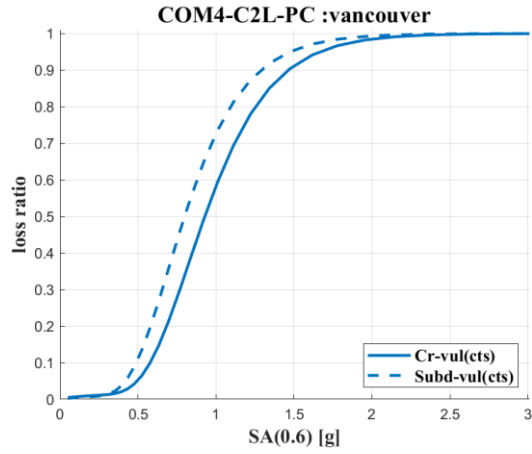


(e)

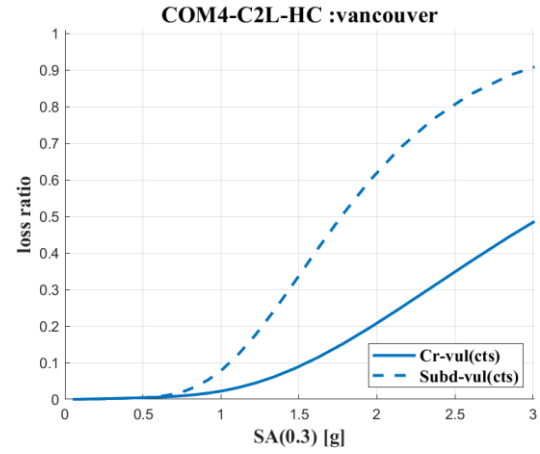


(f)

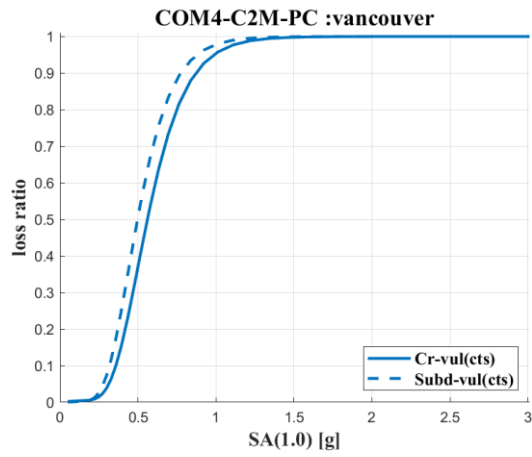
Figure 4.45 Comparison of BC-specific crustal (Cr-) and subduction (Subd-) non-structural vulnerability curves for Vancouver: (a)C2L-PC (b) C2L-HC (c) C2M-PC (d) C2M-HC (e) C2H-PC (f) C2H-HC



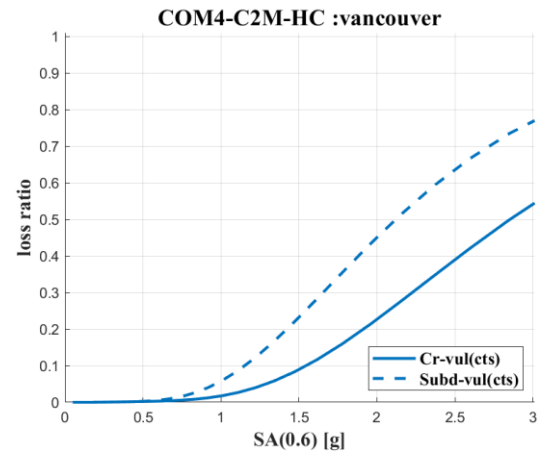
(a)



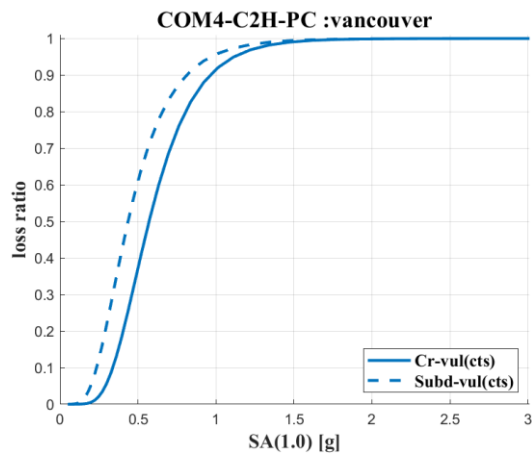
(b)



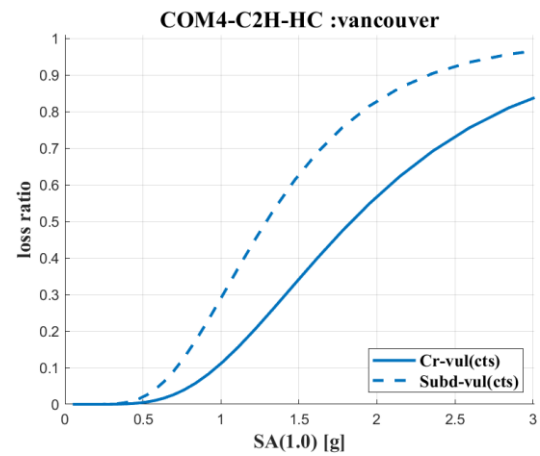
(c)



(d)



(e)



(f)

Figure 4.46 Comparison of BC-specific crustal (Cr-) and subduction (Subd-) contents vulnerability curves for Vancouver: (a)C2L-PC (b) C2L-HC (c) C2M-PC (d) C2M-HC (e) C2H-PC (f) C2H-HC

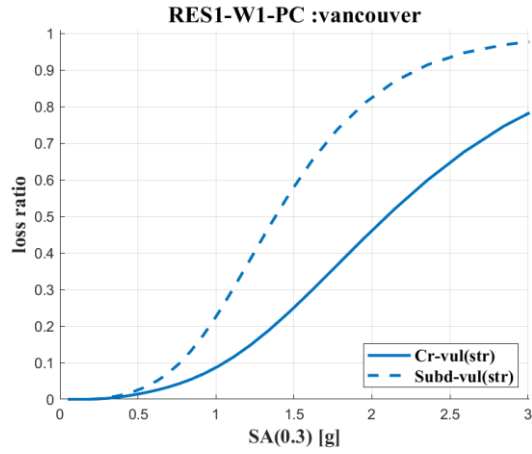
Structural vulnerability functions comparison: From Figure 4.44, it is seen that the median structural loss ratio capacity for BC-specific subduction structural vulnerability functions is lower than corresponding crustal functions by 13% ,9% and 24% for C2L-PC, C2M-PC and C2H-PC typologies (Figure 4.44a, c, e) and by 41%, 25% and 28% for C2L-HC, C2M-HC and C2H-HC typologies (Figure 4.44b, d, f).

Non-structural vulnerability functions comparison: From Figure 4.45, it is seen that the median non-structural loss ratio capacity for BC-specific subduction non-structural vulnerability functions is lower than corresponding crustal functions by 14% ,10% and 24% for C2L-PC, C2M-PC and C2H-PC typologies (Figure 4.45a, c, e) and by 41%, 25% and 29% for C2L-HC, C2M-HC and C2H-HC typologies (Figure 4.45b, d, f).

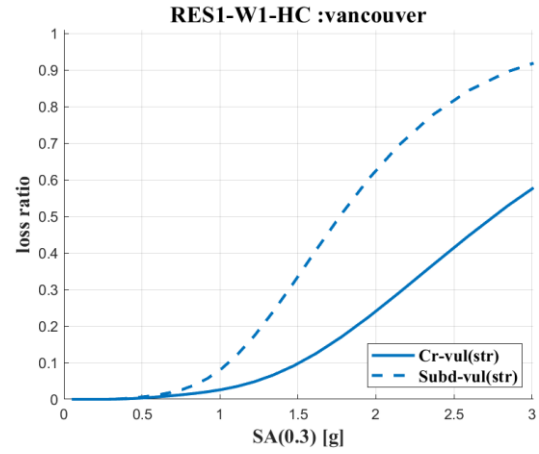
Contents vulnerability functions comparison: From Figure 4.46, it is seen that the median contents loss ratio capacity for BC-specific subduction contents vulnerability functions is lower than corresponding crustal functions by 14% ,11% and 23% for C2L-PC, C2M-PC and C2H-PC typologies (Figure 4.46a, c, e) and by 42%, 25% and 30% for C2L-HC, C2M-HC and C2H-HC typologies (Figure 4.46b, d, f).

4.7.2 Wood typologies

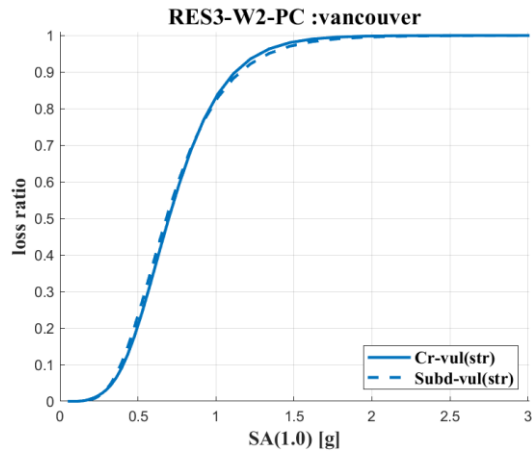
Figure 4.47, Figure 4.48 and Figure 4.49 compares the BC-specific wood crustal (prefix: Cr-) structural, non-structural and contents vulnerability functions to corresponding BC-specific wood subduction (prefix: Subd-) functions for PC and HC typologies, respectively. These figures show that BC-specific subduction vulnerability curves estimate higher losses than corresponding BC-specific crustal vulnerability functions, given an intensity of ground shaking.



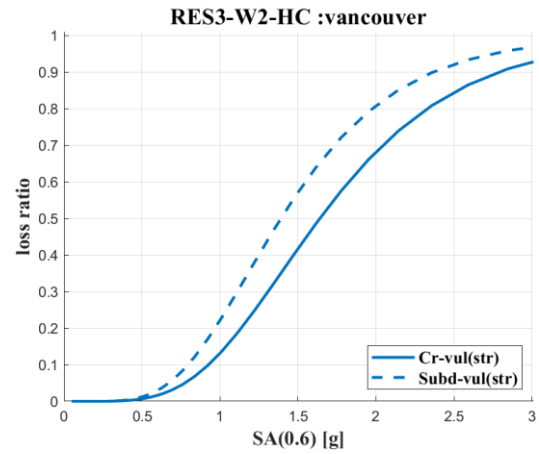
(a)



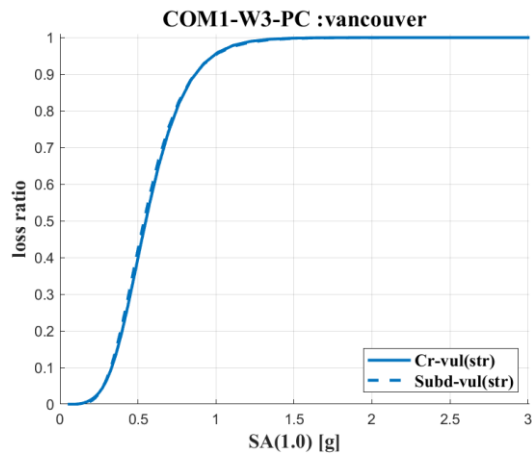
(b)



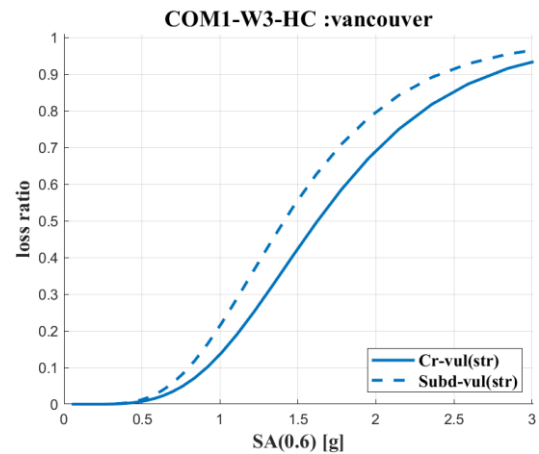
(c)



(d)

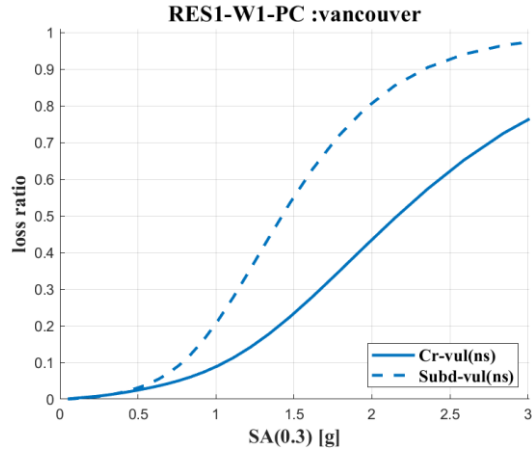


(e)

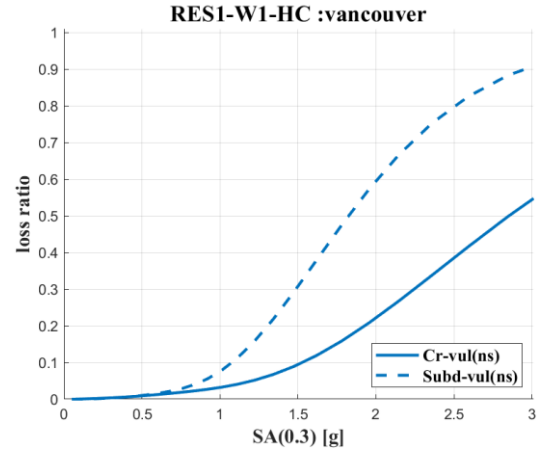


(f)

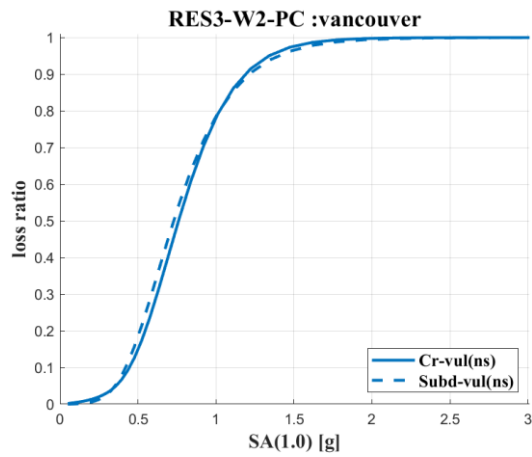
Figure 4.47 Comparison of BC-specific crustal (Cr-) and subduction (Subd-) structural vulnerability curves for Vancouver for (a)W1-PC (b) W1-HC(c)W2-PC (d) W2-HC (e)W3-PC (f) W3-HC



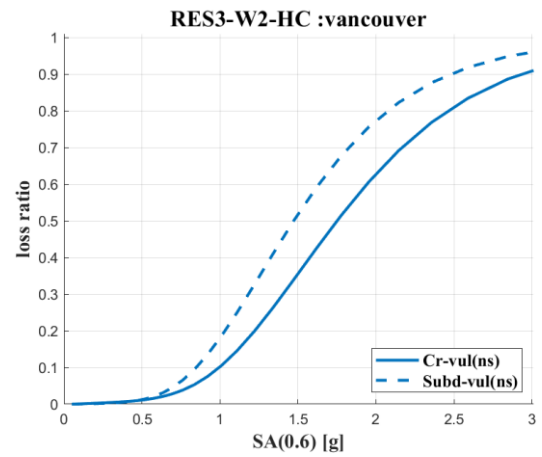
(a)



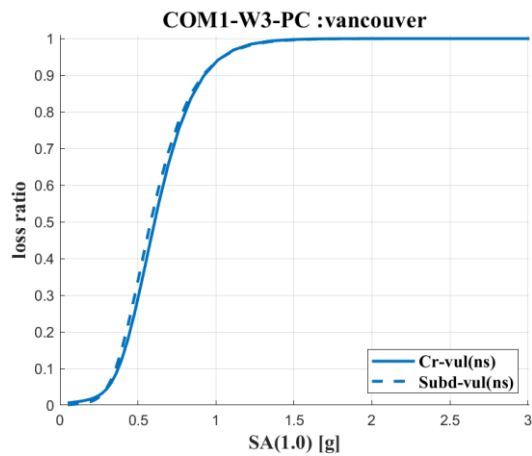
(b)



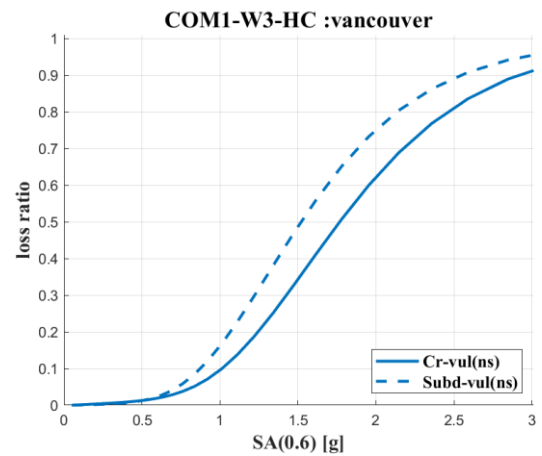
(c)



(d)

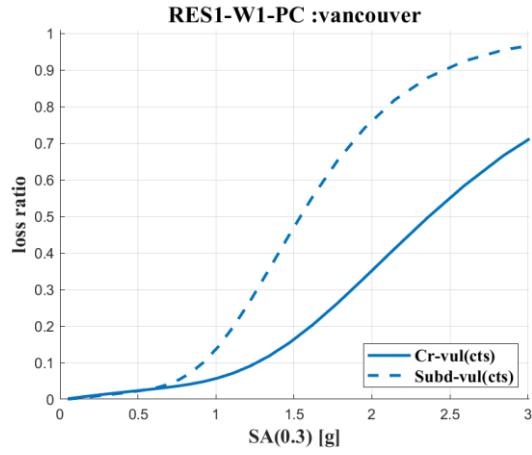


(e)

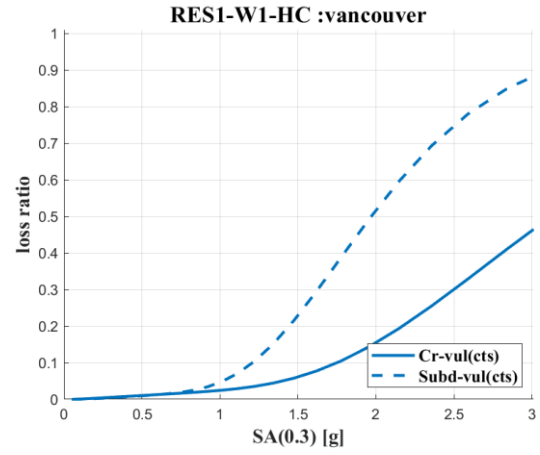


(f)

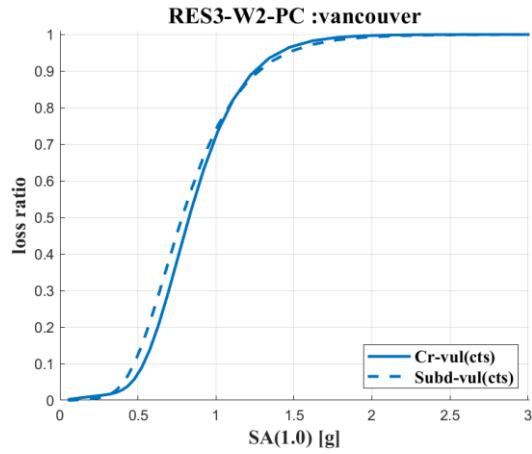
Figure 4.48 Comparison of BC-specific crustal (Cr-) and subduction (Subd-) nonstructural vulnerability curves for Vancouver for (a)W1-PC (b) W1-HC(c)W2-PC (d) W2-HC (e)W3-PC (f) W3-HC



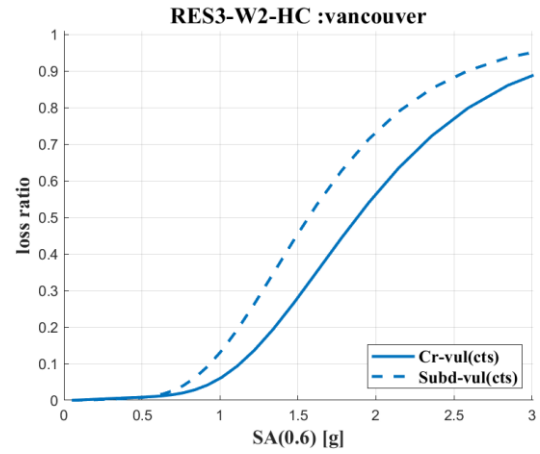
(a)



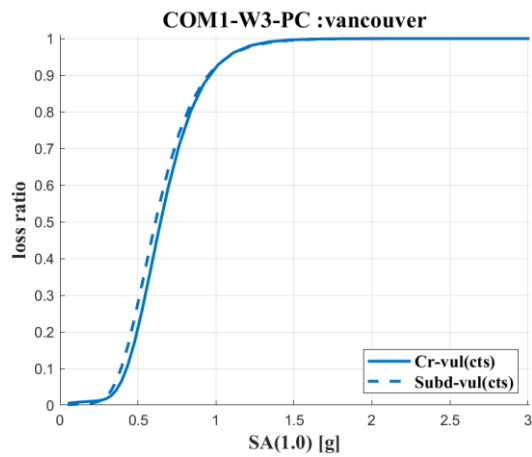
(b)



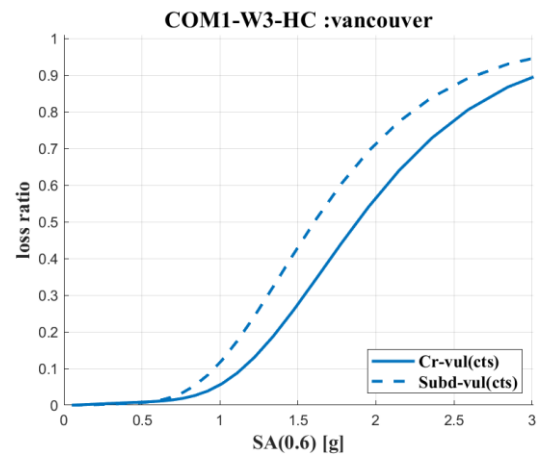
(c)



(d)



(e)



(f)

Figure 4.49 Comparison of BC-specific crustal (Cr-) and subduction (Subd-) contents vulnerability curves for Vancouver for (a)W1-PC (b) W1-HC(c)W2-PC (d) W2-HC (e)W3-PC (f) W3-HC

Structural vulnerability functions comparison: From Figure 4.47, it is seen that the median structural loss ratio capacity for BC-specific subduction structural vulnerability functions is lower than corresponding crustal functions by 34% ,1% and 1% for W1-PC, W2-PC and W3-PC typologies (Figure 4.47a, c, e) and by 36%, 15% and 13% for W1-HC, W2-HC and W3-HC typologies (Figure 4.47b, d, f).

Non-structural vulnerability functions comparison: From Figure 4.48, it is seen that the median non-structural loss ratio capacity for BC-specific subduction non-structural vulnerability functions is lower than corresponding crustal functions by 34% , 5% and 5% for W1-PC, W2-PC and W3-PC typologies (Figure 4.48a, c, e) and by 36%, 15% and 11% for W1-HC, W2-HC and W3-HC typologies (Figure 4.48b, d, f).

Contents vulnerability functions comparison: From Figure 4.49, it is seen that the median contents loss ratio capacity for BC-specific subduction contents vulnerability functions is lower than corresponding crustal functions by 35%, 6% and 5% for W1-PC, W2-PC and W3-PC typologies (Figure 4.49a, c, e) and by 37%, 17% and 15% for W1-HC, W2-HC and W3-HC typologies (Figure 4.49b, d, f).

It is seen that the effect of the long duration subduction ground motions on vulnerability functions is more pronounced in low-rise wood construction (with or without cripple wall and subfloors, than in multi-story residential and commercial and industrial wood construction.

4.8 Verification of vulnerability functions (objective 3)

The average annual loss ratios (AALR) for Vancouver were computed using 200 logic tree branches, 25 stochastic event sets per branch, and a risk investigation time of 1 year for an effective investigation time of 5000 years, using the 2015 GSC seismic hazard model for both GEM and

BC-specific vulnerability curves. Table 4.2 and 4.3 tabulates the AALRs for wood and C2 typologies in Vancouver using BC-specific functions (AALR_BC-specific) and GEM functions (AALR_GEM).

Table 4.2 Comparison of AALR values for wood building typologies in Vancouver, using GEM and BC-specific vulnerability functions

BC-Typology	AALR_GEM [%]	AALR_BC-specific [%]
W1-HC	0.02	0.01
W1-LC	0.05	0.03
W1-MC	0.02	0.01
W1-PC	0.05	0.03
W2-HC	0.02	0.01
W2-LC	0.05	0.03
W2-MC	0.02	0.01
W2-PC	0.05	0.03
W3-HC	0.05	0.01
W3-LC	0.10	0.04
W3-MC	0.05	0.01
W3-PC	0.11	0.04
W4c-HC	0.02	0.03
W4c-LC	0.05	0.07
W4c-MC	0.02	0.03
W4c-PC	0.05	0.07
W4s-HC	0.02	0.01
W4s-LC	0.05	0.03
W4s-MC	0.02	0.01
W4s-PC	0.05	0.03

Table 4.3 Comparison of AALR values for C2 building typologies in Vancouver, using GEM and BC-specific vulnerability functions

BC-Typology	AALR_GEM [%]	AALR_BC-specific [%]
C2H-HC	0.01	0.01
C2H-LC	0.02	0.05
C2H-MC	0.01	0.02
C2H-PC	0.03	0.05
C2L-HC	0.00	0.01
C2L-LC	0.02	0.05
C2L-MC	0.01	0.02
C2L-PC	0.02	0.05
C2M-HC	0.00	0.00
C2M-LC	0.02	0.05
C2M-MC	0.00	0.02
C2M-PC	0.02	0.05

From the global study referred to in section 3.3.4, AALR for wood typologies in a moderate seismic zone (Lisbon) are about 0.03% and for concrete shear wall construction are about 0.04%. A comparison of these AALRs obtained shows that older concrete typologies in Vancouver has a higher-than-expected AALR. This is owing to the definition of non-structural and contents vulnerability functions, which were tied to the probability of exceedance of DS4. It is seen that the older C2 buildings are highly susceptible to damage, and hence, large loss functions are derived for them. This could also be due to the difference in construction practices between these regions. For wood typologies, except for cripple wall cases (W4c) and W3, the AALR is similar to that seen in Lisbon and within reasonable bounds. The AALR seen for W4c is highest, and signifies that low-rise wood construction built over poorly designed cripple walls can drive damage and losses in a region, if it is the primary construction case. Thus, W4c along with C2 and W3 buildings

built before the 1990s in Vancouver are identified as vulnerable building typologies and should be prioritized for seismic retrofitting and upgrading.

4.9 Scenario analysis for Vancouver (objective 4)

The results of scenario analyses for Vancouver are summarized in this section.

The Vancouver building stock distribution by construction year and occupancy is provided in Figure 4.50 to better understand the scenario results. For example, introduction of fragility functions for W4s typology that estimates more damage, when combined with the information in Figure 4.50a means that much more damages will be accounted for when W4s buildings are recognized within the building stock, and from Figure 4.50b, contribution to total damage from residential SFDs increases.

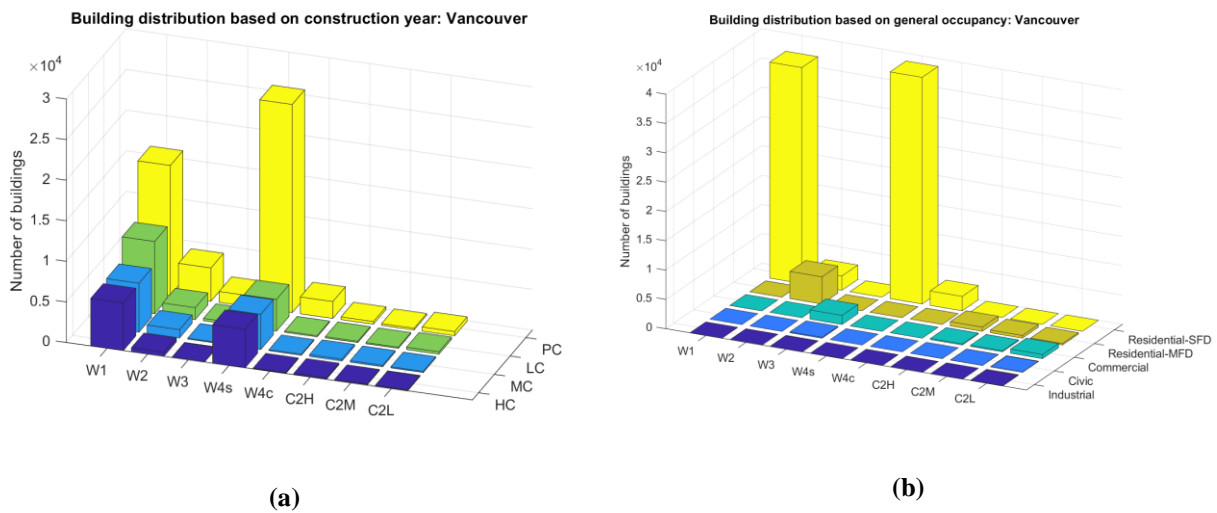


Figure 4.50 Vancouver building stock distribution per per typology based on (a) year of construction (b) general occupancy class

The spatial distribution of building stock in Vancouver is provided in Figure 4.51.

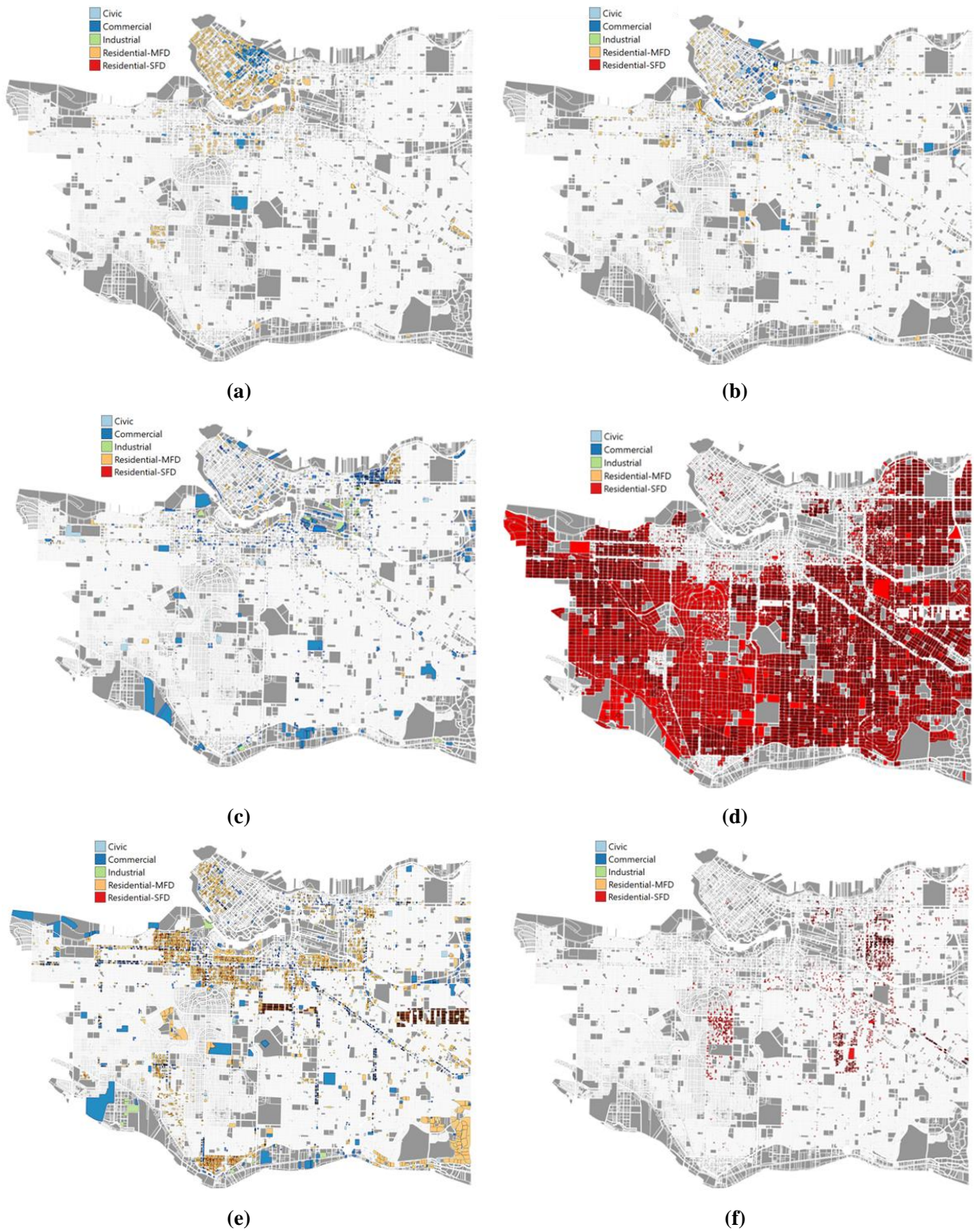


Figure 4.51 Geographic distribution of prominent BC-typologies in Vancouver. (a) C2H (b) C2M (d) C2L (d) W1 and W4s (e)W2 and W3 and (f) W4c

Figure 4.51 shows that older constructions of a specific typology are concentrated to geographical pockets within Vancouver. Older residential C2 construction, mostly high-rise and mid-rise are concentrated in the West-end, Fairview and Kerrisdale, while there are a significant number of older commercial buildings in Downtown Vancouver. Scenario Analysis results pick up these regions as regions of larger damage and loss implications, as well as the cripple wall structures in Shaughnessy, and sub-floor wood construction in West Point Grey and Kitsilano. The W2-PC and W3-PC buildings in south Kitsilano, Sunset, Marpole and Champlain Heights are also identified as pockets in Vancouver that show higher damages and losses.

4.9.1 Crustal scenario (GSM7.3)

A summary of damages and losses to the Vancouver building stock for the three analyses described in section 3.4.1 are shown in Figures 4.52 to 4.57, and the percentage of damage and loss to the building stock estimated for each case are plotted in Figures 4.58 to 4.60. While the damage distribution maps show the distribution of the complete damage state, the loss distribution map highlights the highest individual asset loss that contribute to 50% of the total loss. (Note: The scales of the maps are intentionally set so as to easily and better distinguish the pockets of change in damage and loss analysis when considering the new fragility and vulnerability functions).

Case 1 (GSM7.3, GEM): The Georgia strait M7.3 crustal scenario (GSM7.3) is run using fragility and vulnerability curves developed by GEM for use in Canada. The spatial distribution of complete damage state in Vancouver following the GSM7.3 scenario analysis using the GEM fragility functions is shown in Figure 4.52. The spatial distribution of losses (the highest individual asset losses that contribute to the 50% total loss) in Vancouver following the GSM7.3 scenario analysis using the GEM vulnerability functions is shown in Figure 4.53.

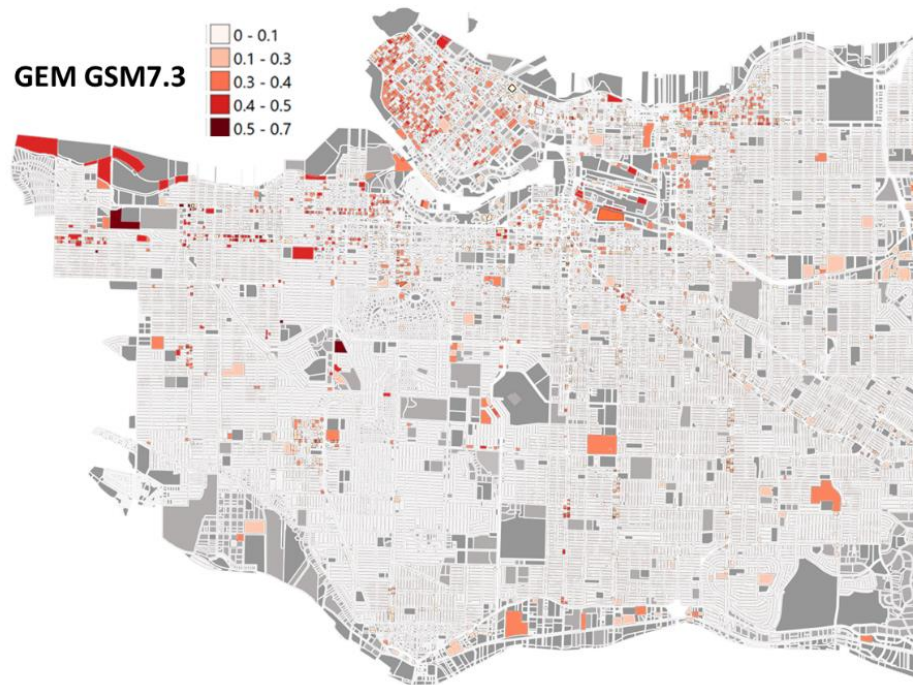


Figure 4.52 GSM7.3 Complete damage state distribution map for Vancouver, using GEM fragility functions

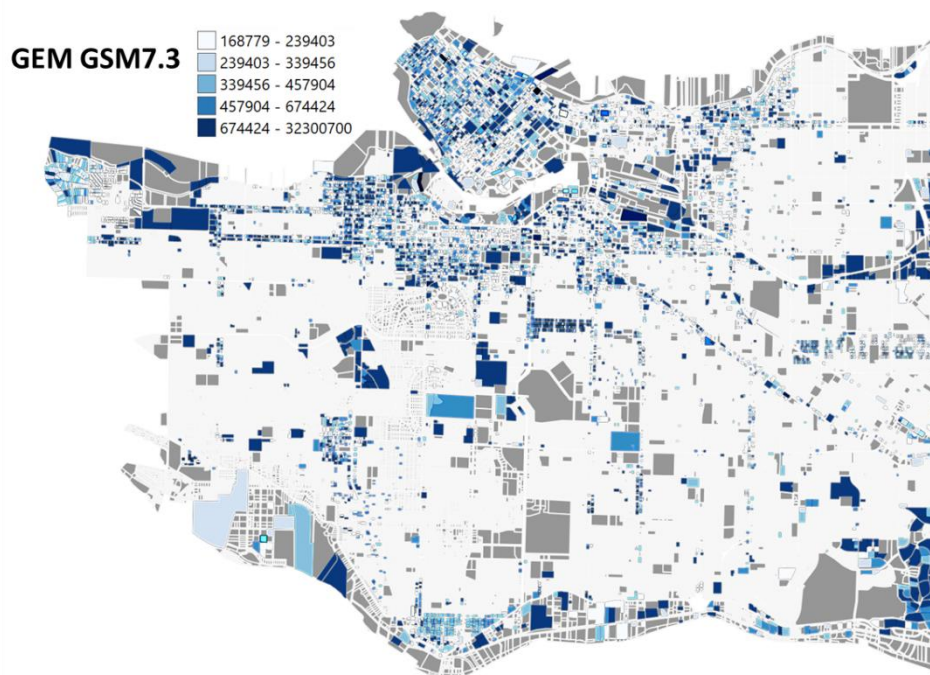


Figure 4.53 GSM7.3 Distribution of highest assets losses that make 50% of total loss, using GEM fragility functions

Case 1 scenario damage analysis shows that 871 buildings (~1.0% of all buildings) are expected to be in complete damage state (Figure 4.58a). Of this, 36% are C2 buildings built before 1973 and 34% are W3 construction built before 1973. Only 6.5% of buildings in the complete damage state are low-rise wood construction (Figure 4.59a). Case 1 scenario loss analysis shows that when using the GEM vulnerability functions, the GSM7.3 event is estimated to create losses of about 7.8 billion CAD. Concrete shear wall buildings built before 1973, and W3 buildings constitute the highest losses. (Figure 4.60a). Figure 4.52 shows that most damages are from C2-PC construction, in the West-end, Downtown Vancouver, Fairview and Kerrisdale and W3-PC buildings in south Kitsilano. W3 and W2 construction in Kitsilano, Fairview, Marpole and Champlain Heights are also identified as pockets in Vancouver that show higher losses, along with the C2-PC constructions in West-end, Downtown Vancouver, Fairview and Kerrisdale (Figure 4.53).

Case 2 (GSM7.3, UBC -no W4): The Georgia strait M7.3 crustal scenario (GSM7.3) is run using BC-specific fragility and vulnerability curves, but without considering the presence of subfloors or cripple walls; i.e., all low-rise wood residential construction is considered as W1.

The spatial distribution of complete damage state in Vancouver following the GSM7.3 scenario analysis using the BC-specific fragility functions is shown in Figure 4.54. The spatial distribution of losses (the highest individual asset losses that contribute to the 50% total loss) in Vancouver following the GSM7.3 scenario analysis using the BC-specific vulnerability functions is shown in Figure 4.55.

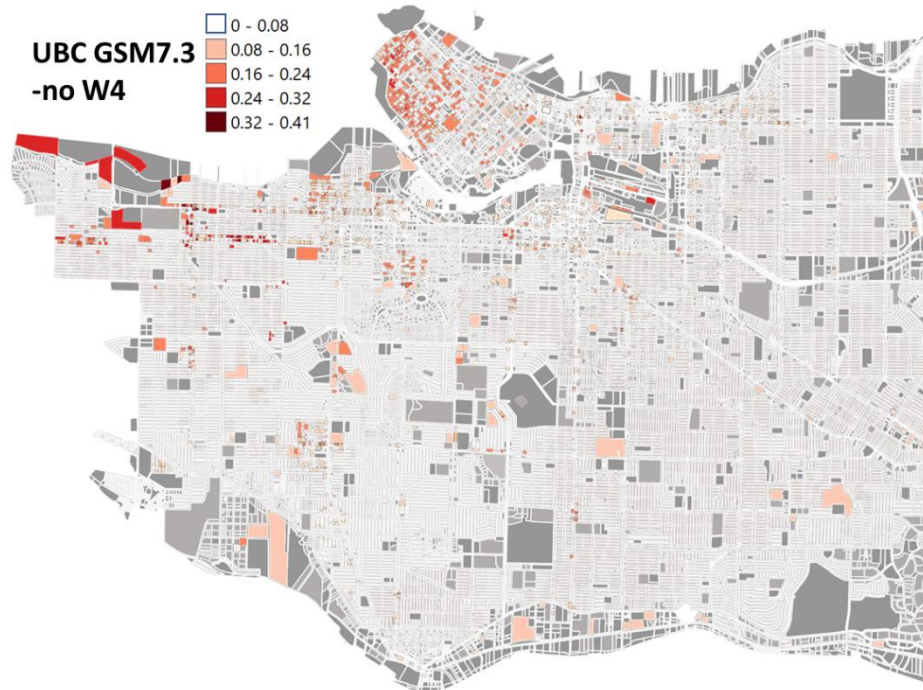


Figure 4.54 GSM7.3 Complete damage state distribution map for Vancouver, using BC-specific fragility functions, without accounting for W4s and W4c.

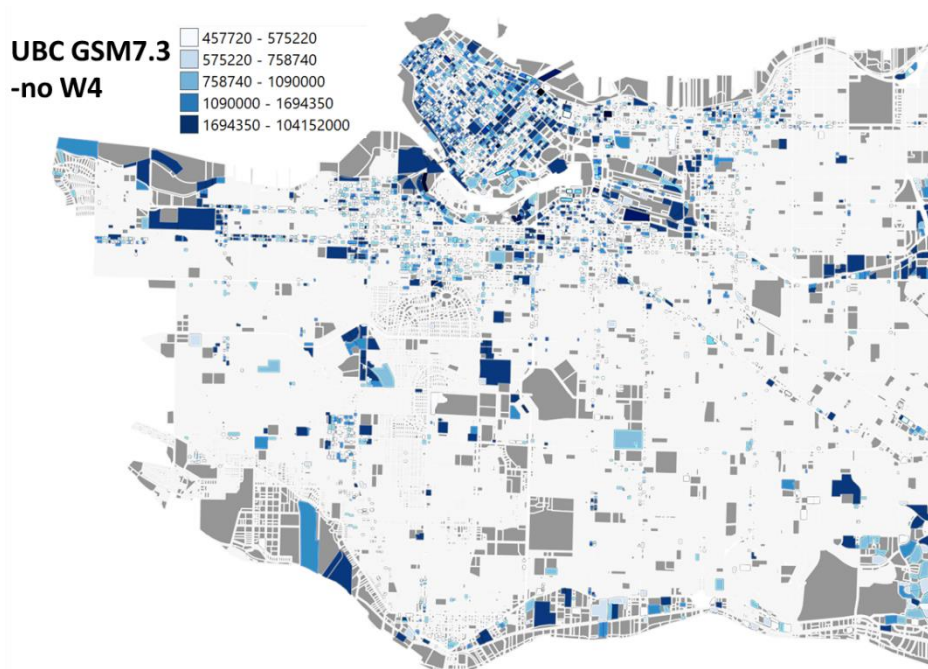


Figure 4.55 GSM7.3 Distribution of highest assets losses that make 50% of total loss, using BC-specific fragility functions, without accounting for W4s and W4c.

Case 2 scenario damage analysis shows that 1083 buildings (~1.2% of the total building stock) are seen to be in complete damage state (Figure 4.58b). Of this, 13% are C2 buildings built before 1973 and 12% are W3 construction built before 1973. 55% of buildings in complete damage state are low-rise wood construction (Figure 4.59b). Case 2 scenario loss analysis shows that when using the BC-specific vulnerability functions, and assuming that no low-rise residential wood buildings have cripple walls or subfloors, the GSM7.3 event is estimated to cost 8.87 billion CAD. Concrete shear wall buildings built before 1973, W2 and W3 buildings constitute the highest losses (Figure 4.60b). From Figure 4.54 and Figure 4.55, it is seen that the pockets identified in Vancouver with largest damage and loss is similar as seen in Case 1, except that the C2-PC buildings shows lower probabilities of bring in complete damage state, and individual asset losses estimated are higher than when using GEM vulnerability functions.

Case 3 (GSM7.3, UBC): The Georgia strait M7.3 crustal scenario (GSM7.3) is run using BC-specific fragility and vulnerability curves, taking into account, the presence of subfloors or cripple walls in low-rise wood residential construction in Vancouver.

The corresponding spatial distribution of complete damage state in Vancouver following the GSM7.3 scenario analysis using the BC-specific fragility functions is shown in Figure 4.56. The corresponding spatial distribution of losses (the highest individual asset losses that contribute to the 50% total loss) in Vancouver following the GSM7.3 scenario analysis using the BC-specific vulnerability functions is shown in Figure 4.57. It is seen in Figure 4.56., that when accounting for W4s and W4c, there is an addition of a large number of damages estimated in the W4s buildings in West point Grey and south Kitsilano (marked in black in Figure 4.56) , as well as the cripple wall pockets in Shaughnessy (marked in blue in Figure 4.56).

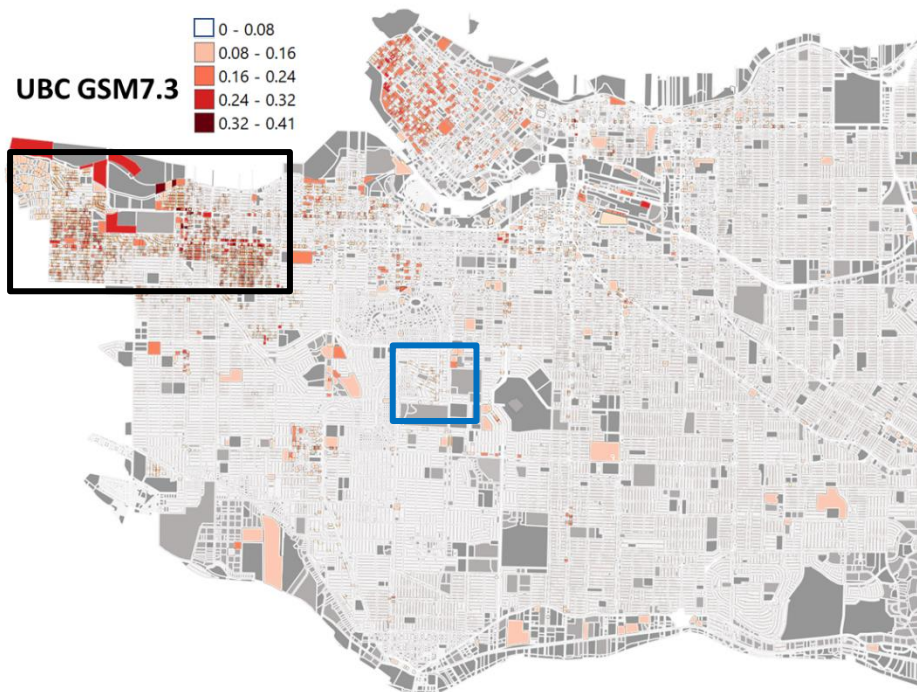


Figure 4.56 GSM7.3 Complete damage state distribution map for Vancouver, using BC-specific fragility functions, accounting for W4s and W4c.

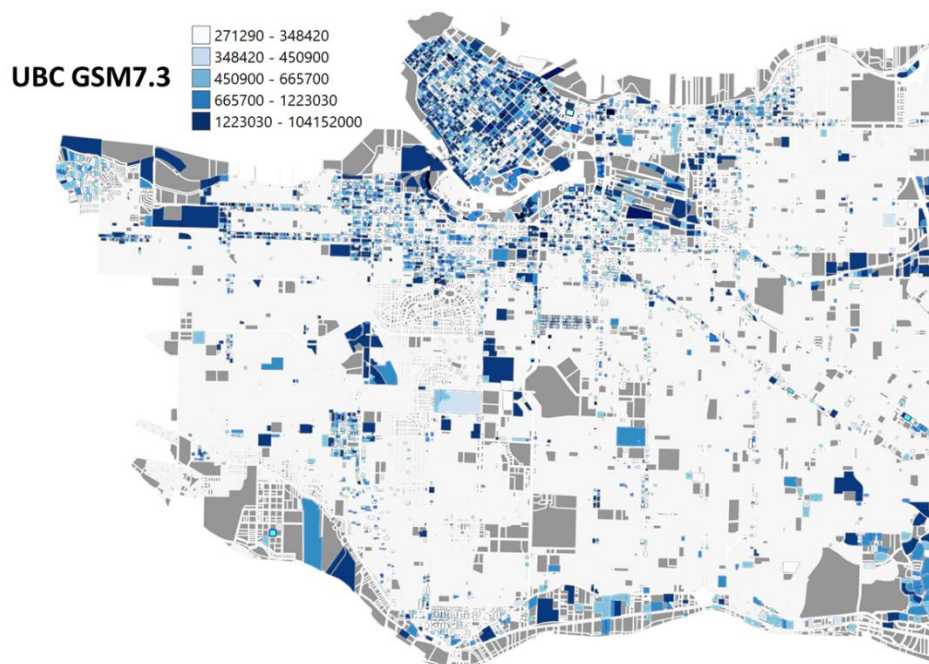


Figure 4.57 GSM7.3 Distribution of highest assets losses that make 50% of total loss, using BC-specific fragility functions, accounting for W4s and W4c.

Case 3 scenario damage analysis shows that 2045 buildings (~2.3 % of the total building stock) are seen to be in complete damage state (Figure 4.58c). Of this, 7% are C2 buildings built before 1973 and 7% are W3 construction built before 1973. 9%, 5% and 62% of buildings in complete damage state are W1, W4c and W4s, respectively (Figure 4.59c). This is since more than half of the W1 in Vancouver are recognized as having subfloors. Case 3 scenario loss analysis shows that when using the BC-specific vulnerability functions, and accounting for the presence of cripple walls and subfloors in low-rise residential wood construction in Vancouver, the GSM7.3 event is estimated to cost 10.5 billion CAD. Concrete shear wall buildings built before 1973, W2 and W3 buildings constitute the highest individual asset losses (Figure 4.60c).

From Figure 4.56 it is seen that the pockets identified in Vancouver with largest damage and loss is similar as seen in Case 2, except that pockets with W4s buildings in West point Grey and south Kitsilano and cripple wall pockets in Shaughnessy become noticeable. This is also reflected in the loss distribution map.

Figure 4.58 summarizes the total damage distribution based on building damage state for the GSM7.3 scenario for the three cases described above. Figure 4.59 summarizes the complete damage (DS4) distribution across the typologies under the three cases discussed above for the GSM7.3 scenario. Figure 4.60 summarizes the total loss distribution across different building typologies for the three cases for the GSM7.3 scenario.

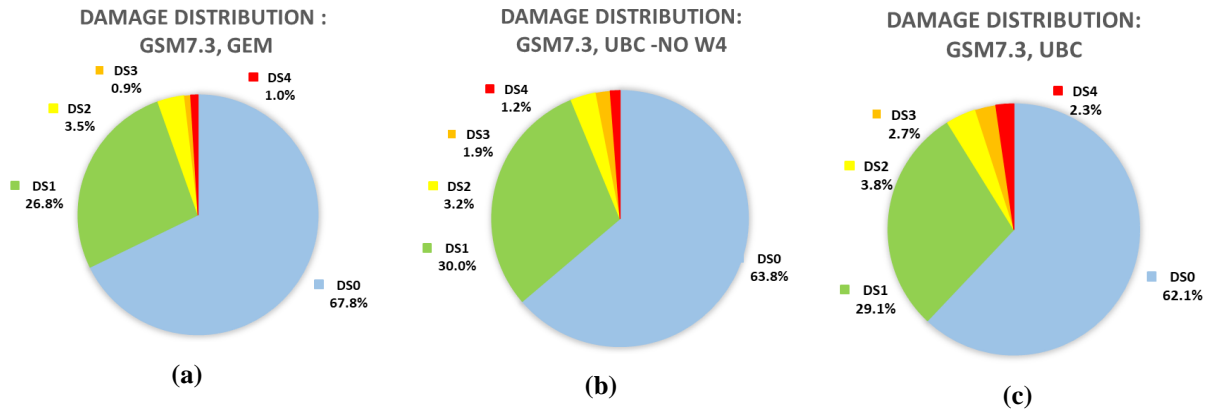


Figure 4.58 Total damage distribution based on building damage state for (a) Case 1 (b) Case 2 (3) Case 3

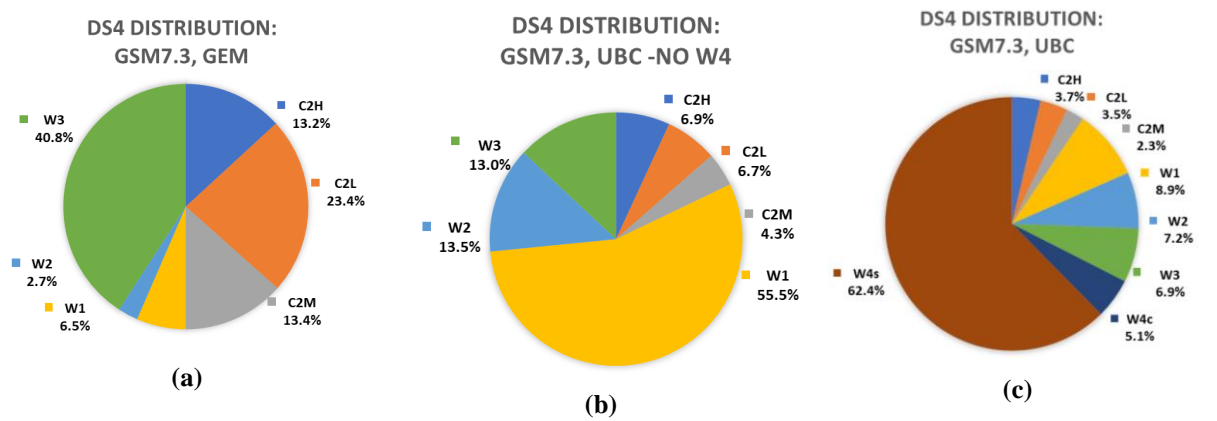


Figure 4.59 DS4 distribution across building typologies for (a) Case 1 (b) Case 2 (3) Case 3

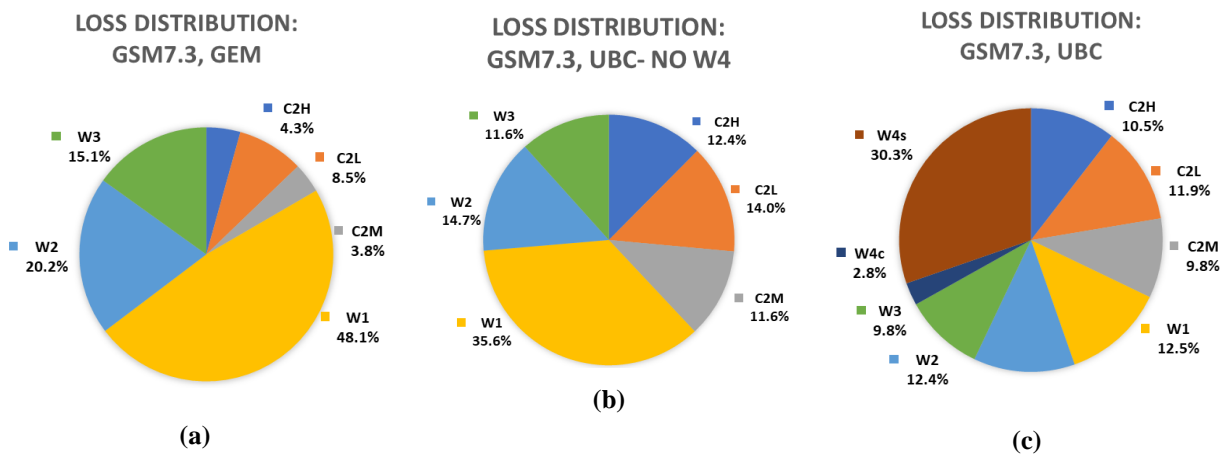


Figure 4.60 Total loss distribution across different building typologies for (a) Case 1 (b) Case 2 (3) Case 3

From the first analysis, complete and extensive damage is mostly localized to the pre-1990 concrete buildings in downtown Vancouver and W3-PC buildings throughout the city. C2L structures in Grandview-woodland, C2H structures in the West End, Kerrisdale and Downtown and W3 in south Kitsilano are seen to be at risk of severe damage. Losses also highlight the W2 construction in Marpole and Champlain Heights.

The second and third scenario analyses that account for BC-specific construction and new wood typologies, reveals a significant increase in damage in single family wood houses. The significant increase in damage predicted for case 2 is accounting for lower shear and displacement capacities of BC wood buildings, and for case 2, due to the inclusion of structures with cripple walls and sub-floors (W4c and W4s), which essentially pushes a W1 building which was previously in an estimated damage state to a higher damage state. The pre-code concrete shear wall buildings show lower damage estimates than case 1, due to the difference in development of vulnerability curves. The increase in damage to the number of concrete buildings built after 1990s is due to the fact that the strength capacity of the moderate code and high code (MC and HC) concrete shear wall buildings were decreased to account for BC building practices.

4.9.2 Subduction scenario (CSZ9.0)

A summary of damages and losses to the Vancouver building stock for the three analyses described in section 3. is shown on the Vancouver map and the percentage of damage and loss - per typology - to the building stock generated under each case is plotted. While the damage distribution maps show the complete damage state distribution, the loss distribution map highlights the highest individual asset loss that contribute to the 50% total loss. (Note: The scales of the map

are intentionally set so as to easily and better distinguish the pockets of change in damage and loss when considering the new fragility and vulnerability functions).

Case 1 (CSZ9.0, GEM): The M9.0 Cascadia subduction scenario is run using fragility and vulnerability curves developed by GEM for use in Canada. The spatial distribution of complete damage state in Vancouver following the CSZ9.0 scenario analysis using the GEM fragility functions is shown in Figure 4.61. The spatial distribution of losses (the highest individual asset losses that contribute to the 50% total loss) in Vancouver following the CSZ9.0 scenario analysis using the GEM vulnerability functions is shown in Figure 4.62.

Figure 4.61 shows that most damages during this scenario occur in C2-PC construction in the West-end, Downtown Vancouver, Fairview and Kerrisdale and W3-PC buildings in south Kitsilano. Figure 4.62 shows that W3 and W2 construction in Kitsilano, Fairview, Marpole, Sunset and Champlain Heights are identified as areas in Vancouver that show high individual asset losses, along with the C2 constructions in West-end, Downtown Vancouver, Fairview and Kerrisdale.

Case 1 scenario damage analysis shows that 396 (~0.4% of the Vancouver building stock) buildings are seen to be in complete damage state (Figure 4.67a). Of this, 41% are C2 buildings built before 1973, and 49.6% are W3 construction built before 1973. Only 1.5% of buildings in complete damage state are low-rise wood construction (Figure 4.68a). Case 1 scenario loss analysis shows that when using the GEM vulnerability functions, the CSZ9.0 event is estimated to create losses of around 2.0 billion CAD. Concrete shear wall buildings built before 1973, and W3 buildings constitute the highest losses (Figure 4.69a). Expected complete damage cases are heavily concentrated on C2 and W3 built before 1973. 90% of the building stock is estimated to be unaffected by the earthquake.

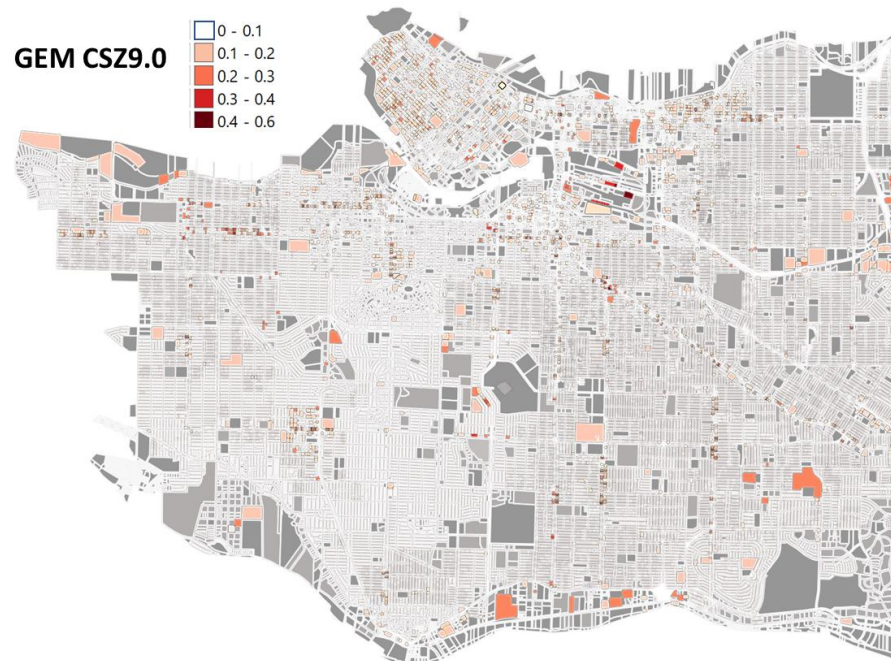


Figure 4.61 CSZ9.0 Complete damage state distribution map for Vancouver, using GEM fragility functions

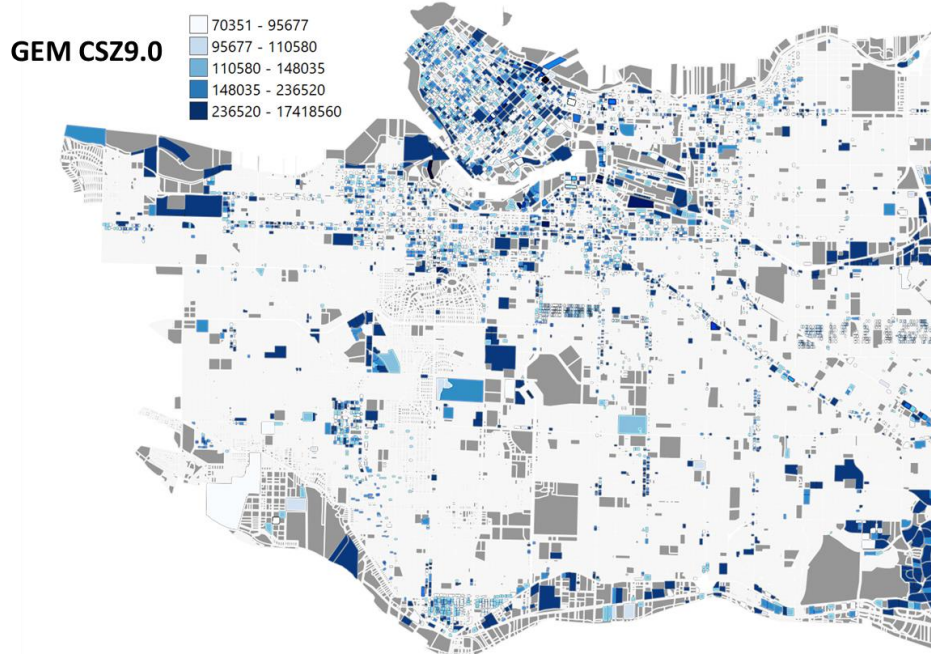


Figure 4.62 CSZ9.0 Distribution of highest assets losses that make 50% of total loss, using GEM fragility functions

Case 2 (CSZ9.0, UBC -no W4): The M9.0 Cascadia subduction scenario (CSZ9.0) is run using BC-specific fragility and vulnerability curves, without considering the presence of subfloors or cripple walls; i.e., all low-rise wood residential construction in Vancouver is considered as W1.

The spatial distribution of complete damage state in Vancouver following the CSZ9.0 scenario analysis using the BC-specific fragility functions is shown in Figure 4.63. The spatial distribution of losses (the highest individual asset losses that contribute to the 50% total loss) in Vancouver following the CSZ9.0 scenario analysis using the BC-specific vulnerability functions is shown in Figure 4.64.

From Figure 4.63 and Figure 4.64, it is seen that the pockets identified in Vancouver with largest damage and loss is similar as seen in Case 1, except that the C2-PC buildings shows lower probabilities of bring in complete damage state, and individual asset losses estimated are higher than when using GEM vulnerability functions.

Case 2 scenario damage analysis shows that 568 buildings are seen to be in complete damage state which is 4.5% of all damaged buildings (Figure 4.67b). Of this, 19% are C2 buildings built before 1973 and 17% are W3 construction built before 1973. 35.4% of buildings in complete damage state are low-rise wood construction, and 20% are W2 construction (Figure 4.68b). Case 2 scenario loss analysis shows that when using the BC-specific vulnerability functions, the CSZ9.0 event is estimated to create losses of around 5.3 billion CAD. Concrete shear wall buildings built before 1973, W2 and W3 buildings constitute the highest losses (Figure 4.69b).

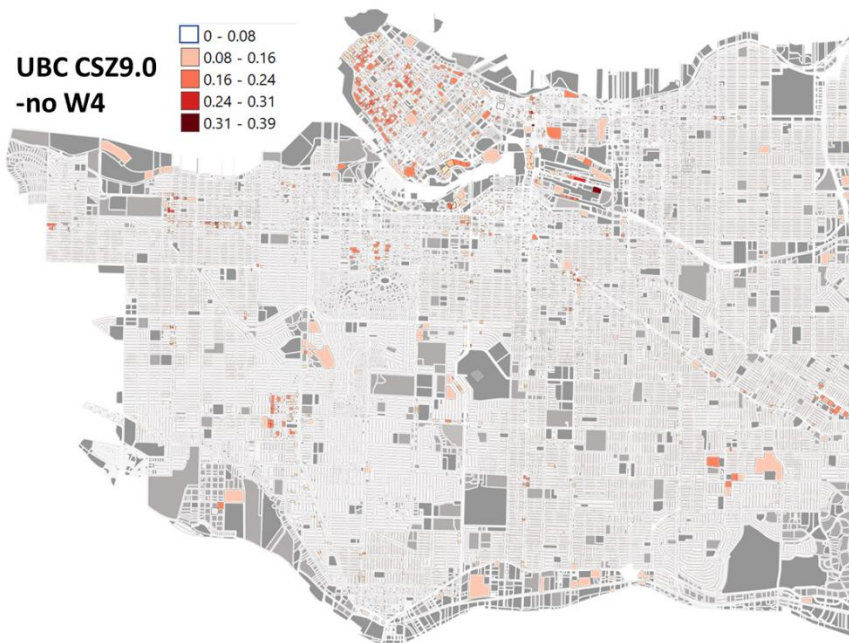


Figure 4.63 CSZ9.0 Complete damage state distribution map for Vancouver, using BC-specific fragility functions, without accounting for W4s and W4c.

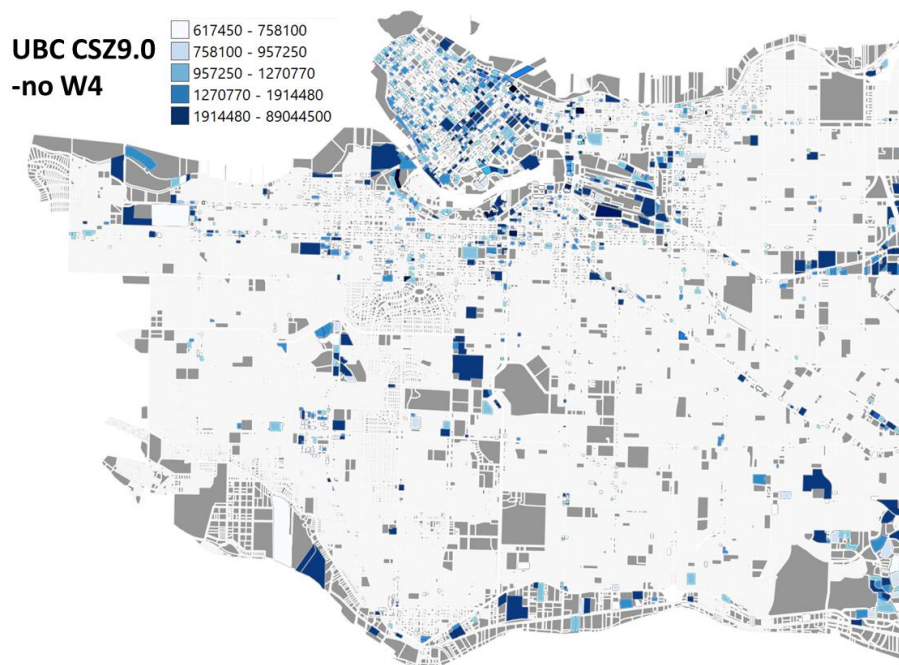


Figure 4.64 CSZ9.0 Distribution of highest assets losses that make 50% of total loss, using BC-specific fragility functions, without accounting for W4s and W4c.

Case 3 (CSZ9.0, UBC): The M9.0 Cascadia subduction scenario (CSZ9.0) is run using BC-specific fragility and vulnerability curves, accounting for the presence of subfloors or cripple wall in low-rise wood residential constructions in Vancouver.

The corresponding spatial distribution of complete damage state in Vancouver following the CSZ9.0 scenario analysis using the BC-specific fragility functions is shown in Figure 4.65. The corresponding spatial distribution of losses (the highest individual asset losses that contribute to the 50% total loss) in Vancouver following the CSZ9.0 scenario analysis using the BC-specific vulnerability functions is shown in Figure 4.66.

Case 3 scenario damage analysis shows that 761 buildings are seen to be in complete damage state (Figure 4.67c). Of this, 14% are C2 buildings built before 1973 and 13% are W3 construction built before 1973. 12%, 4.6% and 35% of DS4 are W1, W4c and W4s respectively (Figure 4.68c). This is since more than half of the W1 in Vancouver are recognized as having subfloors. Case 3 scenario loss analysis shows that when using the BC-specific vulnerability functions, the CSZ9.0 event is estimated to create losses of around 5.64 billion CAD. Concrete shear wall buildings built before 1973, W2 and W3 buildings constitute the highest losses (Figure 4.69c). About 200 low-rise wood structures with subfloors or cripple walls were added to buildings that are assessed to be in complete damage state.

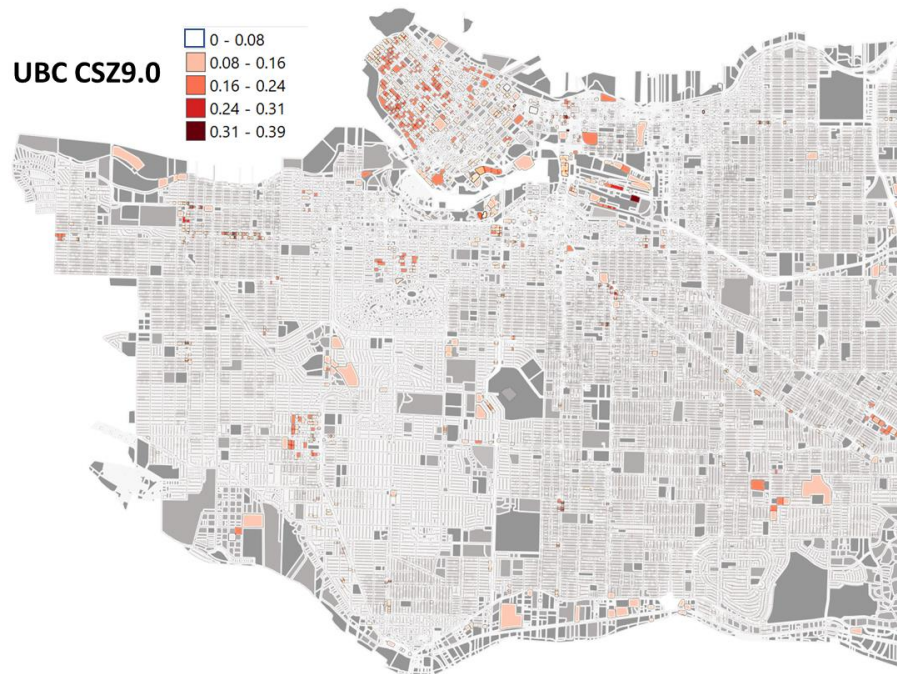


Figure 4.65 CSZ9.0 Complete damage state distribution map for Vancouver, using BC-specific fragility functions, accounting for W4s and W4c.

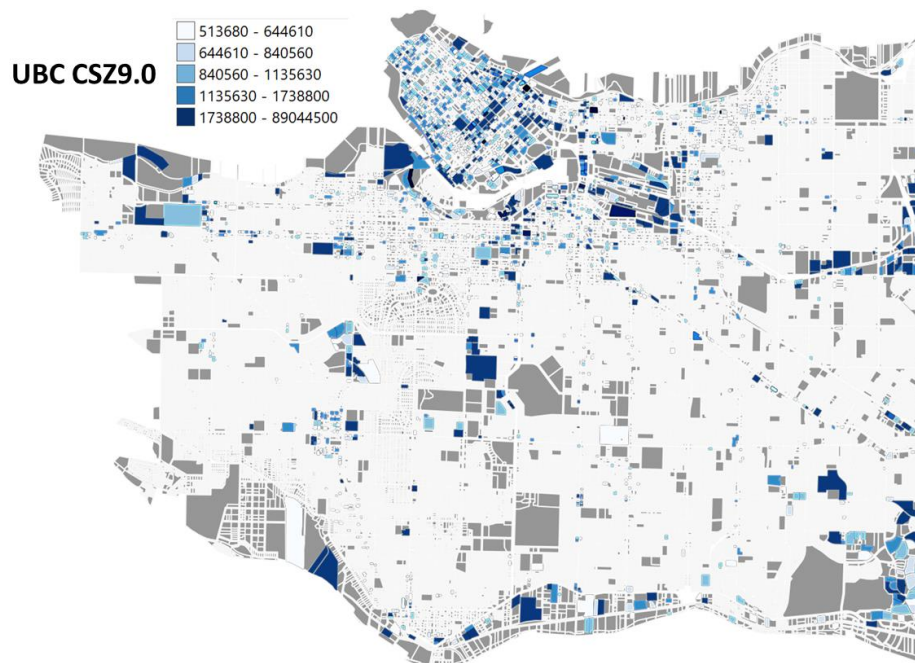


Figure 4.66 CSZ9.0 Distribution of highest assets losses that make 50% of total loss, using BC-specific fragility functions, accounting for W4s and W4c.

Figure 4.67 summarizes the Total damage distribution based on building damage state for the CSZ9.0 scenario for the three cases described above. Figure 4.68 summarizes the complete damage (DS4) distribution across the typologies under the three cases discussed above for the CSZ9.0 scenario. Figure 4.69 summarizes the total loss distribution across different building typologies for the three cases for the CSZ9.0 scenario.

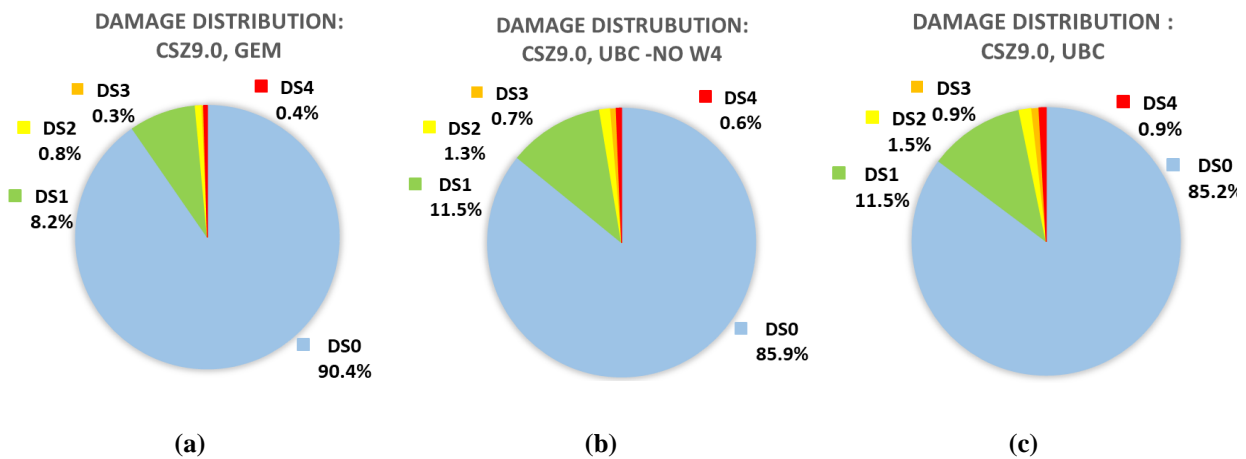


Figure 4.67 Total damage distribution based on building damage state for (a) Case 1 (b) Case 2 (3) Case 3

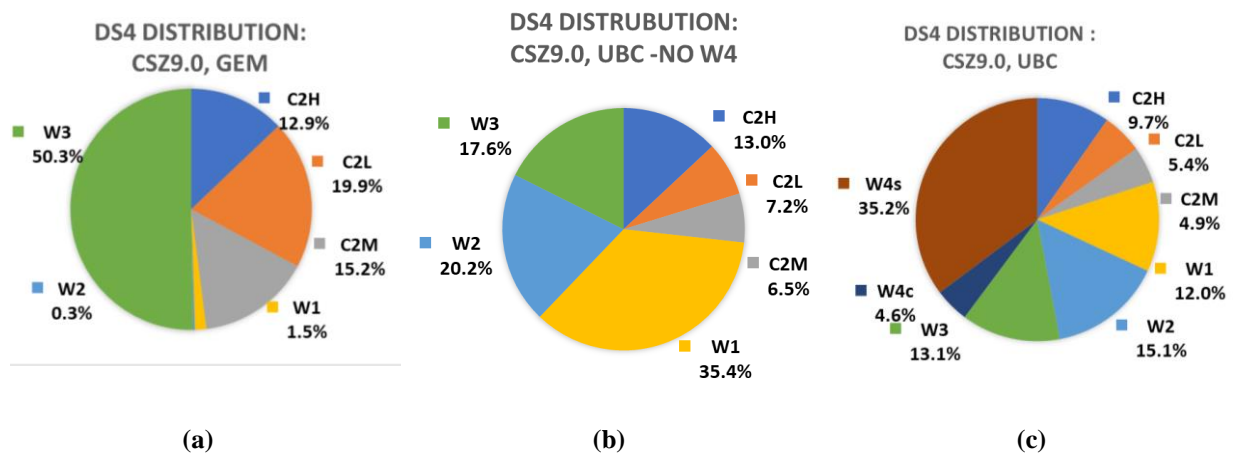


Figure 4.68 DS4 distribution across building typologies for (a) Case 1 (b) Case 2(3) Case 3

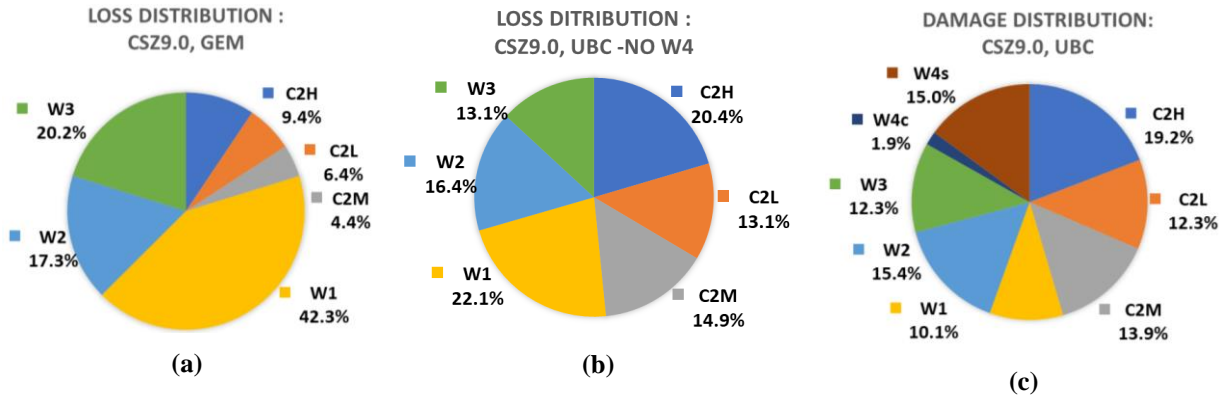


Figure 4.69 Total loss distribution across different building typologies for (a) Case 1 (b) Case 2 (3) Case 3

It is seen that the GEM functions generally estimate lower damages and loss than the BC-specific functions. As is seen in the fragility functions comparisons, the GEM functions predict a large percentage of C2 PC structures to be in DS4. However, the BC functions predict a smaller number, since the BC-specific C2 PC have a higher base shear capacity. At the same time, predicts much lower DS4 numbers in low-rise wood and mid -rise wood structures. Accounting for W4s and W4c increases the damage and loss estimated in Vancouver under both scenarios. Damages from C2 MC and HC are larger, as is seen from the fragility functions.

4.10 Regional Seismic Risk Assessment (RSRA) (objective 5)

The results obtained from Regional Seismic Risk Analysis (RSRA), following the methodology explained in section 3.5 is documented in this section.

It is seen that all the seismic sources described in the 2015 GSC seismic source model do not influence the seismic hazard at the 10 localities chosen. Table 4.4 and Table 4.5 summarizes the sources that influence the seismic hazard at each of the 10 localities, and were compiled from running the OQ event-based risk analysis for each of the ten localities. It identifies sources that do

not contribute to the seismic hazard at a site, based on the magnitude and distance limitations set for each tectonic region type.

Table 4.4 Summary of seismic sources that contribute to the seismic hazard at Chilliwack, Masset, Port Hardy, Prince Rupert and Princeton (based on CanadaSHM5 seismic source model)

Tectonic Region Type	Chilliwack	Masset	Port Hardy	Prince Rupert	Princeton
Active Shallow Crust	✓		✓	✓	✓
Active Shallow Fault		✓	✓	✓	
Active Shallow Offshore		✓	✓	✓	
Stable Shallow Crust	✓			✓	✓
Subduction Interface	✓	✓	✓	✓	✓
Subduction IntraSlab30	✓		✓		✓
Subduction IntraSlab50	✓		✓		✓

Table 4.5 Summary of seismic sources that contribute to the seismic hazard at Daajing Giids (QCC), Sooke, Ucluelet, Vancouver and Victoria (based on CanadaSHM5 seismic source model)

Tectonic Region Type	Daajing Giids (QCC)	Sooke	Ucluelet	Vancouver	Victoria
Active Shallow Crust		✓	✓	✓	✓
Active Shallow Fault	✓		✓		
Active Shallow Offshore	✓	✓	✓	✓	✓
Stable Shallow Crust					
Subduction Interface	✓	✓	✓	✓	✓
Subduction IntraSlab30		✓	✓	✓	✓
Subduction IntraSlab50		✓	✓	✓	✓

For the three localities within mainland BC, Chilliwack, Princeton and Vancouver (Figure 3.25), the Vancouver crustal and subduction fragility and vulnerability functions are used to conduct RSRA. For all other localities on the islands, the Victoria crustal and subduction fragility and vulnerability functions are used for RSRA.

Once the scenario risk (damage and loss) analyses are completed, the changes the BC-fragility and vulnerability models bring are studied and typologies that most influence the damage and loss are identified, RSRA is performed with these BC-specific fragility and vulnerability functions, for the 10 localities. As explained in section 3.5, the results from two cases of RSRA are calculated:

1. **Cr-All** (Baseline): using crustal fragility and vulnerability functions to estimate risk from all seismic sources in the RSRA.
2. **Cr+Subd**: using crustal fragility and vulnerability functions to estimate risk from the crustal and subcrustal events within the RSRA and subduction fragility and vulnerability functions to estimate risk from the subduction events within the RSRA).

These RSRA cases are run considering two exposure cases:

1. Using the site's original exposure model, considering that C2 and Wood assets make 100% of the total exposure of the site.
2. Using a uniform exposure model for Ucluelet at all localities, considering that C2 and Wood assets make 100% of the total exposure of the site.

4.10.1 Compilation of RSRA results for 10 localities using the site's original exposure models

RSRAs were carried out for the 10 selected localities in BC, using the site's original exposure models, and the collapse exceedance curve in terms of collapse fraction and loss exceedance curved at each of the 10 sites are plotted in Figure 4.70 to Figure 4.89.

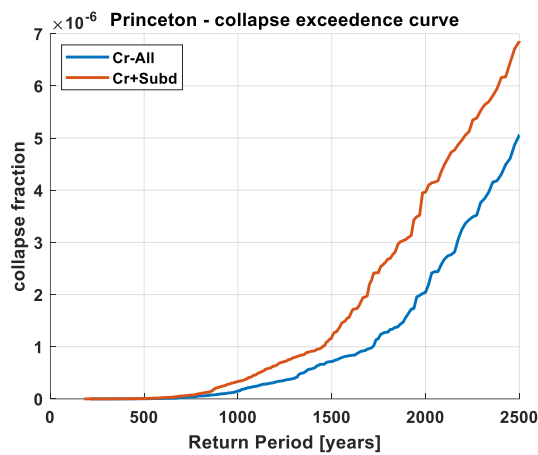


Figure 4.70 Collapse exceedance curve: Princeton

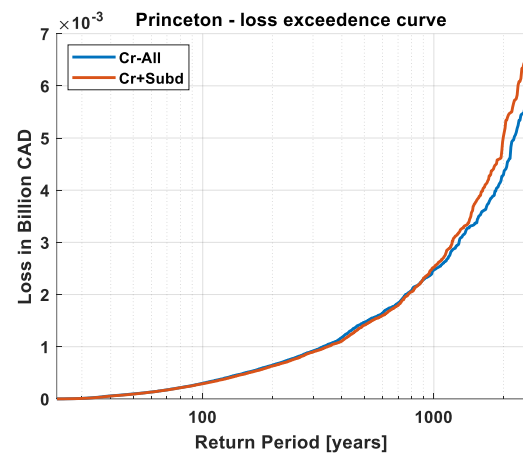


Figure 4.71 Loss exceedance curve: Princeton

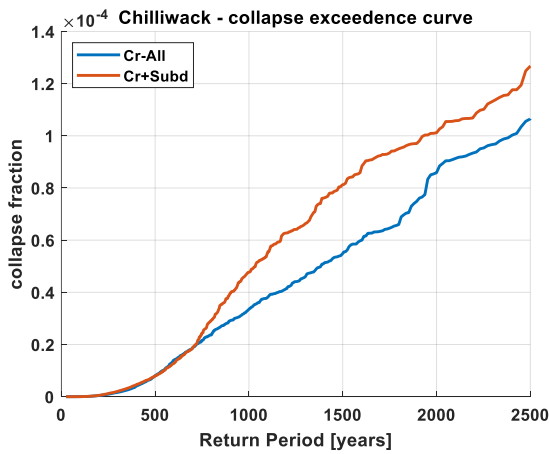


Figure 4.72 Collapse exceedance curve: Chilliwack

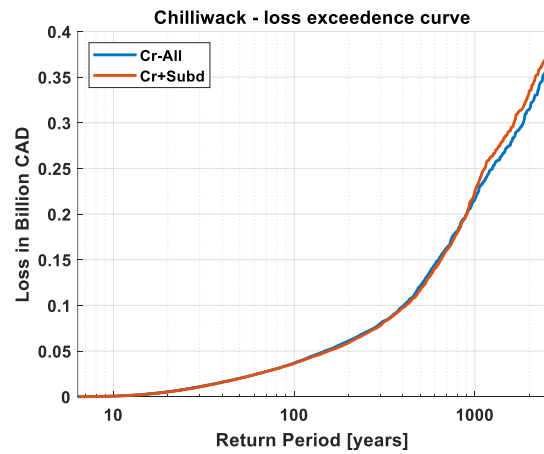


Figure 4.73 Loss exceedance curve: Chilliwack

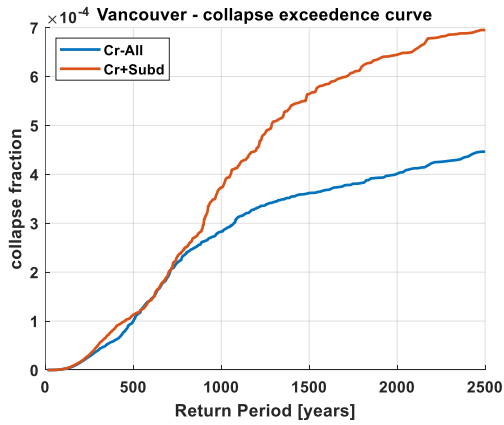


Figure 4.74 Collapse exceedance curve: Vancouver

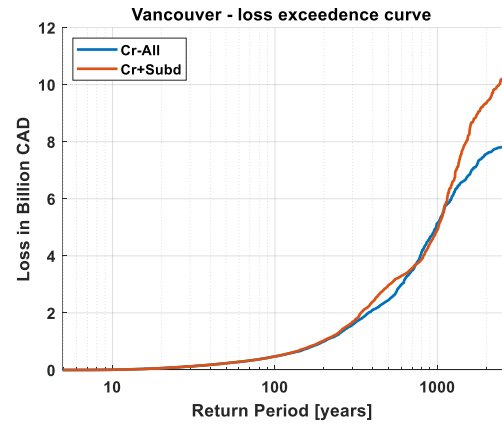


Figure 4.75 Loss exceedance curve: Vancouver

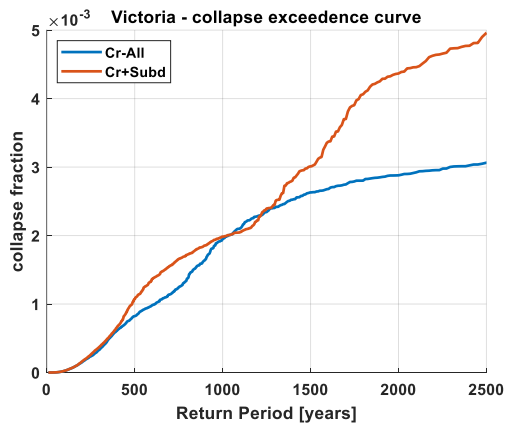


Figure 4.76 Collapse exceedance curve: Victoria

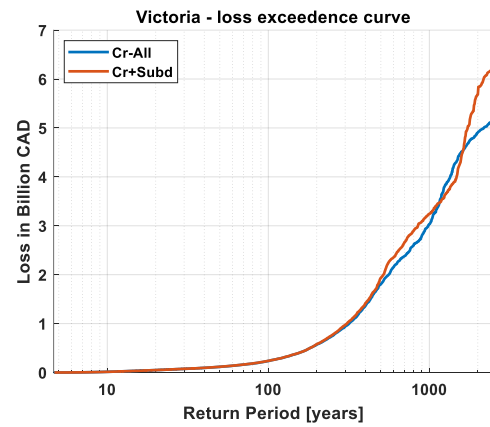


Figure 4.77 Loss exceedance curve: Victoria

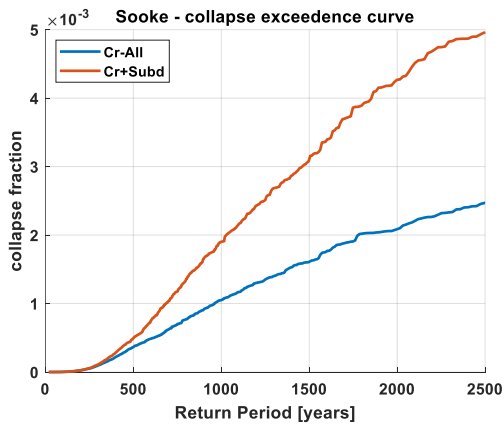


Figure 4.78 Collapse exceedance curve: Sooke

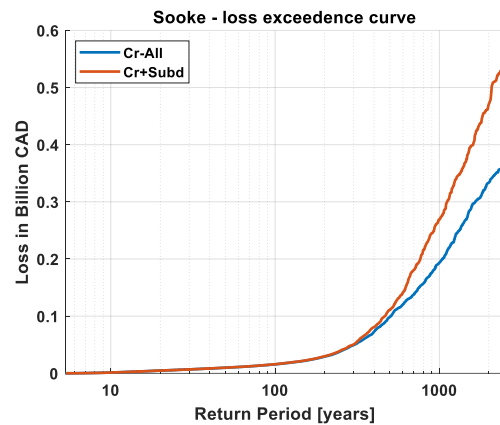


Figure 4.79 Loss exceedance curve: Sooke

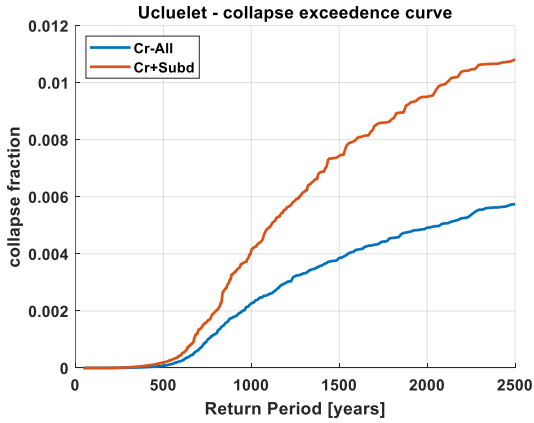


Figure 4.80 Collapse exceedance curve: Ucluelet

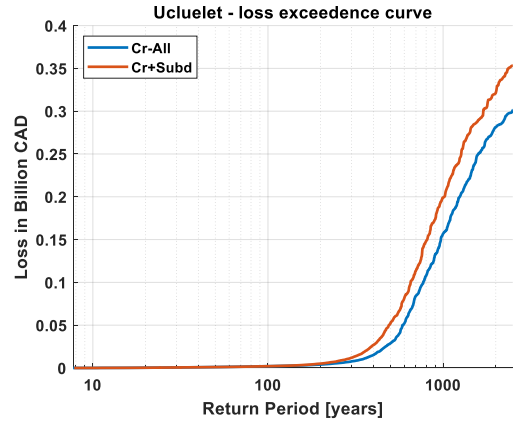


Figure 4.81 Loss exceedance curve: Ucluelet

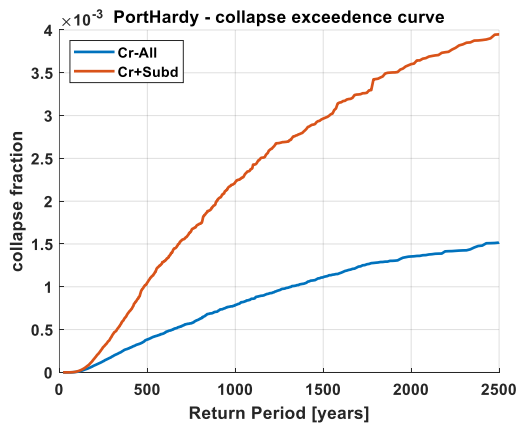


Figure 4.82 Collapse exceedance curve: Port Hardy

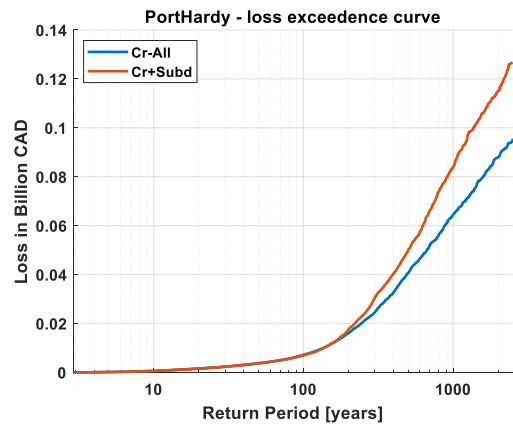


Figure 4.83 Loss exceedance curve: Port Hardy

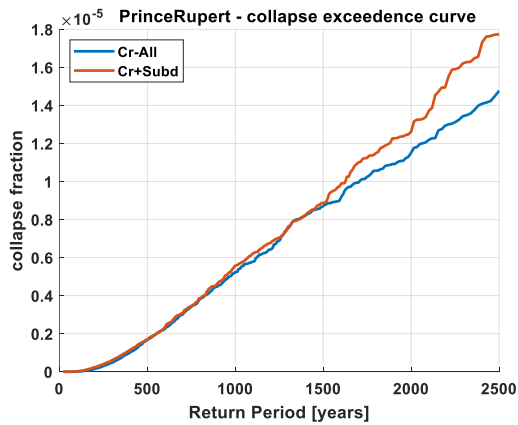


Figure 4.84 Collapse exceedance curve: Prince Rupert

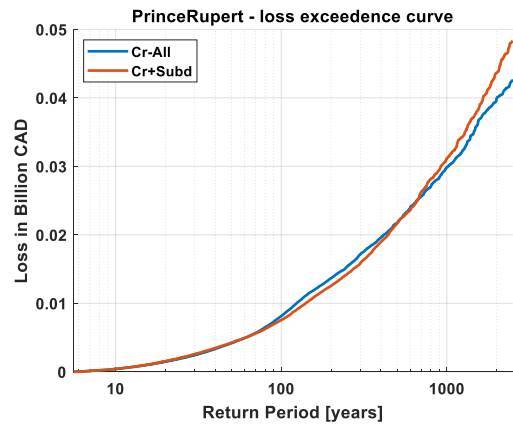


Figure 4.85 Loss exceedance curve: Prince Rupert

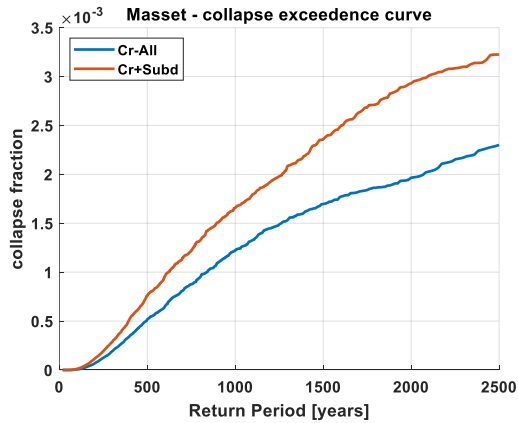


Figure 4.86 Collapse exceedance curve: Masset

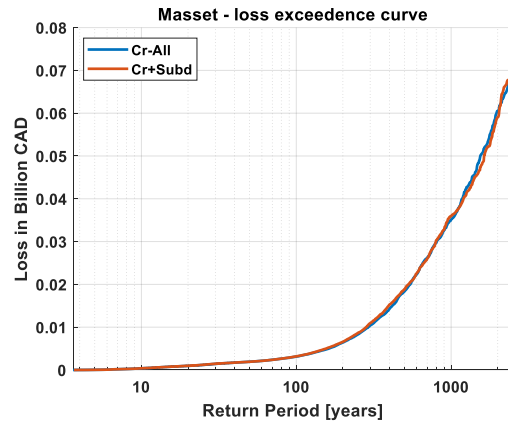


Figure 4.87 Loss exceedance curve: Masset

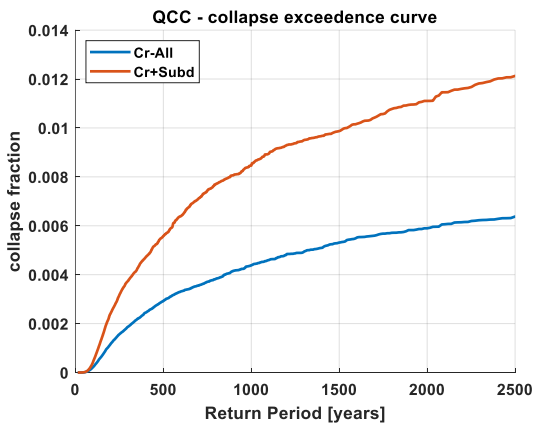


Figure 4.88 Collapse exceedance curve: QCC

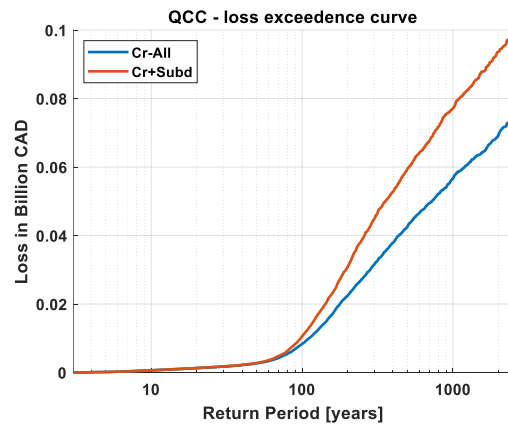


Figure 4.89 Loss exceedance curve: QCC

From Figure 4.70 to Figure 4.89, it is seen that at certain localities, the influence of subduction ground motions on RSRA are more noticeable. For example, at QCC (Figure 4.88 and Figure 4.89), for a return period of 1000 years, the Cr+Subd case estimates an increase of 0.004 in the estimate of collapse fraction (1.9 times the baseline collapse fraction) and 20.6 million CAD in losses (1.4 times the baseline loss) as compared to the Cr-All case respectively. Similar results are also seen in Sooke, Ucluelet and Port Hardy. At Port Hardy, the influence of subduction sources is more pronounced -as seen from the collapse exceedance curve, where at a return period of 1000 years, the Cr+Subd case estimating 2.85 times the collapse fraction and 1.3 times the loss as

compared to the Cr-All case (Figure 4.82 and Figure 4.83). At Vancouver (Figure 4.74 and Figure 4.75), for a return period of 1000 years, the Cr+Subd case estimates an increase of 9×10^{-5} in the estimate of collapse fraction (1.3 times the baseline collapse fraction) and a decrease of 231 million CAD in losses (0.95 times the baseline loss) as compared to the Cr-All case respectively. At Victoria (Figure 4.76 and Figure 4.77) for a return period of 1000 years, the Cr+Subd case estimates an increase of 2.4×10^{-5} in the estimate of collapse fraction and 206.1 million CAD in losses (1.07 times the baseline loss) as compared to the Cr-All case respectively.

The average annual collapse fraction (AACF) of buildings at each locality, Average Annual Loss (AAL) and Average Annual Loss Ratios (AALR) are calculated at each of the 10 localities for the two cases (Cr-All and Cr+Subd) and are tabulated in Figure 4.90 - Figure 4.92.

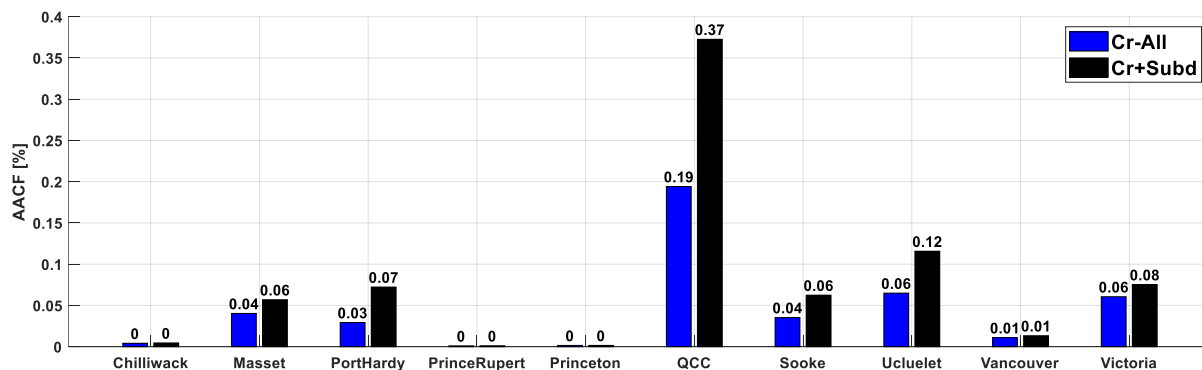


Figure 4.90 Summary of AACF at selected BC localities for Cr-All and Cr+Subd cases when using the locality's exposure model.

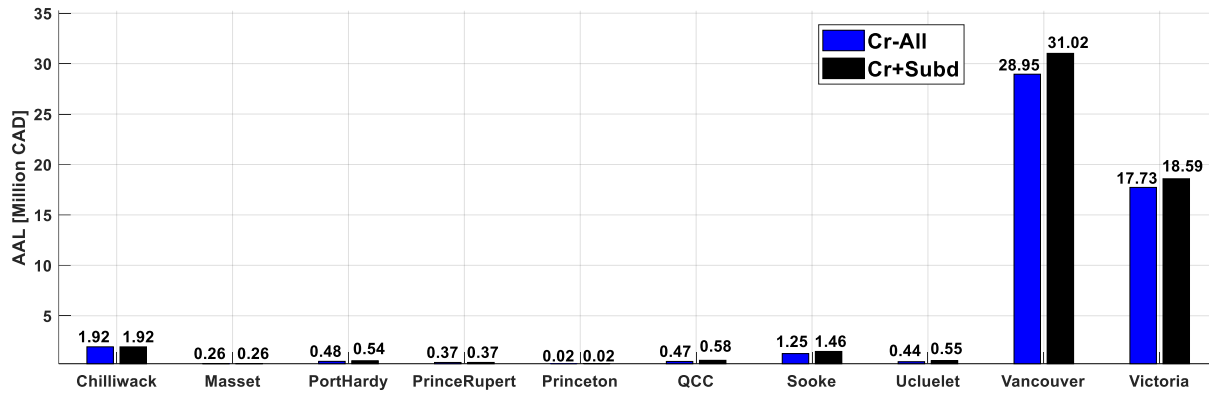


Figure 4.91 Summary of AAL at selected BC localities for Cr-All and Cr+Subd cases when using the locality's exposure model

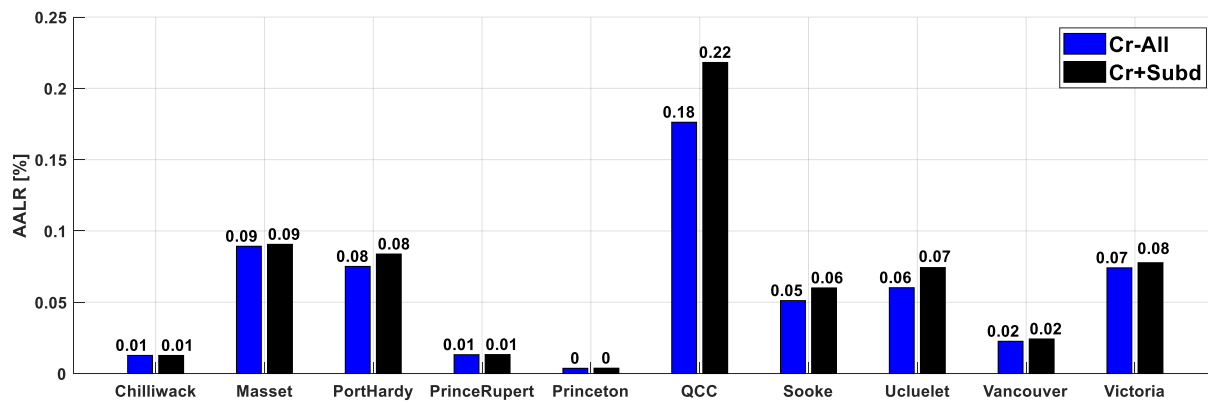


Figure 4.92 Summary of AALR at selected BC localities for Cr-All and Cr+Subd cases when using the locality's exposure model.

From Figure 4.90 to Figure 4.92, the estimated absolute increase in AACF, AAL and AALR for the Cr+Subd case as compared to the baseline Cr-All case at the 10 localities are calculated and summarized in Figure 4.93 to Figure 4.95.

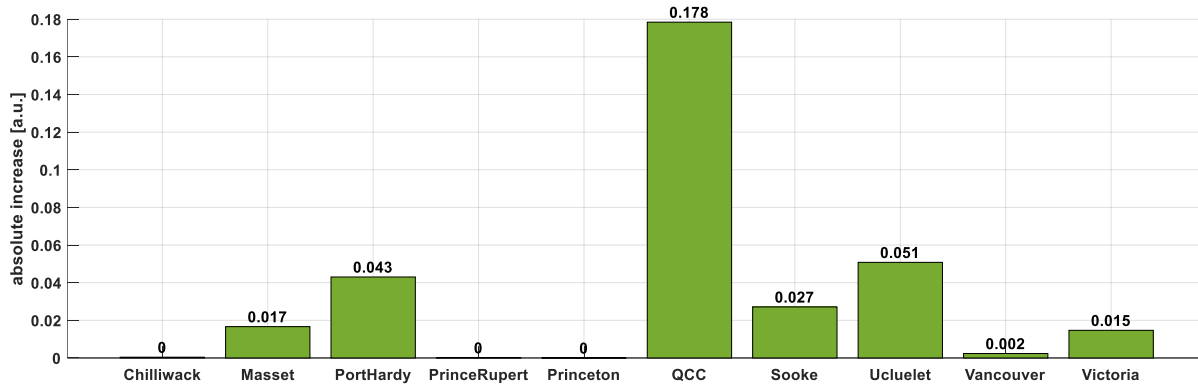


Figure 4.93 Absolute increase in ACF for 10 selected BC sites when using the site's exposure model.

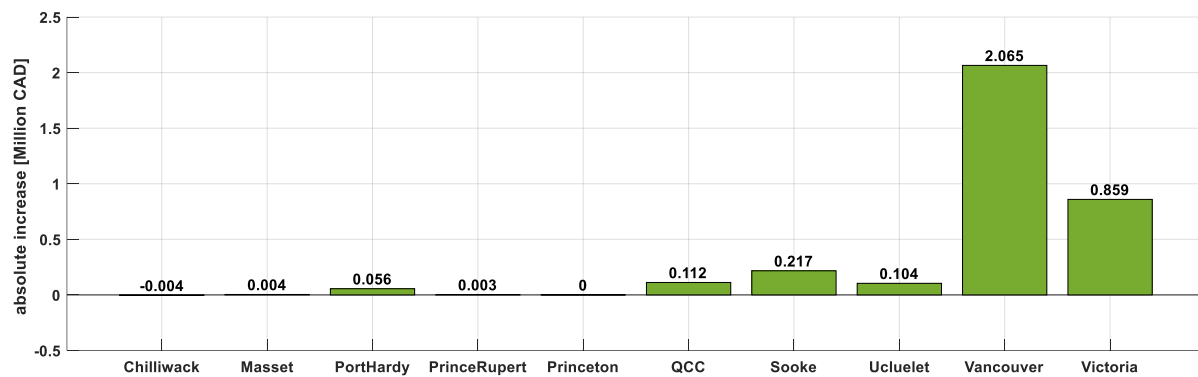


Figure 4.94 Absolute increase in AAL for 10 selected BC sites when using the site's exposure model.

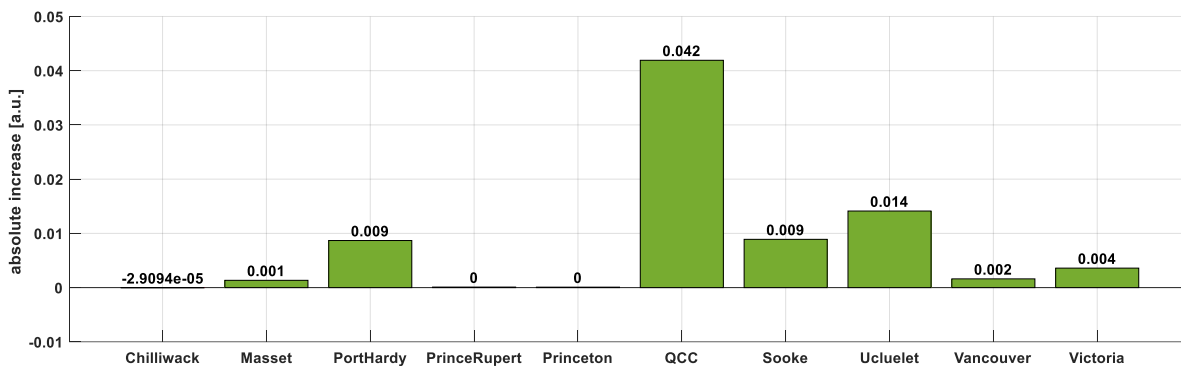


Figure 4.95 Absolute increase in AALR for 10 selected BC sites when using the site's exposure model.

Figure 4.93 depicts that the largest absolute increase in ACF occurs at QCC, followed by Ucluelet, Port Hardy, Sooke, Masset, Victoria and Vancouver as 0.18, 0.05, 0.043, 0.03, 0.017, 0.015 and 0.003 respectively. The contribution of subduction events to ACF at Chilliwack,

Prince Rupert and Princeton are very small. Figure 4.94 shows that largest absolute increase in AAL due to inclusion of subduction vulnerability functions in RSRA, is at Vancouver, followed by Victoria, Sooke, QCC, Ucluelet and Port Hardy, quantified as 2.1, 0.86, 0.22, 0.1, 0.1 and 0.06 million CAD respectively. The AAL at other locations are very small (in thousands of CAD). Figure 4.95 shows that the largest absolute increase in AALR due to inclusion of subduction vulnerability functions is at QCC (from 0.18% to 0.22%), followed by Ucluelet (0.06% to 0.074%), Sooke (0.05% to 0.06%), Port Hardy (0.075% to 0.084%), Victoria (0.074% to 0.075%), Vancouver (0.023% to 0.024%) and Masset (0.089% to 0.09%) respectively. The absolute increase in AALR at other locations are very small.

The estimated relative increase in AACF, AAL and AALR for the Cr+Subd case as compared to the Cr-All case at the 10 localities are summarized in Figure 4.96 and Figure 4.97. Port Hardy is seen to have the largest relative increase in AACF (150%), followed by QCC (92%). However, in absolute terms, the increase in AACF at Port Hardy and QCC are 0.017 and 0.18 respectively. The relative increase at Port Hardy is influenced by the sensitivity of the ‘relative increase in AACF’ metric to the very small baseline (Cr-All) AACF value of 0.03 at Port Hardy, as compared to QCC (0.19). Thus, metrics like the relative increase in AACF and relative increase in AAL and AALR should be explored together with their absolute increase metrics to better quantify the effect of subduction ground motions on RSRA. QCC is seen to have the largest relative increase in AAL and AALR (24%), followed by Ucluelet (23.5%) and Sooke (17%).

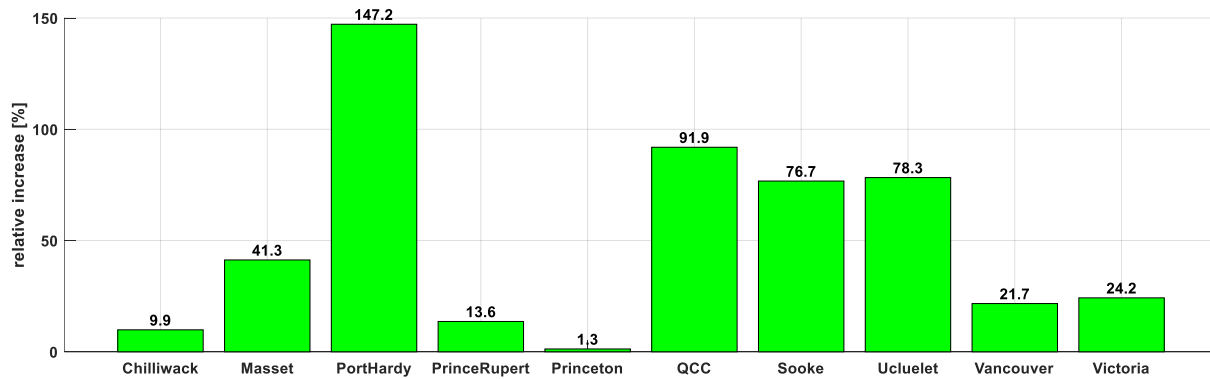


Figure 4.96 Relative increase in AACF across 10 selected BC localities using the site's exposure model.

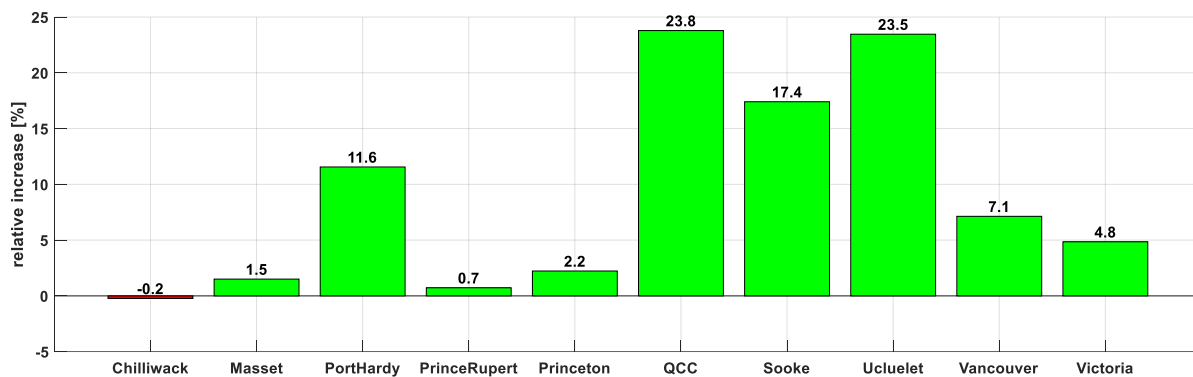


Figure 4.97 Relative increase in AALR across 10 selected BC localities using the site's exposure model.

4.10.2 Compilation of RSRA results for 10 localities using Ucluelet exposure model

The differences in the exposure model (in this study, more percentage of C2 compared to wood) could also have fed into the results observed in section 4.10.1. To remove the variation of the influence of exposure model on the RSRA results, a uniform exposure model is used for all 10 localities, and the procedure explained in section 3.5 was rerun. The Ucluelet exposure model was chosen, as it is the smallest in terms of area, to ensure that assets are defined within landmasses. Once the RSRA was carried out as before for the 10 localities using the Ucluelet exposure model, corresponding collapse exceedance curve and loss exceedance is plotted for each city as shown in Figure 4.98 to Figure 4.117.

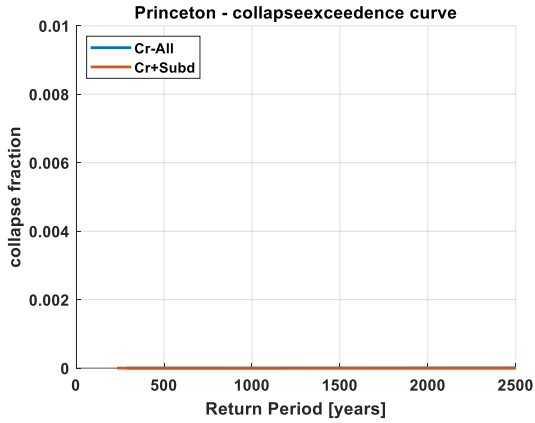


Figure 4.98 Collapse exceedance curve: Princeton

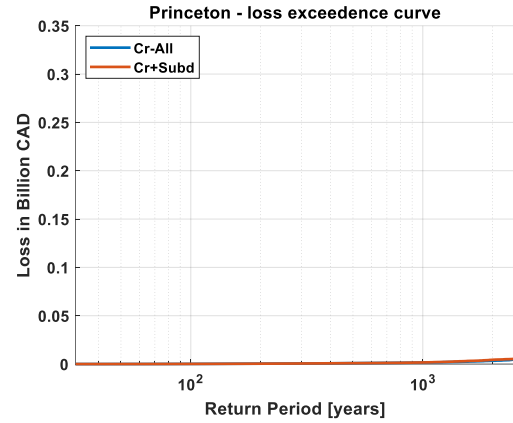


Figure 4.99 Loss exceedance curve: Princeton

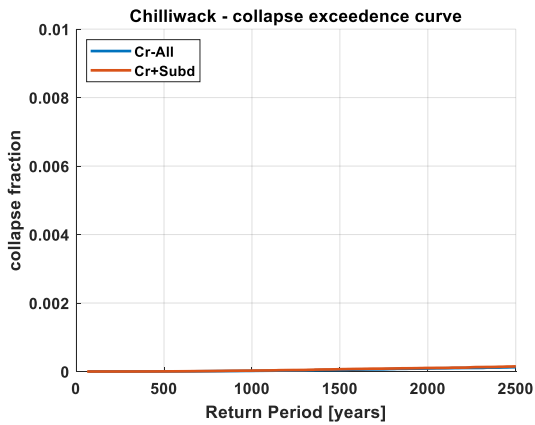


Figure 4.100 Collapse exceedance curve: Chilliwack

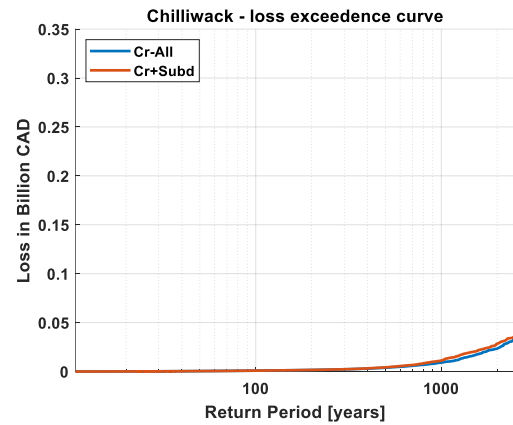


Figure 4.101 Loss exceedance curve: Chilliwack

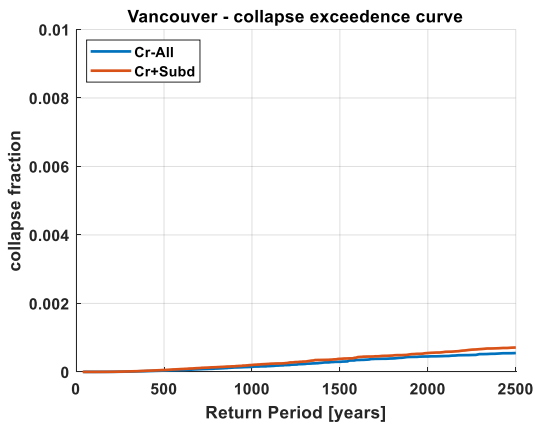


Figure 4.102 Collapse exceedance curve: Vancouver

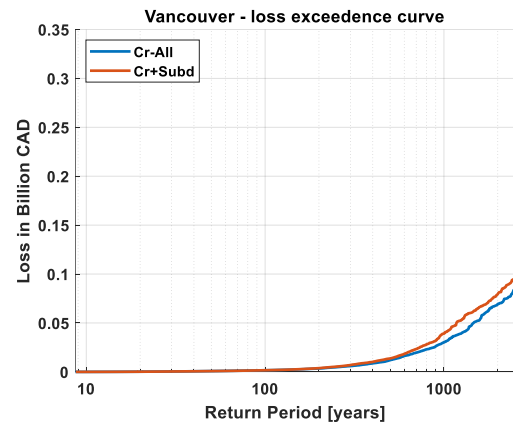


Figure 4.103 Loss exceedance curve: Vancouver

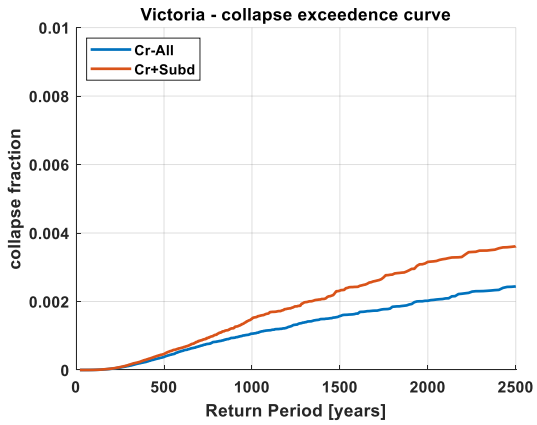


Figure 4.104 Collapse exceedance curve: Victoria

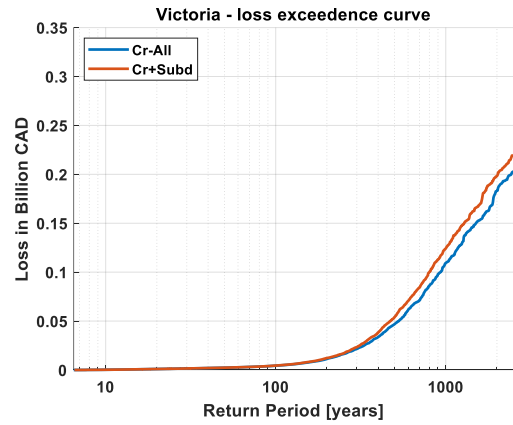


Figure 4.105 Loss exceedance curve: Victoria

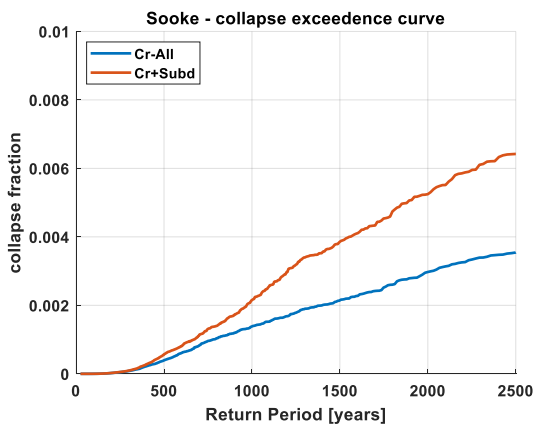


Figure 4.106 Collapse exceedance curve: Sooke

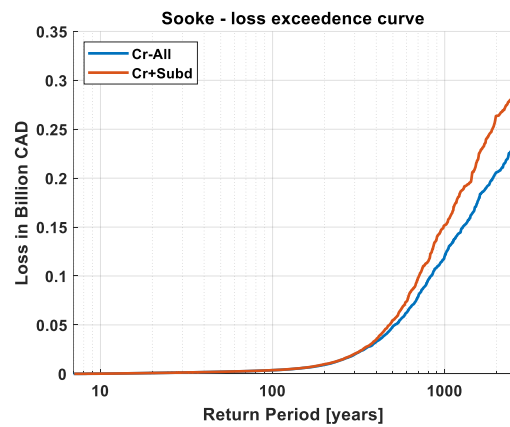


Figure 4.107 Loss exceedance curve: Sooke

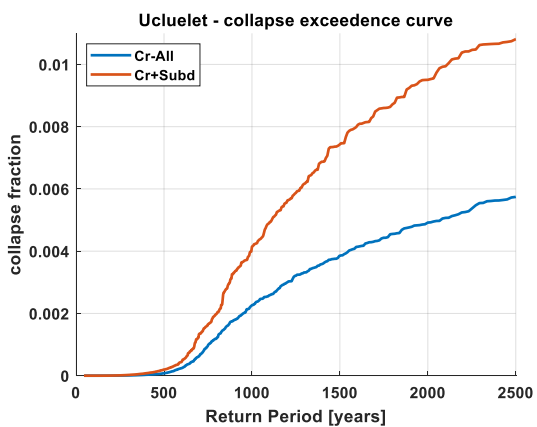


Figure 4.108 Collapse exceedance curve: Ucluelet

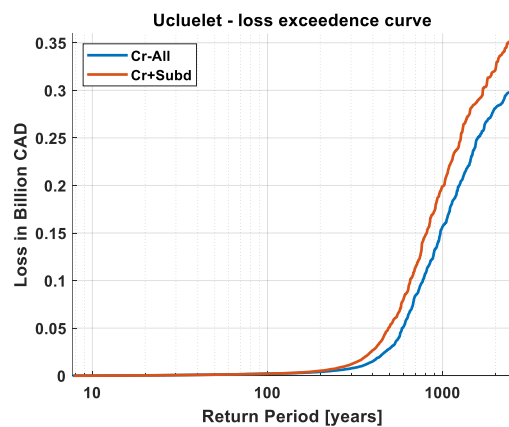


Figure 4.109 Loss exceedance curve: Ucluelet

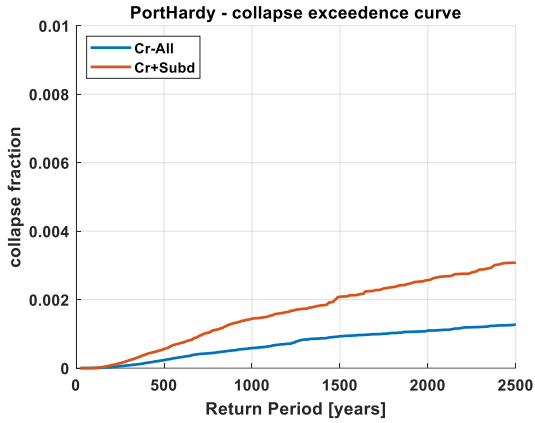


Figure 4.110 Collapse exceedance curve: Port Hardy

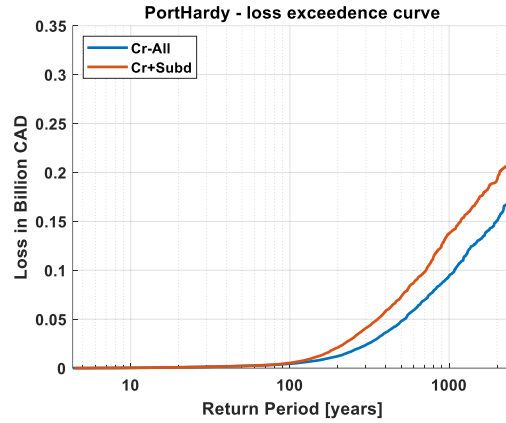


Figure 4.111 Loss exceedance curve: Port Hardy

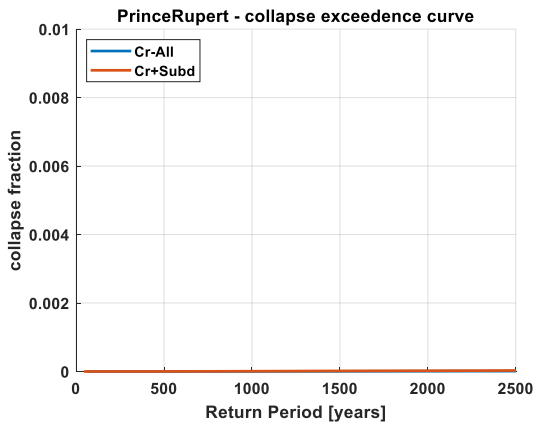


Figure 4.112 Collapse exceedance curve: Prince Rupert

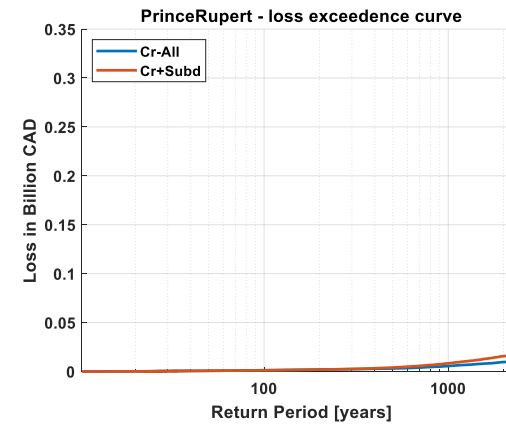


Figure 4.113 Loss exceedance curve: Prince Rupert

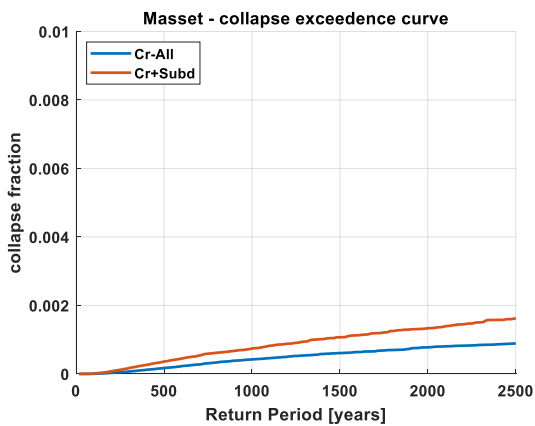


Figure 4.114 Collapse exceedance curve: Masset

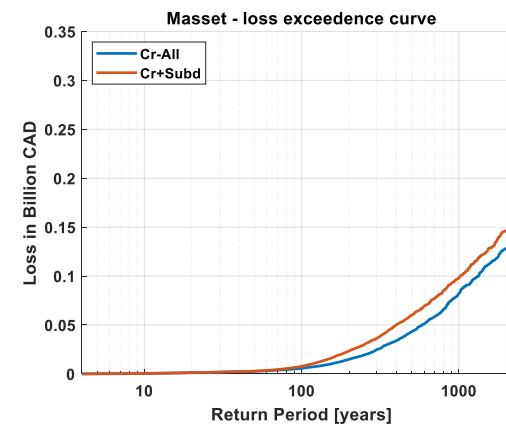


Figure 4.115 Loss exceedance curve: Masset

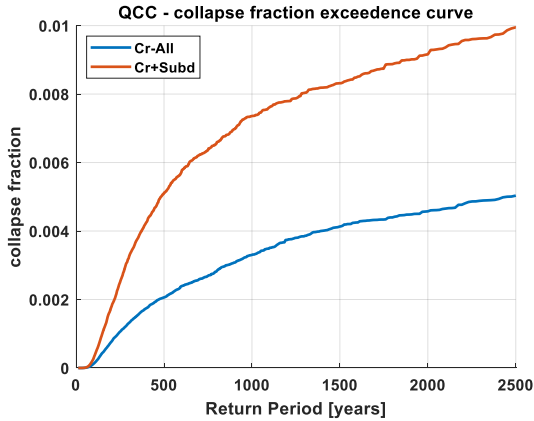


Figure 4.116 Collapse exceedance curve: QCC

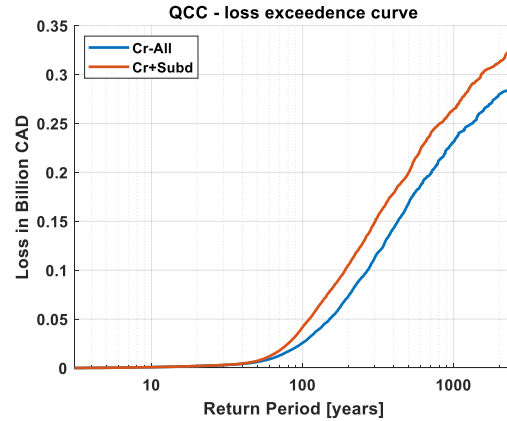


Figure 4.117 Loss exceedance curve: QCC

As compared to the results in section 4.10.1, using a uniform exposure model to conduct RSRA across the 10 sites provides a more direct comparison between the Cr+Subd and the baseline Cr-All case. From Figure 4.98 - Figure 4.117, it is seen that at a return period of 1000 years, the collapse fraction estimated by the Cr+Subd case at Princeton, Chilliwack, Vancouver, Victoria, Sooke, Ucluelet, Port Hardy, Prince Rupert, Masset and QCC are 1.6×10^{-7} , 0.85×10^{-5} , 5×10^{-4} , 4.3×10^{-4} , 7.6×10^{-4} , 1.9×10^{-2} , 8.6×10^{-4} , 5.6×10^{-6} , 3.2×10^{-4} and 4×10^{-3} higher than the collapse fraction estimated by the corresponding baseline Cr-All case. Similarly, at a return period of 1000 years, the loss estimated by the Cr+Subd case at Princeton, Chilliwack, Vancouver, Victoria, Sooke, Ucluelet, Port Hardy, Prince Rupert, Masset and QCC are 8×10^{-5} , 2.7×10^{-3} , 8.8×10^{-3} , 0.015, 0.032, 0.042, 0.043, 2.8×10^{-3} , 0.016 and 0.034 billion CAD higher than the loss estimated by the corresponding Cr-All case. Very clearly, as the subduction hazard increases from Princeton to Chilliwack to Vancouver to Victoria to Sooke to Ucluelet, the increasing effect of the long duration subduction ground motions on the collapse exceedance and loss exceedance curves can be seen from Figure 4.98 to Figure 4.109. As the localities move from mainland BC, toward the subduction

sources, as expected, the influence of subduction fragility and vulnerability curves on the collapse and loss exceedance curves increases.

The AACF, AAL and AALR are calculated at each of the 10 localities for the two cases (Cr-All and Cr+Subd), using the Ucluelet exposure model and summarized in Figure 4.118 to Figure 4.120 and depicts a pattern in the effect of subduction ground motions on RSRA in the 10 BC localities. The increase of AACF, AAL and AALR for the Cr+Subd case increases as you move outward mainland BC, with AACF being more indicative of this change.

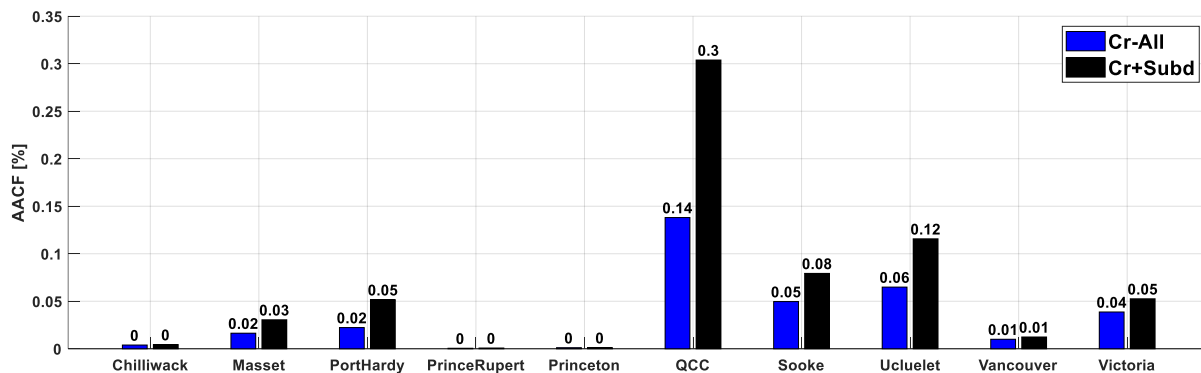


Figure 4.118 Summary of AACF for 10 selected BC localities for Cr-All and Cr+Subd cases using the Ucluelet exposure model.

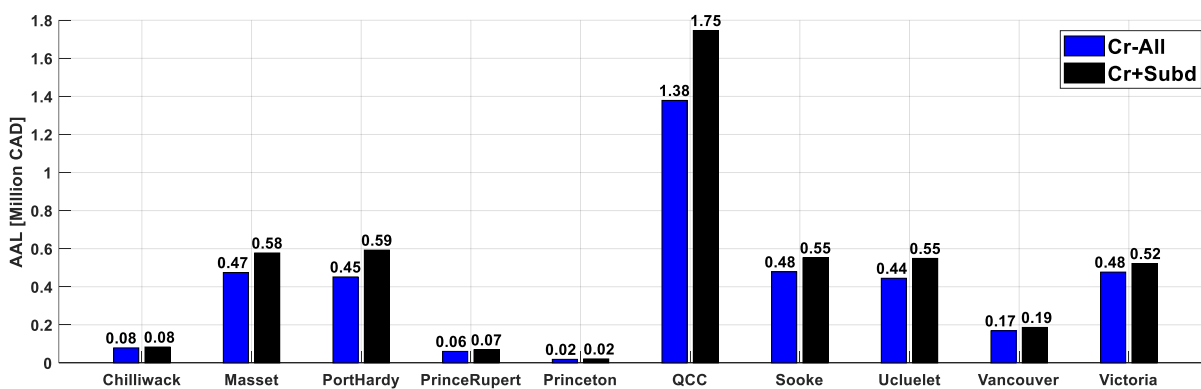


Figure 4.119 Summary of AAL for 10 selected BC localities for Cr-All and Cr+Subd cases using the Ucluelet exposure model.

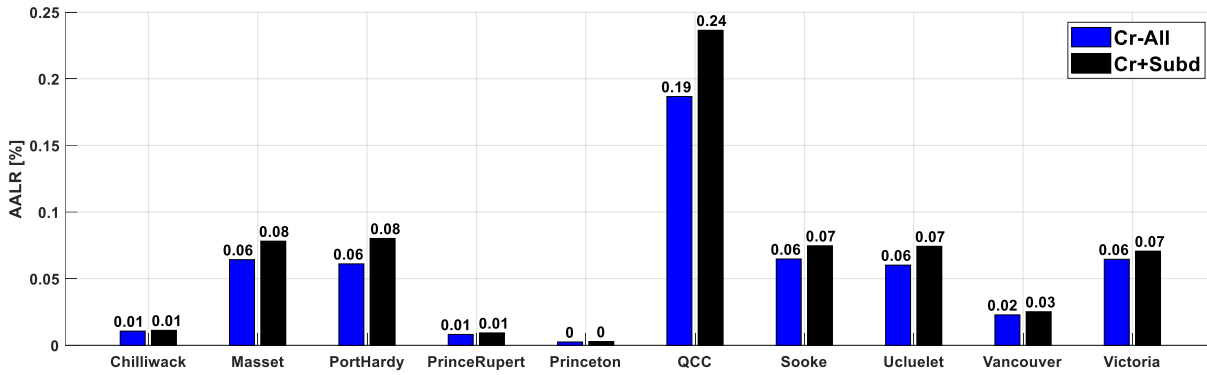


Figure 4.120 Summary of AALR for 10 selected BC localities for Cr-All and Cr+Subd cases using the Ucluelet exposure model.

The inclusion of subduction fragility and vulnerability functions adds to the baseline (Cr-All) results at the 10 localities in different intensities. For example, the AACF at Vancouver is pushed from 0.01 to 0.012, while at Victoria, it goes from 0.039 to 0.053 and the AALR at Vancouver is pushed from 0.023% to 0.025%, while at Victoria, it goes from 0.064% to 0.07%.

From Figure 4.118 to Figure 4.120, the estimated absolute increase in AACF, AAL and AALR are from the Cr+Subd case as compared to the Cr-All case at the 10 localities are calculated and summarized in Figure 4.121 to Figure 4.123.

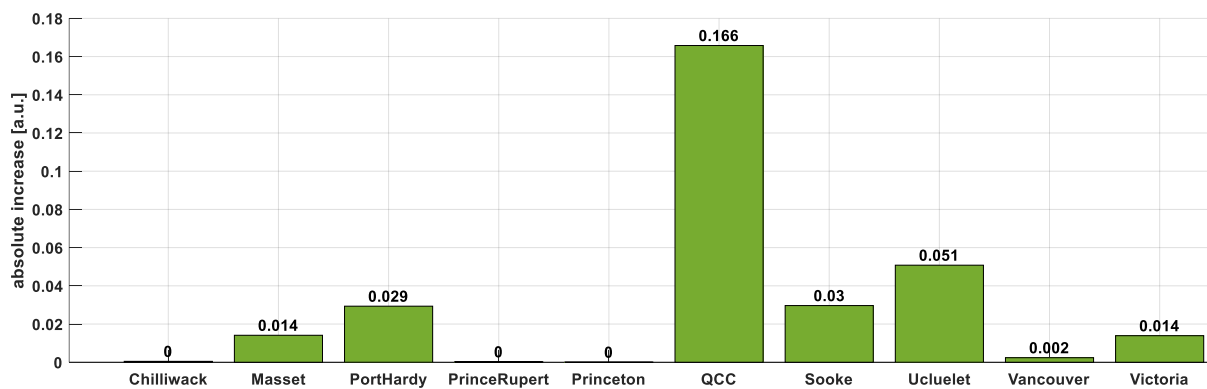


Figure 4.121 Absolute increase in AACF for 10 selected BC sites when using the Ucluelet exposure model.

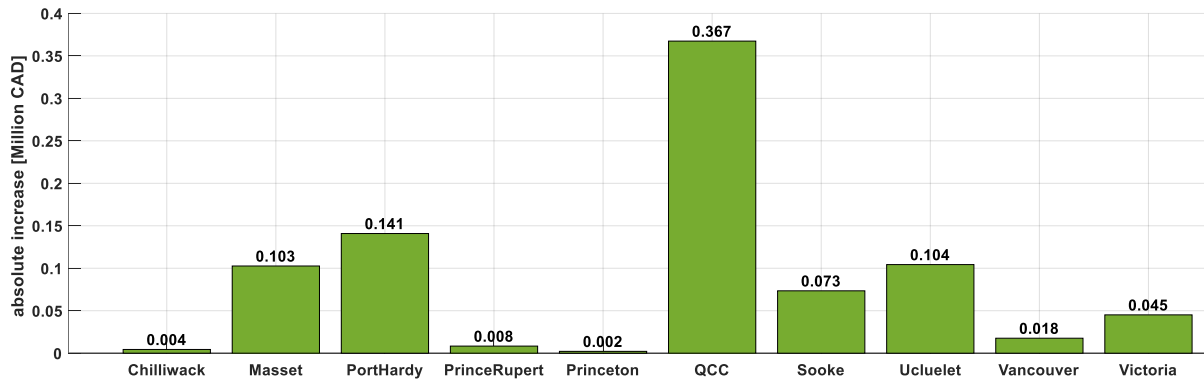


Figure 4.122 Absolute increase in AAL for 10 selected BC sites when using the Ucluelet exposure model.

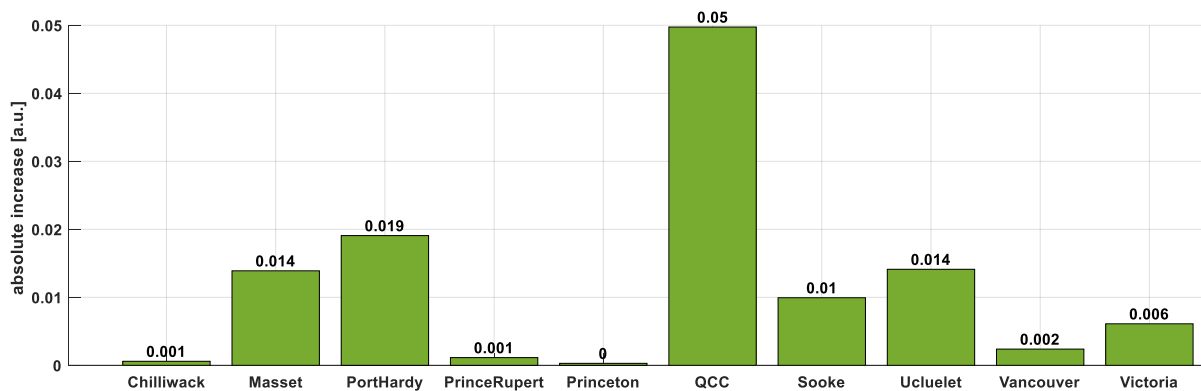


Figure 4.123 Absolute increase in AALR for 10 selected BC sites when using the Ucluelet exposure model.

Figure 4.121 shows that the largest increases in AACF follows QCC, Ucluelet, Sooke, Port Hardy, Victoria, Masset and Vancouver as 0.17, 0.05, 0.03, 0.03, 0.014, 0.014 and 0.002 respectively. Chilliwack, Prince Rupert and Princeton have almost negligible increases in AACF. This means that in QCC, if subduction damage and loss functions are considered in RSRA, the average annual collapse would be 0.3 instead of 0.14 times QCC's building stock (120% increase). Figure 4.122 shows that largest absolute increase in AAL due to inclusion of subduction vulnerability functions in RSRA is at QCC, followed by Port Hardy, Ucluelet, Masset, Sooke, Victoria and Vancouver, quantified as 0.37, 0.14, 0.1, 0.1, 0.07, 0.045 and 0.02 million CAD respectively. The AAL at other locations are very small (in thousands of CAD). Figure 4.123

shows that the largest absolute increase in AALR due to inclusion of subduction vulnerability functions at the 10 sites follows the pattern of increase in AAL. The highest is recorded at QCC (from 0.19% to 0.22%), followed by Port Hardy (0.06% to 0.08%), Ucluelet (0.06% to 0.074%), Masset (0.064% to 0.078%), Sooke (0.065% to 0.075%), Victoria (0.064% to 0.07%) and Vancouver (0.023% to 0.025%) respectively. The absolute increase in AALR at other locations are very small. The estimated relative increase in AACF, AAL and AALR for the Cr+Subd case as compared to the Cr-All case at the 10 localities, when using a uniform exposure model, are summarized in Figure 4.124 and Figure 4.125.

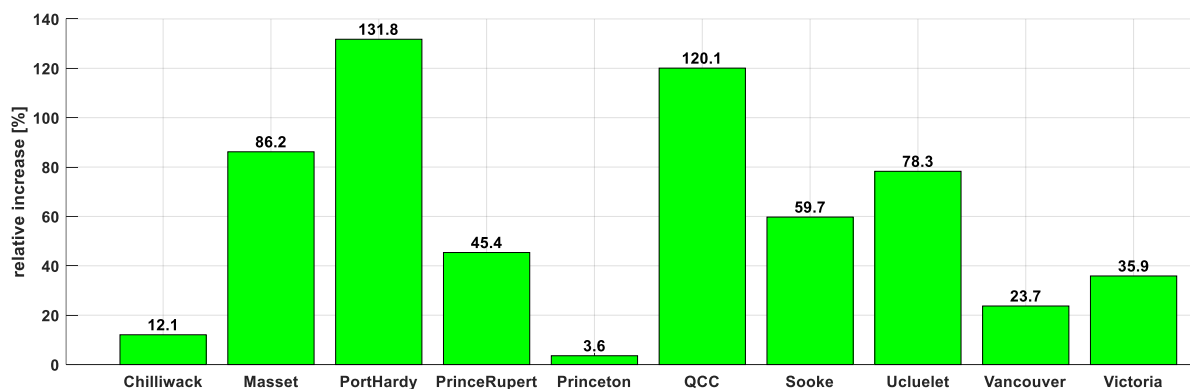


Figure 4.124 Relative increase in AACF across 10 selected BC localities using the Ucluelet exposure model.

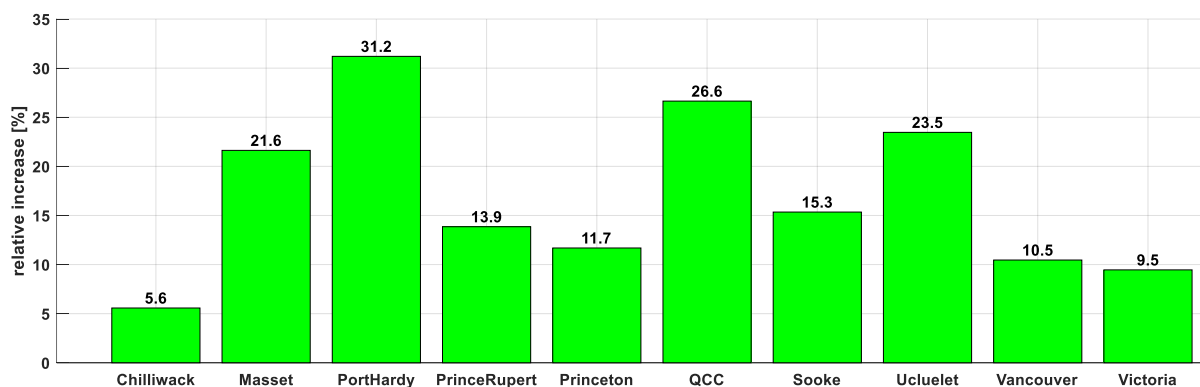


Figure 4.125 Relative increase in AALR across 10 selected BC localities using the Ucluelet exposure model.

Port Hardy is seen to have the largest relative increase in AACF and AALR (~132% and ~31% respectively), followed by QCC (~120% and ~27% respectively). However, in absolute terms, the increase in AACF at Port Hardy and QCC are 0.014 and 0.17 respectively, and AALR, 0.02 and 0.05 respectively.

4.10.3 General summaries drawn from RSRA results

The following general summaries were drawn from sections 4.10.1 and 4.10.2:

1. Localities with larger number of assets have larger AAL and AACF. Vancouver and Victoria show highest AAL. However, regions with lower number of assets, but high seismicity can also have a high AAL, as is the case of Chilliwack and Sooke. (Chilliwack, due to the combination of ~20,000 assets and a low seismicity, Sooke, with ~4000 assets and a very high seismicity) (Figure 4.91).
2. Localities with more W1 and high code/moderate code C2, W2 and W3 shows more influence of subduction ground motions on RSRA. For example, consider Masset (Figure 4.87 and Figure 4.115). Masset originally has ~4.6% C2 PC and ~6.3% W2 and W3 PC assets in its exposure model, while Ucluelet has ~1.1% C2 PC and ~2.9% W2 and W3 PC assets in its exposure model. The fragility and vulnerability functions of these typologies are not influenced much by long duration ground motions, as observed in section 4.4 and hence do not contribute to the influence of subduction ground motions on RSRA. When developing the loss exceedance curves at Masset, first using Masset's exposure model and second with Ucluelet exposure model, a striking increase in the effect of subduction ground motions on RSRA can be seen. This is because Ucluelet has a much higher percentage of W1 in its

exposure model. This influence of exposure model on RSRA results is also evident for loss exceedance curves and collapse exceedance curves for Vancouver, Victoria, Port Hardy and QCC. This means that in the localities where the exposure model is dominated by pre-code C2, W2 and W3 typologies, RSRA can be carried out with the crustal fragility and vulnerability functions alone to get a good estimate of damage and loss.

3. In Figure 4.97, a negative increase in AALR at Chilliwack is seen. This is because, certain typologies like pre-code C2L, W2 and W3 shows a smaller loss ratio from subduction events as compared to crustal events, at lower intensities of ground shaking. Although Chilliwack has a higher seismic hazard than Princeton, the percentage of these specific typologies are higher in Chilliwack (~2.7% of the Chilliwack exposure model vs ~2.4% of the Princeton exposure model). Also, the percentage of W1 -where the effect of subduction ground motions is more pronounced-is lower in Chilliwack (~94.5% in Chilliwack vs ~97.4% in Princeton).
4. AACF and increase in AACF is a more reliable indicator to understand the influence of subduction ground motions on RSRA than AAL and AALR, as it does not have the accumulated uncertainty from definitions of damage states (DS1, DS2 and DS3), consequence models and definitions of vulnerability models affecting the results. (Figure 4.93, Figure 4.96, Figure 4.121 and Figure 4.124)
5. Within the 6 localities marked inside the blue outline shown in Figure 4.126, the influence of subduction ground motions on collapse exceedance curves and loss exceedance curves increases as one moves outward the BC mainland.

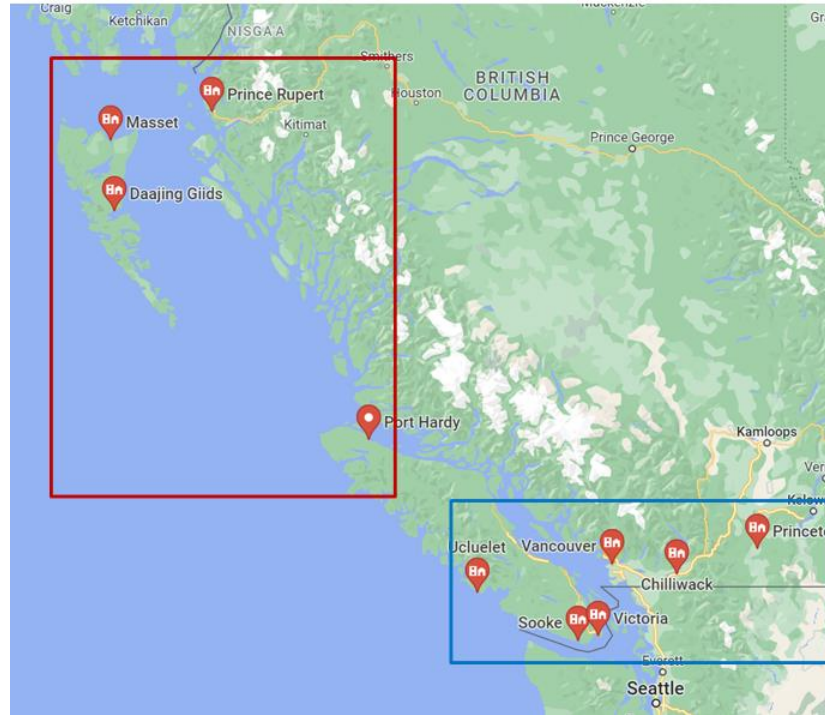


Figure 4.126 Grouping of localities

That is, as one moves from Prince Rupert to Chilliwack to Vancouver to Victoria to Sooke to Ucluelet, the effect of subduction ground motions on RSRA increases steadily. This is reflected in the AACF and increase in AACF comparisons (Figure 4.121 and Figure 4.124).

6. For the four localities marked inside the red outline in Figure 4.126, the influence of subduction ground motions on RSRA cannot be as easily defined, as these four localities have very different exposure to seismic sources, and different soil characteristics. Port Hardy is close to two subduction interface sources (Winona thrust fault and the Explorer section of the CSZ). QCC is closest to the Haida Gwaii thrust fault (Subduction interface source), Queen Charlotte Fault (Active shallow

fault) and the Hecate strait (Active shallow crust) followed by Masset and Prince Rupert.

7. Between the four localities mentioned in 6, assuming a uniform exposure model, the influence of subduction ground motion on RSRA, as seen in the collapse exceedance curve and loss exceedance curve is the highest in QCC, followed by Port Hardy, Masset and Prince Rupert (Figure 4.110 to Figure 4.117). This is also seen in the AACF plotted in Figure 4.118, and absolute increase in AACF, AAL and AALR (Figure 4.121 to Figure 4.123). However, the increase in AACF and AALR is highest in Port Hardy, followed by QCC, Masset and Prince Rupert. (Figure 4.124 and Figure 4.125.).

Chapter 5: Conclusion

5.1 Summary of results

This section summarizes the results obtained. As discussed in the literature review, the effect of subduction ground motions on regional seismic risk assessment (RSRA) in BC has not been studied in detail, prior to this study. This dissertation aimed to bridge this knowledge gap by isolating the influence of subduction ground motions on RSRA in BC by explicitly including subduction fragility and vulnerability functions in RSRA at selected localities within BC, where the contribution of subduction seismic hazard to the total seismic hazard at the site varies significantly. To implement this, the five sub-objectives achieved are:

1. Developed a uniform exposure model for Vancouver and Victoria and identified concrete shear wall and wood buildings as the prominent building typologies (>95%) in these two representative localities. This thesis concentrates on these two typologies.
2. Developed representative simplified models for BC-specific concrete shear wall and wood median building to better characterize BC construction practices, in terms of strength and displacement capacities, and introduced three new wood typologies to represent the BC building stock more accurately.
3. Developed crustal and subduction fragility and vulnerability functions for concrete shear wall and wood typologies in Vancouver and Victoria.
4. Quantified the difference between estimated scenario damages and losses from two scenarios for Vancouver: a crustal (Georgia Strait M7.3) and a subduction

(Cascadia Subduction Zone M9.0), using the BC-specific fragility and vulnerability functions and the current functions used in the national seismic risk map for Canada. This investigation was also extended to study the differences in scenario damage and loss incurred when including low-rise residential wood typologies with cripple walls and sub-floors when running the scenario analyses.

5. Investigated the influence of subduction ground motions on RSRA in BC - using the OQ stochastic event-based damage and loss calculator (a probabilistic seismic risk calculator). First, damage and losses from subduction events and damage and losses from crustal and subcrustal events within the seismic event sets developed within the OQ event-based hazard calculator are calculated separately. These results were then combined to get the total regional risk at the site. This was then compared to a RSRA carried out using only crustal fragility and vulnerability functions to calculate damage and loss from all events, irrespective of source type, to understand how much the inclusion of subduction damage and loss functions affects the RSRA results.

5.2 Key Findings

5.2.1 Key findings regarding exposure

1. BC construction is predominantly made of wood and concrete shear wall construction. From the BC exposure model developed by NRCan, certain BC localities reported more masonry pre-code constructions than concrete shear wall. However, because Vancouver and Victoria were chosen as representative BC localities, masonry construction was excluded in this study.

2. All newer code (after 1990) C2 and wood typologies in BC are weaker than corresponding building typologies described in HAZUS. Design base shear for concrete shear walls in BC have not changed much over the years. Design base shear for wood typologies built after 1990, have only increased by 20% for low-rise residential (W1) and 16.7% for mid-rise residential and commercial wood construction from those built before 1990. Concrete shear wall and commercial and industrial wood construction in BC built before 1990 are stronger than corresponding HAZUS building typologies.

5.2.2 Key findings regarding fragility and vulnerability functions

1. Fragility functions used to develop the CanSRM1 (henceforth referred to as GEM functions) generally estimates lower total damages than BC-specific fragility functions. The median DS4 capacity for BC W1 PC and HC crustal fragility functions are 27.5% and 96.0% lower than corresponding GEM functions respectively. But, fragility functions for concrete shear wall construction and commercial wood built before 1990 estimates higher damages than BC-specific fragility curves. The median DS4 capacity for GEM fragility functions are 41%, 34%, 15% and 39.6% lower than BC-specific crustal fragility functions for C2L, C2M, C2H and W3 PC typologies respectively.
2. BC-specific concrete shear wall vulnerability curves estimate more loss than their corresponding GEM functions. The median structural loss ratio capacity decreases by 35%, 40% and 31% for BC C2L-PC, C2M-PC and C2H-PC typologies and by 36% and 42% for BC C2L-HC and C2M-HC typologies, respectively, as compared

to corresponding GEM typologies. BC-specific wood typology vulnerability curves estimate lower losses than their corresponding GEM functions (except for low-rise wood with cripple wall). The median structural loss ratio capacity decreases by 71.8%, 93.5% and 75% for equivalent GEM W1, W2 and W3 PC typologies and by 41.9%, 52.2% and 58.7% for equivalent GEM W1, W2 and W3 HC typologies, respectively, as compared to corresponding BC typologies. The BC-specific acceleration sensitive non-structural and contents vulnerability functions are tied to the DS4 fragility functions for all typologies.

3. On accounting for the presence of sub-floor and cripple wall cases within the low-rise residential wood construction, much higher damage and loss is seen as compared to cases without cripple walls or subfloors considered. The median DS4 capacity (spectral acceleration at 50% probability of exceedance of DS4), is reduced by 62.5% and 30% when considering the presence of if a cripple wall or subfloor is a W1-PC building. The median loss ratio decreases by 45% in the presence of a cripple wall, and by 28% in the presence of a subfloor to a low-rise residential wood building respectively.
4. Damage estimated at a specified seismic intensity by crustal fragility curves are lower than that estimated by subduction fragility curves for almost all typologies. The difference between the crustal and subduction damage estimates increases as the intensity of ground shaking increases. It is also noted that the long duration subduction ground motions significantly influence the DS4, but its effect

diminishes as the damage state lowers. That is to say, slight damage state is least influenced by long duration effects.

5. The effect of long duration subduction ground motions on fragility and vulnerability curves is more pronounced in buildings built after 1990, that have a larger inherent ductility, than in the non-ductile buildings built before 1973. The higher the ductility of the system, higher the influence of the long duration subduction ground motions on probability of exceedance of a given damage state. For example, the median DS4 capacity for BC-specific C2L-PC and C2L-HC subduction fragility curves decreases by 13% and 43% respectively, when compared to crustal fragility curves.

5.2.3 Key findings from scenario analysis

1. The scenario damage and loss analysis for Vancouver shows that the total damage and loss is governed by residential wood construction. However, the highest individual asset losses are from concrete shear wall, mid-rise residential and commercial and industrial wood construction built before 1990. These are concentrated in Downtown Vancouver, Kerrisdale and the West End, south Marpole and Champlain Heights, and south Kitsilano and Sunset respectively.
2. Comparing scenario analysis results obtained, the use of BC-specific functions for the crustal GSM7.3 scenario shows a 24% increase in complete damage estimates and 13.7% increase in total scenario loss and for the subduction CSZ9.0 scenario, a 43% increase in complete damage estimates and about 2.5 times the total scenario loss using GEM functions.

3. Considering cripple wall and subfloor inclusive low-rise residential wood typologies in scenario analysis drives up damage and loss. In particular, the low-rise wood construction with subfloors in West Point Grey and south Kitsilano and cripple wall cases in Shaughnessy. Considering these two cases would increase the complete damage and loss estimates by 89% and 18% for GSM7.3 scenario and 34% and 6% for CSZ9.0 scenario respectively.

5.2.4 Key findings from Regional Seismic Risk Analysis (RSRA)

1. RSRA was carried out using OQ stochastic event-based damage and loss calculator, using the 2015 GSC seismic hazard model. Given that a uniform exposure model is used in the ten localities and that the seismic sources contributing to the seismic hazard at the localities are the same, generally, the AACF and AALR increase as the location of the selected localities move outward of mainland BC. This is noted between the 6 localities of Princeton, Chilliwack, Vancouver, Victoria, Sooke and Ucluelet and the 3 localities in Haida Gwaii, Prince Rupert, Masset and QCC. At localities where there are isolated seismic sources (e.g., Port Hardy), RSRA has to be conducted more thoroughly to investigate the influence of long duration subduction ground motions.
2. When RSRA is run considering the site's original exposure model and explicitly accounting for subduction fragility and vulnerability functions, the highest AACF and AALR is seen at QCC (0.37 and 0.22%), and lowest at Princeton (0.0015 and 0.004%). The highest absolute increase in AACF and AALR when explicitly accounting for subduction fragility curves is observed at QCC (0.18 and 0.05), and

the least at Princeton (2×10^{-5} and 3×10^{-4}), where there is the least subduction hazard. The highest relative increase in AACF is at Port Hardy (~150%), where there are more subduction sources influencing the total hazard at the site. The highest relative increase in AALR is at QCC (~24%).

3. When the original exposure model of the locality is used, localities with larger number of assets have higher AAL and AACF. Vancouver and Victoria show highest AAL. However, regions with lower number of assets, but high seismicity and vice versa can also have a high AAL, as is the case of Chilliwack and Sooke. (Chilliwack, due to the combination of ~20,000 assets and a low seismicity, Sooke, with ~4000 assets and a very high seismicity).
4. AACF and increase in AACF is a more reliable indicator to understand the influence of long duration ground motions on RSRA than AAL and AALR, as it does not have the accumulated uncertainty from assignment of the different damage states (DS1, DS2, DS3), consequence models and definitions of vulnerability models affecting the results.

5.3 Conclusions

1. It was seen that most BC building typologies (except C2 and W3 pre-code constructions) are weaker than those assumed to develop the CanSRM1. Consequently, the damage and loss estimates using BC-specific fragility and vulnerability functions are higher than when using GEM functions. The presence of subfloor or cripple walls increases the loss and damage estimates in a low-rise wood construction. So, fragility and vulnerability functions for low-rise wood

construction with cripple walls or subfloor has to be developed when a site has a large number of them in its building stock (as in the case for Vancouver).

2. Long duration subduction ground motions influence the fragility and vulnerability functions of constructions built after 1990 more than those built before 1990, due to the larger inherent ductility in the structure. C2, W2 and W3 construction built before 1990 do not show a significant influence of long duration subduction ground motions on their fragility and vulnerability curves, as compared to the short duration crustal ground motions in BC. However, long duration subduction ground motions influence all low-rise residential wood construction.
3. Scenario loss analyses in Vancouver shows that individual assets that contribute to largest losses are concrete shear-wall, multi-family residential and commercial wood construction, while most of the total damage and loss comes from low-rise residential wood construction. The introduction of the new wood typologies doubles the complete damage estimates, due to the recognition of deficiencies like cripple walls and subfloors within the low-rise residential wood structures. Especially so, in Vancouver where 50% of the low-rise residential wood construction was recognized as having subfloors, as per a recent UBC building-by-building survey of Vancouver.
4. RSRA demonstrates that as the relative contribution of subduction hazard to total seismic hazard increases, generally, the influence of the long duration subduction ground motions on regional risk in BC become more pronounced. However, this conclusion is dependent on the exposure model at the locality and the same seismic

sources contributing to the seismic hazard at the sites. Using crustal functions alone for RSRA in mainland BC (say in Princeton) would provide a good estimate of risk (less than 5% increase of AACF and ~10% increase of AAL and AALR if subduction fragility curves were considered). But, in regions on the islands off the coast of mainland BC, it will be severely underestimated (~120% increase of AACF and ~25% increase of AAL and AALR if subduction fragility curves were considered in QCC). The influence of exposure model on the RSRA results is significant. When estimating the influence of the long duration subduction ground motions on RSRA, especially in sites with close subduction seismic sources, much care should be given.

5.4 Significant contributions

1. This dissertation is the first research that investigated the influence of subduction ground motions on RSRA in BC. This work implements a method to identify the extent of influence of subduction ground motions on regional seismic risk at a site using separate crustal and subduction fragility and vulnerability functions in RSRA.
2. To obtain better estimates of the influence of subduction ground motions on RSRA in BC, appropriate crustal and vulnerability functions were developed. To implement this, this work developed appropriate ESDOF models that reflected the BC construction practices, from data provided by the Concrete and Wood groups of the Buildings at Risk Sub-Committee (part of the Seismic Policy Advisory Committee of the City of Vancouver), comprising of members from the academia and industry. Based on discussions with the committees, BC wood typologies were

expanded to 5 structural typologies to better reflect the BC wood building stock. The new structural building typologies introduced are mid-rise residential wood construction (W2), low-rise residential wood construction with subfloor (W4s) and low-rise wood construction with cripple walls (W4c).

3. Crustal and subduction fragility and vulnerability functions were developed for concrete shear wall and wood typologies in Vancouver and Victoria. The crustal and subduction fragility and vulnerability functions were compared to understand the effect of subduction ground motion on damage and loss estimates for these typologies. Generally, the subduction ground motions induce larger estimates of complete damage and by extension, collapses than crustal ground motions, especially for BC construction after 1990.
4. This dissertation has undertaken scenario analysis studies to understand the significance of the changes and decisions made towards developing the BC-specific fragility and vulnerability functions, towards scenario analysis in Vancouver. The scenario analysis results for Vancouver using BC-specific fragility and vulnerability functions were compared to scenario analysis completed using the fragility and vulnerability functions currently used by NRCan.
5. This dissertation carried out RSRA in 10 localities within BC with varying contributions of subduction hazard to total seismic hazard at the site. It concluded that quantifying the effect of subduction ground motions on RSRA requires significant understanding of the exposure model, the seismic sources contributing to hazard at the site and accurate fragility and vulnerability functions that capture

the effect of duration on different typologies within the exposure model. It was determined that of the many metrics considered to quantify the effect of subduction ground motions on RSRA at a site, collapse fraction at a specific return period, AACF, absolute increase in AACF and relative increase in AACF are the metrics that have least uncertainty.

5.5 Recommendations for future research

1. This study addresses only wood and concrete shear wall building typologies in BC. Other building typologies have been excluded, and could be considered for further research in BC, especially masonry construction.
2. Exposure model development includes assumptions assigning buildings to specific structural building typologies, building occupancy types. It requires accurate records of floor area of buildings, component replacement costs and geographic locations of the buildings within the study region. These factors introduce a high uncertainty in risk assessments, through the exposure model, more so for coarser exposure models that involves many aggregation assumptions (as those used to run the RSRA in this study). Contributions to the uncertainty in damage and loss from uncertainties in the assumptions made in the exposure were out of scope of the present study and should be considered in future work, and exposure models used in RSRA should be updated to better represent the locality's building stock.
3. To quantify the effect of subduction ground motions on RSRA, along with AACF, AAL, AALR, loss exceedance curves and collapse fraction exceedance curves, it is also necessary to compute the contribution of subduction hazard at a site. To

calculate this, the subduction contribution at the site at all periods significant to the building stock (periods at which the fragility and vulnerability functions are developed) should be added from deaggregation results. This is beyond the scope of this work, and should be considered for future studies

4. This study developed fragility and vulnerability functions using ground motion suites developed for NBCC 2015. Similarly, the scenario analysis used GMPEs recommended for use in the CanadaSHM5. The RSRA utilizes the CanadaSHM5 for south-west BC, used in NBCC 2015. Future work should consider extending this to NBCC 2020, and use the 6th Generation Seismic Hazard Model of Canada (CanadaSHM6) for RSRA studies.
5. Future research could consider studying the effect of long duration subduction ground motion on RSRA by isolating the long duration effect alone on different building typologies. To do this, the crustal and subduction ground motion suites used for IDA analysis should be developed to consist of spectrally-matched pairs of crustal and subduction ground motions (the ground motions differ only in duration), and the RSRA should be redone.

Bibliography

- Ab-Kadir, M. A. (2014). Experimental And Numerical Study On Softening And Pinching Effects Of Reinforced Concrete Frame. *IOSR Journal of Engineering*, 4(5), 01–05.
<https://doi.org/10.9790/3021-04520105>
- Abrahamson, N., Gregor, N., & Addo, K. (2016). BC Hydro Ground Motion Prediction Equations for Subduction Earthquakes. *Earthquake Spectra*, 32(1), 23–44.
<https://doi.org/10.1193/051712EQS188MR>
- Allen, T., Halchuk, S., Adams, J., & Rogers, G. C. (2017). Canada’s 5th Generation Seismic Hazard Model: 2015 Hazard Values and Future Model Updates. *Proceedings of the 16th World Conference on Earthquake Engineering, Santiago, Chile*.
- Allen, T., Halchuk, S., Adams, J., & Weatherill, G. A. (2020). Forensic PSHA: Benchmarking Canada’s Fifth Generation seismic hazard model using the OpenQuake-engine. *Earthquake Spectra*, 36(1_suppl), 91–111. <https://doi.org/10.1177/8755293019900779>
- Applied Technology Council. (1996). *ATC-40: Seismic Evaluation and Retrofit of Concrete Buildings Volume 1*.
- ASCE. (2010). *ASCE Standard ASCE/SEI 7-10, Minimum design loads for buildings and other structures*. American Society of Civil Engineers.
- Atkinson, G. M., & Adams, J. (2013). Ground motion prediction equations for application to the 2015 Canadian national seismic hazard maps. *Canadian Journal of Civil Engineering*, 40(10), 988–998. <https://doi.org/10.1139/cjce-2012-0544>
- Atkinson, G. M., & Macias, M. (2009). Predicted Ground Motions for Great Interface Earthquakes in the Cascadia Subduction Zone. *Bulletin of the Seismological Society of America*, 99(3), 1552–1578. <https://doi.org/10.1785/0120080147>

- Bebamzadeh, A., Fairhurst, M., Ventura, C. E., & Finn, L. W. D. (2015). Selection of ground motions for the seismic risk assessment of British Columbia school buildings for the proposed 2015 NBCC ground motions. *Proceedings of the 11th Canadian Conference on Earthquake Engineering, Victoria, BC.*
- Bird, A. L., Journeay, J. M., Hobbs, T. E., Hastings, N., Cassidy, J. F., Wagner, C., Bristow, D., Deelstra, A., & Chouinard, P. (2021). *Exercise Coastal Response 2022: Scenario Earthquake & Potential Impacts.*
- Bradley, B. A. (2010). A generalized conditional intensity measure approach and holistic ground-motion selection. *Earthquake Engineering & Structural Dynamics*, n/a-n/a. <https://doi.org/10.1002/eqe.995>
- Capraro, I. (2018). *Damage, collapse potential and long duration effects of subduction ground motions on structural systems* [Doctoral Dissertation]. University of British Columbia.
- Cassidy, J. F. (1986). *The 1918 and 1957 Vancouver Island earthquakes* [Master of Science thesis]. University of British Columbia.
- Chai, Y. H. (2005). Incorporating low-cycle fatigue model into duration-dependent inelastic design spectra. *Earthquake Engineering & Structural Dynamics*, 34(1), 83–96. <https://doi.org/10.1002/eqe.422>
- Chandramohan, R. (2016). *Duration of earthquake ground motion: influence on structural collapse risk and integration in design and assessment practice* [Doctoral dissertation]. Stanford University.
- Chandramohan, R., Baker, J. W., & Deierlein, G. G. (2016a). Impact of hazard-consistent ground motion duration in structural collapse risk assessment. *Earthquake Engineering and Structural Dynamics*, 45(8), 1357–1379.

- Chandramohan, R., Baker, J. W., & Deierlein, G. G. (2016b). Quantifying the influence of ground motion duration on structural collapse capacity using spectrally equivalent records. *Earthquake Spectra*, 32(2), 927–950.
- Chandramohan, R., Baker, J. W., Deierlein, G. G., & Lin, T. (2013). Influence of ground motion spectral shape and duration on seismic collapse risk. *10th International Conference on Urban Earthquake Engineering*.
- Chin, D. H. L., Ventura, C. E., Bebamzadeh, A., & Fairhurst, M. (2015). Effects of subduction ground motions on the probability of collapse on low-rise buildings. *Proceedings of the 11th Canadian Conference on Earthquake Engineering*.
- Cosenza, E., Iervolino, I., & Manfredi, G. (2004). On ground motion duration and engineering demand parameters. . *International Workshop on Performance-Based Seismic Design, Concepts and Implementation*.
- Cruz, C., & Miranda, E. (2017). Evaluation of Damping Ratios for the Seismic Analysis of Tall Buildings. *Journal of Structural Engineering*, 143(1). [https://doi.org/10.1061/\(asce\)st.1943-541x.0001628](https://doi.org/10.1061/(asce)st.1943-541x.0001628)
- CUREE. (2002). *CUREE Publication No. W-17, Seismic Behavior of Level and Stepped Cripple Walls*.
- D'Ayala, D., Meslem, A., Vamvatsikos, D., Porter, K., Rossetto, T., & Silva, V. (2015). *Guidelines for Analytical Vulnerability Assessment of Low/Mid-Rise Buildings, Vulnerability Global Component Project*. .
- Fairhurst, M. (2021). *Effect of long duration motions on the structural response of RC shear wall buildings* [Doctoral Dissertation]. University of British Columbia.

- Fairhurst, M., Bebamzadeh, A., & Ventura, C. E. (2019). Effect of ground motion duration on reinforced concrete shear wall buildings. *Earthquake Spectra*, 55(1), 311–331.
<https://doi.org/10.1193/101117EQS201M>
- FEMA. (2005). *FEMA 440, Improvement of Nonlinear Static Seismic Analysis Procedures*.
- FEMA. (2012). *FEMA P-807, Seismic Evaluation and Retrofit of Multi-Unit Wood-Frame Buildings with Weak First Stories*.
- FEMA. (2014). *Hazus®–MH 2.1 Technical Manual*. www.msc.fema.gov
- FEMA. (2019). *FEMA P-1100-3, Vulnerability-Based Seismic Assessment and Retrofit of One- and Two-Family Dwellings, Volume 3 – Background Documentation*.
- FEMA. (2020a). *FEMA P-2139-2, Short-Period Building Collapse Performance and Recommendations for Improving Seismic Design, Volume 2 – Study of One-to-Four Story Wood Light Frame Buildings*.
- FEMA. (2020b). *Hazus Earthquake Model Technical Manual, Hazus 4.2 SP3*.
- Filiatrault, A., Tremblay, R., Christopoulos, C., Folz, B., & Pettinga, D. (2013). *Elements of earthquake engineering and structural dynamics* (3rd ed.). Presses Internationales Polytechnique.
- GEM. (2022). *The OpenQuake-engine User Manual. Global Earthquake Model (GEM) OpenQuake Manual for Engine version 3.15.0*.
<https://doi.org/10.13117/GEM.OPENQUAKE.MAN.ENGINE.3.15.0>
- Ghofrani, H., & Atkinson, G. M. (2014). Ground-motion prediction equations for interface earthquakes of M7 to M9 based on empirical data from Japan. *Bulletin of Earthquake Engineering*, 12(2), 549–571. <https://doi.org/10.1007/s10518-013-9533-5>

- Goda, K. (2019). Nationwide Earthquake Risk Model for Wood-Frame Houses in Canada. *Frontiers in Built Environment*, 5. <https://doi.org/10.3389/fbuil.2019.00128>
- Goda, K., & Sharipov, A. (2021). Fault-source-based probabilistic seismic hazard and risk analysis for Victoria, British Columbia, Canada: A case of the leech river valley fault and devil's mountain fault system. *Sustainability (Switzerland)*, 13(3), 1–36. <https://doi.org/10.3390/su13031440>
- Goda, K., & Yoshikawa, H. (2013). Incremental dynamic analysis of wood-frame houses in Canada: Effects of dominant earthquake scenarios on seismic fragility. *Soil Dynamics and Earthquake Engineering*, 48, 1–14. <https://doi.org/10.1016/j.soildyn.2013.01.011>
- Goda, K., Zhang, L., & Tesfamariam, S. (2021). Portfolio Seismic Loss Estimation and Risk-based Critical Scenarios for Residential Wooden Houses in Victoria, British Columbia, and Canada. *Risk Analysis*, 41(6), 1019–1037. <https://doi.org/10.1111/risa.13593>
- Goldfinger, C., Nelson, C. H., Morey, A. E., Johnson, J. E., Patton, J. R., Karabanov, E., & Enkin, R. J. (2012). Turbidite event history: Methods and implications for Holocene paleoseismicity of the Cascadia subduction zone. *US Geological Survey Professional Paper*, 1661-F.
- Halchuk, S., Adams, J., & Allen, T. (2015). *Fifth generation seismic hazard model for Canada: grid values of mean hazard to be used with the 2015 National Building Code of Canada*. <https://doi.org/10.4095/297378>
- Halchuk, S., Adams, J., & Allen, T. (2016). *Fifth generation seismic hazard model for Canada: crustal, in-slab, and interface hazard values for southwestern Canada*. <https://doi.org/10.4095/299244>

- Halchuk, S., Allen, T., Adams, J., & Rogers, G. C. (2014a). *Fifth generation seismic hazard model input files as proposed to produce values for the 2015 national building code of Canada*. <https://doi.org/10.4095/293907>
- Halchuk, S., Allen, T., Adams, J., & Rogers, G. C. (2014b). *Fifth generation seismic hazard model input files as proposed to produce values for the 2015 national building code of Canada*. <https://doi.org/10.4095/293907>
- Hancock, J., & Bommer, J. J. (2006). A State-of-Knowledge Review of the Influence of Strong-Motion Duration on Structural Damage. *Earthquake Spectra*, 22(3), 827–845.
<https://doi.org/10.1193/1.2220576>
- Hobbs, T. E. (2021). *A Selection of Earthquake Scenarios for Government Planning Purposes in 2021*. <https://doi.org/10.495/323397>
- Hobbs, T. E. (2022). *Seismic risk in the National Capital Region, Ontario*. Geological Survey of Canada. <https://doi.org/10.4095/329455>
- Hobbs, T. E., Journeay, J. M., & LeSueur, P. (2021a). *Developing a retrofit scheme for Canada's Seismic Risk Model*. <https://doi.org/10.4095/328860>
- Hobbs, T. E., Journeay, J. M., Rao, A., Martins, L., LeSueur, P., Kolaj, M., Simionato, M., Silva, V., Pagani, M., Johnson, K., & Rotheram, D. (2022a). *Scientific basis of Canada's first public national seismic risk model*. <https://doi.org/10.4095/330927>
- Hobbs, T. E., Journeay, J. M., Rao, A. S., Kolaj, M., Martins, L., Simionato, M., Silva, V., Pagani, M., Johnson, K., Rotheram, D., & LeSueur, P. (2022b). The first public national Canadian seismic risk model: scientific underpinnings and preliminary results for the pre-release. *Proceedings of the United States National Conference on Earthquake Engineering*, 1–5.

- Hobbs, T. E., Journeay, J. M., & Rotheram, D. (2021b). *An earthquake scenario catalogue for Canada: a guide to using scenario hazard and risk results*. <https://doi.org/10.4095/328364>
- Homes, C. C. (2023, December 20). *What is a sealed crawl space?* Custom Carolina Homes Blog. Retrieved April 3, 2023, from <https://blog.nccustommodulars.com/the-home-building-process/sealed-crawl-space-benefits>
- Iervolino, I., Manfredi, G., & Cosenza, E. (2006). Ground motion duration effects on nonlinear seismic response. *Earthquake Engineering & Structural Dynamics*, 35(1), 21–38. <https://doi.org/10.1002/eqe.529>
- Jafari, M., Pan, Y., Shahnewaz, M., & Tannert, T. (2022). Effects of Ground Motion Duration on the Seismic Performance of a Two-Storey Balloon-Type CLT Building. *Buildings*, 12(7). <https://doi.org/10.3390/buildings12071022>
- Jalayer, F., De Risi, R., & Manfredi, G. (2015). Bayesian Cloud Analysis: efficient structural fragility assessment using linear regression. *Bulletin of Earthquake Engineering*, 13(4), 1183–1203. <https://doi.org/10.1007/s10518-014-9692-z>
- Journeay, M., LeSueur, P., Chow, W., & Wagner, C. L. (2022). *Physical exposure to natural hazards in Canada*. <https://doi.org/10.4095/330012>
- Lagomarsino, S., & Giovinazzi, S. (2006). Macroseismic and mechanical models for the vulnerability and damage assessment of current buildings. *Bulletin of Earthquake Engineering*, 4(4), 415–443. <https://doi.org/10.1007/s10518-006-9024-z>
- Liu, T., & Hong, H. (2017). Estimation of Seismic Loss for a Portfolio of Buildings under Bidirectional Horizontal Ground Motions due to a Scenario Cascadia Event. *Frontiers in Built Environment*, 3. <https://doi.org/10.3389/fbuil.2017.00061>

- Martins, L., & Silva, V. (2020). Development of a fragility and vulnerability model for global seismic risk analyses. *Bulletin of Earthquake Engineering*. <https://doi.org/10.1007/s10518-020-00885-1>
- Martins, L., Silva, V., Crowley, H., & Cavalieri, F. (2021). Vulnerability modellers toolkit, an open-source platform for vulnerability analysis. *Bulletin of Earthquake Engineering*, 19(13), 5691–5709. <https://doi.org/10.1007/s10518-021-01187-w>
- Mazzoni, S., McKenna, F., Scott, M. H., Fenves, G. L., & Iii, A. (2007). *Open System for Earthquake Engineering Simulation (OpenSees) OpenSees Command Language Manual*.
- Mitchell, D., Devall, R. H., Saatcioglu, M., Simpson, R., Tinawi, R., & Tremblay, R. (1995). Damage to concrete structures due to the 1994 Northridge earthquake. *Canadian Journal of Civil Engineering*, 22(2), 361–377. <https://doi.org/10.1139/195-047>
- Mitchell, D., Paultre, P., Tinawi, R., Saatcioglu, M., Tremblay, R., Elwood, K., Adams, J., & DeVall, R. (2010). Evolution of seismic design provisions in the National building code of Canada. *Canadian Journal of Civil Engineering*, 37(9), 1157–1170. <https://doi.org/10.1139/L10-054>
- Mohammad Noh, N., Liberatore, L., Mollaioli, F., & Tesfamariam, S. (2017). Modelling of masonry infilled RC frames subjected to cyclic loads: State of the art review and modelling with OpenSees. *Engineering Structures*, 150, 599–621. <https://doi.org/10.1016/j.engstruct.2017.07.002>
- Molnar, S. (2004). Comparing Intensity Variation of the 2001 Nisqually Earthquake with Geology in Victoria, British Columbia. *Bulletin of the Seismological Society of America*, 94(6), 2229–2238. <https://doi.org/10.1785/0120030236>

- Molnar, S., Cassidy, J. F., & Dosso, S. E. (2004). Site response studies in Victoria, B.C., analysis of Mw 6.8 Nisqually earthquake recordings and shake modelling. *Proceedings of the 13th World Conference on Earthquake Engineering, Vancouver, BC, Canada*.
- Mulder, M., Ventura, C. E., Bebamzadeh, A., & Fairhurst, M. (2017, January). Long duration effects on wood shear walls. *Proceedings of the 16th World Conference on Earthquake Engineering, Santiago, Chile*.
- National Research Council of Canada. (2015). *National Building Code of Canada*.
- naturally:wood. (2022, May 2). *MEC Head Office*. MEC Head Office | Commercial + Industrial Wood Design + Construction | Naturally:Wood. Retrieved April 3, 2023, from <https://www.naturallywood.com/project/mec-head-office/>
- Nazari, Y. R. (2017). *Seismic fragility analysis of Reinforced Concrete shear wall buildings in Canada* [Doctoral dissertation]. University of Ottawa.
- Nazari, Y. R., & Saatcioglu, M. (2017). Seismic vulnerability assessment of concrete shear wall buildings through fragility analysis. *Journal of Building Engineering*, 12, 202–209. <https://doi.org/10.1016/j.jobbe.2017.06.006>
- O'Brien, F. (2014, October 22). *Adera silences critics of six-story wooden tower*. Business in Vancouver. Retrieved April 3, 2023, from <https://biv.com/article/2014/10/adera-silences-six-story-wooden-tower>
- Onur, T. (2001). *Seismic risk assessment in southwestern British Columbia* [Doctoral Dissertation]. University of British Columbia.
- Onur, T., Ventura, C. E., & Finn, W. D. L. (2005). Regional seismic risk in British Columbia - Damage and loss distribution in Victoria and Vancouver. *Canadian Journal of Civil Engineering*, 32(2), 361–371. <https://doi.org/10.1139/104-098>

- Onur, T., Ventura, C. E., & Finn, W. D. L. (2006). A comparison of two regional seismic damage estimation methodologies. *Canadian Journal of Civil Engineering*, 33(11), 1401–1409. <https://doi.org/10.1139/106-084>
- Otárola, K., Sousa, L., Gentile, R., & Galasso, C. (2023). Impact of ground-motion duration on nonlinear structural performance: Part II: site- and building-specific analysis. *Earthquake Spectra*, 875529302311555. <https://doi.org/10.1177/87552930231155506>
- Pagani, M., Garcia-Pelaez, J., Gee, R., Johnson, K., Poggi, V., Silva, V., Simionato, M., Styron, R., Viganò, D., Danciu, L., Monelli, D., & Weatherill, G. (2020). The 2018 version of the Global Earthquake Model: Hazard component. *Earthquake Spectra*, 36(1_suppl), 226–251. <https://doi.org/10.1177/8755293020931866>
- Pagani, M., Garcia-Pelaez, J., Gee, R., Johnson, K., Poggi, V., Styron, R., Weatherill, G., Simionato, M., Viganò, D., Danciu, L., & Monelli, D. (2018). *Global Earthquake Model (GEM) Seismic Hazard Map (version 2018.1 - December 2018)*. <https://doi.org/10.13117/gem-global-seismic-hazard-map-2018.1>
- Pagani, M., Monelli, D., Weatherill, G., Danciu, L., Crowley, H., Silva, V., Henshaw, P., Butler, L., Nastasi, M., Panzeri, L., Simionato, M., & Viganò, D. (2014). OpenQuake Engine: An Open Hazard (and Risk) Software for the Global Earthquake Model. *Seismological Research Letters*, 85(3), 692–702. <https://doi.org/10.1785/0220130087>
- Pan, Y. (2018). *Effects of ground motion duration on the seismic performance and collapse capacity of timber structures* [Doctoral Dissertation]. University of British Columbia.
- Pan, Y., Ventura, C. E., & Tannert, T. (2020). Damage index fragility assessment of low-rise light-frame wood buildings under long duration subduction earthquakes. *Structural Safety*, 84. <https://doi.org/10.1016/j.strusafe.2020.101940>

- Ploeger, S. K., Atkinson, G. M., & Samson, C. (2010). Applying the HAZUS-MH software tool to assess seismic risk in downtown Ottawa, Canada. *Natural Hazards*, 53(1), 1–20.
<https://doi.org/10.1007/s11069-009-9408-x>
- Porter, K. (2021). *A Beginner's Guide to Earthquake Fragility Vulnerability and Risk*.
<https://www.sparisk.com/pubs/Porter-beginnersguide.pdf>.
- Raghunandan, M., & Liel, A. B. (2013). Effect of ground motion duration on earthquake-induced structural collapse. *Structural Safety*, 41, 119–133.
- Roger, M. F. (2015). House plans with basement apartment. *Drummond House Plans Blog*. Retrieved April 3, 2023, from <https://blog.drummondhouseplans.com/2015/04/25/house-plans-with-basement-apartment/>
- Ryu, H., Luco, N., Baker, J. W., & Karaca, E. (2008). Converting HAZUS capacity curves to seismic hazard-compatible building fragility functions: Effect of hysteretic models. *The Proceedings of the 14th World Conference on Earthquake Engineering, Beijing, China*.
- Satake, K. (2003). Fault slip and seismic moment of the 1700 Cascadia earthquake inferred from Japanese tsunami descriptions. *Journal of Geophysical Research*, 108(B11), 2535.
<https://doi.org/10.1029/2003JB002521>
- Shen, Y.-L., Schneider, J., Tesfamariam, S., Stiemer, S. F., & Mu, Z.-G. (2013). Hysteresis behavior of bracket connection in cross-laminated-timber shear walls. *Construction and Building Materials*, 48, 980–991. <https://doi.org/10.1016/j.conbuildmat.2013.07.050>
- Silva, V., Casotto, C., Vamvatsikos, D., Rao, A., & Villar, M. (2017). Presentation of the Risk Modeller's Toolkit, the open-source software for vulnerability assessment of the Global Earthquake Model. *Proceedings of the 16th World Conference on Earthquake Engineering, Santiago, Chile*.

- Silva, V., Crowley, H., Pagani, M., Monelli, D., & Pinho, R. (2014). Development of the OpenQuake engine, the Global Earthquake Model's open-source software for seismic risk assessment. *Natural Hazards*, 72(3), 1409–1427. <https://doi.org/10.1007/s11069-013-0618-x>
- smallworks. (2022, January 19). *North Vancouver Coach House*. Retrieved April 3, 2023, from <https://smallworks.ca/northvan-coach-house/>
- SRG3. (2016). *Seismic Retrofit Guidelines 3rd Edition, Appendix O, SRG3 Methodology for Ground Motion Selection and Scaling*. (University of British Columbia, Canada).
- Stafford, P. J. (2008). Conditional Prediction of Absolute Durations. *Bulletin of the Seismological Society of America*, 98(3), 1588–1594. <https://doi.org/10.1785/0120070207>
- Stephens, J. E., & Yao, J. T. P. (1987). Damage Assessment Using Response Measurements. *Journal of Structural Engineering*, 113(4), 787–801. [https://doi.org/10.1061/\(ASCE\)0733-9445\(1987\)113:4\(787\)](https://doi.org/10.1061/(ASCE)0733-9445(1987)113:4(787))
- Tesfamariam, S., & Goda, K. (2015a). Seismic performance evaluation framework considering maximum and residual inter-story drift ratios: Application to non-code conforming reinforced concrete buildings in Victoria, BC, Canada. *Frontiers in Built Environment*, 1. <https://doi.org/10.3389/fbuil.2015.00018>
- Tesfamariam, S., & Goda, K. (2015b). Loss estimation for non-ductile reinforced concrete building in Victoria, British Columbia, Canada: Effects of mega-thrust Mw9-class subduction earthquakes and aftershocks. *Earthquake Engineering and Structural Dynamics*, 44(13), 2303–2320. <https://doi.org/10.1002/eqe.2585>
- Turner, R. J. W., Clague, J. J., Groulx, B. J., & Journeay, J. M. (1998). *GeoMap Vancouver, geological map of the Vancouver Metropolitan area*. <https://doi.org/10.4095/209909>

- Vamvatsikos, D. (2011, February 4). *earthquakes, steel, dynamics & probability*. DV - software. Retrieved April 3, 2023, <http://users.ntua.gr/divamva/software.html>
- Ventura, C. E., & Bebamzadeh, A. (2016). *Citywide Seismic Vulnerability Assessment of the City of Victoria - Executive Summary*.
- Ventura, C. E., Bebamzadeh, A., & Fairhurst, M. (2019). *Ground Motion Selection for the UBC Campus*.
- Ventura, C. E., Finn, W. D. L., Onur, T., Blanquera, A., & Rezai, M. (2005). Regional seismic risk in British Columbia-classification of buildings and development of damage probability functions. *Canadian Journal of Civil Engineering*, 32(2), 372–387. <https://doi.org/10.1139/104-099>
- Villar-Vega, M., Silva, V., Crowley, H., Yepes, C., Tarque, N., Acevedo, A. B., Hube, M. A., Gustavo, C. D., & María, H. S. (2017). Development of a fragility model for the residential building stock in South America. *Earthquake Spectra*, 33(2), 581–604. <https://doi.org/10.1193/010716EQS005M>
- Wang, P.-L., Engelhart, S. E., Wang, K., Hawkes, A. D., Horton, B. P., Nelson, A. R., & Witter, R. C. (2013). Heterogeneous rupture in the great Cascadia earthquake of 1700 inferred from coastal subsidence estimates. *Journal of Geophysical Research: Solid Earth*, 118(5), 2460–2473. <https://doi.org/10.1002/jgrb.50101>
- Welch, D. P., & Deierlein, G. G. (2020). *Technical Background Report for Structural Analysis and Performance Assessment (PEER-CEA Project) (Report No. 2020/22)*. https://apps.peer.berkeley.edu/publications/peer_reports/reports_2020/2020_22_Welch_TechnicalBackground.pdf

- White, T. W., & Ventura, C. E. (2006). *Seismic performance of wood-frame residential construction in British Columbia. Earthquake Engineering Research Facility Report No. 06-03. University of British Columbia.*
- Yathon, J. S., Elwood, K. J., & Adebar, P. E. (2014). Seismic Characteristics of Pre-1980 Tall Reinforced Concrete Buildings in Vancouver. *Proceedings of the 10th National Conference in Earthquake Engineering, Earthquake Engineering Research Institute, Earthquake Engineering Research Institute.*
- Yepes-Estrada, C., Silva, V., Rossetto, T., D'Ayala, D., Ioannou, I., Meslem, A., & Crowley, H. (2016). The Global Earthquake Model Physical Vulnerability Database. *Earthquake Spectra*, 32(4), 2567–2585. <https://doi.org/10.1193/011816EQS015DP>
- Zhang, L., Goda, K., de Luca, F., & de Risi, R. (2020). Mainshock-aftershock state-dependent fragility curves: A case of wood-frame houses in British Columbia, Canada. *Earthquake Engineering and Structural Dynamics*, 49(9), 884–903. <https://doi.org/10.1002/eqe.3269>
- Zhao, J. X. (2006). Attenuation Relations of Strong Ground Motion in Japan Using Site Classification Based on Predominant Period. *Bulletin of the Seismological Society of America*, 96(3), 898–913. <https://doi.org/10.1785/0120050122>

Appendices

Appendix A : HAZUS definitions and consequence models

A.1 HAZUS building type classification

HAZUS identifies 36 specific building types used within the HAZUS methodology. GEM uses these typologies to develop the building typologies in Canada, assuming that construction across North America is similar. Using the HAZUS building type classification as reference, the BC building typologies are developed.

Table A. 1 HAZUS building structure types [Source: HAZUS]

No.	Label	Description	Height	
			Range	
			Name	Stories
1	W1	Wood, Light Frame ($\leq 5,000$ sq. ft.)		1-2
2	W2	Wood, ($> 5,000$ sq. ft.)		All
3	S1L	Steel Moment Frame	Low-Rise	1-3
4	S1M		Mid-Rise	4-7
5	S1H		High-Rise	8+
6	S2L	Steel Braced Frame	Low-Rise	1-3
7	S2M		Mid-Rise	4-7
8	S2H		High-Rise	8+
9	S3	Steel Light Frame		All
10	S4L	Steel Frame with Cast-in-Place Concrete Shear Walls	Low-Rise	1-3
11	S4M		Mid-Rise	4-7
12	S4H		High-Rise	8+
13	S5L	Steel Frame with Unreinforced Masonry Infill Walls	Low-Rise	1-3
14	S5M		Mid-Rise	4-7
15	S5H		High-Rise	8+
16	C1L	Concrete Moment Frame	Low-Rise	1-3
17	C1M		Mid-Rise	4-7
18	C1H		High-Rise	8+

Table A. 2 HAZUS building structure types [Source: HAZUS] Continued.

No.	Label	Description	Height	
			Range	
			Name	Stories
19 20 21	C2L C2M C2H	Concrete Shear Walls	Low-Rise Mid-Rise High-Rise	1-3 4-7 8+
22 23 24	C3L C3M C3H	Concrete Frame with Unreinforced Masonry Infill Walls	Low-Rise Mid-Rise High-Rise	1-3 4-7 8+
25	PC1	Precast Concrete Tilt-Up Walls	All	1
26 27 28	PC2L PC2M PC2H	Precast Concrete Frames with Concrete Shear Walls	Low-Rise Mid-Rise High-Rise	1-3 4-7 8+
29 30	RM1L RM1M	Reinforced Masonry Bearing Walls with Wood or Metal Deck Diaphragms	Low-Rise Mid-Rise	1-3 4+
31 32 33	RM2L RM2M RM2H	Reinforced Masonry Bearing Walls with Precast Concrete Diaphragms	Low-Rise Mid-Rise High-Rise	1-3 4-7 8+
34 35	URML URM M	Unreinforced Masonry Bearing Walls	Low-Rise Mid-Rise	1-2 3+
36	MH	Mobile Homes		All

A.2 Detailed description of W1, W2 and C2 HAZUS typologies [Source: HAZUS]

The W1, W2 and C2 typologies description as given in HAZUS (verbatim) is given below.

Wood, Light Frame (W1): These are typically single-family or small, multi-family dwellings of not more than 5,000 square feet of floor area. The essential structural feature of these buildings is repetitive framing by wood rafters or joists on wood stud walls. Loads are light and spans are small. These buildings may have relatively heavy masonry chimneys and may be partially or fully covered with masonry veneer. Most of these buildings, especially the single-

family residences, are not engineered but constructed in accordance with “conventional construction” provisions of building codes. Hence, they usually have the components of a lateral-force-resisting system even though it may be incomplete. Lateral loads are transferred by diaphragms to shear walls. The diaphragms are roof panels and floors that may be sheathed with sawn lumber, plywood or fiberboard sheathing. Shear walls are sheathed with boards, stucco, plaster, plywood, gypsum board, particle board, or fiberboard, or interior partition walls sheathed with plaster or gypsum board.

Wood, Greater than 5,000 Sq. Ft. (W2): These buildings are typically commercial or industrial buildings, or multi-family residential buildings with a floor area greater than 5,000 square feet. These buildings include structural systems framed by beams or major horizontally spanning members over columns. These horizontal members may be glue-laminated (glu-lam) wood, solid-sawn wood beams, or wood trusses, or steel beams or trusses. Lateral loads usually are resisted by wood diaphragms and exterior walls sheathed with plywood, stucco, plaster, or other paneling. The walls may have diagonal rod bracing. Large openings for stores and garages often require post-and-beam framing. Lateral load resistance on those lines may be achieved with steel rigid frames (moment frames) or diagonal bracing.

Concrete Shear Walls (C2): The vertical components of the lateral force-resisting system in these buildings are concrete shear walls that are usually bearing walls. In older buildings, the walls often are quite extensive, and the wall stresses are low but reinforcing is light. In newer buildings, the shear walls often are limited in extent, generating concerns about boundary members and overturning forces.

A.3 HAZUS building occupancy class definition

Table A. 3 HAZUS Building Occupancy Classes [Source: HAZUS]

Label	Occupancy Class	Example Descriptions
Residential		
RES1	Single Family Dwelling	House
RES2	Mobile Home	Mobile Home
RES3	Multi Family Dwelling	Apartment/Condominium
RES4	Temporary Lodging	Hotel/Motel
RES5	Institutional Dormitory	Group Housing (military, college), Jails
RES6	Nursing Home	
Label	Occupancy Class	Example Descriptions
Commercial		
COM1	Retail Trade	Store
COM2	Wholesale Trade	Warehouse
COM3	Personal and Repair Services	Service Station/Shop
COM4	Professional/Technical Services	Offices
COM5	Banks	
COM6	Hospital	
COM7	Medical Office/Clinic	
COM8	Entertainment & Recreation	Restaurants/Bars
COM9	Theaters	Theaters
COM10	Parking	Garages
Industrial		
IND1	Heavy	Factory
IND2	Light	Factory
IND3	Food/Drugs/Chemicals	Factory
IND4	Metals/Minerals Processing	Factory
IND5	High Technology	Factory
IND6	Construction	Office

Table A. 4 HAZUS Building Occupancy Classes [Source: HAZUS] Continued.

Agriculture		
AGR1	Agriculture	
Religion/Non/Profit		
REL1	Church/Non-Profit	
Government		
GOV1	General Services	Office
GOV2	Emergency Response	Police/Fire Station/EOC
Education		
EDU1	Grade Schools	
EDU2	Colleges/Universities	Does not include group housing

A.4 HAZUS damage limit state definition [Source: HAZUS]

The structural damage states for W1, W2 and C2 typologies as given in HAZUS (verbatim), is described below and is used to define the damage states for the BC typologies.

Wood, Light Frame (W1):

- **Slight Structural Damage:** Small plaster or gypsum-board cracks at corners of door and window openings and wall-ceiling intersections; small cracks in masonry chimneys and masonry veneer.
- **Moderate Structural Damage:** Large plaster or gypsum-board cracks at corners of door and window openings; small diagonal cracks across shear wall panels exhibited by small cracks in stucco and gypsum wall panels; large cracks in brick chimneys; toppling of tall masonry chimneys.
- **Extensive Structural Damage:** Large diagonal cracks across shear wall panels or large cracks at plywood joints; permanent lateral movement of floors and roof; toppling of most brick chimneys; cracks in foundations; splitting of wood sill plates and/or slippage of

structure over foundations; partial collapse of “room-over-garage” or other “soft-story” configurations; small foundations cracks.

- **Complete Structural Damage:** Structure may have large permanent lateral displacement, may collapse, or be in imminent danger of collapse due to cripple wall failure or the failure of the lateral load-resisting system; some structures may slip and fall off the foundations; large foundation cracks. Approximately 3% of the total area of W1 buildings with Complete damage is expected to be collapsed

Wood, Commercial and Industrial (W2):

- **Slight Structural Damage:** Small cracks at corners of door and window openings and wall ceiling intersections; small cracks on stucco and plaster walls. Some slippage may be observed at bolted connections.
- **Moderate Structural Damage:** Larger cracks at corners of door and window openings; small diagonal cracks across shear wall panels exhibited by cracks in stucco and gypsum wall panels; minor slack (less than 1/8-inch extension) in diagonal rod bracing requiring retightening; minor lateral offset at store fronts and other large openings; small cracks or wood splitting may be observed at bolted connections.
- **Extensive Structural Damage:** Large diagonal cracks across shear wall panels; large slack in diagonal rod braces and/or broken braces; permanent lateral movement of floors and roof; cracks in foundations; splitting of wood sill plates and/or slippage of structure over foundations; partial collapse of “soft-story” configurations; bolt slippage and wood splitting at bolted connections.
- **Complete Structural Damage:** Structure may have large permanent lateral displacement, may collapse or be in imminent danger of collapse due to failed shear walls, broken brace

rods or failed framing connections; it may fall off its foundations; large cracks in the foundations. Approximately 3% of the total area of W2 buildings with Complete damage is expected to be collapsed.

Concrete Shear Walls (C2):

- **Slight Structural Damage:** Diagonal hairline cracks on most concrete shear wall surfaces; minor concrete spalling at a few locations.
- **Moderate Structural Damage:** Most shear wall surfaces exhibit diagonal cracks; some shear walls have exceeded yield capacity, as indicated by larger diagonal cracks and concrete spalling at wall ends.
- **Extensive Structural Damage:** Most concrete shear walls have exceeded their yield capacities; some walls have exceeded their ultimate capacities, as indicated by large, through the-wall diagonal cracks, extensive spalling around the cracks, and visibly buckled wall reinforcement or rotation of narrow walls with inadequate foundations. Partial collapse may occur due to failure of nonductile columns not designed to resist lateral loads.
- **Complete Structural Damage:** Structure has collapsed or is in imminent danger of collapse due to failure of most of the shear walls and failure of some critical beams or columns. Approximately 13% (low-rise), 10% (mid-rise) or 5% (high-rise) of the total area of C2 buildings with Complete damage is expected to be collapsed.

Appendix B : Pinching4 Material

The Pinching4 material model is used to construct a uniaxial material that characterizes a ‘pinched’ load-deformation response and undergoes degradation when subjected to cyclic loading, (as is observed during an earthquake). OpenSees defines the Pinching4 material as:

```
uniaxialMaterial Pinching4 $matTag $ePf1 $ePd1 $ePf2 $ePd2 $ePf3 $ePd3 $ePf4 $ePd4
<$eNf1 $eNd1 $eNf2 $eNd2 $eNf3 $eNd3 $eNf4 $eNd4> $rDispP $rForceP $uForceP <$rDispN
$rForceN $uForceN > $gK1 $gK2 $gK3 $gK4 $gKLim $gD1 $gD2 $gD3 $gD4 $gDLim $gF1 $gF2
$gF3 $gF4 $gFLim $gE $dmgType
```

Figure B.1 depicts how strength and stiffness degradation are taken into account within this model, considering unloading stiffness degradation, reloading stiffness degradation and strength degradation. The parameters are described in Table B.1. The OpenSees command language manual has further details on how the data points are calculated.

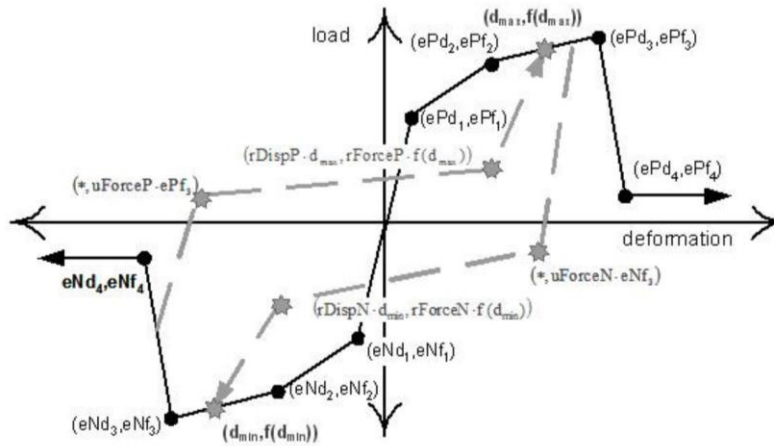


Figure B.1 Definition of Pinching4 Uniaxial Material Model (Mazzoni et al., 2007)

Table B. 1 Description of parameters used to describe the Pinching4 material model in OpenSees

Parameter	Description
\$matTag	unique material object tag (integer)
\$ePf1, \$ePf2, \$ePf3, \$ePf4	force points on the positive response envelope (floating point)
\$ePd1, \$ePd2, \$ePd3, \$ePd4	deformation points on the positive response envelope (floating point)
\$eNf1, \$eNf2, \$eNf3, \$eNf4	force points on the negative response envelope (floating point)
\$eNd1, \$eNd2, \$eNd3, \$eNd4	deformations points on the negative response envelope (floating point)
\$rDispP	ratio of the deformation at which reloading occurs to the maximum historic deformation demand (floating point)
\$rForceP	ratio of the force at which reloading begins to force corresponding to the maximum historic deformation demand (floating point)
\$uForceP	ratio of strength developed upon unloading from negative load to the maximum strength developed under monotonic loading (floating point)
\$rDispN	ratio of the deformation at which reloading occurs to the minimum historic deformation demand (floating point)
\$rForceN	ratio of the force at which reloading begins to the force corresponding to the minimum historic deformation demand (floating point)
\$uForceN	ratio of the strength developed upon unloading from a positive load to the minimum strength developed under monotonic loading (floating point)
\$gK1, \$gK2, \$gK3, \$gK4 \$gKLim	controls cyclic degradation model for unloading stiffness degradation (floating point)
\$gD1,\$gD2, \$gD3, \$gD4, \$gDLim	controls cyclic degradation model for reloading stiffness degradation (floating point)
\$gF1, \$gF2, \$gF3, \$gF4, \$gFLim	controls cyclic degradation model for strength degradation (floating point)
\$gE	maximum energy dissipation under cyclic loading. Total energy dissipation capacity is defined as this factor multiplied by the energy dissipated under monotonic loading (floating point)
\$dmgType	type of damage (“cycle”/ “energy”) (string)

Appendix C : Ground motion suites used for development of fragility and vulnerability functions

The ground motion suites used to develop the fragility and vulnerability functions are tabulated in this section C.1 and C.2. These suites were provided by Dr. Armin Bebamzadeh, and were developed for SRG3 (Bebamzadeh et al., 2015b; UBC, 2016).

C.1 Crustal ground motion suites

Table C. 1. Crustal ground motion records summary for Vancouver (Low) $T_c = 0.5\text{sec}$

Name	Year	Record	Mw	Depth (km)	SF
Baja, CA	1987	BAJA_CPE251	5.5	6	0.64
Cape Mendocino, CA	1992	CAPEMEND_FOR090	7	9.5	2.86
Chi-Chi, Taiwan	1999	CHICHI03_CHY029-E	6.2	7.8	3.52
Chi-Chi, Taiwan	1999	CHICHI03_TCU122-E	6.2	7.8	2.42
Chi-Chi, Taiwan	1999	CHICHI04_CHY074-N	6.2	18	0.59
Chi-Chi, Taiwan	1999	CHICHI06_CHY035-N	6.3	16	2.65
Chi-Chi, Taiwan	1999	CHICHI06_CHY087-N	6.3	16	3.99
Chi-Chi, Taiwan	1999	CHICHI06_TCU129-E	6.3	16	1.81
Kobe, Japan	1995	KOBE_NIS090	6.9	17.9	0.69
Loma Prieta, CA	1989	LOMAP_CLS000	6.9	17.5	0.52
Loma Prieta, CA	1989	LOMAP_G06000	6.9	17.5	3.29
Manjil, Iran	1990	MANJIL_ABBAR--T	7.4	16	0.79
Morgan Hills, CA	1984	MORGAN_CLS310	6.2	8.5	2.81
Northridge, CA	1994	NORTHR_5080-360	6.7	17.5	3.48
Northridge, CA	1994	NORTHR_5108-360	6.7	17.5	1.54
Northridge, CA	1994	NORTHR_MU2125	6.7	17.5	1.1
Northridge, CA	1994	NORTHR_PKC090	6.7	17.5	0.96
San Salvador, El Salvador	1986	SANSALV_GIC180	5.8	10.9	0.69
San Fernando, CA	1971	SFERN_ORR291	6.6	13	1.4
Whittier Narrows, CA	1987	WHITTIER_A-PKC090	6	14.6	2.87

Table C. 2 Crustal ground motion records summary for Vancouver (Low) $T_c = 1.0\text{sec}$

Name	Year	Record	Mw	Depth (km)	SF
Cape Mendocino, CA	1992	CAPEMEND_FOR090	7	9.5	2.27
Cape Mendocino, CA	1992	CAPEMEND_PET090	7	9.5	0.43
Chi-Chi, Taiwan	1999	CHICHI03_CHY028-N	6.2	7.8	1.8
Chi-Chi, Taiwan	1999	CHICHI03_CHY035-N	6.2	7.8	3.25
Chi-Chi, Taiwan	1999	CHICHI03_CHY074-E	6.2	7.8	3.87
Chi-Chi, Taiwan	1999	CHICHI03_TCU082-N	6.2	7.8	3.8
Chi-Chi, Taiwan	1999	CHICHI03_TCU129-E	6.2	7.8	1.04
Chi-Chi, Taiwan	1999	CHICHI06_CHY041-N	6.3	16	2.04
Coyote Lk, CA	1979	COYOTELK_G06230	5.7	8	0.73
Duzce, Turkey	1999	DUZCE_1061-N	7.1	14	2.83
Imperial Valley, CA	1979	IMPVALL_H-CPE237	6.5	10	1.43
Landers, CA	1992	LANDERS_LCN260	7.3	7	0.88
Loma Prieta, CA	1989	LOMAP_GIL067	6.9	17.5	1.73
Nahanni, Canada	1985	NAHANNI_S1280	6.8	8	0.87
Northridge, CA	1994	NORTHR_0655-022	6.7	17.5	0.75
Northridge, CA	1994	NORTHR_5108-090	6.7	17.5	1.77
Northridge, CA	1994	NORTHR_ALH090	6.7	17.5	3.13
Northridge, CA	1994	NORTHR_CHL070	6.7	17.5	2.04
San Fernando, CA	1971	SFERN_PDL210	6.6	13	3.62
Taiwan SMART1	1986	SMART1_45E02NS	7.3	15	2.84

Table C.3 Crustal ground motion records summary for Victoria (High) $T_c = 0.5\text{sec}$

Name	Year	Record	Mw	Depth (km)	SF
Chi-Chi, Taiwan	1999	CHICHI03_TCU122-N	6.2	7.8	3.75
Chi-Chi, Taiwan	1999	CHICHI03_TCU138-N	6.2	7.8	3.02
Chi-Chi, Taiwan	1999	CHICHI06_CHY028-N	6.3	16	3.57
Chi-Chi, Taiwan	1999	CHICHI06_CHY041-E	6.3	16	3.28
Chi-Chi, Taiwan	1999	CHICHI06_TCU129-E	6.3	16	2.8
Coyote Lk, CA	1979	COYOTELK_G06230	5.7	8	1.62
Hector Mine, CA	1999	HECTOR_HEC000	7.1	14.8	2.85
Imperial Valley, CA	1979	IMPVALL_H-CPE147	6.5	10	2.49
Irpinia, Italy	1980	ITALY_A-CTR000	6.9	9.5	2.73
Kobe, Japan	1995	KOBE_NIS090	6.9	17.9	1.07
Loma Prieta, CA	1989	LOMAP_CLS000	6.9	17.5	0.81
Loma Prieta, CA	1989	LOMAP_LGP000	6.9	17.5	0.6
Manjil, Iran	1990	MANJIL_ABBAR--T	7.4	16	1.22
Morgan Hills, CA	1984	MORGAN_CYC285	6.2	8.5	0.68
Northridge, CA	1994	NORTHR_5108-360	6.7	17.5	2.38
San Salvador, El Salvador	1986	SANSALV_GIC090	5.8	10.9	0.92
San Fernando, CA	1971	SFERN_ORR291	6.6	13	2.17
Taiwan SMART1	1986	SMART1_45E02NS	7.3	15	2.97
Victoria, Mexico	1980	VICT_CPE315	6.3	11	1.76
Whittier Narrows, CA	1987	WHITTIER_A GRV060 -	6	14.6	2.29

Table C.4 Crustal ground motion records summary for Victoria (High) $T_c = 1.0\text{sec}$

Name	Year	Record	Mw	Depth (km)	SF
Cape Mendocino, CA	1992	CAPEMEND_FOR090	7	9.5	3.64
Cape Mendocino, CA	1992	CAPEMEND_PET090	7	9.5	0.68
Chi-Chi, Taiwan	1999	CHICHI03_CHY028-N	6.2	7.8	2.89
Chi-Chi, Taiwan	1999	CHICHI03_TCU076-E	6.2	7.8	1.1
Chi-Chi, Taiwan	1999	CHICHI06_CHY028-N	6.3	16	3.78
Chi-Chi, Taiwan	1999	CHICHI06_CHY029-E	6.3	16	3.68
Hector Mine, CA	1999	HECTOR_HEC000	7.1	14.8	1.91
Imperial Valley, CA	1979	IMPVALL_H-CPE237	6.5	10	2.29
Landers, CA	1992	LANDERS_LCN260	7.3	7	1.41
Loma Prieta, CA	1989	LOMAP_AND250	6.9	17.5	3.17
Loma Prieta, CA	1989	LOMAP_CYC195	6.9	17.5	2.11
Loma Prieta, CA	1989	LOMAP_GIL067	6.9	17.5	2.77
Loma Prieta, CA	1989	LOMAP_LGP090	6.9	17.5	1.57
Nahanni, Canada	1985	NAHANNI_S1280	6.8	8	1.39
Northridge, CA	1994	NORTHR_5108-360	6.7	17.5	3.61
Northridge, CA	1994	NORTHR_LDM064	6.7	17.5	0.95
Northridge, CA	1994	NORTHR_ORR090	6.7	17.5	1.26
Santa Barbara, CA	1978	SBARB_SBA222	5.9	12.7	3.84

C.2 Subduction ground motion suites

Table C.5 Subduction ground motion records summary for Vancouver (Low) $T_c = 0.5\text{sec}$

Name	Year	Record	Mw	Depth (km)	SF*
Hokkaido, Japan	2003	HKD0950309260450-EW	8	42	3.29
Hokkaido, Japan	2003	HKD0980309260450-NS	8	42	1.58
Hokkaido, Japan	2003	HKD0990309260450-EW	8	42	2.14
Hokkaido, Japan	2003	HKD1050309260450-NS	8	42	3.04
Hokkaido, Japan	2003	HKD1090309260450-NS	8	42	2.33
Hokkaido, Japan	2003	HKD1250309260450-EW	8	42	2.3
El Maule, Chile	2010	matanzas1002271-L	8.8	35	0.78
El Maule, Chile	2010	SJCH-360	8.8	35	1.36
Michoacan, Mexico	1985	AZIH8509_191_N00W	8.1	15	3.82
Michoacan, Mexico	1985	SUCH8509_191_N00W	8.1	15	3.83
Tohoku, Japan	2011	CHB0051103111446-EW	9	24	3.7
Tohoku, Japan	2011	FKS0011103111446-EW	9	24	1.14
Tohoku, Japan	2011	GNM0081103111446-NS	9	24	3.3
Tohoku, Japan	2011	GNM0131103111446-EW	9	24	2.23
Tohoku, Japan	2011	IBR0081103111446-NS	9	24	1.33
Tohoku, Japan	2011	IBR0091103111446-NS	9	24	2.42
Tohoku, Japan	2011	IWT0111103111446-NS	9	24	2.41
Tohoku, Japan	2011	MYG0131103111446-NS	9	24	0.58
Tohoku, Japan	2011	MYG0161103111446-EW	9	24	2.22
Tohoku, Japan	2011	TCG0061103111446-EW	9	24	1.12

Table C.6 Subduction ground motion records summary for Vancouver (Low) $T_c = 1.0\text{sec}$

Name	Year	Record	Mw	Depth (km)	SF
Hokkaido, Japan	2003	HKD0830309260450-NS	8	42	3.47
Hokkaido, Japan	2003	HKD0840309260450-NS	8	42	1.47
Hokkaido, Japan	2003	HKD0950309260450-EW	8	42	2.7
Hokkaido, Japan	2003	HKD0980309260450-EW	8	42	0.8
Hokkaido, Japan	2003	HKD0980309260450-NS	8	42	0.88
Hokkaido, Japan	2003	HKD0990309260450-EW	8	42	1.45
Hokkaido, Japan	2003	HKD1040309260450-NS	8	42	2.79
Hokkaido, Japan	2003	HKD1050309260450-EW	8	42	1.86
Hokkaido, Japan	2003	HKD1070309260450-EW	8	42	3.86
Hokkaido, Japan	2003	HKD1090309260450-NS	8	42	2.04
El Maule, Chile	2010	matanzas1002271-T	8.8	35	1.64
Michoacan, Mexico	1985	AZIH8509_191_N90W	8.1	15	3.71
Tohoku, Japan	2011	AOM0211103111446-EW	9	24	2.65
Tohoku, Japan	2011	CHB0051103111446-EW	9	24	1.99
Tohoku, Japan	2011	GNM0081103111446-NS	9	24	3.71
Tohoku, Japan	2011	IBR0091103111446-NS	9	24	2.65
Tohoku, Japan	2011	IBR0141103111446-NS	9	24	1.45
Tohoku, Japan	2011	IWT0111103111446-NS	9	24	2.57
Tohoku, Japan	2011	KNG0101103111446-NS	9	24	3.44
Tohoku, Japan	2011	SIT0021103111446-NS	9	24	3.08

Table C.7 Subduction ground motion records summary for Victoria (High) $T_c = 0.5\text{sec}$

Name	Year	Record	Mw	Depth (km)	SF
Hokkaido, Japan	2003	HKD0840309260450-NS	8	42	0.83
Hokkaido, Japan	2003	HKD0940309260450-NS	8	42	3.25
Hokkaido, Japan	2003	HKD0990309260450-NS	8	42	1.71
Hokkaido, Japan	2003	HKD1030309260450-NS	8	42	2.24
Hokkaido, Japan	2003	HKD1050309260450-EW	8	42	2.1
Hokkaido, Japan	2003	HKD1070309260450-NS	8	42	2.96
El Maule, Chile	2010	matanzas1002271-L	8.8	35	0.5
Michoacan, Mexico	1985	AZIH8509_191_N00W	8.1	15	2.47
Michoacan, Mexico	1985	SUCH8509_191_N00W	8.1	15	2.48
Tohoku, Japan	2011	AOM0141103111446-NS	9	24	3.2
Tohoku, Japan	2011	FKS0141103111446-EW	9	24	1.42
Tohoku, Japan	2011	GNM0071103111446-EW	9	24	2.54
Tohoku, Japan	2011	GNM0081103111446-EW	9	24	1.92
Tohoku, Japan	2011	GNM0131103111446-EW	9	24	1.44
Tohoku, Japan	2011	IBR0081103111446-NS	9	24	0.86
Tohoku, Japan	2011	IBR0091103111446-NS	9	24	1.56
Tohoku, Japan	2011	KNG0061103111446-EW	9	24	2.95
Tohoku, Japan	2011	KNG0101103111446-EW	9	24	3.21
Tohoku, Japan	2011	SIT0011103111446-NS	9	24	3.43
Tohoku, Japan	2011	TCG0061103111446-EW	9	24	0.72

Table C.8 Subduction ground motion records summary for Victoria (High) $T_c = 1.0\text{sec}$

Name	Year	Record	Mw	Depth (km)	SF
Hokkaido, Japan	2003	HKD0540309260450-NS	8	42	3.74
Hokkaido, Japan	2003	HKD0550309260450-NS	8	42	2.69
Hokkaido, Japan	2003	HKD0950309260450-EW	8	42	1.69
Hokkaido, Japan	2003	HKD1040309260450-EW	8	42	1.5
Hokkaido, Japan	2003	HKD1050309260450-EW	8	42	1.16
Hokkaido, Japan	2003	HKD1070309260450-EW	8	42	2.41
Hokkaido, Japan	2003	HKD1210309260450-NS	8	42	3.94
El Maule, Chile	2010	matanzas1002271-L	8.8	35	0.57
El Maule, Chile	2010	SJCH-90	8.8	35	0.84
Michoacan, Mexico	1985	AZIH8509_191_N00W	8.1	15	2.35
Tohoku, Japan	2011	AOM0141103111446-NS	9	24	1.6
Tohoku, Japan	2011	AOM0211103111446-EW	9	24	1.65
Tohoku, Japan	2011	AOM0281103111446-NS	9	24	2.53
Tohoku, Japan	2011	GNM0081103111446-NS	9	24	2.32
Tohoku, Japan	2011	IWT0111103111446-NS	9	24	1.61
Tohoku, Japan	2011	KNG0051103111446-NS	9	24	3.98
Tohoku, Japan	2011	KNG0071103111446-EW	9	24	3.28
Tohoku, Japan	2011	KNG0101103111446-NS	9	24	2.14
Tohoku, Japan	2011	NIG0071103111446-EW	9	24	3.79
Tohoku, Japan	2011	YMT0031103111446-EW	9	24	3.68

C.3 D_{5-95} and SED characteristics of SRG3 ground motion suites

The D_{5-95} and SED characteristics of the SRG3 ground motion suites not mentioned in the section 3.3.2.3.3 are plotted below:

SRG3 Vancouver crustal and subduction ground motion suites, conditioned at 0.5s:

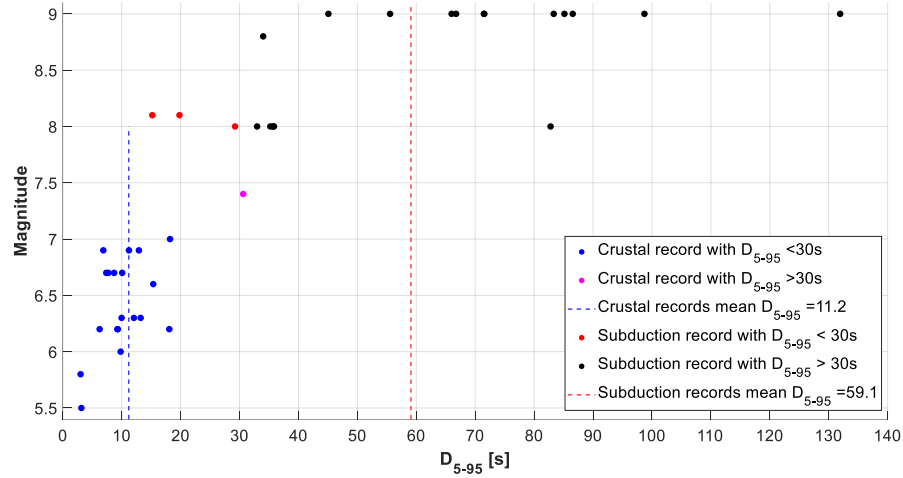


Figure C.1 Distribution of D_{5-95} of the records in the Vancouver crustal and subduction ground motion suites conditioned at 0.5s, across relevant magnitudes.

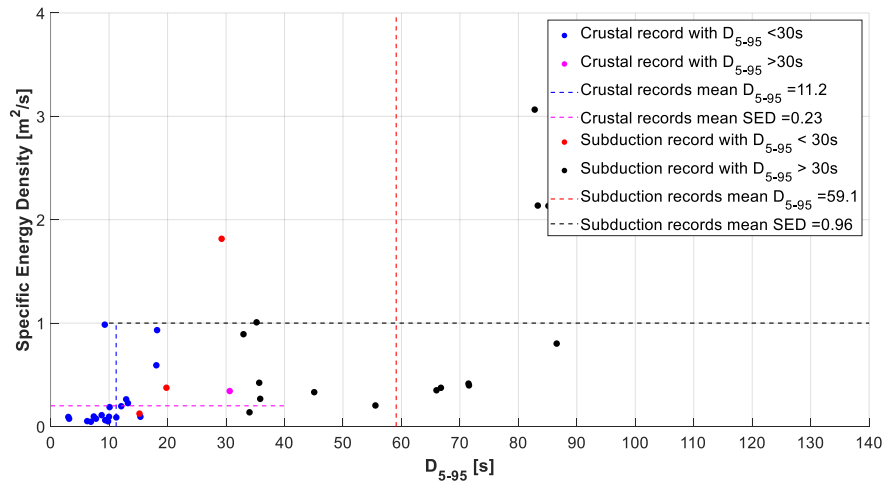


Figure C.2 Plot of D_{5-95} vs. SED of the records in the Vancouver crustal and subduction ground motion suites conditioned at 0.5s

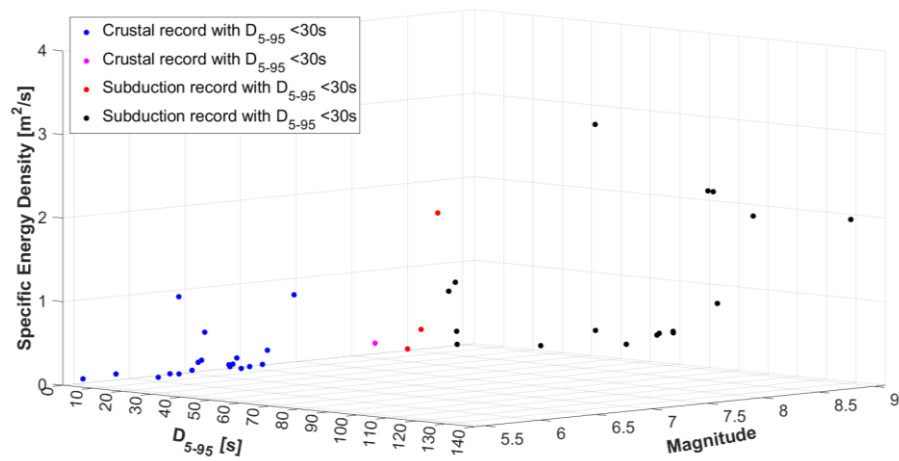


Figure C.3 Distribution of D_{5-95} vs. SED of the records in the Vancouver crustal and subduction ground motion suites conditioned at 0.5s, across relevant magnitudes.

SRG3 Victoria crustal and subduction ground motion suites, conditioned at 0.5s :

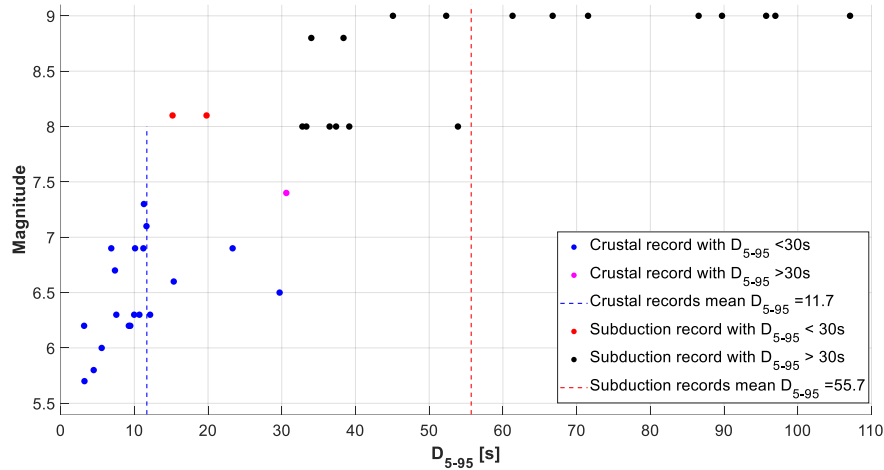


Figure C.4 Distribution of D_{5-95} of the records in the Victoria crustal and subduction ground motion suites conditioned at 0.5s, across relevant magnitudes.

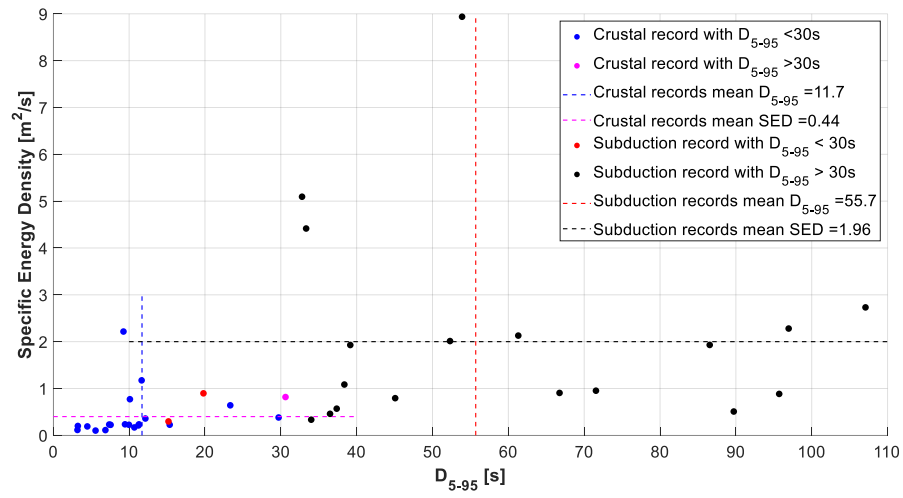


Figure C.5 Plot of D_{5-95} vs. SED of the records in the Victoria crustal and subduction ground motion suites conditioned at 0.5s

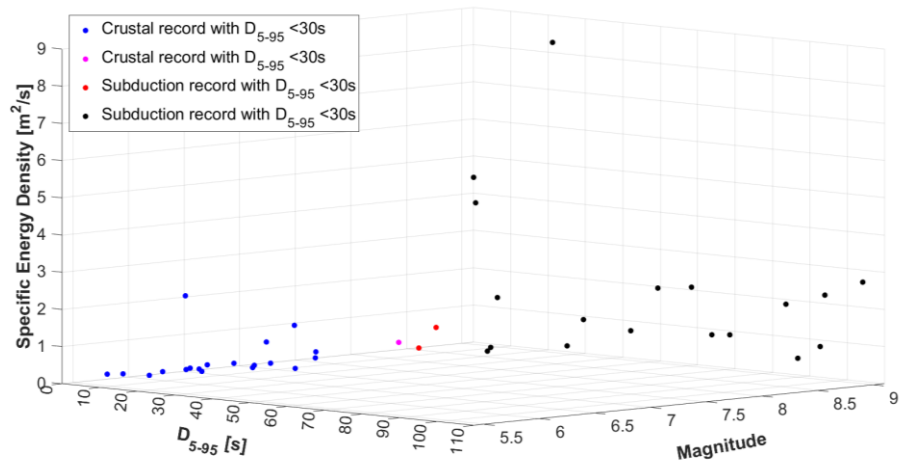


Figure C.6 Distribution of D_{5-95} vs. SED of the records in the Victoria crustal and subduction ground motion suites conditioned at 0.5s, across relevant magnitudes.

SRG3 Victoria crustal and subduction ground motion suites, conditioned at 1.0s :

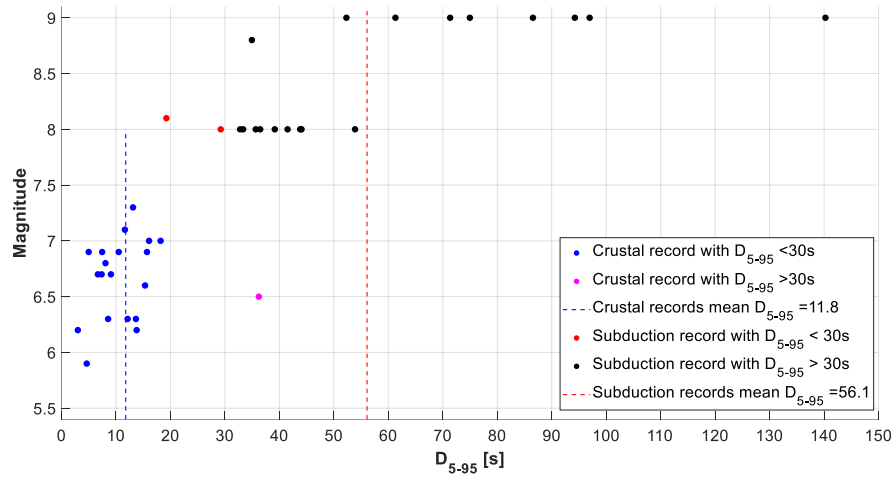


Figure C.7 Distribution of D_{5-95} of the records in the Victoria crustal and subduction ground motion suites conditioned at 1.0s, across relevant magnitudes.

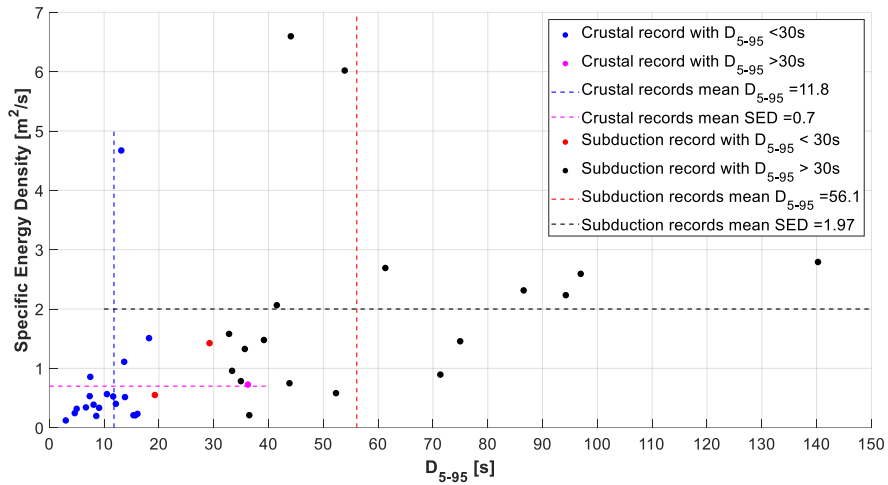


Figure C.8 Plot of D_{5-95} vs. SED of the records in the Victoria crustal and subduction ground motion suites conditioned at 1.0s

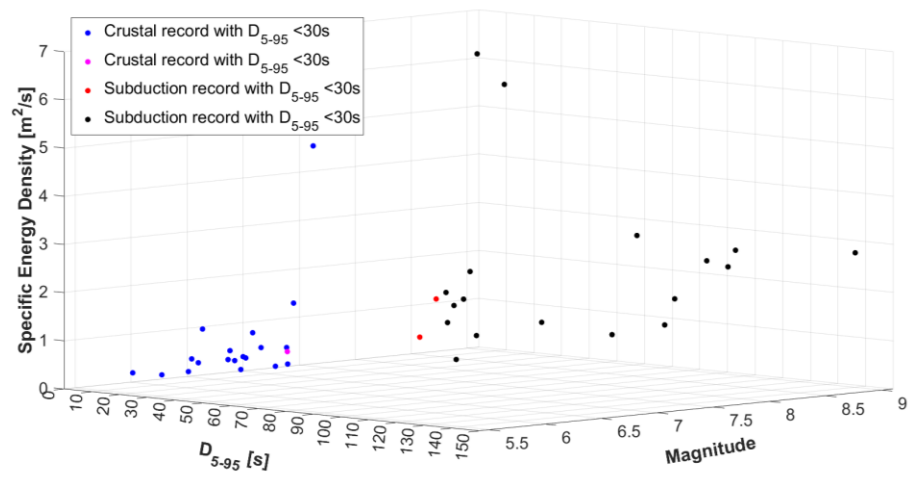


Figure C.9 Distribution of D_{5-95} vs. SED of the records in the Victoria crustal and subduction ground motion suites conditioned at 0.5s, across relevant magnitudes.

Appendix D : Additional tables and figures

D.1 Comparison of damage state thresholds

Table D.1 Comparison of Spectral displacement at Damage state thresholds used in Hazus, GEM and in the current study for concrete shear wall (C2) typologies

Sd at Damage state thresholds[cm]: GEM					
C2L	HC	2.7	8.5	14.3	21.9
	MC	2.7	5.9	9	13.2
	LC	2.7	6.9	11	16.5
	PC	2.2	4.7	7.2	10.5
C2M	HC	4.6	14.2	23.8	36.6
	MC	4.6	9.8	15	21.9
	LC	4.6	11.5	18.3	27.4
	PC	3.6	7.8	12	17.5
C2H	HC	6.6	20.4	34.2	52.7
	MC	6.6	14.1	21.6	31.6
	LC	6.6	16.5	26.3	39.5
	PC	5.3	11.3	17.3	25.3
Sd at Damage state thresholds[cm]: BC					
C2L	HC	0.8	6.6	12.5	18.3
	MC	0.8	4.5	8.2	11.9
	LC	0.8	3.6	6.4	9.1
	PC	0.8	3.6	6.4	9.1
C2M	HC	1.5	12.4	23.4	34.3
	MC	1.5	7.8	14.2	20.6
	LC	1.5	5.4	9.3	13.1
	PC	1.5	5.4	9.3	13.1
C2H	HC	3.7	23.7	43.6	63.6
	MC	3.7	17.1	30.5	43.9
	LC	3.7	10.2	16.7	23.2
	PC	3.7	10.2	16.7	23.2

Table D.2 Comparison of Spectral displacement at Damage state thresholds used in Hazus, GEM and in the current study for Wood typologies

Sd at Damage state thresholds[cm]: GEM					
W1	HC	1.9	7.1	12.3	19.2
	MC	1.9	4.6	7.2	10.8
	LC	1.9	5.7	9.4	14.4
	PC	1.5	4	6.5	9.8
W2	HC	3.3	12.2	21.1	32.9
	MC	3.3	7.9	12.4	18.5
	LC	3.3	9.7	16.1	24.7
	PC	2.6	6.9	11.1	16.8
Sd at Damage state thresholds[cm]: BC					
W1	HC	0.9	3.1	5.3	15
	MC	0.9	3.1	5.3	15
	LC	0.8	2.5	4.3	12.5
	PC	0.8	2.5	4.3	12.5
W2	HC	1.2	4.5	7.9	17.3
	MC	1.2	4.5	7.9	17.3
	LC	0.7	3.5	6.2	14.5
	PC	0.7	3.5	6.2	14.5
W3	HC	0.9	3.6	6.3	16.3
	MC	0.9	3.6	6.3	16.3
	LC	0.5	3.5	6.4	15.6
	PC	0.5	3.5	6.4	15.6
W4s	HC	1	2.2	3.5	8.5
	MC	1	3.7	6.3	8.5
	LC	0.9	3.6	6.4	7
	PC	0.9	3.6	6.4	7
W4c	HC	0.5	3	5.5	10.4
	MC	0.5	3	5.5	10.4
	LC	0.5	3	5.5	10.2
	PC	0.5	3	5.5	10.2

D.2 Consequence Models

Table D.3 Structural consequence model

Occupancy Class	DS1	DS2	DS3	DS4
RES1	0.02	0.10	0.50	1.00
RES2	0.02	0.10	0.30	1.00
RES3	0.02	0.10	0.50	1.00
RES4	0.02	0.10	0.50	1.00
RES5	0.02	0.10	0.50	1.00
RES6	0.02	0.10	0.50	1.00
COM1	0.02	0.10	0.50	1.00
COM2	0.02	0.10	0.50	1.00
COM3	0.02	0.10	0.50	1.00
COM4	0.02	0.10	0.50	1.00
COM5	0.02	0.10	0.50	1.00
COM6	0.01	0.10	0.50	1.00
COM7	0.02	0.10	0.50	1.00
COM8	0.02	0.10	0.50	1.00
COM9	0.03	0.10	0.50	1.00
COM10	0.02	0.10	0.50	1.00
IND1	0.03	0.10	0.50	1.00
IND2	0.03	0.10	0.50	1.00
IND3	0.03	0.10	0.50	1.00
IND4	0.03	0.10	0.50	1.00
IND5	0.03	0.10	0.50	1.00
IND6	0.03	0.10	0.50	1.00
AGR1	0.02	0.10	0.50	1.00
REL1	0.02	0.10	0.50	1.00
GOV1	0.02	0.10	0.50	1.00
GOV2	0.02	0.10	0.50	1.00
EDU1	0.02	0.10	0.50	1.00

Table D.4 Drift sensitive non-structural consequence model

Occupancy class	DS1	DS2	DS3	DS4
All Classes	0.02	0.10	0.50	1.00

Table D.5 Acceleration sensitive non-structural consequence model

Occupancy class	DS1	DS2	DS3	DS4
All Classes	0.02	0.10	0.30	1.00

Table D.6 Contents consequence model

Occupancy class	DS1	DS2	DS3	DS4
All Classes	0.02	0.10	0.50	1.00

D.3 Capacity curves and fragility functions for C2-MC typology

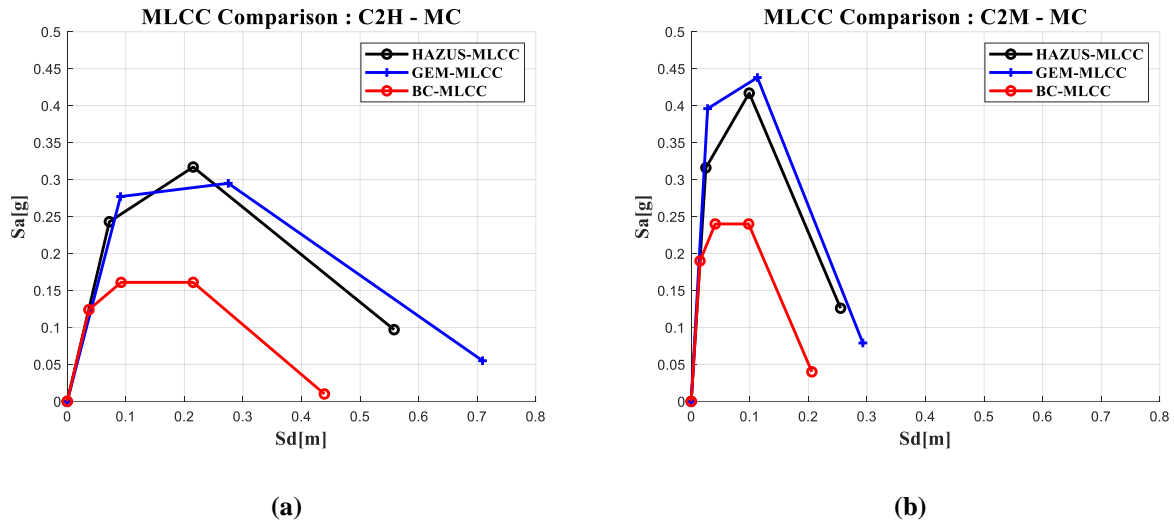


Figure D.1 Comparison between capacity curves- GEM, HAZUS and BC-specific for (a) C2H-MC (b) C2M-MC

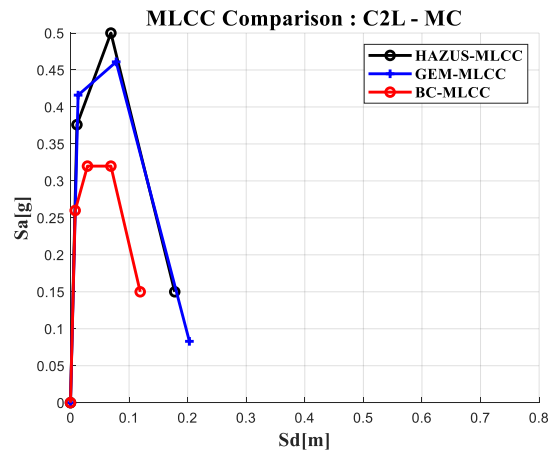
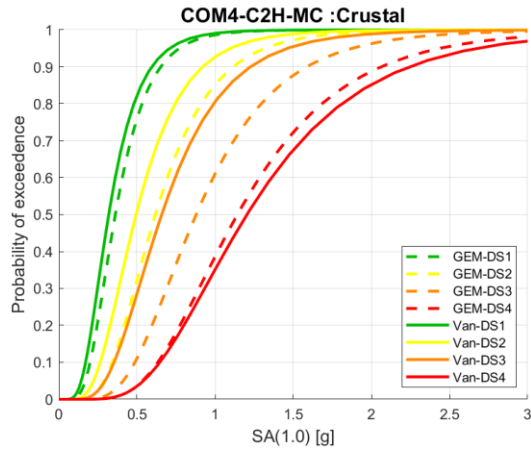
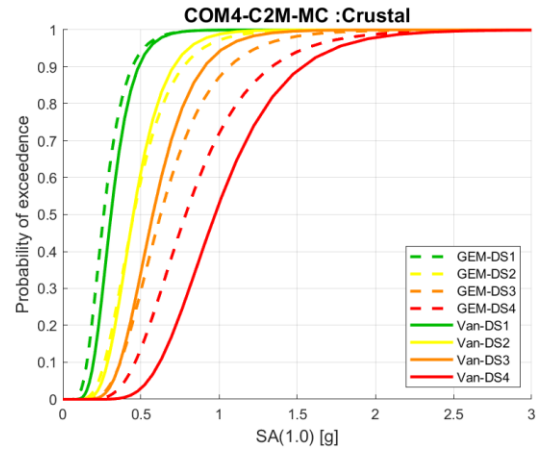


Figure D.2 Comparison between capacity curves- GEM, HAZUS and BC-specific for C2L-MC



(a)



(b)

Figure D.3 Comparison of current fragility curves (GEM-) to new BC specific fragility curves (Van-) for (a) C2H-MC (b) C2M-MC

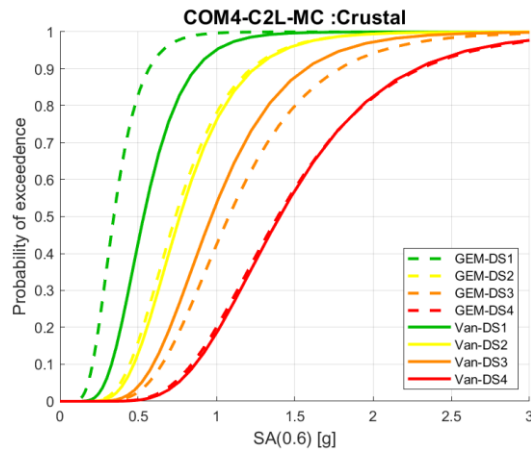


Figure D.4 Comparison of current fragility curves (GEM-) to new BC specific fragility curves (Van-) for C2L-MC

D.4 Building taxonomy description in CanSRM1






Hazus Building Taxonomy (FEMA P547)						
Model	Construction Material	Typology	Height	Wall Type	Description	Design Epoch
	Concrete	C1H	> 8 Floors	C1: Moment Frame	Consists of concrete framing, either a complete system of beams and columns or columns supporting slabs without gravity beams. Lateral forces are resisted by cast-in-place moment frames that are stiffened by mechanical connections of the column and beams.	PC: < 1973, LC: 1974-1989, MC: 1990-2004, HC: 2005-present
		C1M	4-7 Floors			
		C1L	< 3 Floors			
		C2H	> 8 Floors	C2: Shear Wall	Consists of concrete with flat slab or precast plank floors and concrete bearing walls. Little, if any, of the gravity loads are supported by the beams and columns. Building Type C2f has a column and beam or column and slab system that essentially carries all gravity load. Lateral loads are resisted by concrete shear walls surrounding shafts, at the building perimeter, or isolated walls placed specifically for lateral resistance.	PC: < 1973, LC: 1974-1989, MC: 1990-2004, HC: 2005-present
		C2M	4-7 Floors			
		C2L	< 3 Floors			
		C3H	> 8 Floors	C3: Masonry Infill	Consists of older buildings with an essentially complete gravity frame assembly of concrete columns and floor systems. The floors can consist of a variety of concrete systems including flat plates, two-way slabs, and beam and slab. Exterior walls, and possibly some interior walls, are constructed of unreinforced masonry, tightly infilling the space between columns horizontally and between floor structural elements vertically, such that the infill interacts with the frame to form a lateral force-resisting element.	PC: < 1973, LC: 1974-1989
		C3M	4-7 Floors			
		C3L	< 3 Floors			
	Manufactured	MH	< 2 Floors	MH: Light Frame	Consists of buildings constructed using self-supporting steel chassis or frames that are designed to support transportation on wheels from one location to another. They are integral structures but can be designed in sections and assembled on-site. Floor and roof framing are most commonly wood-frame joists and rafters supported on wood stud walls.	PC: < 1973, LC: 1974-1989, MC: 1990-2004, HC: 2005-present
	Precast	PC1	< 3 Floors	PC1: Tilt-Up	Consists of buildings constructed with concrete walls, cast on site and tilted up to form the exterior of the building. They are used for many occupancy types including warehouse, light industrial, wholesale and retail stores, and office. The majority of these buildings are one story; however, there are tilt-up buildings of up to three and four stories, and a limited number with more stories exist. Lateral forces in PC1 buildings are resisted by flexible wood or steel roof diaphragms and tilt-up concrete shear walls. Floor diaphragms are most commonly composite steel decking.	PC: < 1973, LC: 1974-1989, MC: 1990-2004, HC: 2005-present
		PC2H	> 8 Floors	PC2: Shear Wall	Consists of buildings that include wide ranging combinations of precast and cast-in-place concrete elements. Precast members may be limited to a floor system of hollow core or T-beam construction, or may include all elements of the gravity and lateral load systems. PC2 includes concrete wall or frame buildings in which any of the horizontal or vertical elements of the lateral load system are made of precast concrete.	PC: < 1973, LC: 1974-1989, MC: 1990-2004, HC: 2005-present
		PC2M	4-7 Floors			
		PC1L	< 3 Floors			
	Reinforced Masonry	RM1M	4-7 Floors	RM1: Wood/ Metal Diaphragm	Consists of buildings that are constructed with reinforced masonry perimeter walls with a wood or metal deck flexible diaphragm. RM1 construction can be separated into two categories. RM1u is a multi-story structure and typically has interior concrete masonry unit walls and shorter diaphragm spans, and RM1t structures are large, typically one-story buildings similar to concrete tilt-ups.	PC: < 1973, LC: 1974-1989, MC: 1990-2004, HC: 2005-present
		RM1L	< 3 Floors			
		RM2H	> 8 Floors	RM2: Precast Diaphragm	Consists of buildings made of reinforced masonry walls and concrete slab floors that may be either cast-in-place or precast. This building type is often used for hotel and motels and is similar to the concrete bearing wall type C2.	PC: < 1973, LC: 1974-1989
		RM2M	4-7 Floors			
		RM2L	< 3 Floors			
	Steel	S1H	> 8 Floors	S1: Moment Frame	Consists of buildings characterized by a complete frame assembly of steel beams and columns. Lateral forces are resisted by moment frames that develop stiffness through rigid connections of the beam and column created by angles, plates, and bolts, and/or welding. Floors are cast-in-place concrete slabs or metal decks infilled with concrete. Some S1 structures may have floors and roofs that act as flexible diaphragms such as wood or un-topped metal deck.	PC: < 1973, LC: 1974-1989, MC: 1990-2004, HC: 2005-present
		S1M	4-7 Floors			
		S1L	< 3 Floors			
		S2H	> 8 Floors	S2: Braced Frame	Consists of buildings with a frame assembly of steel beams and columns. Lateral forces are mainly resisted by diagonal steel members placed in selected bays. Floors are cast-in-place concrete slabs or metal decks infilled with concrete. Some S2 buildings may have floors and roofs that act as flexible diaphragms such as wood or un-topped metal deck.	PC: < 1973, LC: 1974-1989, MC: 1990-2004, HC: 2005-present
		S2M	4-7 Floors			
		S2L	< 3 Floors			
		S3	< 3 Floors	S3: Light Frame	Consists of buildings with a frame assembly of flexible steel studs, joists and rafters that are used to establish a complete structural system. They are designed to support axial loads other than self-weight and the weight of attached finishes, which can include masonry veneer, metal cladding, stucco, synthetic veneers and integrated exterior insulation and finish systems	PC: < 1973, LC: 1974-1989, MC: 1990-2004, HC: 2005-present
		S4H	> 8 Floors	S4: Concrete Shear Wall	Consists of buildings with an essentially complete frame assembly of steel beams and columns. The floors are concrete slabs or concrete fill over metal deck. These buildings feature a significant number of concrete walls effectively acting as shear walls, either as vertical transportation cores, isolated in selected bays, or as a perimeter wall system. The steel column and beam system may act only to carry gravity loads or may have rigid connections to act as a moment frame to form a dual system.	PC: < 1973, LC: 1974-1989, MC: 1990-2004, HC: 2005-present
		S4M	4-7 Floors			
		S4L	< 3 Floors			

Figure D.5 Description of building taxonomies used in CanSRM1: [Source Journey et al., 2022] (wood and concrete shear wall typologies were updated from HAZUS, based off this work)




Hazus Building Taxonomy (FEMA P547)						
Model	Construction Material	Typology	Height	Wall Type	Description	Design Epoch
		S5H	> 8 Floors	S5: Unreinforced Masonry Infill	Consists of buildings with an essentially complete gravity frame assembly of steel floor beams or trusses and steel columns typical of older construction practices. The floor consists of masonry flat arches, concrete slabs or metal deck and concrete fill. Exterior walls, and possibly some interior walls, are constructed of unreinforced masonry, tightly infilling the space between columns and between beams and the floor such that the infill interacts with the frame to form a lateral force-resisting element.	PC: < 1973, LC: 1974-1989
		S5M	4-7 Floors			
		S5L	< 3 Floors			
	Unreinforced Masonry	URMM	4-7 Floors	URM: Unsupported	Consists of unreinforced masonry bearing walls, usually at the constructed along the building perimeter. The floors are typically made of wood joists and wood sheathing supported on the walls and on interior post and beam construction.	PC: < 1973, LC: 1974-1989
		URML	< 3 Floors			
	Wood	W1	< 2 Floors	W1: Light Frame	Consists of one- and two-family detached dwellings of one or more stories. Floor and roof framing are most commonly wood-frame joists and rafters supported on wood stud walls. The first floor may be slab-on-grade or framed. Lateral forces in W1 buildings are resisted by wood-frame diaphragms and shear walls.	PC: < 1973, LC: 1974-1989, MC: 1990-2004, HC: 2005-present
		W2	3-6 Floors	W1A/W2: Light Frame		
		W3	< 4 Floors	W3: Heavy Frame	Consists of commercial, institutional, and smaller industrial buildings constructed primarily of wood framing. The first floor is most commonly slab-on-grade, but may be framed. Floor and roof framing may include wood joists, wood or steel trusses, and glulam or steel beams, with wood posts or steel columns. Lateral forces in W2 buildings are primarily resisted by wood-frame diaphragms and shear walls, sometimes in combination with isolated concrete or masonry shear walls, steel braced frames, or steel moment frames. Diaphragm spans may be significantly larger than in W1, W1A and W2 buildings.	PC: < 1973, LC: 1974-1989, MC: 1990-2004, HC: 2005-present
		W4	< 2 Floors	W4: Light Frame/Cripple Wall	Consists of buildings that are similar in construction to W1 light frame structures, but distinguished by wood cripple wall frames built on irregular foundations and/or open subfloor crawl spaces. Lateral forces are resisted by wood-frame diaphragms and shear walls in structural elements above the main floor level. However, cripple wall and subfloor wall systems are often unsupported and not bolted to the foundation and subfloor creating a structural weakness to lateral forces.	

Figure D.6 Description of building taxonomies used in CanSRM1: [Source Journeay et al., 2022] (wood and concrete shear wall typologies were updated from HAZUS, based off this work)